CRANFIELD UNIVERSITY

CITLALLI ELIZABETH RUIZ TREJO

FEASIBILITY STUDY ON MAIZE HUSK AS RESOURCE FOR A NOVEL COMPOSITE MATERIAL

SCHOOL OF WATER, ENERGY AND ENVIRONMENT

PhD/ Full Time
Academic Year: 2014 - 2017

Supervisor: Dr Adriana Encinas-Oropesa
Dr Nigel Simms
August 2018

CRANFIELD UNIVERSITY

SCHOOL OF WATER, ENERGY AND ENVIRONMENT

PhD/Full Time

Academic Year 2014 - 2017

CITLALLI ELIZABETH RUIZ TREJO

FEASIBILITY STUDY ON MAIZE HUSK AS RESOURCE FOR A NOVEL COMPOSITE MATERIAL

Supervisor: Dr Adriana Encinas-Oropesa
Dr Nigel Simms

August 2018

This thesis is submitted in partial fulfilment of the requirements for the degree of PhD

ABSTRACT

Over the past decades, a dramatic increment on the production of maize husk (MH) in Mexico has been observed. Encouraging the study of this copious material as an alternative for the manufacture of composite materials, thereby enabling the use of MH. Offering advantages such as availability, renewability and more importantly the possibility to reduce local pollution levels without compromising the environmental integrity.

The purpose of this research was to develop a maize husk-based composite (MHC) at a lab scale through a transdisciplinary systemic design approach (SDA). The SDA framework was developed from a designer point of view to confront the concerns of MH overproduction, including social, environmental, technical and economic implications. The investigated fibres were obtained from two harvesting methods: manual (MASH) and mechanical (ASPROS). Both MHF's performance was lower than other natural fibres. ASPROS fibres showed a steadier mechanical performance with a cross-section area of 0.14 mm^2, an ultimate tensile strength of 45.75 MPa, a 7.65 % of elongation and Young's modulus of 1.95 MPa.

Nineteen different MHC blends were manufactured, at a concentration of 70/30 MH/binder. Four MH sizes with three binding systems were tested; the sizes were (1) whole husk, (2) chopped, (3) milled and (4) 10 % NaOH alkalinised fibres. The binding systems included: (A) a board made rearranging MH's natural components through thermal fusion, (B) MH mixed with lignin for the production of non-resin MHC boards, and (C) MH blended with a super SAP® CPM epoxy resin (SSE). The size-reduction (milled and alkali) improved MHF' surface interfacial bonding with SSE resin, however, only alkali treated presented enhanced tensile properties. Overall, the M30 boards met the properties of general purpose fibreboards for use under humid conditions (BS EN622-5:2009). The AK30 and M20 boards properties remained within the general-purpose fibreboards for use in dry conditions (BS EN622-5:2009).

Keywords: Agro-waste, maize husk, non-wood fibreboard, mechanical properties, physical properties, natural fibres, bio-based material, systemic design, sustainable innovation.

ACKNOWLEDGEMENTS

This PhD has been the most challenging experience I have had on both academic and personal level. I would not have completed this academic journey without the support of a number of people that guided me through these years.

First, I would like to thank my supervisor Dr Adriana Encinas-Oropesa for having confidence in the project and her recommendations to take me through during this PhD. Second, I would like to extend my thanks to my second supervisor Dr Nigel Simms for his advice and patience. It goes without saying that this PhD would not have been possible without their support and guidance.

Third, I would like to thank Raúl Díaz Arellanes and Aspros *Semillas* for believing and supporting this research. I would also like to thank Andrew Milles for his advice, and to the Cranfield technical staff for their help during the materialisation of the experimental work. Special thanks to Steve Pope for his openness to new (quirky) try-outs in the laboratory, and Rafael Diazgonzález Plata for his extremely useful help to complete the thesis.

Fourth, I would like to extend a warm and special thanks to my Mom, my brother Sergio and my friends. This PhD would not have been possible without their love and advice during my time in Cranfield. Last but not least, to express my gratitude to my beloved husband Omar, for his love, and continuous encouragement during my struggle with the PhD monster.

This PhD was sponsored by the Mexican government, through the National Council of Science and Technology (CONACYT).

"To eliminate the concept of waste means to design things-products, packaging and systems- from the very beginning on the understanding that waste does not exist."

W. McDonough

TABLE OF CONTENTS

LIST OF FIGURES

LIST OF TABLES

LIST OF FIGURES IN APPENDICES

LIST OF TABLES IN APPENDICES

LIST OF EQUATIONS

LIST OF ABBREVIATIONS

%E	Apparent elongation
AA	Accelerated ageing
AK	Alkali
AR	As received
ASTM	American Society for Testing and Materials
AW	Agricultural waste
AZ	Enzymatic extraction
BC	Bio-composites
Bs	Binderless
BT	Billion Tonnes
C2C	Cradle to cradle
C2G	Cradle to grave
CI	Confidence interval
CIMMYT	International Maize and Wheat Improvement Centre
CM	Composite material
CPA	Composite Panel Association
CSA	Cross section area
DfBP	Design for the base of the pyramid
DfS	Design for sustainability
DfSI	Design for sustainability innovation
DT	Design thinking
E	Young’s modulus
FAO	Food and Agriculture Organization of the United Nations
FM	Flexural Modulus
GC	Green composites
GHG	Greenhouse gas emissions
HDF	High-density fibreboard
HP	Hand-picked
IT	Impact test
L	Lignin
M	Milled
MASH	Market sourced husk
MD	Material development

MDF	Medium density fibreboard
MDP	Medium density particleboard
MF	Melamine formaldehyde
MH	Maize husk
MHC	Maize husk composite/ fibreboard
MHF	Maize husk fibres
MOR	Modulus of elasticity
MP	Machine-picked
MR&D	Material research and development approach
MRD	Material research and development
MRL	Manufacturing readiness level
MT	Million tonnes
NF	Natural fibres
OECD	Organization for Economic Co-operation and Development
OW	Organic waste
PF	Phenol formaldehyde
PP	Polypropylene
SAGARPA	Mexican Secretariat of Agriculture, Livestock, Rural Development, Fisheries and Food
SD	Standard deviation
SDA	Systemic design approach
SEMARNAT	Secretariat of Environment and Natural Resources
SSE	Super Sap® CPM epoxy resin
TES	Techno-economical study
UF	Urea formaldehyde
UMF	Melamine urea formaldehyde
UN	United Nations
UTS	Ultimate tensile test
VOC	Volatile organic compound
WBF	Wood-based fibreboard
WM	Waste management
wt.%	Water uptake

GLOSSARY

Design thinking

The thought processes of designers capable of transforming products, companies, and even social issues [1].

Sustainability

Derived from the sustainable development definition from the World Commission on Environment and Development, 2016 [2], sustainability is defined as the ability to make development sustainable, to ensure that it meets the needs of the present without compromising the ability of future generations to meet their own needs.

Transdisciplinary research

Transdisciplinarity according to Lawrence and Després, 2004 [3] is the articulation among disciplines to address issues relevant to society; in contrast to multidisciplinarity or interdisciplinarity that implies the articulation of different types of knowledge.

Autopoiesis

The self-maintenance of an organised entity through its own internal processes; Also defined by Barbero (2011) [4] as a self-maintaining system that sustains itself by reproducing automatically.

Peel failure in a composite

Failure initiated as transverse tension may progressively change to peel as the fracture moves away from the origin.

Resin maturing

Is the time it takes the chemical reaction during a two-phase resin preparation; it is also known as ambient temperature *"maturing"*.

Trilobal

tri = three and *lobal* = sides. Fibres that have three distinct sides.

Carreteros

Colloquial name for scavengers.

Polymerisation

A chemical reaction in which two or more molecules are combined to form larger molecules that contain repeating structural units.

Bast

Fibrous material from a plant. The phloem or vascular tissue of a plant.

Hygroscopicity

The capacity of a material to react to the moisture content of the air by absorbing or releasing water vapour.

Delignification

The removal of lignin from woody tissue, through natural enzymatic or industrial chemical processes.

1 INTRODUCTION

The increasing demand for wood-based fibreboard materials (WBF) has considerably impacted the forests in Mexico. The Food and agriculture organisation (FAO) reported in 2016 Mexico's timber wood production of 5.3 million m^3, in contrast to WBF production that dropped 15 % during the same year [5]. Making evident the current wood fibre scarcity in the country. Thus, the potential use of alternative cellulosic materials, particularly agricultural waste (AW) fibres, as a reinforcement for composite materials (CM) has opened new possibilities for the local industry due to their availability and low cost.

As the origin place of maize, Mexico occupies the third place in maize consumption per capita, since it covers 33 % of their daily caloric intake. The Mexican Secretariat of agriculture, livestock, rural development, fisheries and food (SAGARPA) has forecasted a 5.5 % increment in the annual maize production, however, that will be reflected as nearly 3 million tonnes (MT) of MH waste by 2020 per year [6]. This situation put the local waste management (WM) efficiency under the spotlight; in the last years, the agricultural WM has been proven deficient according to the Secretariat of Environment and Natural Resources (SEMARNAT) reports [7]. Local and international institutions have indicated crop burning remains as the primary disposal method in the country as shown in Figure 1. Despite the government efforts to reduce this practice, crop burning in Mexico releases 600 tonnes of CO_2 per year, from which 90 % is directly related to maize harvesting (FAO [8]).

A number of disciplines related to natural fibre-based composites have increased considerably in recent years. This awareness has not only aroused among academics but also from stakeholders, consumers, designers, economists, sociologists and environmentalists according to Karana et al. [9]; thus, demonstrating that to achieve material science innovation is necessary to have a different approach towards raw materials and processes. Thereby increasing the chances to obtain a novel material in a shorter period. In search of innovation, the material sciences have turned to other disciplines. Muratovski [10] places design and design thinking (DT) as the most outstanding contributions to innovative research methodologies. In this manner, my experience working with materials together with my background as an Industrial Designer have become the required link to carry out the present research.

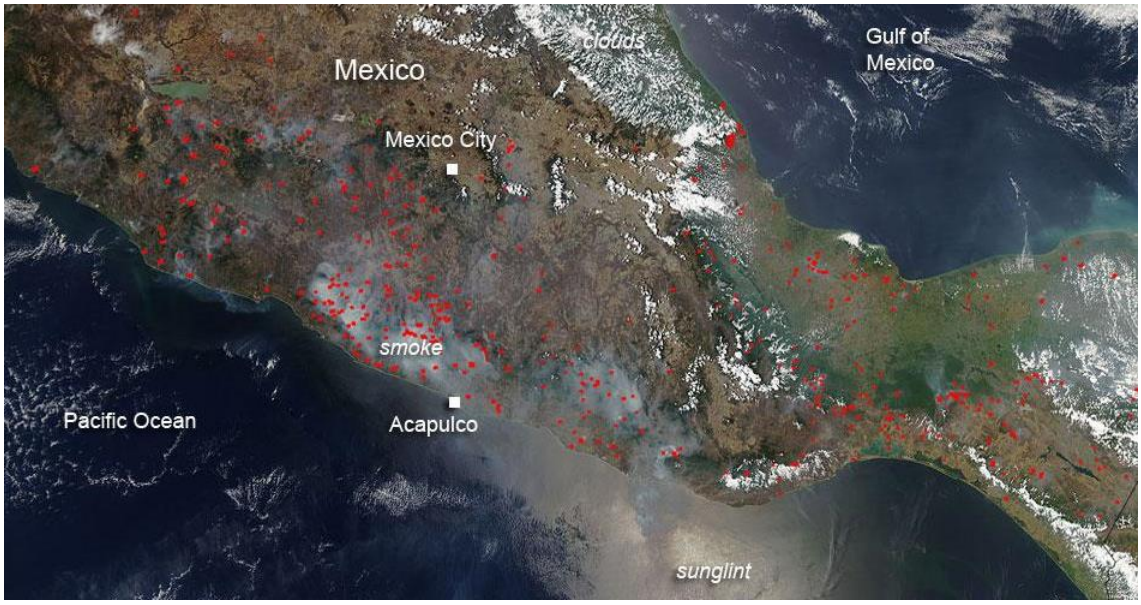

Figure 1 Fires detected during the burning season (March-May) in Southwestern of Mexico, (NASA [11])

The focus of the first chapter is to establish the grounds for the development of a novel CM from the perspective of an SDA. Thus, the SDA framework aims to encourage a shift towards a more sustainable and affordable MHC development and eventual manufacture, besides raising the environmental consciousness among stakeholders involved and the local people affected by the AW recovered. Following this, the SDA was divided into four sections: design for sustainable innovation (DfSI), design for the base of the pyramid (DBoP), material research and development (MR&D), and techno-economic study (TES). Each methodology assisted not just to add value to an existent waste, but to tackle the MH overproduction in Mexico from more sustainable development as Figure 2 depicts.

Research interest in natural fibres (NF) has increased in the past decade, driven mainly by the raw materials shortage and the increment of food production, e.g. wheat, maize and rice [12]. The potential of renewable lignocellulosic materials from AW, as an alternative to wood-based fibres, has been widely explored by Youngquist et al. [13]; however, the study of MH' fibres remains very scarce to date.

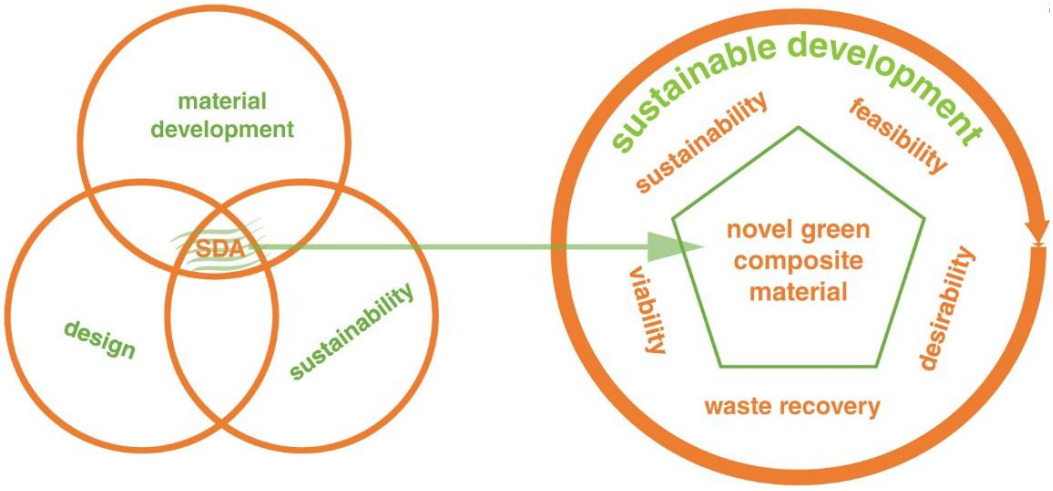

Figure 2 Drivers to achieve sustainable development through an SDA in the manufacture of a novel composite material

Therefore, this research focused on two types of MH (ASPROS and MASH) produced in the State of Mexico. The assessment covered whole MH and extracted fibres morphology, tensile strength, moisture content, as well as diverse extraction methods. Moreover, MHC boards were manufactured and assessed according to WBF's international evaluation standards. Nineteen combinations were made using four different husk states (whole, chopped, milled and alkali) with three different bio-based binding systems (binderless (Bs), lignin (L) and an SSE resin).

The final section of the thesis draws upon the obtained data tying up the various aspects studied from the SDA perspective, i.e. MH selection, production processes, production volume, current technologies used and the estimated cost for the MHC boards. Thereby, the MHC boards manufactured were analysed and selected based on qualitative and quantitative properties from an SDA transdisciplinary perspective; thus, by doing so, a comprehensive understanding of the MHC manufacture has been obtained. Together with the TES, the MHC pilot plant setting-up provided additional data to discuss aspects to consider, such as the social impact, price fluctuation and technical feasibility of a large-scale MHC manufacture, and production volume.

Overall, the SDA framework assesses the MHC manufacture from a transdisciplinary perspective to determine whether the design intervention helped to create a transferable methodology for material design innovation; besides covering the whole life-cycle of the MHC material.

1.1 AIM AND OBJECTIVES

1.1.1 Aim

To maximise agricultural by-products used in Mexico, through a feasibility study on MH as a raw material source for a novel composite material.

1.1.2 Objectives

The objectives of this thesis are as follows:

- To define and apply a systemic design approach (SDA) for the development of a novel green composite based on discarded maize husk.
- To investigate the overall physical and mechanical characteristics of the MH.
- To manufacture of an MHC based on three different bio-based binders.
- To increase the understanding of MHC's core physical properties (flexural and tensile strength, density, impact resistance, thickness swelling and accelerated ageing) through standardised testing.
- To carry out a preliminary techno-economical study to analyse MHC pilot plant feasibility and MHC manufacture costs.

Figure 3 shows a summary of objectives and the accomplished outcomes per chapter.

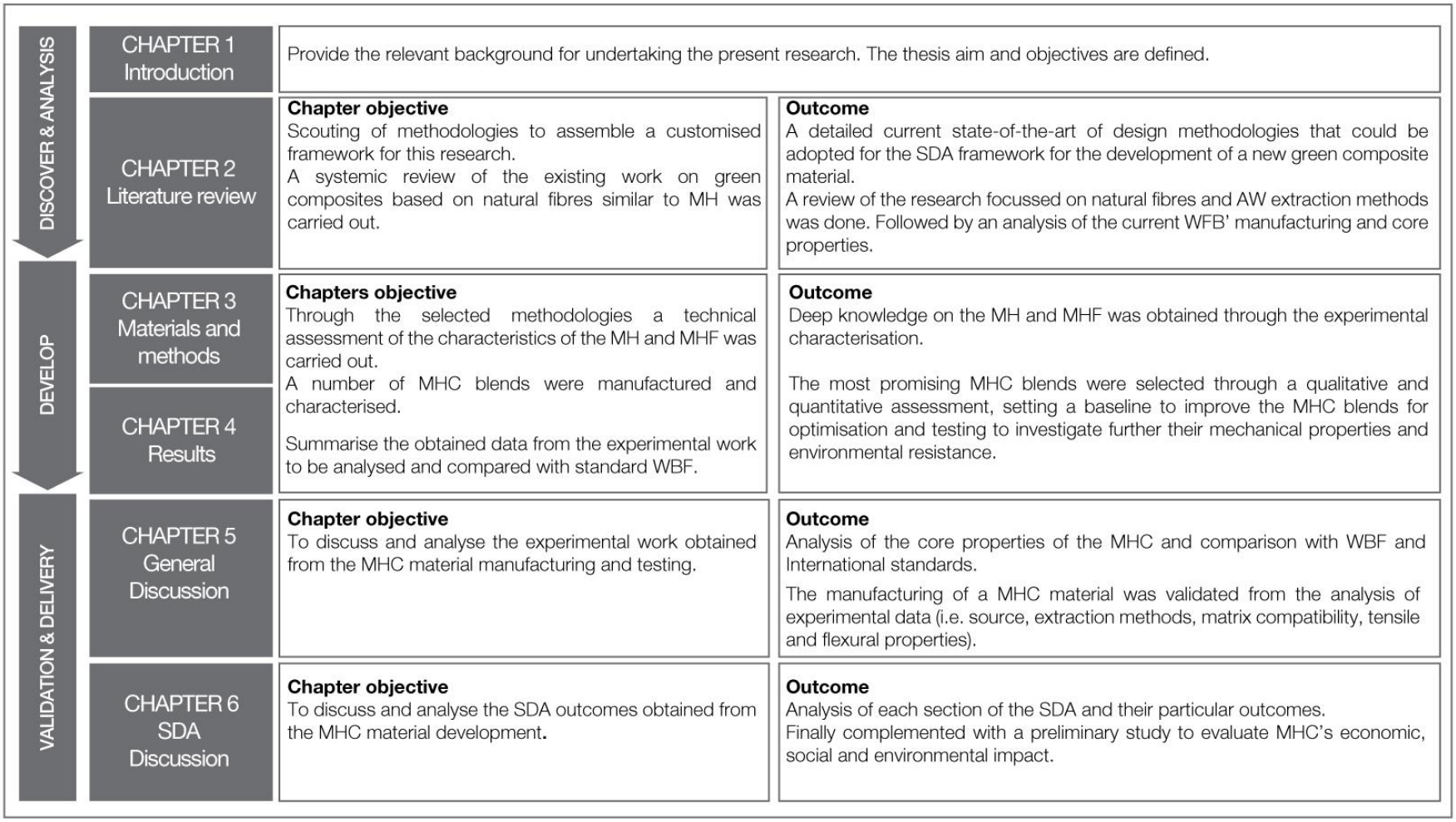

Figure 3 Thesis outline of each research phase, objectives and obtained outcomes throughout each chapter

2 LITERATURE REVIEW

The present literature review outlines the rationale for undertaking an SDA to develop a novel composite material. The proposed SDA framework (Figure 55) is based on four methodologies: DfSI (section 2.1.2), DBoP (section 2.1.3), MR&D (section 2.1.1) and TEC (2.1.1); and from there builds up into an interdisciplinary approach for the development of a novel AW based CM. The rationale behind the selected methods is discussed, along with the particulars of the context such as AW types and availability, environmental, social and economic impact. Thus, the research scope is adequate and able to meet the research objectives.

A general overview of similar natural fibres composite (NFC) materials, NF extractions, methods, CM manufacturing processes, and, core physical and mechanical properties are also presented. However, these are limited to the scope of the present research.

2.1 Systemic design for novel material development

To date, there has been little agreement on the role of a designer as a researcher. However, as Muratovsky [10] presents, designer's artistic-oriented skills are shifting towards a conceptual and problem-solving discipline. Thus, to overcome a broader range of challenges, companies and clients are turning to designers not only to deal with product related issues but also to bring them into social, data generation, policy-making, education and logistics projects [14]. As a result, according to the Design Council's 2010 report [14], 51 % of the load work of design businesses in the UK is carried out in collaboration with other disciplines. Demonstrating the relevance of cross-disciplinary insights to achieve significant innovation in diverse fields such as finance (40 %), education and retail (31 %), and manufacturing (30 %).

Thereby the proposal of a novel transdisciplinary methodology through the implementation of DT principles will allow the application of Lawrence and Després [3] adaptative approach. On their work presented a series of cases that

challenged structured methodologies with a more flexible and interlinked approach, by using these creative tools to move freely and exchange information between academics, policy decision-makers and users. This approach enables designers to understand whether they are following the right path to reach a solution. Hence, as in Brown's [15] *human-centered* approach, the interaction between disciplines becomes the "real problem" identifier. Thence, the project' technical aspects offer the right inputs, and consequently innovative results are reached. Overall, Luchs et al. [16] study is a compelling explanation of how DT strategies can be applied by design professionals, but also by any other professional open to doing so. Thus, the SDA framework as an academic tool may be used by designers, chemists, lawyers, engineers and sociologists, to mention a few.

Figure 4 schematic provides valuable insight into how an iterative system draws upon four main questions, and from there it moves back and forth in a flexible non-linear sequence in search of insightful results. Therefore, as previously mentioned, DT encourages the interaction between stages and disciplines at any point in the research to obtain non-conventional solutions, that can be reviewed and proven from diverse points of view. Thereby, the use of a DT approach in the present research could be seen as a collaborative job between design, material sciences, waste management and sustainability.

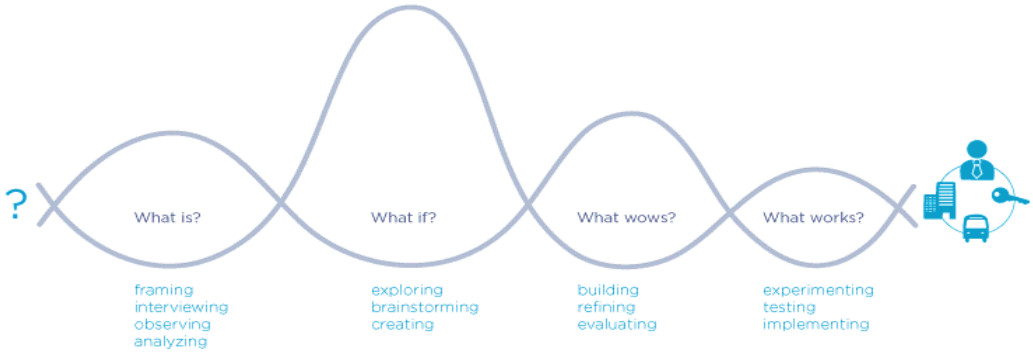

Figure 4 Design thinking framework [16]

Moreover, the results of earlier studies have demonstrated the strong link between the application of design methodologies and the acquisition of

unconventional (innovative) contributions. For example, Peters [17] documented how DT emerged as a powerful cross-disciplinary platform tool for a wide range of companies in the last decades. On the other hand, the difference between multidisciplinary and transdisciplinary research was extensively discussed by Lawrence and Després [3], emphasising that multidisciplinarity is a fixed arrangement, e.g. systematic product design process, where the disciplines work parallelly towards the same objective. Whereas in the transdisciplinarity or lateral perspective, e.g. DT, the objective/problem is approached by a non-linear knowledge interconnection of diverse disciplines; hence, a wider perspective is covered and an interconnected solution can be reached. Therefore, the proposal of a holistic and interdisciplinary methodology to assemble an SDA for the development of a novel CM based on AW and broaden the approach for a cleaner and more efficient production. Consequently, allowing this research to achieve innovative solutions based on Brown's (2009) [1] design approach. Figure 5 is a good illustration of the three "needs" according to *human-centered design*: desirability, feasibility, and viability. Therefore, the application of an SDA in the development and testing of a novel AW based CM will expand the boundaries of apparent opposing disciplines, such as design, sustainability and material science to demonstrate its adaptive capabilities.

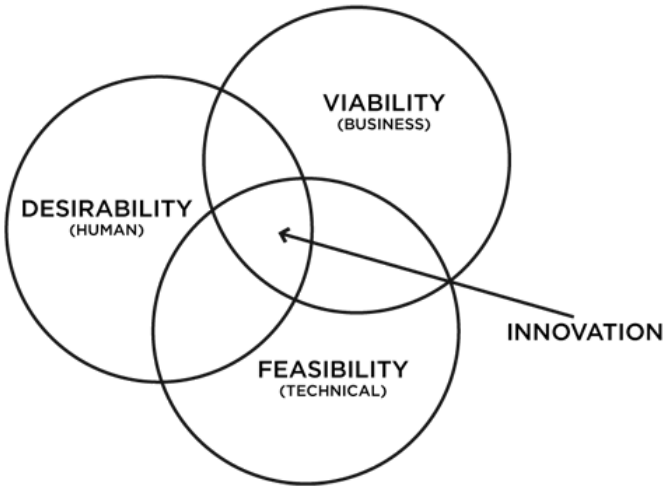

Figure 5 IDEO's design thinking *human-centered* approach [18]

Roos [19] elaborates on the relevance of design-based innovation approaches, by developing a four-value creation strategy, shown in Figure 6, to create a tailored approach for the manufacturing sector. Most of his case studies were focused mainly on mass-produced objects. Whilst Friedman [20] reworked Roos's approach to demonstrate the advantages of the designer's transdisciplinary proficiency and technical skills to solve complex and diverse problems; by integrating Natural Sciences; Humanities and Arts; Social and Behavioural Sciences; Human Professions and Services; Creative and Applied Arts; and Technology and Engineering. On the other hand, IDEO's previous studies have considered transdisciplinarity as the primary tool to draw new paths for innovation in social challenges such as the lack of in-home toilets, access to clean water [21] and even in building health literacy in developing areas [22]. In the same fashion, Karana's et al. (2015) [9] addressed the perception and development of materials.

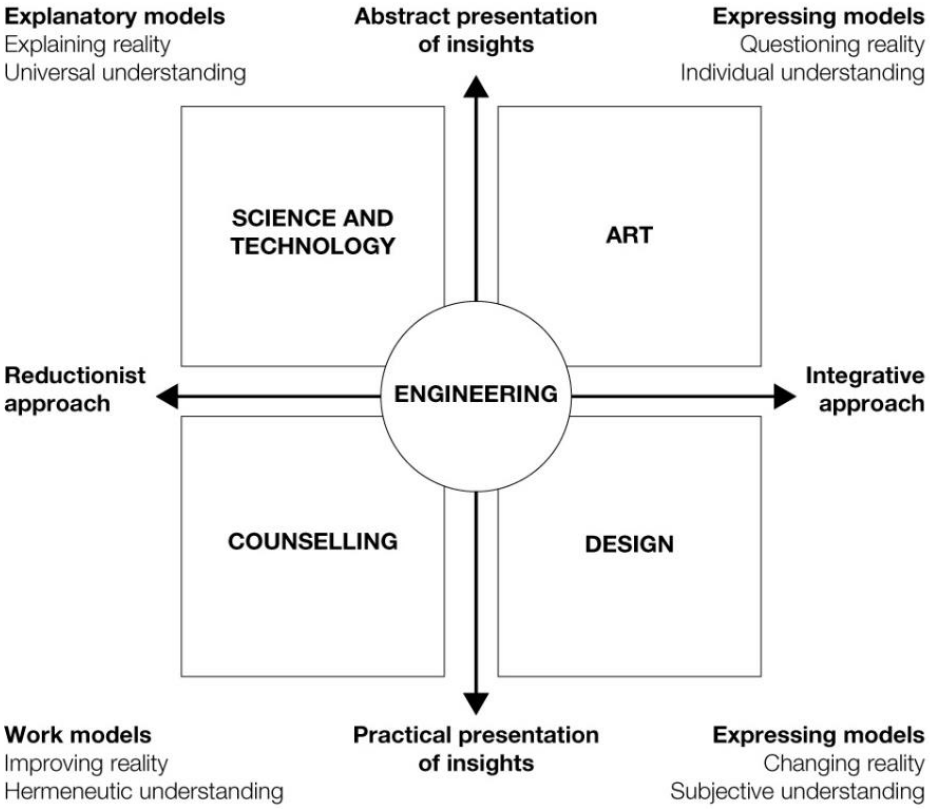

Figure 6 Freidman's redraw Roos's [23] value creation approaches and added engineering [20]

Whilst several studies have shown sustainability as a key element to compensate the current environmental damages, it has been demonstrated that it will not make a significant change if treated as an isolated phenomenon, but as an interconnected natural system. In the same way, the SDA approach aims to develop a manufacturing model inspired by the natural systems, where all the elements are interconnected in a closed loop by exploring synergies with other disciplines. Furthermore, based on Karana's et al. [9] research on material driven design, it has been demonstrated the need to consider not only the composite's technical characteristics but its long-term impacts on the society and natural environment.

To date, only a few studies have assessed design-driven cross-sectional methodologies focused on AW-based material developments. A prominent example is Barbero and Toso's [24] coffee waste recovery study which validated a successful merge of systemic design [25] and design for sustainability (DfS) [26,27]. That resulted in a transferable methodology for other industries than material development (MD). Therefore, the trend of DfS studies has evolved from incremental innovation applied to existent products, i.e. green design [28], to product life extension, i.e. emotionally durable design [29]. It is evident the lack of interaction and communication between disciplines from different backgrounds, resulting in the omission of the product's long-term impact. Ceschin and Gaziulusoy [29] have reported that much of the DfS research to date pinpoints to lowering industrial environmental impact throughout innovation. Similarly, Thorpe's [30] research has spanned sustainable development throughout a DT perspective. In some way, these approaches have initiated a shift towards a more sustainable and cleaner society; however, their contribution to CM development remain not yet fully understood.

The SDA methodologies were selected based on their particular scope, emphasising their capability to take part in an innovative interlinked system. Based on Castillo's et al. [31] innovation drivers to reach an integral product development are shown below in Figure 7.

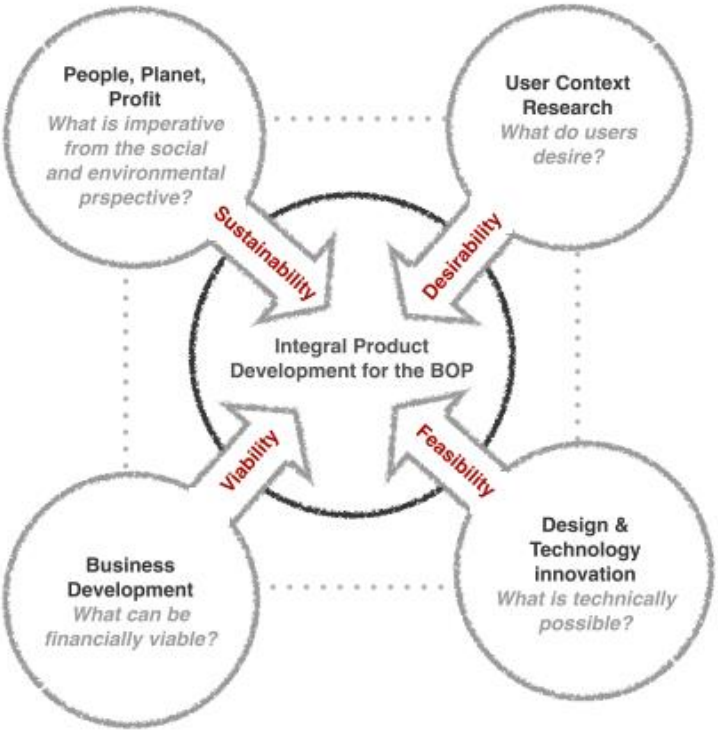

Figure 7 Castillo's et al. [31] integral product development approach for the base of the pyramid

To date, very few studies have held the study of MD, design and sustainability simultaneously, with the sole focus of contributing to the identification and application of specific approaches to promote their use as a basis for future research framework. The closest comparable case study to this research is the presented by Karana et al. [9]. In this example, they tested the materials from three different perspectives: a relatively known material, an unknown material and a material proposal (new material); measuring material's physical properties and user's emotional perception. Other researchers, however, gave preference to traditional material research and development (MRD) approach to optimise and test novel CM, facing lengthy development processes, e.g. Martínez García et al. [32] and Madurwar et al. [33].

The collaborative nature of the SDA approach offers a number of advantages over the individual use of each methodology. However, to fully understand

SDA's extent, the relevant characteristics of the four methods selected will be reviewed further ahead.

2.1.1 Material research and development

The MRD approach objective is to identify and evaluate the physical and mechanical characteristics of a specific material. Following a Stage-Gate™ [34] scheme, scientific method and material engineering, to meet specific requirements according to industry demands. Although these methodologies have been proven to be efficient and accurate, they are considerable lengthy and expensive.

The US Air Force technology program has widely used the first of these approaches, the Stage-Gate™ model (Figure 10). However, despite great efforts, the MRD timeline remains between 14-18 years from the initial exploration up to the material launch to the market [35]. This linear MRD approach strength lays on the technical features of the material, rather than on its long-term environmental impact or users' perception [29].

Overall, the MRD approach will provide the objective and analytic basis for the manufacturing of an MHC. While to attain quality data during earlier stages from a novel material in a short time frame may result very challenging, Roos [36] acknowledges design' ability to lead to behavioural changes within engineering processes, yet not specifically in the MRD area.

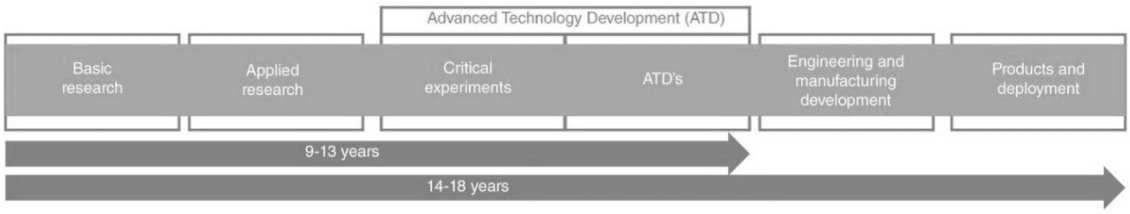

Figure 8 US Air Force material development program [35]

2.1.2 Design for sustainability

Papanek's [28] work on design competence to address social and environmental challenges, is complemented by Chick and Micklethwaite's [26],

research where they discussed further the design systems. Suggesting a disciplines crossover to tackle a wider scope of challenges, such as manufacturing, scientific and even policy advice.

Moreover, according to Ceschin and Gaziulusoy [29] in the last decades DfS approach has become the main driver to increase society's awareness and interest in local sustainability challenges. Transforming the stationary perception of sustainable development, into an interactive system. In the same fashion, DfS has evolved into an essential element of the longed shift towards a cleaner and sustainable manufacturing culture. The sustainable material development was considered by Chick and Micklethwaite [26] as the approach that best integrates sustainability and design, where the main objective is not "designing for" but "designing with". Although some research on environmental awareness and DT has been carried out; only a few controlled studies have been reported on AW CM developments (e.g. banana [37], coconut shell [38] and pineapple [39] residues), even less in Mexico (e.g. agave bagasse [40], henequen [41], and coconut shell [41] residues).

The socio-technical innovation system of DfS is focused on supporting the transition to the new SDA framework. Its wide scope encourages not only the ideas transference but also to rethink the raw material through experimentation, the manufacturing systems, and stakeholders perspectives. Manzini and Vezzoli [42]; and Vezzoli [43] have forecasted in the SDA diversity based on the individual outcomes of each methodology; the synergy between them is what characterises the approach.

Perhaps the most thorough review on DfS evolution and reach is to be found in the work of Ceschin and Gaziulusoy [29]; where they analyse the transition of green design towards a systemic design approach. The latter's approach goal of designing locally-based productive systems was used as a baseline for the purposed SDA framework (Figure 55). Supported by cradle to cradle (C2C) system and the 7R's golden rule to encompass to reach a cleaner material manufacturing system.

Before proceeding to explain the C2C system, it is necessary to understand that since the industrial revolution in the 1800's the manufacturing processes have been operating as a one-way system of resources consumption (shown in Figure 9(a)). The process is known as cradle to grave (C2G) material flow system, still widely used globally despite the fact of the current natural resources shortage. This system also has a number of serious ecologic and social drawbacks. Many studies have investigated the causes of C2G's failure, one of the most remarkable is the United Nations (UN) committee's report "*Our Common Future*" [2], where humanity's ability to deflect the current environmental depletion is questioned and challenged by an overall sustainable development shift. Thus, not only social and ecological awareness and involvement is of paramount importance for an adjustment for sustainable human development; but a comprehensive transformation including all the actors, i.e. industries, redirection of investments, refocus the technological development, and public policies adjustment.

While the "take-make-dispose" system [44] increases companies operation costs and environmental depletion; the introduction of a natural regenerative system known as C2C [45] boosts the raw material production and waste is minimum or non-existent. As it can be observed in Figure 9(b), the C2C system most significant advantages are the acknowledgement of environmental limits. Thus, the industries can allow the ecosystems to recover at their own pace; and the system's adaptability to suit multiple conditions, as a "one-size fits all" system is no longer an option as it was in the linear manufacturing systems [45].

Consequently, some manufacturing companies, e.g. construction materials, textiles, health and beauty products, home and office supplies to mention some, have started implementing and certifying their productive system following C2C principles. Even despite the economic risk that expensive processes, undefined methodologies, and producers and consumers' lack of interest in products origin may represent. However, the company Method© [46] has successfully implemented these apparent drawbacks from the C2C principles including green chemistry, closed-loop design, recyclability, and biodegradable

ingredients in all their cleaning products. Demonstrating the viability and market openness for this kind of products and services.

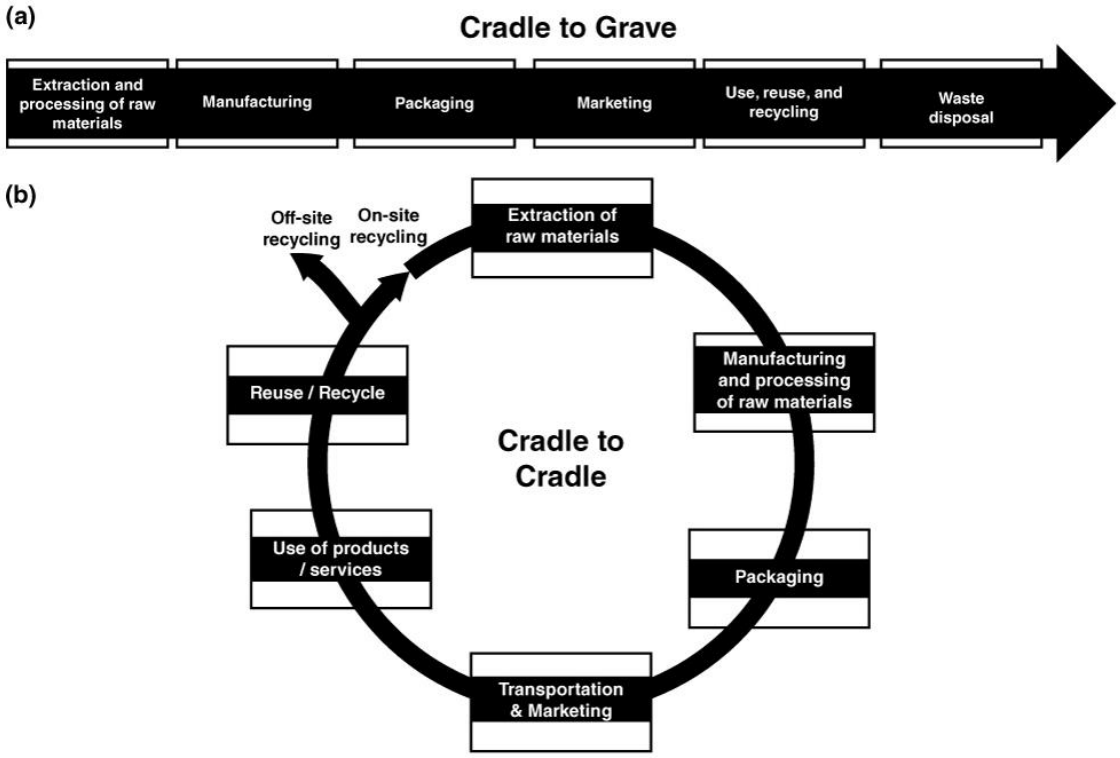

Figure 9 Material flow cycles. (a) C2G cycle, and (b) C2C cycle, compiled from [47]

C2C system gives an alternative view of reaching more accurate handling of AW overproduction in Mexico's central area. As the raw material availability, collection and ecological consequences of using this valuable resource are integrated into a closed loop for the whole process of the CM manufacturing system. A reassessment of the new material's path in the circular economy will be necessary, as suggested in the report "*Towards a circular economy"* [44], to guarantee a comprehensive interpretation of C2C principles. The technologic and economic affordability was incorporated to underpin MH's feasibility to be transformed into a CM through a TES.

Moreover, WM plays a vital role as a complement to the circular economy, and particularly if the raw material comes from an AW. Figure 10 illustrates El-Haggar's [47] categorisation for the WM known as the 7R's phases. He

classified waste's path regarding material source, durability, reparability, disposal system (if any), and finally the three last stages lead towards a zero pollution and waste production policies.

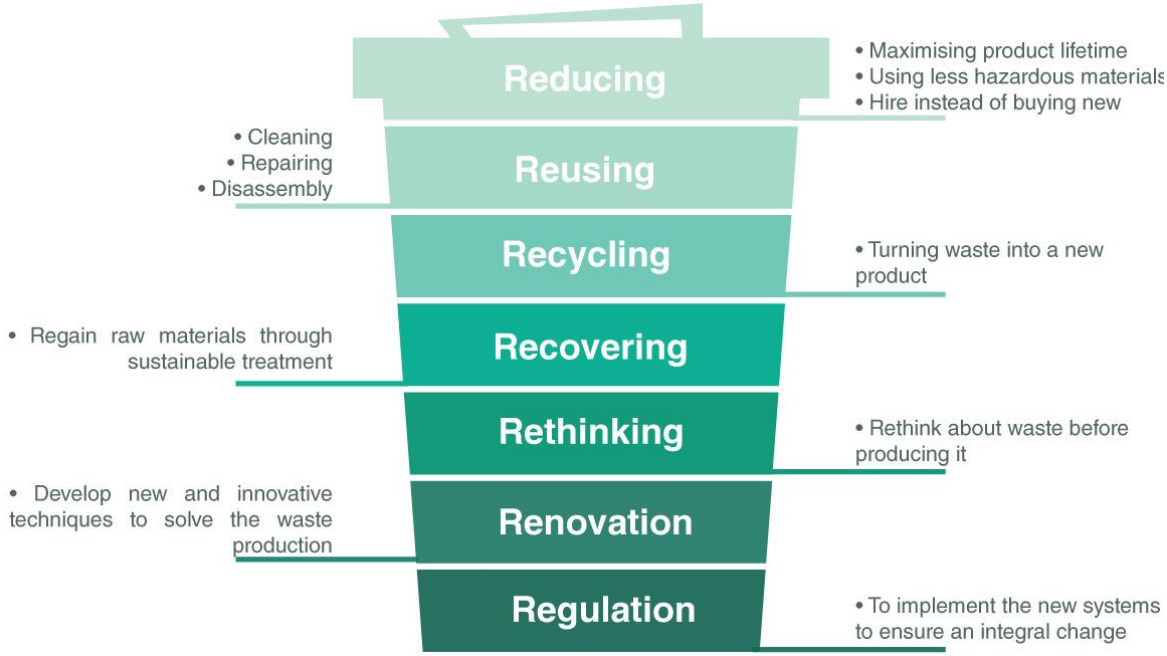

Figure 10 7R's Golden Rule diagram [47]

The 7R's golden rules have been successfully implemented in the C2G manufacturing processes. However, it will require a profound effort and investment for the manufacturing industries to be taken into a C2C manufacturing cycle. Not only because of the lifecycle product follow-up up elevated costs but for the struggle that represents to encompass not only raw material producers, suppliers, goods manufacturers, final users and local authorities to assume their responsibility along the product's path.

2.1.3 Design for social innovation

Whilst DfS opens the design scope towards technological developments; the DfSI approach is more focused on the social implications of these novel processes. Thus, the people considered within the base of the pyramid, are those with an income below USD 1.90/day as the international wellbeing threshold established by the World Bank in 2017 [48]. There is, therefore, a definite need to enable the 53.3 million people [49] living in poverty in Mexico to

take part and own attainable productive projects. However, the generalisability of this approach, as discussed by Castillo et al. [31], is limited to the local resources and subjects' openness to external intervention in their economic growth.

Although one of the strengths of this approach is the inclusion of a great number of actors (farmers, manufacturing industry, government, academics), it has certain limitations due to the lack of information flow, reduced or inexistent infrastructure and low literacy levels in the study area. Thus, making more complex the communication among the communities, investors, and governmental institutions; and consequently, determining the impact of MH overproduction and exploitation in Mexico, as well as its future environmental effects.

Therefore, more information on social-economic development in an emerging economy, by involving the community as co-owners and co-creators of a maize husk-based composite material pilot plant, would help to establish a greater understanding on the application of the DfSI approach. Even though a DfSI model per se was not found in the literature, Barbero [4] adopted five nature-based principles to assess the application of a systemic design methodology: *output>input, relationship, act locally, autopoiesis, and the man at the centre of the project*. She implemented the methodology in seven case-studies, where the disciplines' interaction was proven through the local development.

In contrast, Castillo et al. [31] summarised the main tools employed to take forward social innovation and entrepreneurship with a strong base on design for the base of the pyramid (DfBP). Their framework is based on five steps: *preparation, contextualization, concept development, implementation* and finally *managing* as shown in Figure 11. Castillo's et al. approach is one of the most practical methods for its comprehensive problem treatment, which includes practical tools for each phase in order to address local socio-economic development.

Altogether these methodologies serve as theoretical guidelines to underpin the foundations of the SDA framework focused on MD. This review has helped to have a thorough insight into different disciplines and its reach. However, the SDA framework illustrates the flexible knowledge transferability, suggesting its efficacy when looking for a sustainable solution for the current AW overproduction in Mexico. The SDA provides a method to assess the outcome of four different approaches to obtain a solution that fits them all; in other words, a way towards sustainable development.

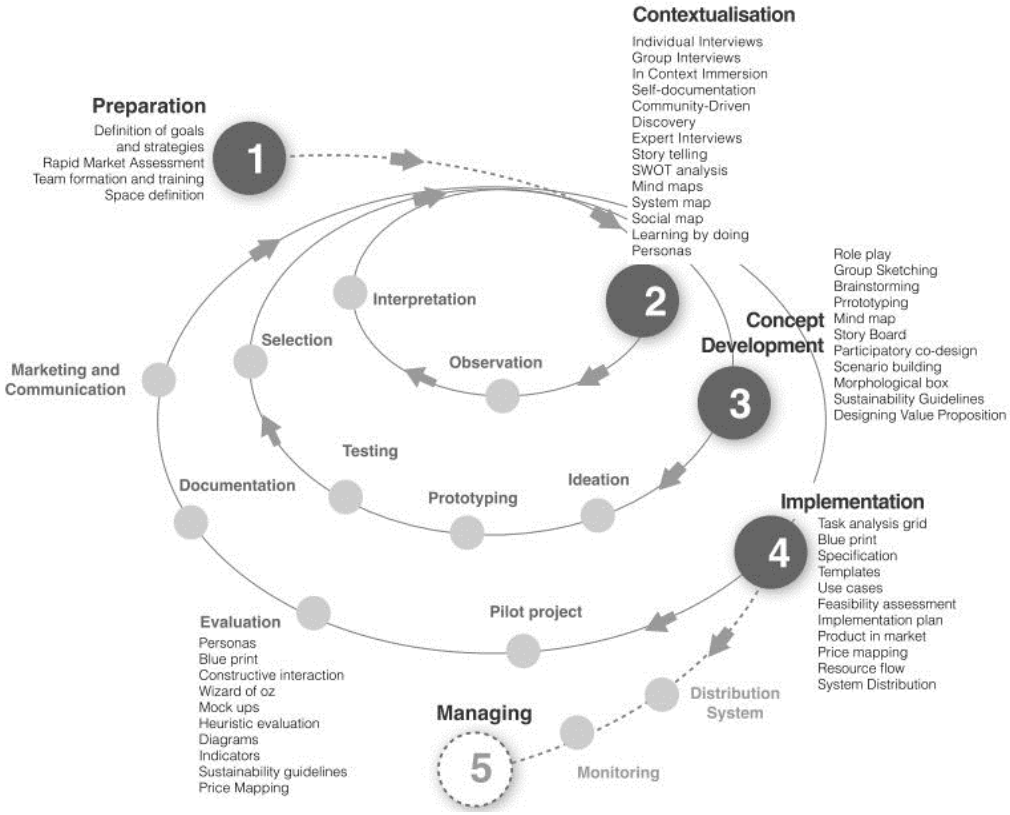

Figure 11 DfBP framework and tools [31]

2.2 Waste management

WM has been an object of research in the last decades, while several studies have underpinned waste handling relevance as the main driver for social, economic and environmental change, capable of not only to avoid further environmental damages but to atone for the current depletion [50]. Other studies have emphasised the low effectiveness of current disposal methods, as

the World's Bank [51] report that estimated annual production of 1.3 billion tonnes (BT) of solid waste. Most of these studies have typically concentrated on plastics, metal and wood, even despite that 46 % of the waste stream is integrated of natural materials (organic and agricultural residues).

The irreversible effects of poor WM programmes, such as public health problems, air, water and soil pollution, have become an issue of concern for local policymakers all over the world, and Mexico is not the exception. Thence, government and stakeholders have begun a reassessment for the implementation of a new AW management system. Based on the 17 sustainable development goals set out by the UN and local governments in 2015 [52]. However, despite the launch of waste disposal programmes, an average of 41% per kilogram of raw material recovery (for re-use and recycling) [51,53] remains within the countries Organization for Economic Co-operation and Development (OECD) as shown in Figure 12. This is certainly true in the case of Mexico, Slovenia and Turkey, countries where the lack of WM and correspondent policies stands out [51].

Mexico produces 44 MT of waste per year, from which only 9.6% is recycled as a result of the almost inexistent waste classification system [7]. Comparison of the OCDE findings with those of Jacinto Nieves [50] confirms that generalised efforts are still scarce particularly regarding AW, due to the lack of a proper residues system handling. Hence, Mexico has become one of the worldwide top greenhouse gas emissions (GHG) emitters from waste disposal (i.e. landfilling) as described in Table 1.

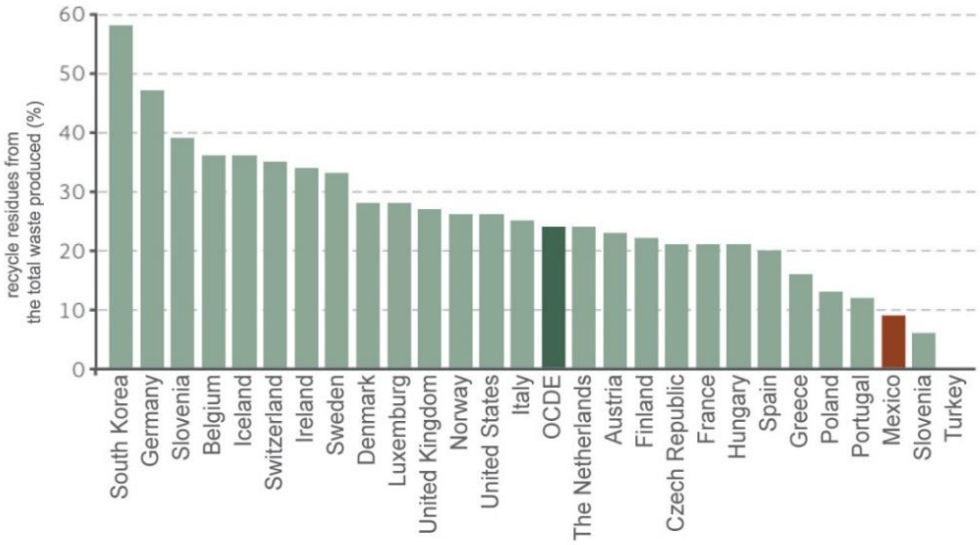

Figure 12 Recycling percentage in the OECD countries, 2012 [7]

Table 1 Landfill methane emissions and GHG, compiled from [12,51]

Country	Methane emissions from post-consumer municipal waste disposal ($MTCO^2e$)	GHG (CO^2, CH_4, N_2O) ($MTCO^2e$)	Methane percentage from disposal sites relative to total GHG (%)
Brazil	16	659	2.4
China	45	3,650	1.2
India	14	1,210	1.1
Mexico	31	383	8.1
S. Africa	16	380	4.3

Moreover, the World Bank [54] has reported energy and manufacturing industries to hold the highest levels of CO_2 emissions (27 and 19 %); agriculture, forestry and fishing had a steady rise of 8.5 % in the last decade due to the increasing global food demand [12]. Although agriculture-related emissions have reached only 12 % of the overall GHG, the present research will focus in the 6 % from the large quantities of AW produced and the deficient disposal methods adopted, i.e. burning of by-products in the open air [55–57].

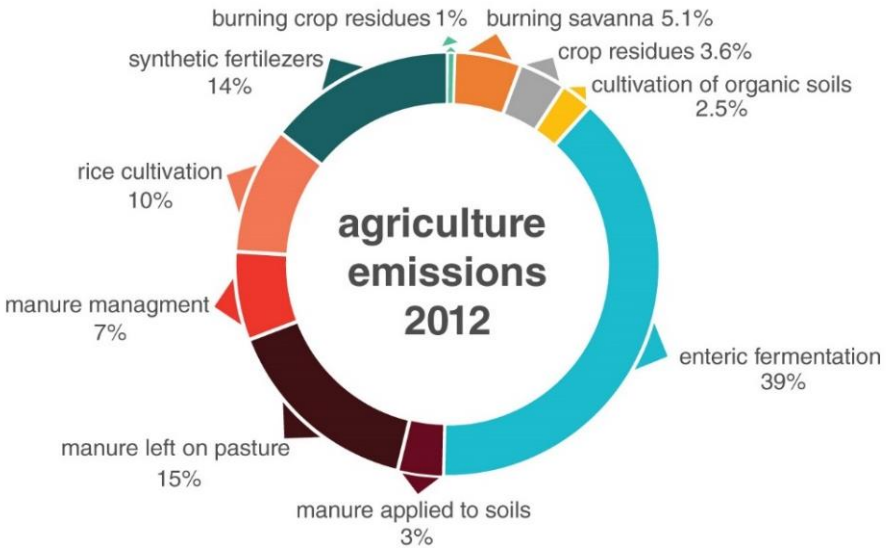

Figure 13 WW CO_2 agriculture emissions report, 2012 [54]

In 2016, FAO revealed that globally wheat (27%), rice (26%) and maize (23%) were the most contaminating crops, as Figure 14 shows. Despite the steady rise of worldwide crop production, the UN sustainable development goals [58] did not consider it. Some countries have already in place a WM system prepared to tackle the current AW generated, however, they are not for the expected increment of AW.

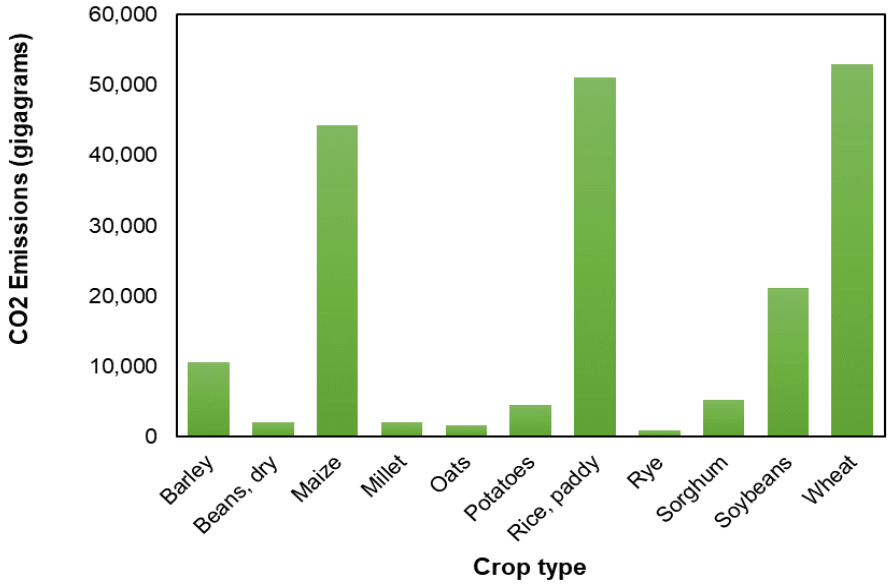

Figure 14 Global CO_2 emissions from agricultural activities as per crop type 2006-2016 [59]

The GHG emissions levels in Mexico have increased considerably in the like manner as the maize harvest in the last years. The country is the eighth on CO_2 emissions from crop burning worldwide according to FAO [60], contributing with 659,000 tonnes from which 90 % come from maize production (Figure 15). All this is a consequence of the government's programme *MasAgro* [6], which intends to increase in 10 years the annual maize production at 2.5 %. However, this programmed maize harvest growth to recover the country's food security represents an oncoming WM issue. Being that currently over half of the agriculture GHG emissions produced are directly linked to maize production and its by-products [12,61].

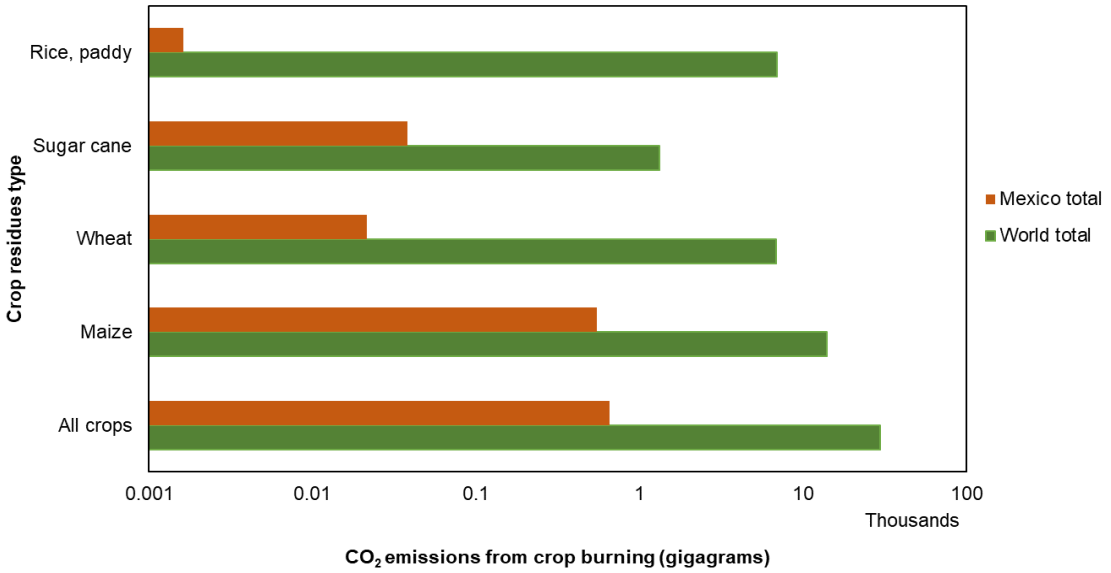

Figure 15 Comparison of global and Mexico's CO_2 emissions per crop burning practices as per crop type in 2016 [62]

As mentioned above, the waste treatment strategies commonly used in Mexico are not the optimal as discussed by El-Haggar [47] and Garcia et al. [63]. The alternative waste processing methods proposed (e.g. 7R's golden rules (Figure 10), manual sorting, automated sorting and disassembly) seem to be efficient recovering valuable raw materials, e.g. aluminium, different plastics, steel, among others. However, Figure 16 demonstrates that these methods have not yet reached Mexican rural areas, where over 90% of unclassified residues are sent to uncontrolled dumps [51]. Thus, the lack of infrastructure can be

attributed to the assumption that a WM system is not necessary since the waste stream in rural areas is mainly derived from agricultural activities.

Moreover, the General Law for the Prevention and Integral Management of Waste in Mexico (2018) [64] establishes as essential instruments: waste reduction and efficient management and social inclusion. This, based on the local waste disposal practices that led 75 % of the total waste generated into controlled landfills, whereas 21 % ended up in unknown dumps and only 4 % was recycled or recovered [7].

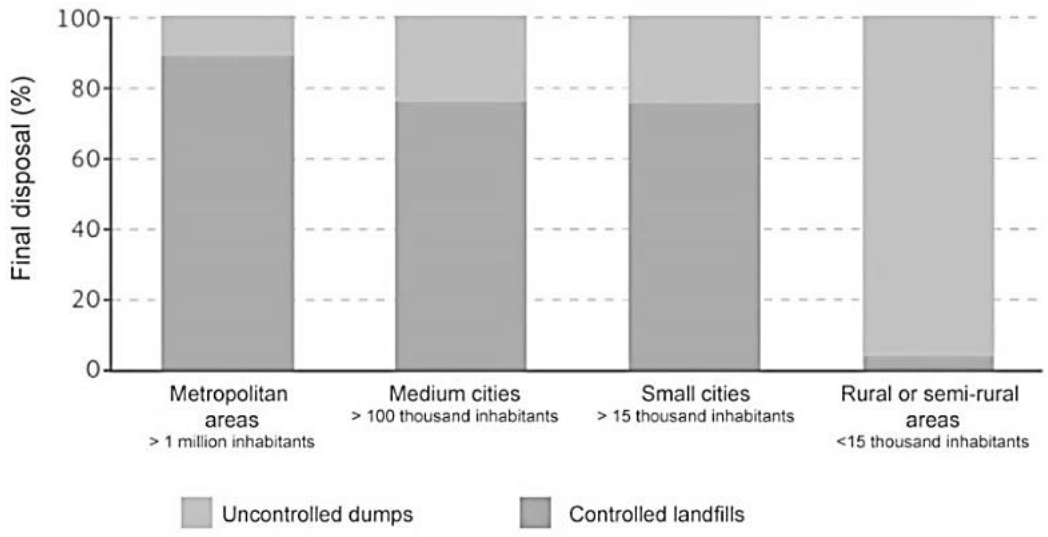

Figure 16 Percentage of controlled and uncontrolled landfills by settlement type in Mexico, 2012 [7]

Social inclusion plays a vital role in forestalling any damages to the population' well-being and environmental balance. A good example of this is the waste crisis in "*Bordo de Xochiaca dump*", the biggest open landfill in Mexico City. Thereby, more than 1.2 million people were affected by the 150 hectares of unclassified rubbish for more than 30 years, while a number of families risked their health dedicating its life to rubbish scavenging (Figure 17).

Figure 17 Rubish scavengers in the landfill, "*Bordo de Xochiaca*" Nezahualcoyotl, Mexico (2007) [65]

Overall, these findings highlight the importance of a comprehensive waste management plan (CWMP) in the rural areas, to efficiently deal with the copious amounts of agricultural by-products generated annually. Understanding the WM not only as a method to transform residues into less harmful waste but mainly as an approach to avoid waste production as shown in Figure 18 [45,47]. As a consequence, raw material re-evaluation has gained importance among the goods' producers since they realised that re-using and recycling materials represent considerable savings in the production processes and final costs. Encouraging the shift towards cleaner manufacturing processes, where companies avoid not only the generation of waste but also become carbon neutral.

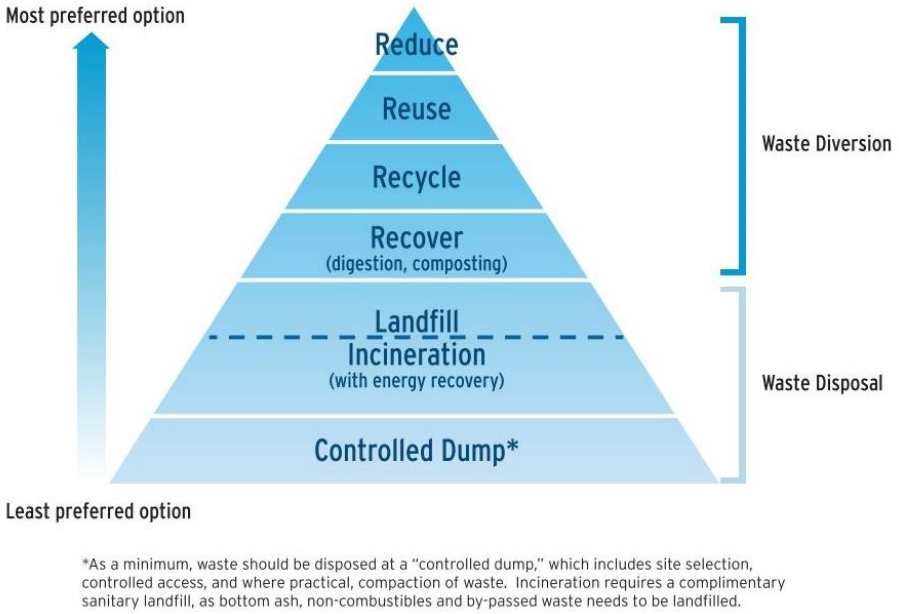

Figure 18 Waste hierarchy [51]

2.2.1 Agricultural waste in Mexico

Different methods have been proposed for waste assortment, though the World Bank waste classification, shown below, is the most widely used. Table 2 helps distinguish waste composition and origin, same that is directly correlated to the economic and cultural context. For instance, the amount of inorganic waste discarded in an urban zone is twice as much than the produced in a rural area, where the organic waste (OW) represents 60% of the total waste produced [66].

Moreover, the *"Global Review of Solid Waste Management"* report [51] the percentage of OW falls below 46 % of the solid waste stream. However, SAGARPA [7] reported a 52.4 % of the produced waste is organic as Figure 19 reveals.

Table 2 Waste categorisation as per type and sources [66]

Type	Sources
Organic	Food leftovers, garden waste (leaves, grass, brush) and wood from the household.
Paper	Paper scraps, cardboard, newspapers, magazines, bags, boxes, wrapping paper, telephone books, shredded paper, paper beverage cups. Strictly speaking, paper is organic, but unless food residue contaminates it, the paper is not classified as organic.
Plastic	Bottles, packaging, containers, bags, lids, cups.
Glass	Bottles, broken glassware, light bulbs, coloured glass.
Metal	Cans, foil, tins, non-hazardous aerosol cans, appliances (white goods), railings, bicycles.
Other	Textiles, leather, rubber, multi-laminated, e-waste, appliances, ash, other inert materials.

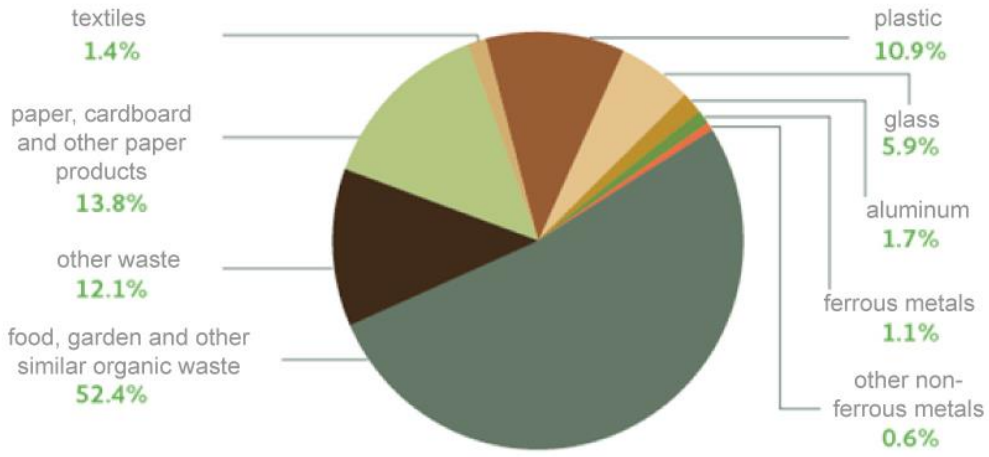

Figure 19 Waste composition in Mexico, 2012 [7]

Thus, not only understanding the type and origin of waste is of paramount importance to guarantee appropriate waste management, but also to distinguish OW and AW. The first consists of household residues, mainly food leftovers and garden waste; Whereas the AW is classified as the remnants produced as a result of various agricultural operations [67] and mainly formed by the leftovers from the harvest, around 40-50 % of the picked plant's weight. It is considered

AW once the edible part (grains) has been collected, e.g. straws, husks, stalks, shells, seeds grounds, leaves, grasses [51,63].

To set a more precise outlook on Mexico's crop and AW production, that has 21 million hectares dedicated to agriculture; divided in the two main farming systems: irrigation land (6.5 million hectares) and rain-fed (14.5 million hectares) [68]. The wide spectrum of climates and farmland allow growing of around 200 crops across the country, placing it among the worldwide top ten food producers according to the FAO's report [12]. Figure 20 shows Mexico's most harvested crops in 2016, were sugar cane, maize and sorghum stand out with an annual yield of 56, 28 and 5 MT respectively [34,37].

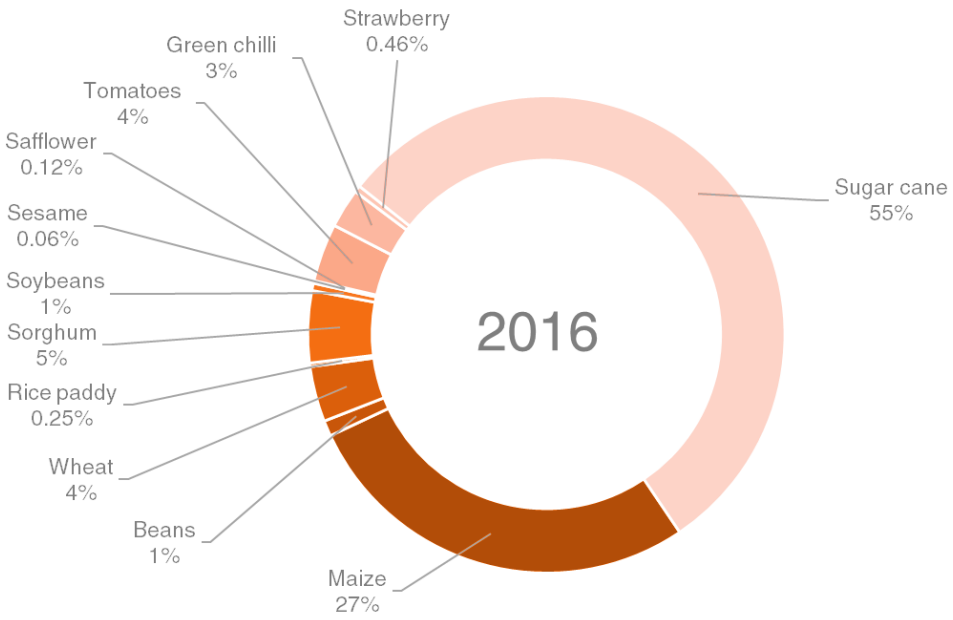

Figure 20 Crop production in Mexico in 2016, compiled from [12,68]

According to SAGARPA [6] in 2015 the generation of by-products came near to 45 MT, even though most of the harvesting processes utilise all the crop components as described in Table 3. However, despite the good use given to the residues, a considerable amount of AW remains unexploited resource; that, if exploited, it could have a significant impact on both local producers' economy and local environmental impact.

Although this may be true, currently the main use of AW in Mexico is mainly on livestock food enhancement and cheap biofuel for rural kitchens [70] (Figure 21), leaving a great amount of fibrous material to be exploited. The sugarcane producers are the best example, they have managed to reach a nearly zero-waste system, by making use as livestock food of all the remaining bagasse from the sugar extraction use [71,72].

Figure 21 Rural kitchen where coconut and maize stubble are the main sources of biofuel

Moreover, several studies on AW have been carried out to explore their limitations and capabilities mainly as biomass but also as alternative applications are being pursued such as construction materials, natural soil fertilisers, fillers, textiles fibres and source of biochemicals, e.g. coconut [73,74], maize cobs [13,75,76] and sugarcane [76]. Notwithstanding, MH remains unexploited cellulose; particularly there are not many studies on Mexico's MH.

Granted that the AW availability has been covered, the second aspect that cannot be missed is the material cost. As detailed in Table 3, residues' prices will always depend on the market offer-demand; thence, it is important to highlight that at least 70%, mainly those from maize, can be obtained free of charge from the producers, as their major concern is to clear the field as soon as possible [61].

Table 3 Uses of agricultural by-products in Mexico, compiled from [71]

Agricultural by-products	Production (Tone/Year)	Uses (%)					Price (£/Tone) *
		Export	Cattle Food	Fertilizer	Biomass	Waste	
Rice husk	101,318	/	/	/	/	100	Free
Coconut coir	178,853	/	/	/	20	80	Free
Forage maize	804,531	/	100	/	/	/	Free
Sorghum	331,074	/	100	/	/	/	Free
Alfalfa	1'238,097	/	100	/	/	/	3,117.08
Sugarcane bagasse	26'942,501	/	100	/	/	/	4,933.72
Maize cob	2'860,976	/	/	/	/	100	Free
Sugarcane stalk	1'084,680	/	/	/	/	100	Free
Maize husk	2,260,000	/	/	5	5	90	Free
Maize stover	23'468,019	/	/	/	20	80	6,080.61

***24.67 MXN to 1 GPB exchange rate 05/05/2017**

To date, 45 MT of annual crops wastes produced in Mexico, from which the producers are exploiting only 45 %. The lack of information may be related to AW typology and availability in the country. Several studies have documented AW mean estimate as per each kilo of grain one kilo of AW is obtained [68]. Nevertheless, each AW's crop yield is affected by different factors, e.g. grain type, fertilisers used, type of tillage and irrigation mode. Therefore, as the ordinance to Mexico's agenda for sustainable development [58], the AW production volume has been recalculated based on SAGARPA and SIAP [68,69] data with the following results in Table 4.

Table 4 Agricultural waste generation in Mexico, based on 2016 crop production

Crop	Total Annual production (ton)*	Total AW yield (ton)	AW generated ton/h (%)	Percentage from the total AW (%)
Beans	1,088,767	950,122.51	53.4	1.0
Green chilli	2,737,028	2,737,028	50	3.0
Maize	28,250,783	24,653,305.01	53.4	26.8
Rice paddy	254,043	225,283.41	53	0.2
Safflower	121,764	121,764	50	0.1
Sesame	59,412	54,841.84	52	0.1
Sorghum	5,005,837	4,439,138.47	53	4.8
Soybeans	509,114	509,114	50	0.6
Strawberry	468,248	702,372	40	0.8
Sugar cane	56,446,821	50,056,614.85	53	54.5
Tomatoes	4,047,171	4,047,171	50	4.4
Wheat	3,862,914	3,425,602.98	53	3.7
Total	102,851,902	91,922,358.09	/	100

* data collected from [77]

2.3 Maize: production, harvest and waste generation

Maize is one of the most widely used grains worldwide, and certainly the most important in Mexico. As shown in Figure 22 2016 the global maize production reached 1.04 BT. Placing Mexico as the sixth largest producer with an annual yield of 27.4 MT [12,78], and the first importer of 16.7 MT with a total value of USD 2.61 billion [79].

Correspondingly, the International Maize and Wheat Improvement Center (CIMMYT) has reported a global rise of 30-50 % in food demand by 2020, impacting crop and AW production directly. The increasing food has a direct effect on the global AW production. In accordance, [80]. Figure 23 displays the country's struggle coping to satisfy the internal food demand (maize) in the last decade [69,81,82]. Under those circumstances, the government has launched the *MasAgro* program with the objective of boosting Mexico's' maize production by 20 % by 2020 [6].

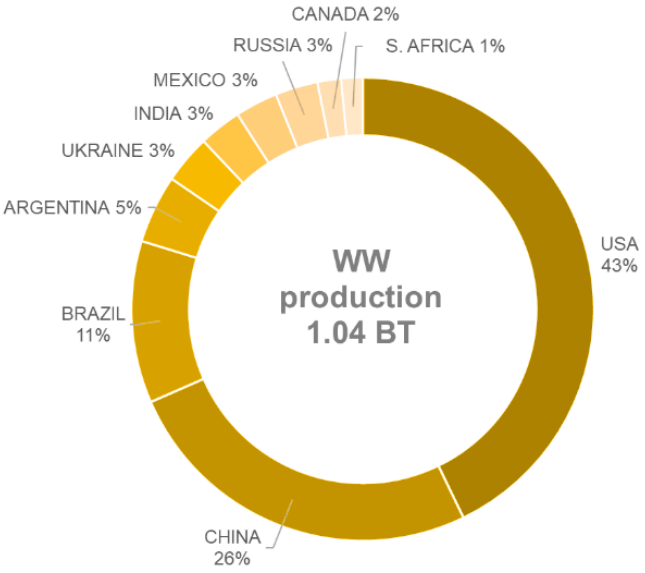

Figure 22 Maize producers ten top in 2016, from [12,78]

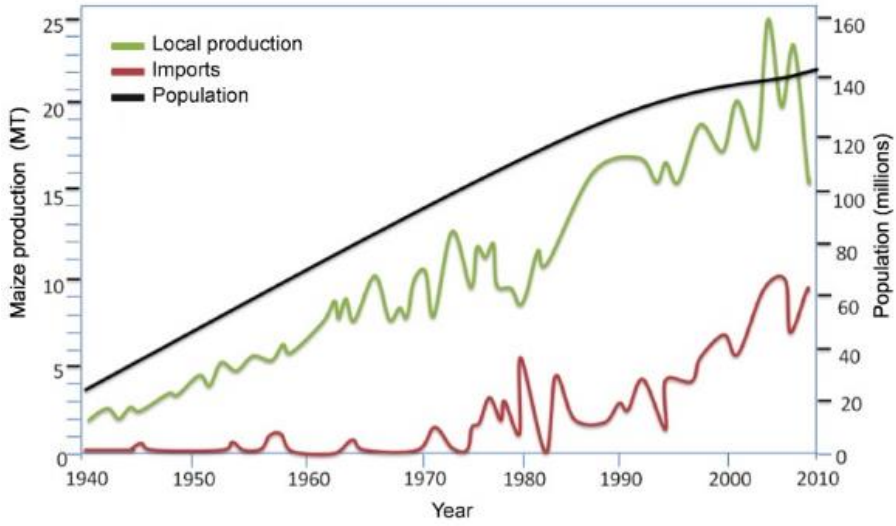

Figure 23 Mexico's maize production, imports and population growth from 1940-2010 [6]

Furthermore, the 59 native maize landraces (Figure 24) have made this perennial the main nutritional base grain in Mexico, contributing 47 % of the daily caloric intake [83,84]. Due to this great diversity, a brief anatomical and structural description of white maize will be included to identify the type of maize studied in this research.

Figure 24 Examples of some of the maize native Mexican landraces (CYMMYT, 2010) [85]

The white maize (*Zea Mays*) plant belongs to the *Poaceae* family, originated in the Americas and has been recognised as the most popular edible grain in Latin America [80]. Figure 25 below provides a simplified schematic of a white maize plant, showing the plant's structural frame is the cane (stalk), that consists of a solid stem. Thus, under the right conditions provides enough strength, that the plant can reach up to six-metres long. The vegetative part is composed of leaves (husks), which are long and narrow with sharp wavy margins, and spaced alternately on opposite sides of the stem. From the leaves, two to three very dense ears (cobs) wrapped in husks protrude; the ears elongate with a hairy pointy end, and their surface is rougher by the stem. The stem (tassel) of

the plant is topped at the end by a small male flower panicle; that has a crystalline yellow colour, and eventually becomes dry and brownish once the pollen has been winnowed [88]. The fertilised pistillate (female) inflorescence develops to become the maize cob, producing grain rows (kernel) on each ear that can vary from eight to thirty.

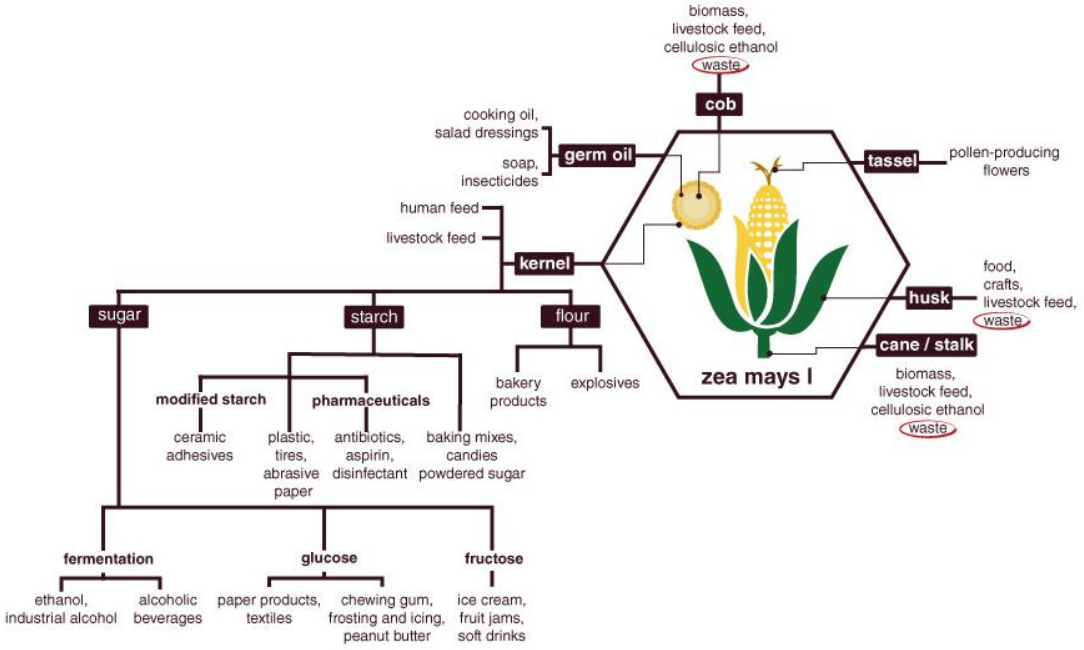

Figure 25 Anatomy of the maize plant and current uses in various industries, from [86]

As shown in the schematic above (Figure 25) nearly every component resulting from maize plant have an application within diverse industries. However, the cob, husks and stalks are still discarded. Much of the literature reviewed on the exploitation of AW, faces the challenge of handling a dormant waste problem while demonstrating its real potential to be exploited. To date, a large number of published studies have been carried out using maize and most of its by-products in several industries, such as food [83,87], biofuels [55,76], bioplastics [88], pharmaceutical precursors [89], and even explosives [86]. Examples such as Tomerlin's [90] that made a maize-based biofuel by taking advantage of the waste decomposition state, to yield ethyl alcohol; thereby opening AW new opportunities to diverse industries.

On the other hand, a limited number of studies have used maize husk and stalk fibres despite the material abundance. Though some researchers have explored cellulose extraction [91], and fibre for composite materials [92–94], perhaps the most comprehensive study on maize residues were found in the work of Youssef et al. [95]. That focuses on the raw materials recovery (low-density polyethene and maize husk fibres) through the manufacturing optimisation of a CM and thus proving maize AW's broad scope if utilised in further studies as fibreboard reinforcement.

2.3.1 Maize husk

As explained before, the increasing food demand has led to an overproduction of maize, resulting in 26.8 % of the AW produced in Mexico [80]. Whereas, on the one hand, are the farmers and producers with the urgency to prepare the soil for the following growing season; and on the other, the unfit WM and local regulations in the rural areas, carelessly increasing pollution levels. Despite all that, MH waste represents a significant and available natural supply, which can be utilised to obtain valuable products.

According to SAGARPA maize concentrates 33 % of the cultivated area in the country (Figure 26), which are mainly produced in the state of Jalisco, Michoacán, State of Mexico, Chiapas and Veracruz [68]. From which 74 % is rain-fed with an average yield of 2.2 ton/h; whereas the irrigation fields produce 3.4 times more (7.5 ton/h) [77]. In the "Waste management plan for agricultural activities, first stage" [68] the maize by-products (stover, stalks, grasses, leaves and husks) production is calculated in a relation of 3 tonnes per cultivated hectare and confirmed by Quintero and Moncada [61].

Figure 26 Maize cultivated area in Mexico, from [68]

In contrast to earlier findings, however, not much evidence of MH production was detected. Nevertheless, Reddy and Yang [96] estimated MH's yield of 7.1% of the total produced weight. Even though waste crop burning in situ and illegal open landfills disposal seem like a small portion of the waste generated, as shown in Figure 27 they have had severe environmental impacts in the region as mentioned before.

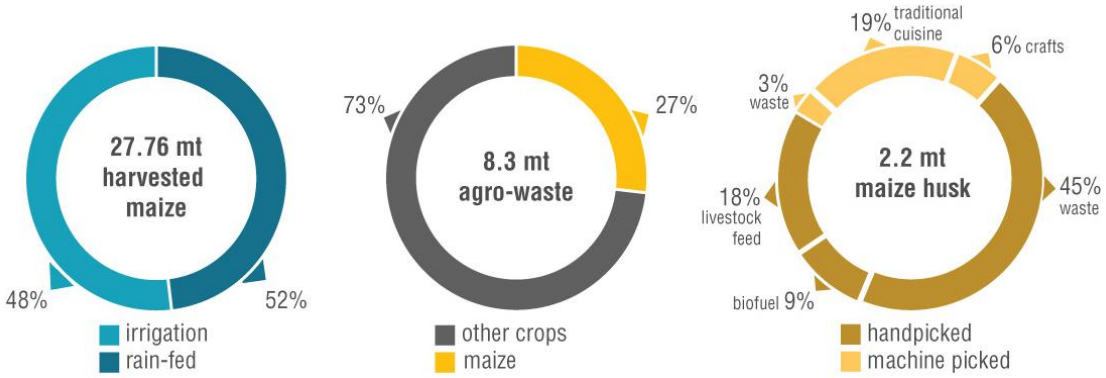

Figure 27 Maize, agro-waste and husk production, including diverse collection methods and applications in Mexico in 2017, from [77]

Although several studies have shown the extent of the soil damage and levels of GHG emissions on account of the current disposal practices in Mexico (FAO [12]); Quintero Núñez et al. [61] work investigated more in detail MH's burning and its potential to be fully exploited. Therefore, is necessary to deepen the knowledge on the maize residues and how they are obtained. To eventually utilise them wisely so that the noxious impact could turn positive by adding value to these copious lignocellulosic resources.

Maize by-products (stover, stalks, grasses, leaves and husks) represent around 30% of the total yield, which so far has been considered a useless material by the farmers. Giving a result of damaging disposal practices such as waste crop burning in situ and illegal open landfills disposal (Figure 28), without any consideration of the environmental impacts and secondary effects on the soil [12,61]. Hence, is necessary to deepen the knowledge on the maize residues and how they are obtained; to eventually be utilised in such way that it could not only diminish the GHG emissions but represent a positive impact by adding value to these existing lignocellulosic resources.

Figure 28 Maize waste management. (a) AW burnt in the fields [80]. (b) a mound of accumulated AW in Mexico

As explained before, the increasing food demand has led to an overproduction of unwanted by-products, turning into a rising concern with severe environmental consequences. Furthermore, the particular case of Mexico, where on the one hand are the farmers with the urgency to prepare for the

following growing season, and on the other are blurry WM regulations in the rural areas, carelessly increasing pollution levels. Despite all that, MH waste represents a significant and available natural supply, which can be utilised to obtain valuable products.

2.3.2 Harvest techniques

In Mexico, as in many other countries, maize harvest is carried out mainly through two techniques. The first one and the most traditional is manual harvest or hand-picked (HP). The HP method does not require any specific tools; and consists of recognising the mature cobs by removing first the ears above from the standing stalk and leaning the corncob to one side of the steam, leaving it almost perpendicular, so it follows from the stalk (Figure 29). The rest of the plant is left in the field until it is time to prepare the field for the next sowing. The harvesting with this technique takes around 25-30 days per hectare [97].

Figure 29 Maize harvest. (a) HP harvesting [82], (b) field post-harvest in San Juan de las Huertas, Mexico, 2014

The HP technique has been used since ancient times to use the MH as food plates (Figure 30(a)), food wrap (Figure 30(b)) and in some areas to manufacture of crafts (Figure 30(c)) [69]. Moreover, it is important to mention that this MH goes through a steaming process with small quantities of sulphur (SO_2) [98]. Hence the husk is clear of fungi, germs and insects. As an addition

to the mentioned benefits, there is bleaching and fibre softening effect, that helps to keep its natural shape while in use.

Figure 30 MH uses. (a) traditional food wrapped up in MH. (b) MH used as a plate. (c) Traditional crafts made with MH (Ontiveros [99])

The steaming process starts right after the MH collection, first the husks are cropped 3 to 4.5 cm from the base with a mechanical blade as shown in Figure 31(a), secondly they are stacked in 20 to 25 kg bales (Figure 31(b)); thirdly, the bales are piled up on wooden pallets in the centre of the oven and subjected to 24 hours to sulphured. Lastly, the MH's is selected manually into first and second class husk, so that they can be sold in local markets [98].

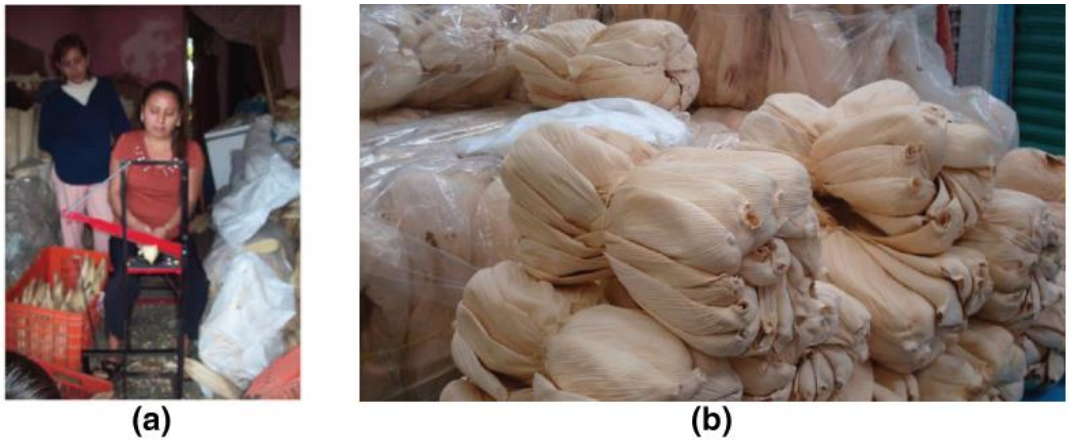

Figure 31 MASH treatments. (a) MH manual trimming, (b) maize husk storage and piling for transportation [87]

On the other hand, the mechanised harvest (MP) technique is carried out by a tractor which detaches the maize ears from the standing stalks, to finally remove the kernel from the cob while moving across the field as shown in Figure 32(a). Commonly a multi-row machine is used to make the process economically efficient. In contrast to the manual harvest, the MP method can cover about two hectares per hour, when using a 3-row sheller harvester (Figure 32(b)); whereas to obtain the same quantity with the HP method would take about two months [87].

Figure 32 Maize sheller. (a) diagram [69], (b) in operation [100]

2.4 Composite materials

This section draws upon and integrates from diverse literature domains, definition and categorisation of CM, the developments on AW as reinforcement, and technical performance of conventional CM. The literature highlights the definition of CM as the materials that can be found both in nature, e.g. wood, bamboo, as well as result of human intervention, e.g. steel, reinforced concrete, carbon fibre, engineered wood, etc. [101].

CM has been studied widely since the early years of the Industrial Revolution in search of more efficient and reliable materials [102], while other definitions can be complex, this study uses Hull's [101] CM definition *"a material made of two or more separable elements (phases), when mixed results in a stronger and enhanced material"*. Figure 33 shows the five basic types of CM according to the changes in the reinforcement; each sample has a different set of properties and applications [101].

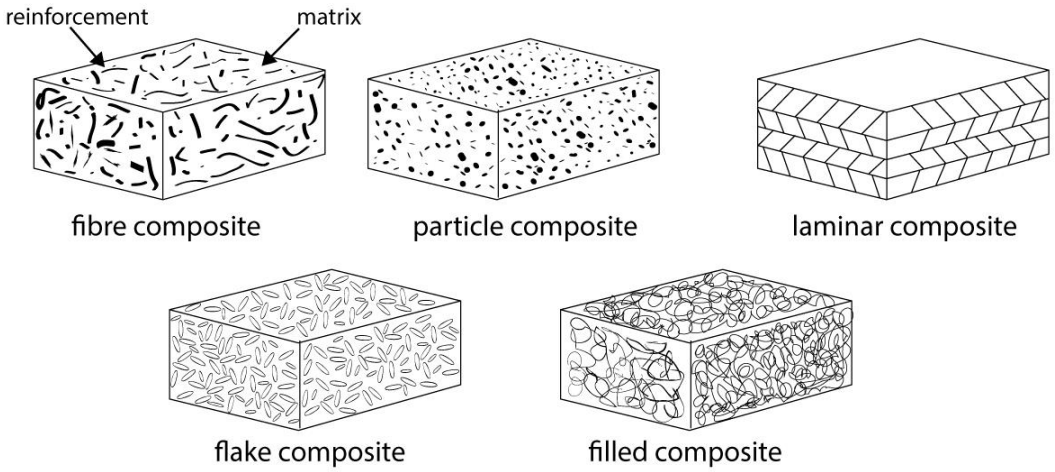

Figure 33 Types of composite materials; and, structural phase (matrix) and structural load phase (reinforcement)

Comparatively, Ibrahim's et al. [103] categorisation, shown in Figure 34, classifies CM based on matrix and reinforcement. Thus, the materials' properties can be tailored according to its application.

Beyond the CM's phases composition there is another classification, but this is divided by their origin: bio-composites (BC), green composites (GC). GC have both matrix and reinforcement come from renewable sources [104], while only one biological-source integrate BC materials, either the matrix or reinforcement [105]. This classification, shown in Figure 34, allows a deeper understanding of the phases' interaction and properties, while Ibrahim's focuses more on the engineering applications and specific characteristics of both matrix (e.g. particles percentage, matrix bonding, flexural strength) and reinforcement (e.g. fibre dispersion, size, distribution and orientation) that together, can help to determine CM's physical and mechanical features [105].

This study aims to contribute to this growing area of research by exploring MH's feasibility as reinforcement fibre, as a response to the increasing demand for less harmful materials in the GC manufacturing. At the same time that an alternative thermosetting matrix is being tested, thus a novel CM is developed.

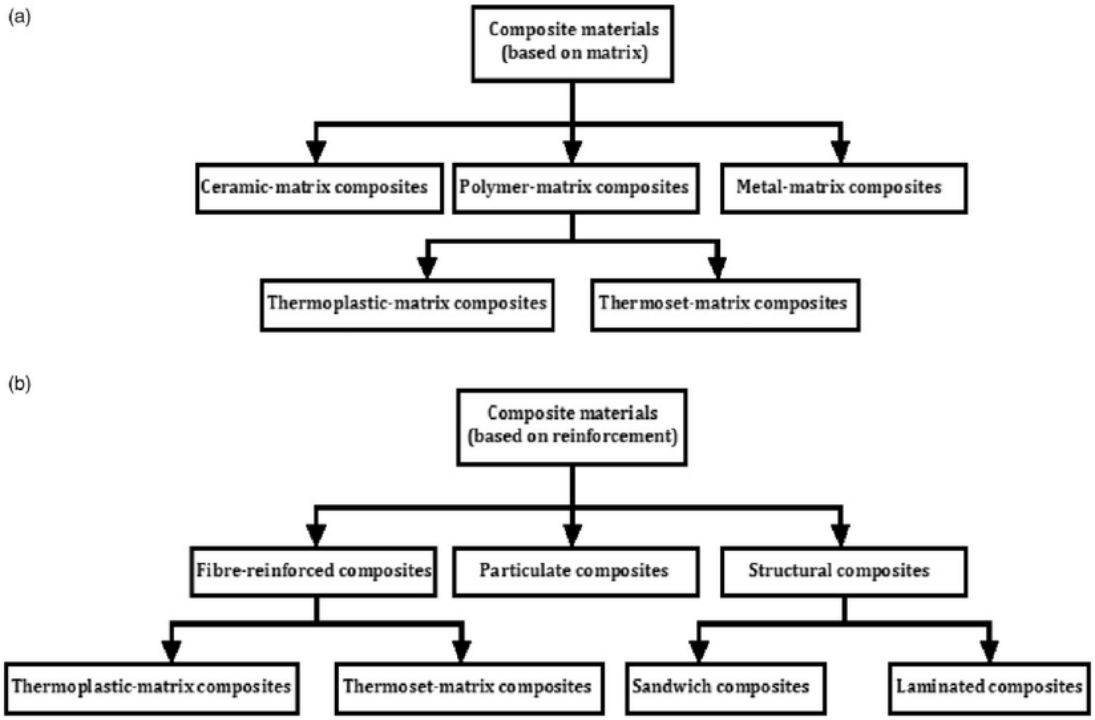

Figure 34 Classification of composite materials. (a) based on matrix and (b) based on reinforcement, from [103]

Therefore, as Baillie [106] emphasised the most relevant features in composite manufacturing are the fibre content, size, orientation and matrix interaction, as they directly impact the material mechanical properties. For this reason, the study will focus only on thermoset-natural fibre reinforcement composites. Thence as Zini et al. [104] and Kalia at.al [107] studies that focused only in one fibre to enable a more profound knowledge of the core physical and mechanical properties of the manufactured CM. This research will focus on MH extraction, fibre/matrix adhesion and a thorough composite characterisation to get the most of both phases (matrix and fibre) similarly to Aziz and Ansell [108] work.

2.4.1 Natural fibres as composite reinforcement

NF is currently widely used as CM reinforcement, because of its renewability and low cost [106]. However, due to the extensive variety, they are classified according to their source into three categories: plant, animal and wood (Figure 35); and the subdivision is based on the source's morphology [105].

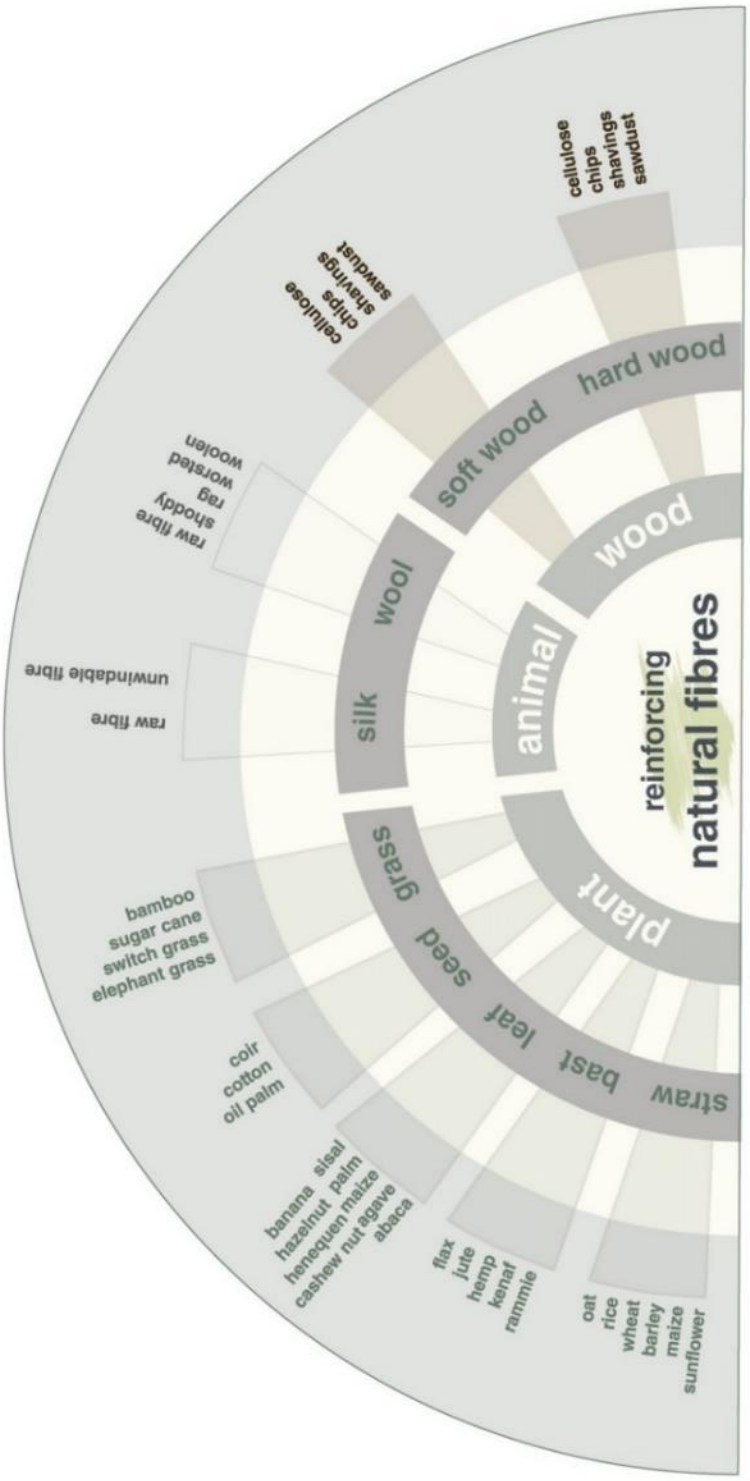

Figure 35 Origin of natural fibres used as reinforcement, compiled from [109]

Therefore, several studies have reported the use of specifically grown and harvested NF (i.e. flax and cotton) for the manufacturing of GC. However, the recovery and use of NF from other industrialised primary processes have risen considerably in the past decade. An example of this is Youngquist et al. [13] work, which outlined a significative number of studies on non-wood plant materials, mainly from AW, to produce fibre based panels. All this couple to the growing environmental concern resulted in an important number of NF studies, e.g. sugarcane bagasse, rice and coir, with 255, 219 and 101 reports respectively [13]. Other sources studied too are ramie fibre [110], pineapple leaf [111], banana leaf [37,72,112], sisal [113], jute [114], rice husk/stalk [115–117], flax [118–120], cashew nut shells [111,121], coffee grounds [122], kenaf [109,123], wheat straw [113,124,125] and soy stalk [126] to mention the most relevant.

Furthermore, to get the most of the NF as reinforcement, it is essential to know its properties [106] and structure, so when compared the differences are easily spotted. The NF properties among studies vary depending on the plant type, climate, soil and watering method; thus, the chemical compound and structure will always vary within specimens, and even more between batches, resulting in significant GC variations.

2.4.1.1 Fibre structure

Fibres from leaf tissue (Figure 36(a)) and bast tissue (Figure 36(b)) will always discern; whereas the first one presents a grainer structure, the other has a coarser and compact structure [107]. Thence, the presence of these two types of tissue is essential to the structure of any vegetal-sourced fibre.

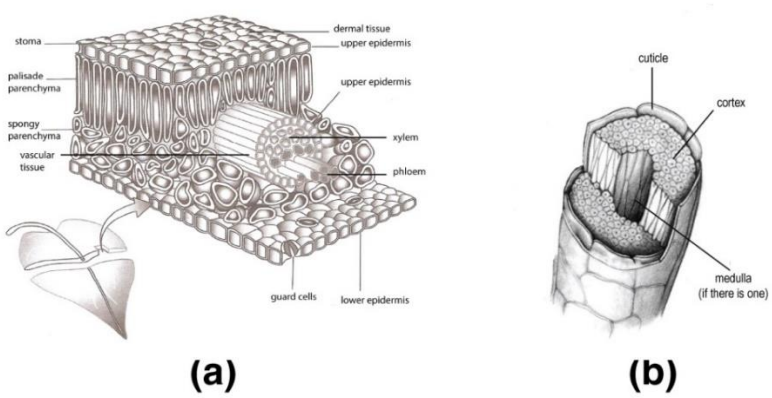

Figure 36 Structural arrangement of fibre cells (a) leaf structure, and (b) bast structure [107]

Therefore, the relevance of maize husk fibre (MHF) structure and physical variations (Figure 37), will determine the composite manufacturing process as they impact the composite features [96]. Reddy and Yang [96] studies of MHF have shown a ribbon-like structure with reversal twists through the strand length (Figure 37 (a) and (b)). Demonstrating its cohesive properties to be transformed into yarns; however, the fibre's shape had severe modifications due to the different extraction methods used. On the other hand, Kalia et al. [107] and Yilmaz et al. [127] demonstrated that no matter the harvest method (handpicked or machine-picked) the MHF' hierarchical fibrils alignment abides, as their strong link with the bonding cellulosic elements naturally embedded in the fibres.

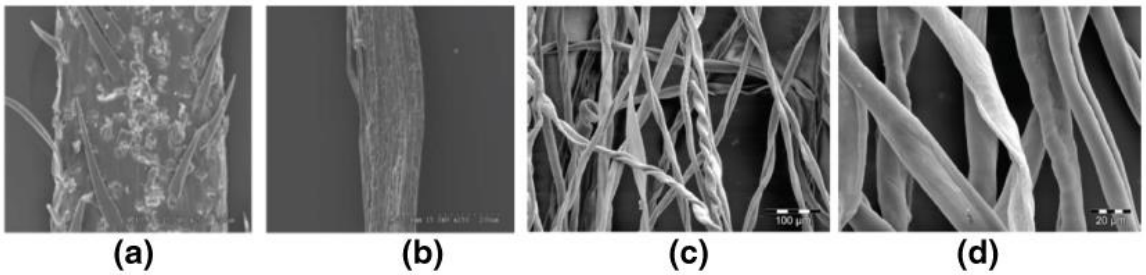

Figure 37 Micrographs from mechanically extracted from maize husk fibres. (a) showing lignin and other elements remained on the surface, (b) fibre surface modification after treatment [96]. (c) and (d) show immature cotton fibres from a length view [128]

Several studies on post-harvest MHF have been undertaken the extraction methods for residual wood fibres. Despite their differences in fibre size (MHF 2 to 20 mm [96] and softwood fibre 1.5-5 mm [104]) and structure, it was concluded that both fibres could be broken down similarly into a homogeneous material to enhance the adhesion with the strengthening agent (matrix) [129,130].

Nechwatal et al. [131] NF characterisation covering the essential fibre properties, if they are to be used as a CM reinforcement; contemplating among others tensile strength (i.e. Young's modulus), cross-section calculation, strain and elongation percentage. Complemented by the micrographic analysis (optical and electronic microscopes) widely used in NF.

2.4.1.2 Fibre chemical composition

NFs chemical composition has been extensively evaluated, a clear example of this is Larrauri et al. [132] and Zhuanzhuan et al. [133] work on fibre modification. Their studies have drawn under the assumption that raw fibre's chemical composition (Table 5) is based on cellulose, lignin, pectin and hemicellulose, as well as waxes, inorganic and nitrogenous salts, these last considered non-structural components [105]. Thus, when the structure is altered these levels serve as a guide for their extent of its application as a CM reinforcement. In this way, they proved that not only fibre structure is influenced by weather, soil composition, plant age and harvesting procedure but also affects its overall composition [72,116,134–137].

Furthermore, one of the arguments against the use of NF in the composite industry comes from its low performance, i.e. low density, poor mechanical properties, moisture sensibility, assorted fibre shape, unstable supply and heterogeneous composition [138], when used in GC material. Casting a heavy shadow over their positive features, i.e. renewability, nontoxic and low cost [106], rather than focussing on the possibility of structural and chemical modifications, i.e. plasma treatment, silane, enzyme, alkaline treatment, [110], thus the negative effects on the GC can be addressed.

Table 5 Natural fibres chemical composition and physical characteristics

wt.% / Fibre	Cellulose	Lignin	Hemi-cellulose	Pectin	Wax	Moisture	Ash	Crystallinity	Colour	Ref.
Rice husk	38	23	12	-	-	-	25	46.8	Brown	[116]
Banana leaf	83	5	-	-	-	10.7	-	-	Green	[137]
Cotton	82.7	-	3	-	.6	7.85	-	65-75	Off-white	[105]
Flax	64.1	2.0	29.6	1.8	1.7	.8	-	65-70	Creamy withe	[139]
Jute	64.4	12	9.9	.2	.5	12.5	.5	65-70	Brownish	[33]
MH	42.3	12.58	-	-	-	-	4.16	48-50	Yellowish - white	[117,127]
Bamboo	26	1-31	30	-	-	9.16	-	-	Brownish	[139]

Equally important is to explore less harmful and polluting methods to maintain the multiple forms of added value the use of NF have, whether they are used as reinforcement, chemical precursor or bio-fuel source the NF relevance in the manufacturing industries is certain. Particularly the derived from agricultural residues as the 507 different fibres listed by Youngquist [13]. Therefore, the study of MH characteristics and comparison with other NF's is an unmissable step towards a shift in the manufacturing industry mindset.

2.4.2 Matrices

As mentioned before, the responsible of the CM external characteristics matrix is known to be the structural phase (Figure 33), while the reinforcement responds to the structural loads. Faruk et al. conducted a comprehensive study on the polymer-based matrices, analysing their source, availability, performance and environmental impact in the CM manufacturing, and despite the robust offer

of oil-based epoxy resins, their emphasis is in alternative greener solutions. Supported by significant data on the hazardousness of oil-based resins. i.e. urea formaldehyde (UF) resins (considered a 1B class carcinogenic [140]).

Whilst, the CM industry has been working in the last two decades to mitigate the formaldehyde fumes produced during the resin curing as well as the volatile organic compound (VOC) levels produced during the material's lifecycle as reported *"Cradle to Cradle"* [45] interior emissions case-study. Supported by the VOC standards update in 2011 (BIFMA e3 sustainability standard), especially directed to wood-based fibreboards manufacturing and transformation due to their popularity [141,142]. Hence, triggering the research on formaldehyde-free composites, even despite the widespread and low prices of the polymeric matrices.

Faruk's et al. [110] analysis of bio-based plastics and alternative binding materials is detailed below in Figure 38; showing further evidence that the obvious collateral effects that these may bring such as CO_2 emissions reduction, an increase of biodegradability in CM to be reintegrated into the natural system. Which is the exploitation of existent resources, therefore the CM manufacturing will be able to prevent the health dangers while getting rid of other industry's waste. Transforming the CM productive cycle into a closed loop, and most importantly one that works within the means of the planet.

Moreover, bio-polymer sourcing can come in diverse forms, such as bio-resins extracted from AW and vegetable oils, e.g. soybean [120], triglyceride [143], cashew nut shell [143], bio-based glycerol [88], to mention some. It has also been demonstrated that when blended with natural fibres and certain additives competitive GC materials can be produced, e.g. flax [144], banana [37], sugarcane bagasse [72], hemp, sisal and kenaf [143]. However, the extent to which bio-based polymers procurement can be guaranteed will directly affect the CM entry to the mass-market [143].

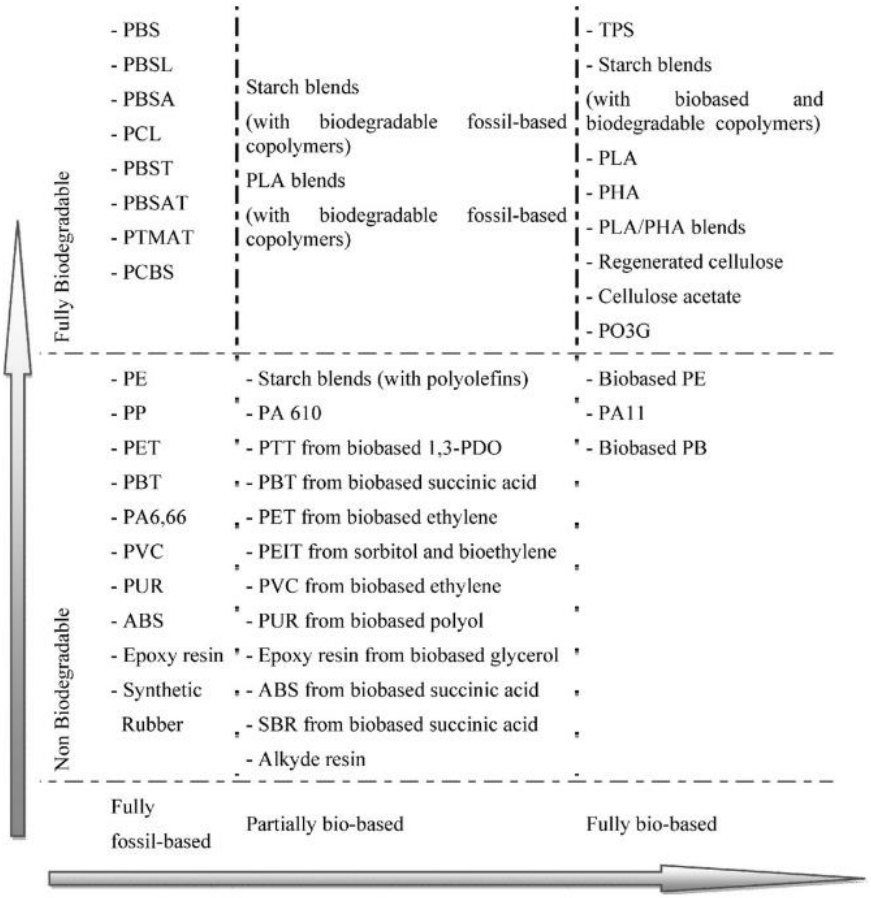

Figure 38 Current and emerging plastics and their biodegradability, from [110]

Biopolymers can be either thermoplastics or thermosets, but also, they may be classified into three types: biosynthetic, semi-biosynthetic, and chemosynthetic. The biosynthetic ones are considered the closest to being entirely biodegradable, as the semi and chemosynthetic require certain conditions to be reintegrated into the ecosystem [144]. Most of the bio-based polymers developed to date are based on fatty acids of seed oils, e.g. soybean [124], castor [104], and cashew nuts shell [145], anhydrides and polyurethanes.

As for the core properties of the GC, the main limitations are related mainly to fibre moisture absorption, the interference of chemical components other than lignin, cellulose and hemicellulose with the matrix, and low mechanical performance [13,110,146,147]. In the view of that, this study will compare the effects and performance of three bonding agents (Table 6) for the MHC

manufacturing. The rationale for the selection of each matrix can be found in the following section.

Table 6 Selected bio-polymers as composite matrix [122,148]

Bio-matrix	Abbrev.	% bio-based	Origin	Applications
Cellulose & hemicellulose	Bs	100	Natural fibres, agricultural waste, wood bark and bagasse	Fibreboards, cardboard
Lignin	L	100	Pulping liquor Wood shavings	Wood panels, e.g. plywood
Natural phenols resin	BE	50- 90	Pine oil waste	Surfboards, boats

2.4.2.1 Binderless

In previous studies of self-binding or binderless fibreboards manufacturing, different variables have been found to be associated with the final properties of the material such as particle size, shape, chemical structure (lignin and cellulose content), pressing time and temperature [37,149–151]. These studies focused on better use of the elements naturally present in the raw material through a process, unfortunately, manufacturing elevated prices, and low material performance has discouraged the industry from self-binding processes implementation.

However, a low-cost manufacturing process patented by Shen [152], gave the non-woody plants a second chance to be explored and further analysed. He showed how preparing the surface of the fibre can create a chemical bonding between them and its self-contained carbohydrates and saccharides during the curing process to obtain functioning fibreboards.

Furthermore, bonding may play a central role in the fibreboard manufacturing. Research done by Halvarsson [153] on straw medium density fibreboard (MDF), explains how during the board's pressing phase the NF's are linked with the matrix by the reactive hydroxyl groups. However, the fibre/matrix adhesion

strength can be affected by fibre' surface porosity (e.g. presence of cracks, cavities). Thus, fibre chemical pre-treatments (e.g. alkalisation, acetylation) and additives (e.g. maleic anhydride-modified polypropylene (PP)) might raise the cross-linking degree (only the thermoset matrices) [106,121]. A deep understanding of this modification and their relevance on the final composite will increase not only the fibre/matrix bonding but the surface tension (strength), wetting resistance, swelling, adhesion and matrix compatibility of the MH [104].

Table 7 Binderless composites raw materials and manufacturing processes

Source	Manufacturing process	Pre-treatments	Additives	Ref.
Coir	Hot pressing	Enzymatic Alkali	Kraft lignin	[155,156]
Banana bunch	Hot pressing	Steam explosion	/	[37]
Wheat straw	Hot pressing	Alkali Fenton's reagent	/	[153]
Sugarcane stalks	Hot pressing	Milling Enzymatic	/	[75,152]
Kenaf	Hot pressing	Alkali	/	[123]
Cotton stalks	Hot pressing	Enzymatic	/	[147,157]
Flax	Hot pressing	Alkali Acetylation Silane Enzymatic Esterification	Kraft lignin	[118,152]
Maize stalks	Hot pressing	Milling Alkali Enzymatic (Laccase)	/	[94,152]
Agave bagasse	Hot pressing	Acetylation Alkali Enzymatic	/	[110]
Maize husk	Hot pressing	Alkali Enzymatic	/	[155,158]

Table 7 summarises several pre-treatments and manufacturing processes that have investigated the mechanical properties of NF self-bind composites, where evidence suggests that the formation of a stable bond at chemical level is reached by a hot-pressing process [104]. For instance, the implementation of a

steam explosion to break down the fibres in the composite manufacturing process has been enhanced by improving internal bond structure; hence, overall material performance. Additionally, this strategy has broadened the composite application range, thus its possibilities to be commercialised, yet the method is still considered out of reach [37,154].

Since most of the work carried out on Bs composites suggest the need to investigate MH's viability further to be used in this process, this work will contribute to the expand of knowledge and determine its possibilities to be transformed into a Bs composite.

2.4.2.2 Lignin

Lignin together with cellulose from annual crops is considered the most abundant renewable materials available on the planet. Even though lignin has been mainly extracted from softwoods and wood bark, due to their high content [147,159,160], herbal lignin has also been studied since the 1960s; and principally used in pulping processes, yet other applications, such its adhesive properties in the papermaking industry have been explored as well [75,159]. Some other studies have investigated the implications of levels of lignin to be exploited as a natural bio-matrix, yet lignin quality and yield depend largely on the source, e.g. various wood types and annual crop residues; and also to the extraction method [159,161].

As mentioned before in 2.4.1, NF with a higher lignin content can be used either as a source or self-bonding composite core. Though, the use of technical lignin has also been explored as an alternative for the NF with deficient lignin levels, showing interesting results enhancing the final composite tensile and internal bonding strength [161].

Moreover, Anglès et al. [162] pointed out that the addition of different lignin types (lignosulphonate, Kraft) in combination with the curing process, resulted in less hygroscopic fibre. Hence the composite obtained reported significant

improvements in the mechanical performance such as water absorption (WA), modulus of rupture (MOR), modulus of elasticity (MOE).

2.4.2.3 Bio-based epoxy resin

Formaldehyde airborne toxic control on MDF and thin MDF has been reduced by half in 2011, to be left in 0.11 and 0.13 parts per million (ppm) respectably [141]. Thus, the formaldehyde-free or bio-based resins have indeed increased its chance to enter into the CM industry.

Furthermore, bio-based polymers are obtained from biological sources and hold a measurable ^{14}C content, which results in being partly or wholly biodegradable [104]. The development of both thermosetting and thermoplastic bio-polymers reached 20 % of the global production in 2009 [88]. Consequently, research suggests that as their renewable origin and naturally occurring chemical links are a viable alternative to current pollution issues due to oil-based composites [163,164].

While a variety of bio-polymer matrices have been proposed in fibreboard manufacturing, this research will focus on a thermoset chemosynthetic resin, due to its similitude to other oil-based polymers used within the industry [106]. The SSE resin system was designed for press moulded composites and wood laminates, e.g. skies, snowboards and surfboards.

2.4.3 Fibreboards

The Composite Panel Association (CPA) defines fibreboard as a composite made of extracted cellulosic fibres from various sizes of wood, that are bonded together with an adhesive through heat and pressure [165]. Fibre reinforced CM, fibreboards for short, take an important role in the engineering and materials sciences. Altenbach et al. [166] places fibreboards as the most complex and studied composite to the fact that not only NF have been used but a list of synthetic ones as well. According to the European Committee Standardisation (EN 622-5:2009 [167]) fibreboards are classified as shown in Table 8.

Table 8 Properties and manufacturing processes of different WBF [153,165]

Production process	Composite	Density (kg/m^3)	Thickness (mm)	Additives	Grade
Wet ≥ 20% MC*	Hardboards (HB)	≥ 900	3-18	Fire retardant Moisture & fungi resistant Tempered	Commercial Industrial Exteriors Construction Underlayment Perforated
	Medium density boards (MDB)	≥ 400 to 900	3-32	Fire retardant Moisture resistant	Commercial Industrial Interiors Exterior Construction Underlayment
	Softboards (SBo)	≥ 230 to 400	6-40	Fire retardant Moisture resistant Strength enhancement	Commercial Door core Underlayment Perforated Thermal & Acoustic insulation
Dry ≤ 20% MC	Ultra-light MDF**	≤ 550	3-12	Fire retardant Moisture resistant	Commercial Interiors Non-structural underlayment
	Light MDF	≤ 650	3-12		
	High-density fibreboard (HDF)	≥ 800	6-32	Fire retardant Moisture resistant	Furniture Door core Stair treads Floor Underlayment Thermal & acoustic insulation
	Particleboard (PB)	≥ 620 to 740	6-40	Moisture resistant	

*** moisture content**
**** medium density fibreboard**

Furthermore, in Mexico the construction industry is the principal consumer of the WBF, e.g. timber, plywood, veneers, and MDF; holding around 2.2 % of the total market value [137,168]. However, in the last decade, timber production decreased 3.1 % [168], a consequence of the rampant deforestation. In the view of that, Youngquist et al. (1994) [95] concerned by the predicted wood pulp shortage, compiled 734 studies on the use of alternative fibres; giving a wider view to the engineering of greener WBF.

2.4.4 Fibreboard manufacturing and properties

The manufacture of WBF is based on different and complex steps, divided into wet and dry methods (Figure 39). Even though the wet process allows the manufacture of binderless boards, it was discontinued because of the environmental concerns due to the large amounts of water required for the process [165].

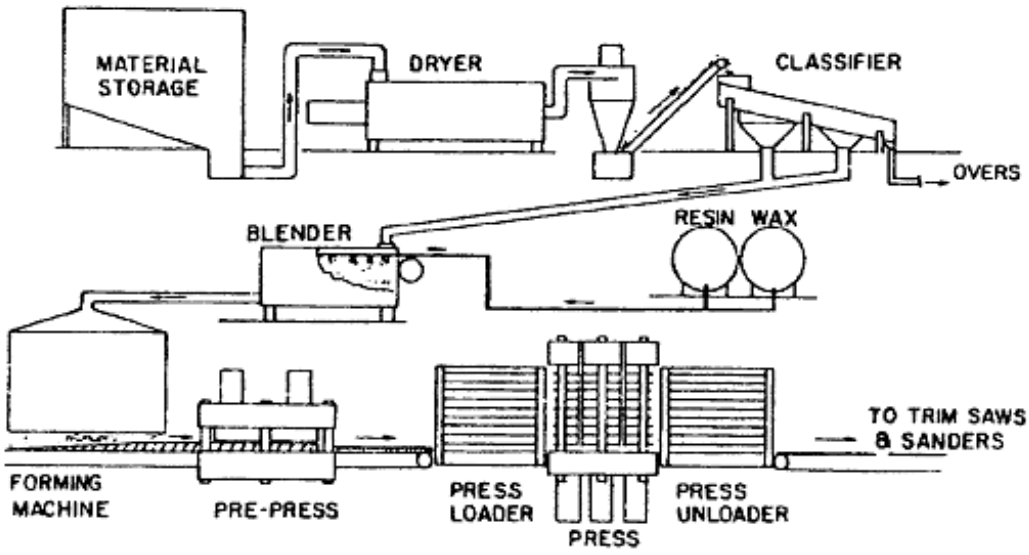

Figure 39 WBF dry production line, from [169]

The wood chips are sized-reduced (flaking), screened, cleaned, dried, blended or resin spreading. Generally, the adhesives used are thermosetting resins (UF and MF), in a range of 3-18% depending on the WBF type. The resin spreading is carried out via a blowline blending methods, although it can also be sprayed manually right after the drying process.

The impregnated fibres are transported to the mat-forming section and followed by a set of pre-pressing rounds. Once the mat is placed and reached the right temperature, the board is hot-pressed and left there for the resin curing. Once the compression/consolidation is reached, the boards are left for cooling, sizing and labelling.

Therefore, in this work, the dry method is adopted and described for maize husk-based composites. The average density obtained with this process is between 650-110 kg/m^3, as mentioned above in the WBF properties [153]. A report from the Society of Plastic Industries showed that only in North America (Canada, United States and Mexico) 60% of the adhesives used to manufacture WBF were amino resins, e.g. UF and melamine formaldehyde (MF) [121,169]. Limiting the range of alternative adhesive, only to thermosetting ones.

The manufacturing differences between MDF's dry process and an MHC are mainly founded on the raw material treatment and extraction [170]. The feasibility of the MHC manufacturing process is a fundamental element of the herein project as it will allow the producers to initiate a pilot-plant with equipment already available on the market and if possible to optimise the processes.

Even though maize by-products have been thoroughly studied as potential raw materials for the CM industry, to date there is no knowledge of any commercial production of MHC. Among several studies, Youssef et al. [95] demonstrated the advantages and viability of MH as composite reinforcement when blended with low-density polyethene; although some properties did not perform well, the composite had acceptable performance.

MHC's performance will be directly reliant on the fibre size and extraction; thus, the proposed MHC manufacturing processes will be compared to a lab scale fibreboard manufacturing [125,171]. Therefore, as shown in Table 9 the MHC properties will be corresponding to WBF, i.e. MDF and OSB boards.

Table 9 MHC proposed manufacturing steps

Step	Description	ASPROS and MASH MH fibre
1	Size reduction	Whole husk
		Chopped
		Milled
2	Wetting	Alkali extraction
		Alkali, 120 min
3	Defibration	Milled, 5 min
4	Binder impregnation	Binderless
		Lignin
		Super Sap® CPM epoxy resin
5	Mat-forming	Frame 250 X 250 mm
6	Hot pressing	According to binder

For the obtention of a comprehensive view of MHF' adhesion properties, the husks were tested in four sizes: complete husk (W), chopped into swatches (CH), milled (M) and alkali extracted (Ak), same that will be detailed later on. The fibre size scrutinisation was carried out to explore not only the composite features but also to analyse the equipment suitability, handling logistics and costs [171]. The subsequent steps were analysed in the same fashion, not only considering performance but viability as a cost-effective process.

Density and resin content determine the core physical and mechanical properties of fibreboards. Halvarsson [153] confirmed the rise in fibreboard's mechanical and physical properties, to higher density and matrix ratio. Even though the fibreboard thickness may vary between 3-40 mm, for the MHC manufacturing, a 3 mm board will be used to obtain the typical properties measured in any WBF (Table 10). Moreover, the existent literature on MHF is focused on textile applications; thus, single fibre tests have to be considered to measure MH properties. Thereby, the MHC could be equated to existent materials, i.e. wood-based fibreboards and non-wood-based fibreboards.

Table 10 Proposed standards to obtain MH, MHF and MHC overall properties

	Test	MH Tensile	MH wt.%	MH CSA	MHF tensile	
Fibre	Reference	ASTM D 5035-11[172]	ASTM D1348-94 [173]	[174]	ASTM D 3822M-14 [175]	
	Outcome	Breaking force Apparent elongation (%E)	Moisture content	Diameter Cross-section area (CSA)	Tensile strength Tensile strain Tensile Modulus Stress-strain	
	Test	Semi-static 3 point-bending (3PB)	Tension parallel (TP)	Water Absorption (WA)	Accelerating Ageing (AA)	Impact Test (IT)
MHC	Reference	ASTM D 1037-12 [176]				ASTM D4812-11 [177]
	Outcome	MOR MOE	Tensile stress (TS) MOE	% of WA % swell	TS and MOE after severe exposure environmental conditions	Impact resistance (IR)

2.5 Key findings in the literature review

Most studies in the field of green composites, particularly AW-based, have not been developing following an SDA approach. Perhaps the closest cross-sectional study is Karana's et al. (2015) [9], investigated the emotional response to new materials, drawn upon the user-material-product relationship using a material driven design approach. However, there is still very little understanding of the development of an MH-based composite. The most relevant gaps found in the literature revised are the following:

- Lack of an SDA approach for the manufacturing of novel material composites
- Merge of three study areas with one objective through design methodologies
- Concern for the current environmental, economic and social of the AW generation, and its implications in the Mexican context
- Analysis of the MH collection methods and their effects on the fibre properties
- MHF mechanical and physical properties related to the extraction method performed
- MHF overall performance as a fibreboard-like composite
- Use of natural and bio-based thermoset matrices for the MHC manufacturing
- Similarities and comparison of AW fibre-based fibreboards and WBF.

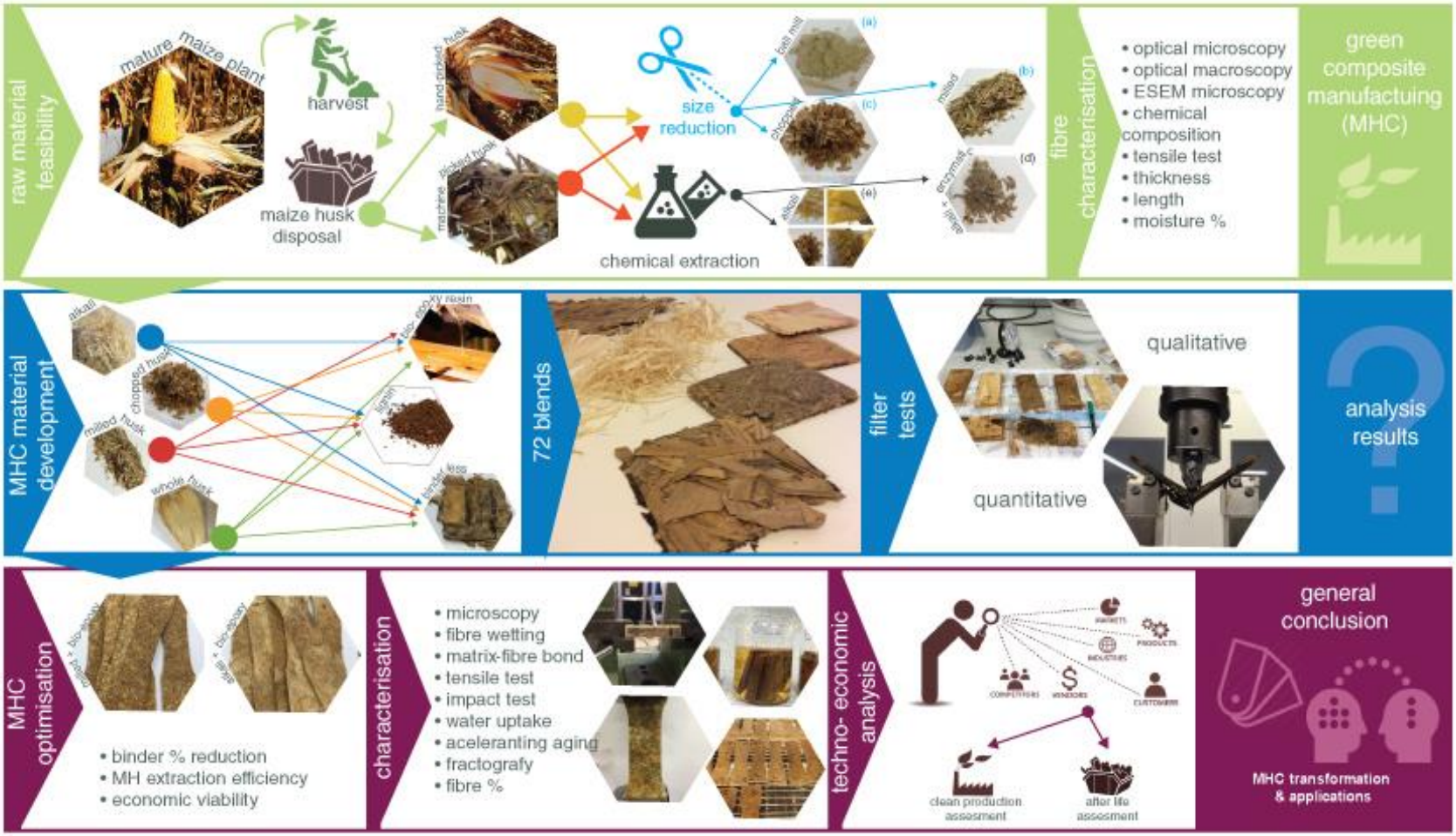

Figure 40 Experimental procedures followed to MHC sample manufacture

3 MATERIALS AND METHODS

The present chapter covers MD&D methodology; thus the SDA approach achieves its goal of manufacturing a viable MHC. This section describes raw materials, design and experimental methods, as well as the measurement instruments used throughout the different stages of the research (Figure 40).

3.1 MATERIALS

3.1.1 Maize husk

MH availability was assessed in the State of Mexico area; this is fully explained in section 2.3. For this research, the samples were divided into two groups shown in Table 11; both husk types were analysed according to the source, harvest method, production yield, husk length, flexural strength and chemical composition. Thus, only the best samples were tested as a composite reinforcement.

Table 11 Maize husk samples codification

Code		Source	Harvest method	Location
ASPROS	A	ASPROS *Semillas*	Mechanic	Zacatecas, Mexico
MASH	M	Local farmers market	Manual	Toluca, Mexico

ASPROS samples were “Sultan” maize seed harvested in 2013 produced by ASPROS *Semillas*. Husks were mechanically collected from fully mature maize plants (Figure 41(a)). ASPROS meets the characteristics of a major agricultural producer in Mexico, with more than 500 ha of sown land and a maize yield of approximately 3,000 tonnes per annum. MASH samples are from the 2013 harvest and were obtained from a local farmers’ market. Samples were hand-picked in Toluca Valley (Figure 41(b)). The product comes from micro-producers with 5 ha or less of sown land with an annual yield of 40 tonnes. It is important to mention that MASH specimens have been treated with steam and sulphur to bleach and soften the surface [97] for traditional food wrapping and craft purposes. Both sample husks were stored at room temperature (20 °C ± 1 °C) prior to characterisation.

Figure 41 Maize husk samples. (a) ASPROS sample as received (AR) from the field. (b) MASH sample AR from the local market

3.1.2 Maize husk fibre extraction

Alkali (AK) extraction was carried out using sodium hydroxide (NaOH) pellets (Fisher Chemicals, UK) at 97 % purity. They were used at two concentrations of 5 (0.125 M) and 10 g/l (0.125 M). Then, acetic acid ($C_2H_4O_2$), diluted to a concentration of 10 % solution mixed with deionised water, was used to neutralise the alkalisation process, which is explained in detail further ahead.

Subsequently, some samples underwent an enzymatic extraction (AZ) which was carried out using Pentopan ® Mono BG (xylanase from *Thermomyces lanuginosus*) to remove the remains of lignin and hemicellulose, improving the fibre-matrix bonding. Celluclast ® (cellulase) was used to remove the short fibres from the obtained slurry; Sigma-Aldrich Company Ltd, UK supplied both.

3.1.3 Maize husk-based composite manufacturing

The adhesives and chemicals used for the manufacture of MHF have been selected following the results obtained from size reduction trials. All husk sizes detailed in Table 12, were tested with both the chosen matrices, lignin and an SSE epoxy resin, at 20/80 and 30/70 w/w ratios of matrix and MH, respectively. Table 19 summarises the manufactured blends.

3.2 METHODS

3.2.1 Microscopy

Microscopy observations were performed at every step of MHF manufacturing, from the raw material as received, fibre and bundles obtained from the size reduction processes to the different MHF obtained.

3.2.2 Optical microscope and macroscope

A Nikon Optiphot optical microscope and a Leica EC3 macroscope were used to analyse the morphological structure and diameter of both ASPROS and MASH bundles and fibres. The MHF obtained were observed to compare and analyse matrix bonding, fibre wetting, voids formations and eventual fractures after the performed tests.

3.2.3 Environmental Scanning Electron Microscope

Both samples ASPROS and MASH, and selected MHF specimens obtained were analysed using an FEI XL30 Environmental Scanning Electron Microscope (ESEM). The parameters used for observation were as follows: no coating, magnification between 100-5000x depending on the sample; 20 kV of acceleration voltage; 15-30 mm working distance; stubs alumina 12.5 mm diameter [128]. A pre-requisite for the ESEM was to dry the specimens in the Harvard/ LTE convection oven for 12 hours at 80 °C, to make the samples electrically conductive.

Image J software was used to analyse the cell geometry of different boards to provide the information to understand the effect of matrix/fibre interaction and to evaluate fracture types after the mechanical test (Figure 42). Three-plane (XY, YZ and XZ planes) investigation was applied to each specimen.

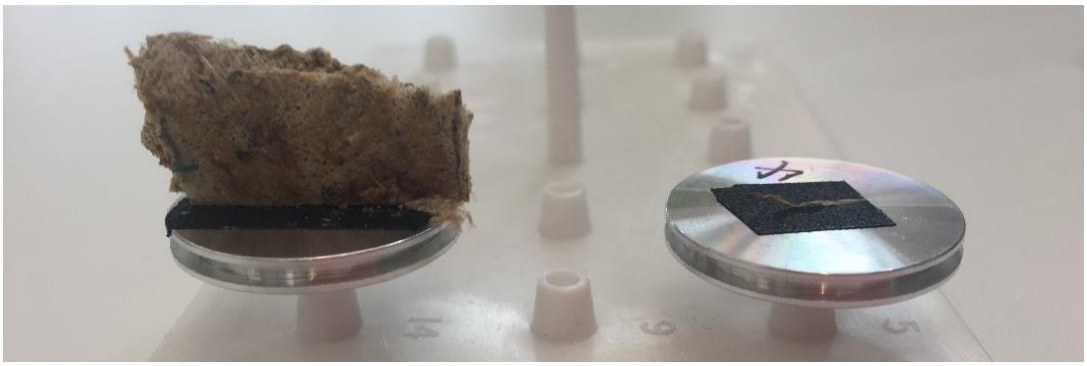

Figure 42 MHF and fibre specimens mounted on aluminium stubs using double-sided electrically conductive carbon adhesive tabs

3.2.4 Maize husk cleaning

To reduce variation, dark green mature leaves were not included. Both ASPROS and MASH husks were hand-washed with tap water at room temperature (20 °C ± 1 °C) to remove dust and other contaminants from the field, dried in a Harvard/ LTE convection oven for 12 hours at 80 °C, and finally packed in seal plastic bags to be kept in a desiccator at 20 °C ± 2 °C.

3.2.5 Maize husk and fibre characterisation

3.2.5.1 Maize husk length

The as-received husk length was measured with a Vernier calliper to the nearest 0.1 mm. For each batch, an average of ten husks specimens were measured.

3.2.5.2 Maize husk fibre cross-section area

To determine MHF diameter a Nikon Optihot microscope was used at 50x magnification. Measurements from the obtained images were taken in mm. Due to MHF's natural waviness, specimens were measured in three different places lengthwise to identify the edges; thus, the fibre's diameter could be determined. The MHF and bundles were considered both round and oval and contrasts with each other for the sake of accuracy [174]. Ten bundles of each batch were analysed.

3.2.5.3 Maize husk moisture content

MH moisture content was measured following the American Society for Testing and Materials (ASTM) D 1348-94 [173]. It was performed on bulk samples (10 g) of both ASPROS and MASH husks. The samples were cut into small pieces and left overnight in a sealed glass container to obtain its moisture equilibrium before initiating the test. Samples were weighed to the nearest 0.001 g and then dried in a Harvard/ LTE convection oven at 103 °C ± 3 °C for 4 hours and finally weighed again to the nearest 0.001 g. Later, the specimens were returned to the oven for another hour, until weight difference was no more than 0.005 g. Moisture content was calculated, as follows:

$$moisture\ content, \% = \left[\frac{M - D}{M - T}\right] * 100 \qquad \textbf{Equation 1}$$

Where:

M = original mass of the specimen plus container (g)

D = oven-dry mass of the specimen plus container (g), and

T = mass of the empty weighing container (g)

3.2.6 Maize husk size reduction

Five different methods for size reduction were carried through as shown in Table 12. The whole husks were used as a control.

Table 12 MH size reduction and fibre extraction codification

Abbrev.	Husk size	Husk type
W	Whole	ASPROS & MASH
CH	Chopped	ASPROS & MASH
BM	Ball milled	ASPROS & MASH
M	Hammer-milled	ASPROS & MASH
AK	Alkali extraction	ASPROS & MASH
AZ	Alkali & enzymatic extraction	ASPROS & MASH

Mechanical processes aim to break down a semi-dry plant or wood residues into smaller pieces and eventually into single fibres. Hence, chopping and milling are commonly used in the WBF industry. The obtained fibres are expected to be coarse and considerable thicker than those acquired with any chemical method.

3.2.6.1 Chopped

Both MH types were trimmed by hand into swatches of 30 mm approximately, using regular scissors; then, packed in sealed plastic bags and kept in a desiccator at 20 °C ± 2 °C to avoid any moisture uptake before the MHF compounding.

3.2.6.2 Ball mill

An alternative method for breaking down the MH involved using a *Pulverisette 5* ball mill. AR husks were cut into halves, then placed into the ceramic container and ground for 3 hours at a medium speed. Samples were checked every 30 minutes. The obtained mix was bagged and sealed to be kept in a desiccator at 20 °C ± 2 °C.

3.2.6.3 Milling

The cleaned husks were ground in a powered mill using cutting blades at 25,000 RPM for 4-10 minutes to mid power until the dried husks reached a uniform size. The milled husks were bagged and sealed to be kept in a desiccator at 20 °C ± 2 °C.

3.2.6.4 Alkali fibre extraction

Different authors have used the alkali treatment for fibre extraction [110,114,116,145,178]. Yilmaz et al. [179], as well as Reddy and Yang [180], identified an increment of fibre roughness by disrupting hydroxyl groups (–OH), removing lignin, wax, and oils from the surface of fibre cell wall, depolymerising cellulose, and exposing crystalline regions. This method has been applied in several case studies using flax [118], softwood [126], maize husk [180], rice husk [116], jute [135], sisal [139] and pineapple leaf [109], showing a sufficient

fibre yield. To determine the effect of the alkali extraction on MHC's tensile strength and breaking strength, several mechanical tests were performed, same that will be explained further ahead in section 3.2.7.

Both husk types were soaked in a NaOH solution in 5, and 10 g/L diluted in distilled water for 60 and 120 minutes under boiling temperature (Table 13). The alkalinisation was followed by rinsing five times with tap water and neutralised with acetic acid ($C_2H_4O_2$) solution at 10 %, then rinsed again until pH 7 was reached. The obtained slurry was dried in a Harvard/LTE convection oven for 12 hours at 80 °C, and finally packed in sealed plastic bags and kept at 20 °C ± 2 °C in a desiccator to avoid moisture uptake.

Table 13 Routes and codification of alkali extractions

Code*	Husk	NaOH (g/l)	time (min)	Temp (°C) ± 5
A-AK01	ASPROS	5	60	90
M-AK01	MASH	5	60	90
A-AK02	ASPROS	5	120	90
M-AK02	MASH	5	120	90
A-AK03	ASPROS	10	60	90
M-AK03	MASH	10	60	90
A-AK04	ASPROS	10	120	90
M-AK04	MASH	10	120	90

*** Refer to section Figure_Apx 7-1 for key code**

3.2.6.5 Enzymatic extraction

Enzymatic extraction was carried out using first alkali extraction followed by the prepared enzymes, as reported Reddy and Yang [96]. The extractions were made in triplicate with an enzyme concentration of 5 % of Pentopan ® Mono BG and 3 % of Celluclast ®, the amounts were calculated based on the 5 % fibre weight (w/v) in the enzymatic solution; incubations were done for 60 minutes at 90 °C ± 1 °C (Table 14). All enzymatic treatments were performed simultaneously to avoid any variables. Extraction was followed by rinsing five times with tap water and drying in a Harvard/LTE convection oven for 12 hours

at 80 °C. Samples were finally packed in sealed plastic bags and kept in a desiccator at 20 °C ± 2 °C.

Table 14 Routes and codification of MH enzymatic extractions

Code*	Husk	NaOH (g/l)	time (min)	temp (°C) ± 5	Xylanase (%)	Cellulose (%)	time (min)	temp (°C) ± 3
A-AZ01	ASPROS	10	120	90	5	3	60	90
M-AZ01	MASH	10	120	90	5	3	60	90

*** Refer to Figure_Apx 7-1 for key code**

3.2.7 Tensile properties of maize husk

Tensile properties of both MH and MHF were grouped into four batches: (1) AR MH swatches; (2) untreated MH fibre bundles; (3) alkali extracted MH fibres; and (4) mechanically MH obtained fibres. ASTM D 3822M-14 [175] was adapted for the single fibre test.

Table 15 Routes and codification of MH swatches

Code*	# samples	Husk type	Husk state	Husk direction
A-Tr	10	ASPROS	as received	transversal
A-L	10	ASPROS		longitudinal
M-Tr	10	MASH		transversal
M-L	10	MASH		longitudinal

*** Refer to Figure_Apx 7-2 for key code**

The tensile test for husk strips was based on ASTM D 5035-11 standard [172], it was adapted to test the breaking strength and %E of both MH types. The husks were cut into strips in both directions longitudinal and transversal, taking the husk veins as a reference as shown in Figure 43. The specimen size was 150 x 25 mm for the transversal ones and 75 x 25 mm for the longitudinal. The tensile test was conducted with a gage length of 75 mm at a loading rate of 2 mm/min, using a 5 KN load cell. At least ten specimens were tested for each sample type.

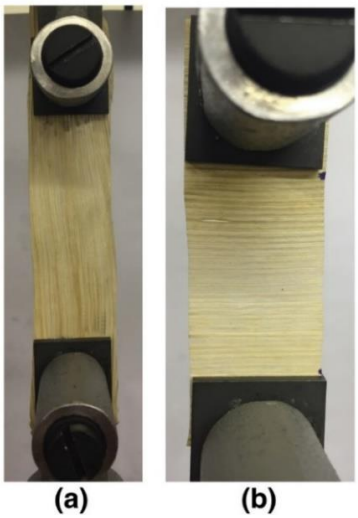

Figure 43 Tensile test setting. (a) Longitudinal husk strip mounted for the tensile test. (b) Transversal husk strip mounted for tensile test

3.2.8 Tensile properties of maize husk fibre

MH bundles were manually drawn from the cleaned husk. According to ASTM D 3822M –14 [175] the preparation procedure was as follows: MH fibres were cut at the required distance and glued into a 25 x 25 mm paper tabs with a die cut of 14 mm using an epoxy resin as shown in Figure 44. During mounting, the specimens were handled with tweezers to avoid sample contamination. The tests were carried out on an electromechanical Instron 5/100 KN 5500 R machine. Load-displacement curves were recorded during the test. Once the sample was mounted in the clamps, the paper frame was cut, allowing the fibre bundle to receive without interferences the loading as seen below in Figure 45.

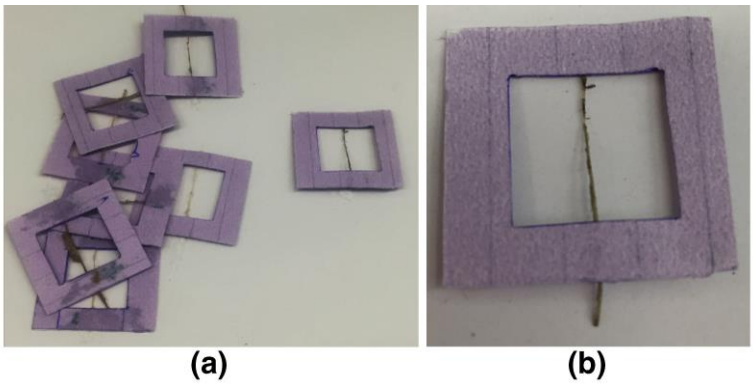

Figure 44 MHF tensile samples (a) and (b) MHF AR fixed on a paper frame

Tensile testing was performed at ambient temperature with a deformation rate of 1 mm/min with a load cell of 5 KN. At least 20 fibre bundles were tested separately with a clamping length of 14 mm as depicted in Figure 45. The specimen numbers were calculated, so the statistical model had sufficient samples for analysis.

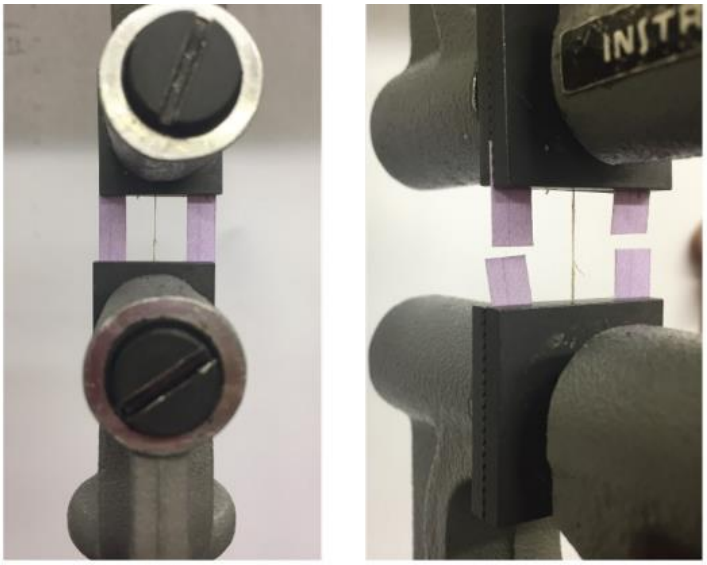

Figure 45 MHF tensile test set-up (a) clamped paper frame, (b) released paper frame ready to start the test

Following ASTM D 3822M –14 [175] the MHF breaking tenacity was calculated using the formula:

$$\gamma = F/D_L \qquad \textbf{Equation 2}$$

Where:

γ = breaking tenacity (mN/diameter)

F = breaking force (N), and

D_L = linear density (mm)

3.2.9 Maize husk composite manufacturing

The manufacturing of natural fibre-based composite materials is based on several steps, as previously mentioned in section 0. Therefore, for the MHC manufacturing, the steps followed were taken from the current method used in the WBF composites dry process and adapted to a lab scale (Table 16).

Table 16 MHF manufacturing steps

#	Description
1	Size reduction
2	Cleaning
3	Drying
4	Binder preparation
5	Fibre impregnation
6	Mat-forming
7	Hot pressing

Albeit in the first phase of the research the MH went through cleaning and selection, to complete the production processes the closest to the original WBF, all the MH were treated as if they were received from the field. Thus, the size reduction and cleaning were performed as previously explained in section 3.2.6.

3.2.9.1 Binder selection and maize husk composite configuration

MH was tested as raw material to manufacture fibreboard samples in combination with three different binders used for this study (Table 19). Regardless of the binder used, the mixing was performed after the MHF was dried and kept from moisture uptake to ensure a better blending. Previous studies on MHF-based fibreboards reported the use of PP [92], UF [123,153], phenol formaldehyde (PF) [181] and some other modified binders like melamine urea formaldehyde (UMF) [182]. However, the usage of MHF natural elements as an adhesive agent has been studied from a self-bonding [147] methods; yet, other alternative methods have not explored to date the use of MHF, e.g. steam explosion [37,154], starch [183], lignin [159], natural oils [26,27]. Offering an excellent opportunity to diminish and even eliminate the toxic fumes and side-

effects caused by the use of oil-based resins in fibreboards production. Consequently, before commencing the manufacturing process, a series of possible binders were considered and evaluated as explained in Table 18, under the premise that the chosen binder had to be reliable, available, cost-effective, and environmentally friendly.

The MHC samples were manufactured with the chosen three binding schemes SSE, L and Bs at 80/20 % w/w relation MHF/binder, to assess properties further. MHF/matrix performance, manufacturing process and MHC boards properties. Once the MHF was mixed with the different adhesive agents, then it was hot-pressed. All the pressure loads, time and generated heat to consolidate the MHC varied as detailed in Table 17. Additionally, to avoid adhesion of boards to the press plates and frame, Teflon sheets were indispensable during pressing, this because the use of a press-release agent sprayed was discarded avoid cross contamination as low as possible.

Table 17 Compression moulding cycles and settings per binder

	Pre-heating	**Pre-press**		**Hot-pressing**			**Cooling**
Binder	(°C ± 3)	(s)	(ton)	(°C ± 3)	(ton)	(min)	(min)
Bs	100	30	10	130-160	25-30	5-20	10
L	130	-	-	150-170	25-30	20-25	10
SSE	130	20	10	180	25-30	20-35	15 -20

Table 18 Binder selection criteria for MHC manufacture [92,144,145,147,153,159,185–188]

	Binder	UF	Greenpoxy 56	PP	Super SAP® CPM epoxy	Cashew resin	Tannin	Lignin	Steam explosion	Binderless
Criteria	Chemical nature	TS	TS	TS	TS	TS	TS	-	-	-
	Source	Oil	Plants	Oil	Pine oils	Cashew shell oil	Pinus bark	Biomass	Steam	Fibre chemicals
	Density (g/cm^3)	1.5	1.2	0.905	1100 - 1200	/	-	1.3	/	/
	Curing (min/ °C)	30/120	240/40	/210	2-40/180	3* / 60-100	+	+		
	Tensile strength (N/mm^2)	30.3	3,200	0.95-1.3	3006.1	24.5	/	/	/	/
	Elongation (%)	1.0	1.6	150	6	/	+	/	/	/
	Fire resistance	Additive	X	X	/	/	X	X	X	X
	Moisture resistance	Additive	✓	✓	✓	/	Additive	X	X	X
	Bio-based carbon content (%)	X	56	X	31	70	60	60	100	100
	Colour	Milky	Clear	White opaque	Clear - pale yellow	/	Brown	Dark brown	/	/
	Appearance	Liquid	Liquid	Liquid	Liquid	Liquid	Powder	Powder	/	/
	Toxic emissions	✓	X	✓	Low	/	Low	X	X	X
	Biodegradable	X	✓	X	/	✓	/	✓	✓	✓
	Availability in Mexico	✓	X	✓	✓	X	✓	✓	✓	✓
	Price (£/L)	1.10	14.74	0.75	11.97	8.40	24**	132**	/	/
	Supplier	Arclin	Sicomin	AVG	Entropy	GTM	Hach	Pholser	/	/

TS= Thermoset resin *days **kg / not available

3.2.9.2 Binder preparation and fibre impregnation

The MH in the four different sizes were manually impregnated and blended as shown below in Table 19. To make clear and help the results interpretation, the sample code is explained in Figure 46.

Table 19 MHC manufactured blends and codification

Binder	MH type	ASPROS	MASH
	MH size		
Binderless (Bs)	Whole husk	WB-A	WB-M
	Chopped	CHB-A	CHB-M
	Milled	MB-A	MB-M
Lignin (L)	Whole husk	WL-A	WL-M
	Chopped	CHL-A	CHL-M
	Milled	ML-A	ML-M
Super Sap ® CPM epoxy resin (SSE)	Whole husk	WE-A	WE-M
	Chopped	CHE-A	CHE-M
	Milled	ME-A	ME-M
	Alkali	AKE-A	AKE-M

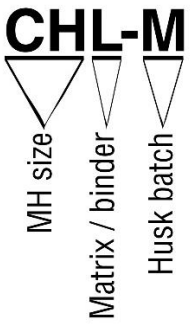

Figure 46 MHC blends key code

The binder mixing was carried out with an impregnation tool pack from Entropy Resins EU, an analytical balance and a wooden mixer. The binder solution was calculated per total fibre weight, at concentrations of 30/70 and 20/80 % w/w, respectively. Impregnation was carried out by spreading and squeezing the binder mix carefully onto the lignocellulosic material while mixing manually until a homogeneous mix was obtained. Once the fibres were covered with a binder, they were left at room temperature for 5 minutes before the pressing, so the fibre wetting was completed.

3.2.9.3 Binderless

The husk was manually moistened with tap water using an atomiser; then the mix was placed randomly by hand in the steel frame ready for the pressing.

3.2.9.4 Lignin

The lignin powder was dissolved in warm distilled water at 30 °C; the mixture was stirred using a magnetic stirrer at room temperature (20°C ± 1 °C) for 10 minutes. Then the prepared lignin was sprayed with water and mixed with the MH to be manually placed in the steel frame for the hot-pressing.

3.2.9.5 Bio-epoxy resin

The Super Sap ® CPM epoxy resin (SSE) preparation was done at a 1:2 ratio of epoxy/hardener at room temperature 20 °C ± 1 °C, as suggested by the supplier. The resin maturing took 10-15 minutes. Once the resin was stirred well, the solution was sprayed and mixed with the husk until a homogeneous blend was obtained, then it was placed by hand in the pre-heated frame.

3.2.9.6 Maize husk fibreboard hot-pressing

The pressing cycle was guided by a systematic trial test designed for the first and second batches, in which the first batch was considered fast prototypes. To explore the MH resistance and response to the hot-press and the binders, due to lack of actual data. The samples for the filter tests were obtained from the second batch. Thence the MHC samples were tested and classified with a Pugh matrix (section 4.7.3), to later be improved for the following tests. The third batch was the optimised blends, ready to perform further mechanical studies.

The pressing method is comparable to the one used by the wood-based panel industry. This procedure has been adjusted in previous researches to non-wood fibres, e.g. kenaf [123], wheat straw [125], pineapple leaf, flax and hemp [104]. Moreover, the research on MH's utilisation using the hot-pressing has been very limited and scarce in Mexico, although Youssef et al. [95], Huda and Yang [92] and Padkho [117] studies have shown MH's endurance when hot-pressed and mixed with another NF

The MHC laminates were produced in a 40T laboratory manual hydraulic hot-press machine. Figure 47 diagram describes the pressing process indicating temperature and pressure ranges to obtain the laminates. The MH blends were

put into a steel frame and placed between stainless steel plates, so they work as support and the frame as a mould. The frame dimensions are shown in Figure 48. After the pressing, the frame was left at room temperature conditions to allow the MHF obtained to be de-moulded.

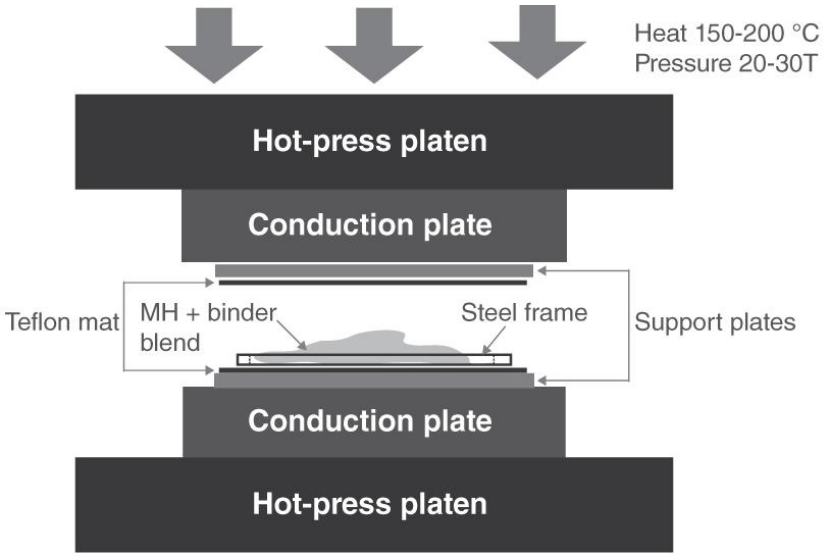

Figure 47 MHC hot-pressing process diagram

The boards pressing time was 3-5 minutes per millimetre of the total panel thickness. The panel thickness aimed was 3 mm. The total pressing time had a variation between 5 and 30 minutes, depending on the binder used. The press-plates temperature was set to 150 °C. The maximum temperature in the core of the fibre mat was kept between 180 to 200 °C, and it was monitored with a small-diameter thermocouple placed as close as possible to the board's centre to avoid MH's cellulose, hemicellulose and lignin degradation. Prior to the pressing stage, a Teflon mat was placed between the plates and the steel frame to ease the de-moulding process.

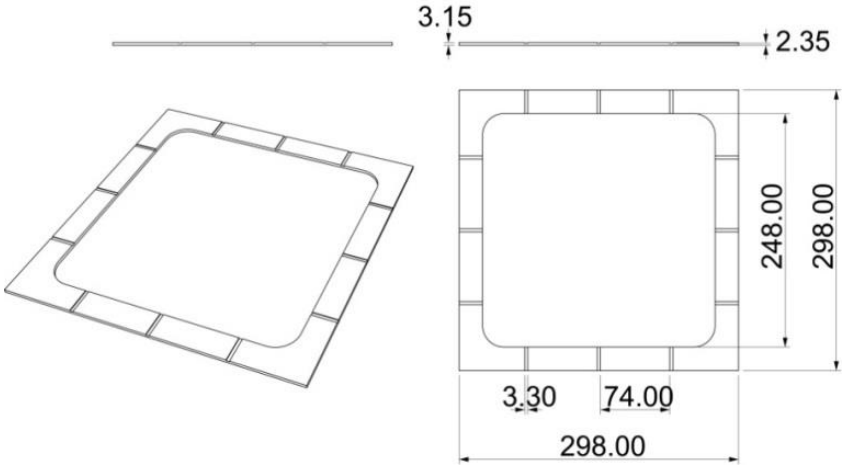

Figure 48 General measurements in millimetres of the used steel frame

3.2.10 Maize husk composite characterisation

Traditionally fibreboards have been assessed by measuring mechanical properties, however, for the assessment of the MHC boards various qualitative and quantitative characteristics were considered and will be explained further ahead. The performed tests helped to classify the MHC specimens so they could be compared with other NF-based fibreboards. The variance of matrix/ binder compatibility, fibre dispersion and fibre wetting in MHC samples were taken into consideration, inasmuch as the chemical compounds (cellulose, hemicellulose, pectin and waxes) percentages changed in each extraction method applied. Together with this, the different binders used showed a different result in the MHC specimens.

MHC boards were cut according to each test requirements. The assessment tests flexural modulus (FM), MOR, MOE, water absorption (WA) and the AA were determined and adapted to a lab scale from the ASTM D 1037-12 [176]. The IT was carried out according to ASTM D 4812-11 [177].

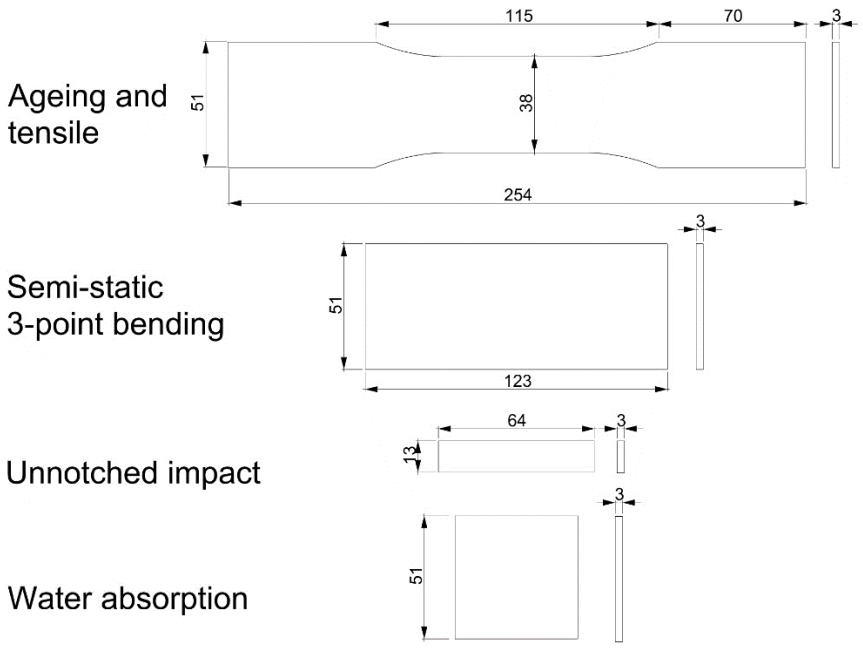

Figure 49 MHC specimen' dimensions (mm)

MHC specimens were cut with a CNC Roland Modela MDX-40A milling machine using a 3 mm carbide coated end mill cutter at a feed rate of 3 mm/sec (Figure 49). Details on the optimised machining programme and parameters are shown in Appendix B. Before testing, the specimens were dried at 80 °C for 24 hours and kept in a desiccator to reduce the moisture uptake.

3.2.11 Maize husk composite moisture content

For the measure of MHC specimens moisture content, the ASTM D 1348-94 [173] was followed. The MHC boards from both ASPROS and MASH husks were cut (51 x 51 mm) and weighted to the nearest 0.001 g before any procedure. Then, the samples were left at room temperature 20 °C (± 1 °C) with a relative humidity of 60 % (± 5 %) overnight in aluminium foil containers, to reach its moisture equilibrium before initiating the test. Samples were weighed to the nearest 0.001 g and then dried in a Harvard/ LTE convection oven at 100 °C (±3 °C) for 24 hours, and weighed after 2,4,12 and 24 hours to the nearest 0.001 g. The moisture content was calculated, as follows:

$$moisture\ content, \% = \left[\frac{M - D}{M - T}\right] * 100$$ **Equation 3**

Where:

M = original mass of the specimen plus container (g)

D = oven-dry mass of the specimen plus container (g), and

T = mass of the empty weighing container (g)

3.2.12 Semi-static 3-point bending

The semi-static 3-point bending test was used as a filter test to select the most resistant MHC blends from the first and second batches manufactured. Burge's (2009) [189] decision tool was used to handle the complex quantitative and qualitative data obtained during the testings, hence an objective evaluation of the MHC mechanical features and manufacturing process. Consequently, further studies could be implemented to broaden the MHC characterisation.

The rectangular MHC coupon size was 123×51 mm according to the ASTM D1037-12. The evaluation was performed with an Instron 5/100 kN with a 100 N load cell with a speed rate of 1 mm/min, for which an adapter was designed and manufactured (Appendix C). Rounded supports were used with a span distance of 24:1 of the MHC thickness (Figure 50). At least three specimens were tested for each blend, to average the flexural results. Sixty-three specimens were tested.

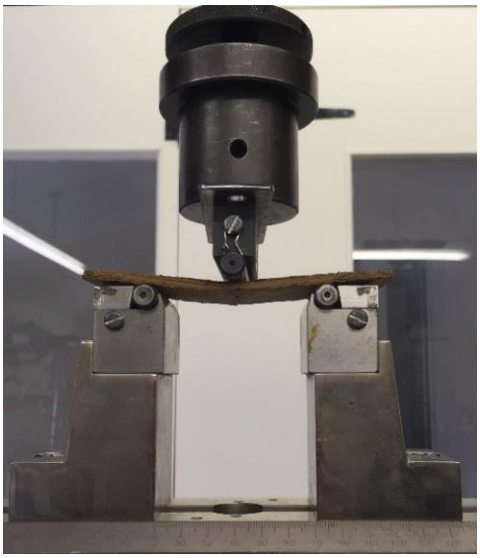

Figure 50 Semi-static 3-point bending test setting for MHC samples

From the data obtained MOR was calculated using the formula:

$$R = \frac{3P_{max}L}{2bd^2}$$ **Equation 4**

Where:

B= specimen width (mm)

d = specimen thickness (mm)

L= span length (mm)

P_{max} = maximum load (N)

R= modulus of rupture (kPa)

The FS was calculated as follows:

$$\delta = \frac{6Dd}{Ld^2}$$ **Equation 5**

Where:

D = maximum deflexion of the centre of the specimen

L= support span (mm), and

d= specimen thickness (mm)

3.2.13 Tensile test

The tensile test was performed in an Instron 5/100 kN machine at a 1 mm/min rate with a 100 N load cell. ASTM D 1037-12 was followed for the testing settings and calculations. Dog-bone-shaped specimens were cut as shown in Figure 51.

Figure 51 MHC sample placed in the testing machine for tensile test

Seven specimens were tested for each composite blend to average the results. The MOE was calculated in accordance to the following equation:

$$E_t = \frac{l_g}{bd} * \frac{\Delta P}{\Delta y}$$ **Equation 6**

Where:

E_t = modulus of elasticity in tension (MPa)

l_g= gage length (mm)

b= specimen width (mm)

d= specimen thickness (mm), and

$\frac{\Delta P}{\Delta y}$ = slope of the straight-line portion of the load-deformation curve (N/mm).

3.2.14 Accelerating ageing

This test was chosen with the purpose of comparing and examining MHC attrition of the optimised blends, leading to further understanding of the material' behaviour. The specimens were cut as per ASTM D1037-12 into dog-bone shaped pieces as Figure 52 shows. Seven specimens were tested for each composite blend to average the results.

Figure 52 MHC specimens distributed in the ambience chamber

Table 20 summarises the ageing cycle to which MHC specimens were exposed; the test simulated environmental conditions that the material could be exposed to during its life cycle. The specimens were exposed to six complete cycles, using a Design Environmental FS1100-70V environmental chamber.

Table 20 MHC ageing cycle

Step	Process	Temperature (℃)	Humidity (%) ± 2 %	Time (h)
1	Steam and water vapour	93 ± 3	100	3
2	Freezing	-12 ± 3	100	20
3	Dry air heating	99 ± 2	0	3
4	Steam and water vapour	93 ± 3	50	3
5	Dry air heating	99 ± 2	0	18
6	Test conditioning	20 ± 3	65	48

Finally, a tensile test was conducted after conditioning the specimens to report the mechanical properties changes in MHC. The calculations were made by taking dimensions and weight after the ageing exposure and following the same procedure previously detailed in section 3.2.13.

3.2.15 Water absorption

The WA test was implemented to report MHC moisture uptake, and thickness swelling since it is one of the most significant drawbacks in NF-based composites as Zini and Scandola [104] reported. The test was carried out following the ASTM D 1037-12 standard, and specimens were weighed and measured with ± 0.2 % accuracy using an electronic calliper and electronic balance. Squared shaped samples of 51 mm were cut. Once all the specimens were measured and marked, they were submerged horizontally under 25 mm of water and temperature was kept at 20 °C (± 1 °C) for 2 hours. After immersion, samples were measured, weighed and put back into the clean water for 22 hours; the procedure was repeated twice. Five specimens were tested for each composite blend. To calculate the moisture content percentage of MHC, the initial and final weights were used. The thickness swelling was reported as the incremented percentage of the initial thickness.

$$moisture\ content, \% = \left[\frac{M - D}{M - T}\right] * 100 \qquad \textbf{Equation 7}$$

Where:

M = original mass of the specimen plus container (g)

D = oven-dry mass of the specimen plus container (g), and

T = mass of the empty weighing container (g)

3.2.16 Unnotched impact test

There have been only limited studies on the impact behaviour of fibreboards. For instance, Huda and Yang [92] utilised the IT to investigate the fracture energies for PP/split maize husk fibres boards, thus the understanding of this particular blend. Therefore, the study of MHC impact response seems relevant for this research scope. The impact test was based on the ASTM D 256-10 [190] and performed using a Zwick pendulum with a 1J hammer (Figure 53). Five 65.5 x 12.7 mm specimens were tested for each sample type. Impact strength was calculated using the following equation:

$$I = \frac{E_c}{hb} \times 10^3 \qquad \textbf{Equation 8}$$

Where:

E_c = corrected energy absorbed by the specimen (J)

h= specimen thickness (mm)

b= specimen width (mm)

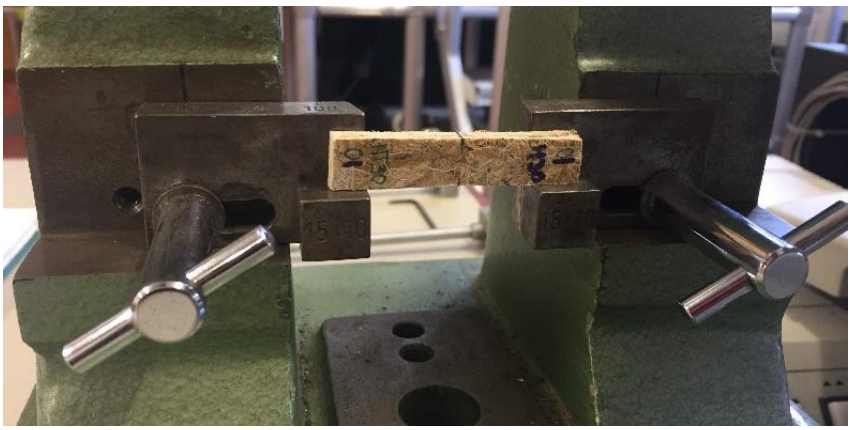

Figure 53 MHC sample placed in the pendulum for impact test

3.2.17 Pugh decision matrix

This methodology developed by Burge [189] is generally used when a number of products or designs are pairwise for an objective comparison. The benefit of this matrix is that also allows the creation of hybrid candidates and the re-evaluation of the subjects with the same criteria, thus, the information crossover may include qualitative data (price, fibre length, density, thickness) as well as quantitative characteristics (user perception, easy to use).

The Pugh matrix (PM) assembling process consists in 5 steps:

1. Criteria/requirements identification
2. Baseline material selection and core features/ requirements
3. Compare each candidate (material) against the baseline and score adequately as follows:

   S = same

   ++ = much better

   + = better

   -- = much worse

   - = worse

4. Once all the candidates have been scored (by adding the number of +'s or –'s), hybrids can be made by combining features from each candidate. Though, candidates first filter comprises twenty different blends a weighing scale was added. The weighing scale used goes from 1- 5, being 1 the less significant to the MHC development and 5 extremely important.
5. Decide and record the rationale behind the selection. This step is fundamental for the outcome validation. As the PM would not deliver a clear "winner", thus it is of fundamental to continue the iterations to obtain the most suitable candidate (material).

Table 21 Pugh matrix criteria

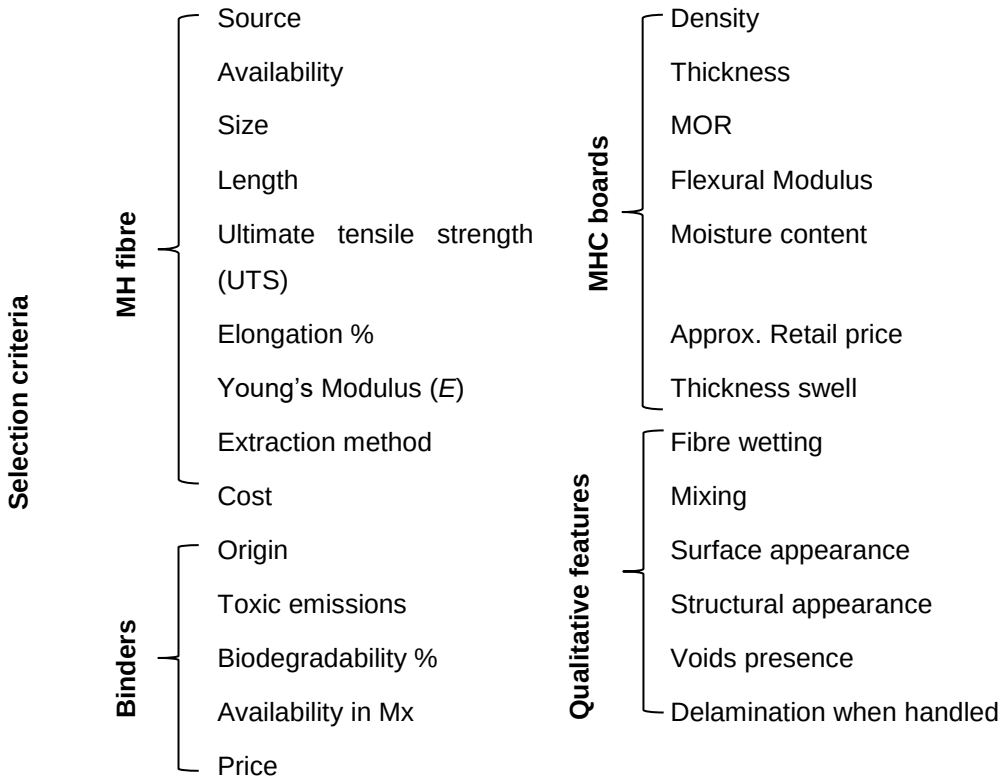

The scoring criteria used for MHC boards selection is based on the data obtained from MH and MFB availability and characterisation and MHC early stage characterisation. Albeit the features available were overly broad, the PM's focus was on the most remarkable per section as shown in Table 21. As for the baseline materials (light MDF and medium density particleboard (MDP)), chosen were determined by the information found in the literature. Therefore, each criterion was assigned a score in relation to its relevance to the overall material features or the manufacturing processes. It is noteworthy that the baseline material in each iteration has overall competitive features, not necessarily the best ranked in previous iterations. It is important to mention that this selection method does not aim to find an optimal MHC blend but to enhance the MHC materials.

4 RESULTS

This chapter objective is to present the SDA framework proposed for this research, as well as the outcome from the studies performed to test MH's viability in four different sizes to be used as a reinforcement for a green composite fibreboard.

The initial studies were focused on MH's physical and mechanical features, as well as the different methods followed to extract more efficiently the MHF. The MHC manufacturing trials were conducted with the different MH/binder blends. The obtained MHC boards were set up for characterisation and testing. Finally, all the collected data was summarised and analysed, thus the most competent MHC specimens could be optimised and paired with other commercial NF-based composites in accordance with their overall performance.

4.1 Systemic design approach

The first stage of this research was to conduct a systematic literature review to identify design and sustainability methodologies so that they could be applied across disciplines. Given the breadth of the proposal, this research will only focus on a sustainable design approach for novel material development, specifically using MH waste.

The literature highlighted a number of study-cases pursuing the "ideal innovation process" (Figure 5), including thorough testing for all three characteristics are of paramount importance. Hence, based on Roos's [23] value creation approaches an early innovative framework for the MH case-study was integrated as depicted in Figure 54.

The model draws from DT's innovation theory in a combined effort with other disciplines as Roos's case study in manufacturing industries [19]. Where he discusses the relevance of an adequate deployment system, so the new approach proposed could be fully embraced by all the actors involved: industry, market, government and users. Therefore, to conduct a comprehensive exploratory study of the innovation effectiveness and reach of a new methodology. Measure throughout the appraisal value of the five key innovation enablers: monetary, physical, rational, organisational and human [19].

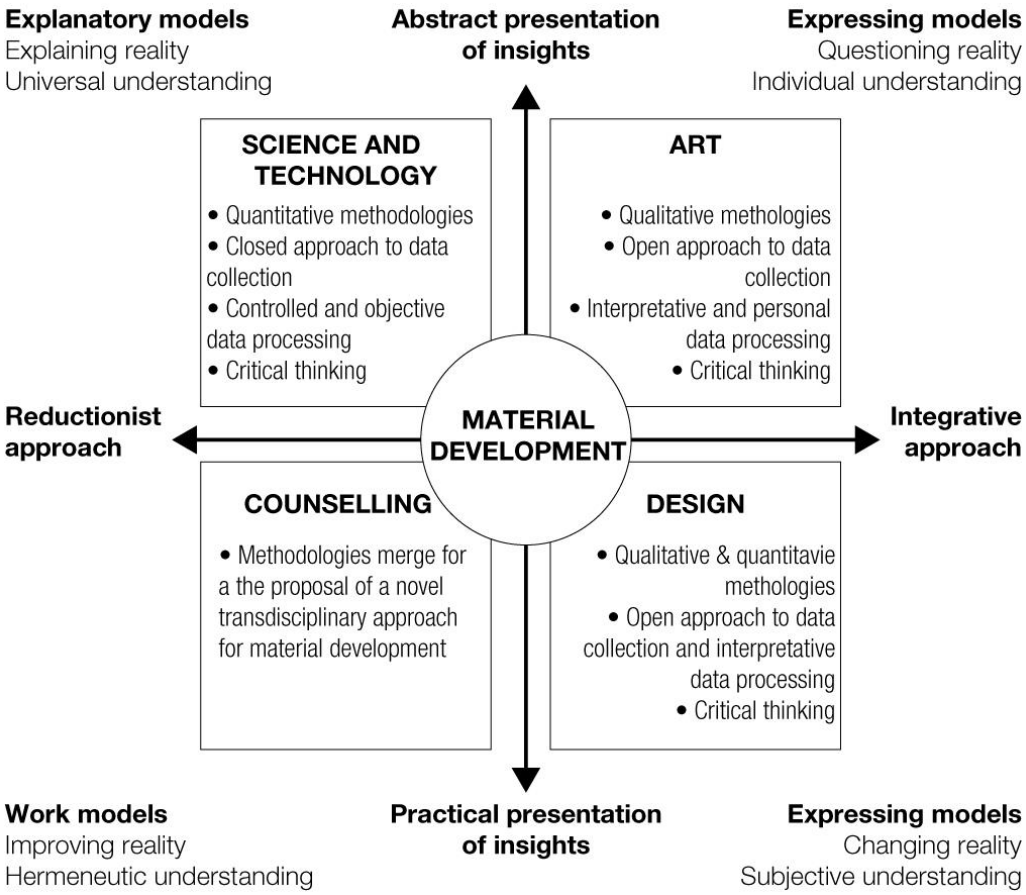

Figure 54 Transdisciplinarity framework for the development of a novel composite material based on Roos's [23] value creation approach

Thence, to enable a more straightforward and synthesised method to study further MH waste production in Mexico's central area the following SDA approach was proposed (Figure 55). This framework draws upon the transdisciplinarity of design, material sciences and sustainability. The four methodologies chosen are MR&D; DfS; TES; and DfSI. All sections interact freely with each other, as the coloured arrows show. Furthermore, delving into the framework the innovation drivers flow (grey arrows) indicate the possibility of knowledge transference between methodologies and compliance of IDEO's [18] innovation trifecta.

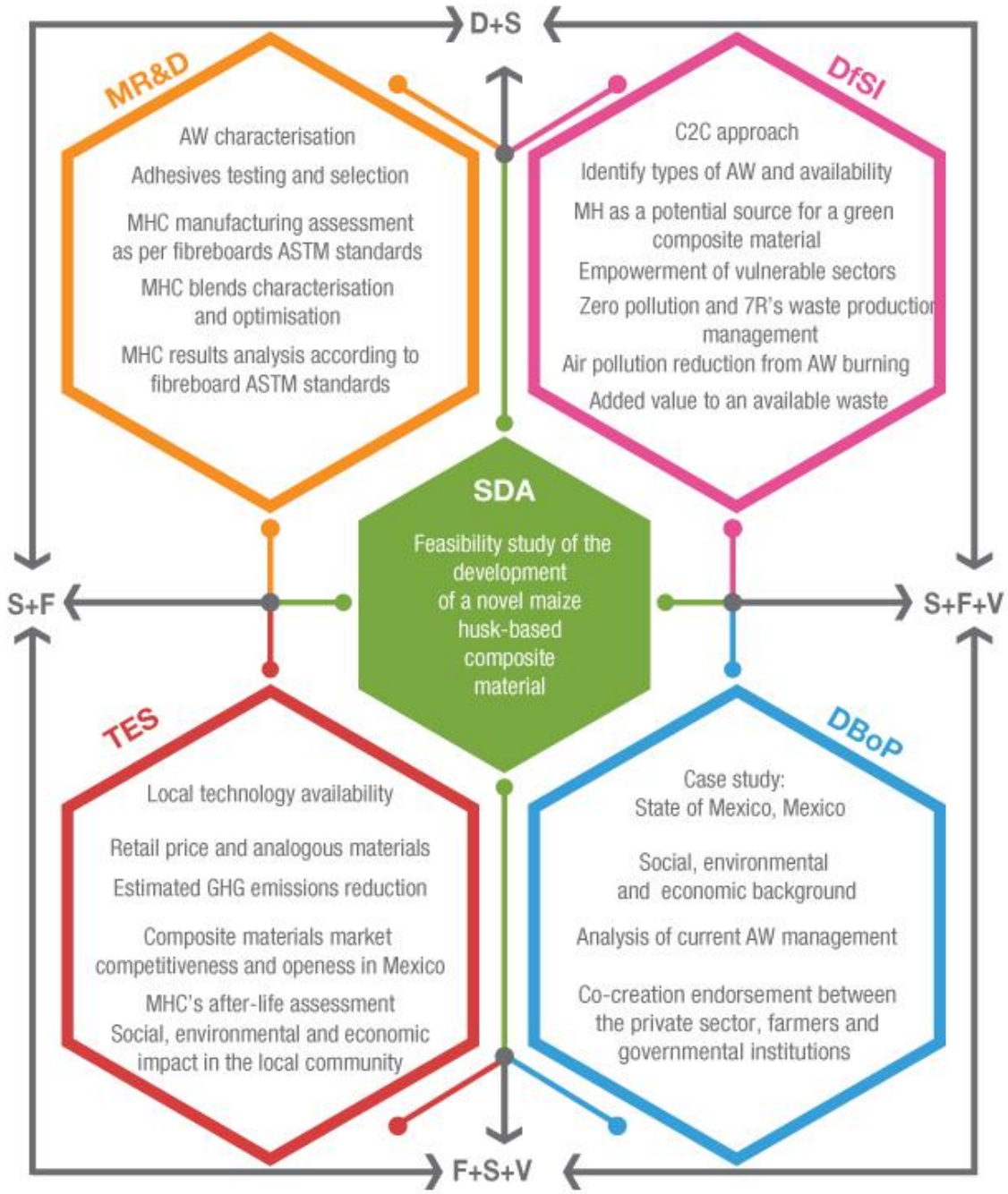

Figure 55 Proposed SDA framework for the development of a maize husk-based composite. The colour arrows show the learning synergies between methodologies; whereas, the grey arrows show the innovation drivers [29] (D= desirability, F= feasibility, V= viability and S= sustainability)

4.2 Maize husk characterisation

Studies on composite materials using post-harvest residues have shown their potential as a viable replacement for wood-based materials. As it has been discussed before in section 2.4.1, the fibre structure is associated with different factors, e.g. plant variety, growth location, harvesting method and humidity. Therefore, the observations on both MH types, ASPROS and MASH, were of fundamental importance to set the starting point in the measurement of MHF general parameters, i.e. density, moisture content, chemical composition and elasticity.

Thus far, previous studies on AW have begun to examine the source from the state in which it was obtained, e.g. bagasse [110], chips [191], split husk/stalk [13,92], leaf or fibre bundles [110]. The authors set out different methods, however for the MH evaluation only the tests summarised in Table 22, so they could be contrasted with other AW fibres used in the composites industry.

Table 22 MH and MHF tests and obtained features

	MH Tensile	**MH wt.%**	**MH CSA**	**MHF tensile**
Standard	ASTM D5035-11	ASTM D1348-94	ASTM D3822/ D3822M	ASTM D 3822M-14
Ref.	[172]	[173]	[174,192,193]	[175]
Outcome	Breaking force Apparent elongation (%)	Moisture content (%)	Diameter CSA	Tensile strength Tensile strain Tensile Modulus Stress-strain
Sample size	150x25 mm vertical 75x25 mm horizontal	10 g per each husk type	10 fibre bundles per husk extraction treatment	25x25 mm
# samples	10	2	10	20

ASPROS specimens were assessed right after the harvest, though due to its curled nature and length they had to be manually washed and sorted lest the husk would not be damaged (Figure 56(a)). Whilst MASH husks presented a more consistent shape and size (Figure 56(b)), this is because the specimens were already manually pre-selected, trimmed and exposed to a softening treatment, detailed in section 2.3.2, by the time they were analysed.

Figure 56 ASPROS (a) and MASH (b) husks AR

The leaf structure constitutes an 80-90% of the total dry weight of the MH, whereas the bast structure represents the remaining 10-20%, based on Sreekumar and Thomas [194] plant fibres classification it can be concluded that ASPROS husk can yield both stem and leaf cell structures. Even though both tissues can be found in both husks, in this trial MASH samples only yielded the leaf tissue. Other researchers, however, who have looked into hand-picked AW, have found that the structural tissue (bast) is removed to ease its handling and transformation [97]. Hence, MASH specimens were not expected to have other tissue structure than vascular (leaf). The correlation between the fibre structure and its location within the plant remains clear.

Figure 57(a) exhibits a macro view of an ASPROS specimen bast section, from which the following macro shots were taken. It can be observed in Figure 57(b) the cuticle as the outer layer that gives structure to the husk and holds the fibre bundles together, whereas in Figure 57(c) the bast' cross-section fibre bundles arrangement is shown. The later would determine the cell development by the water uptake and soil composition [195]. This husk section is characterised to have fine fibres, known to be stiff and brittle as Augusto et al. [196] have reported.

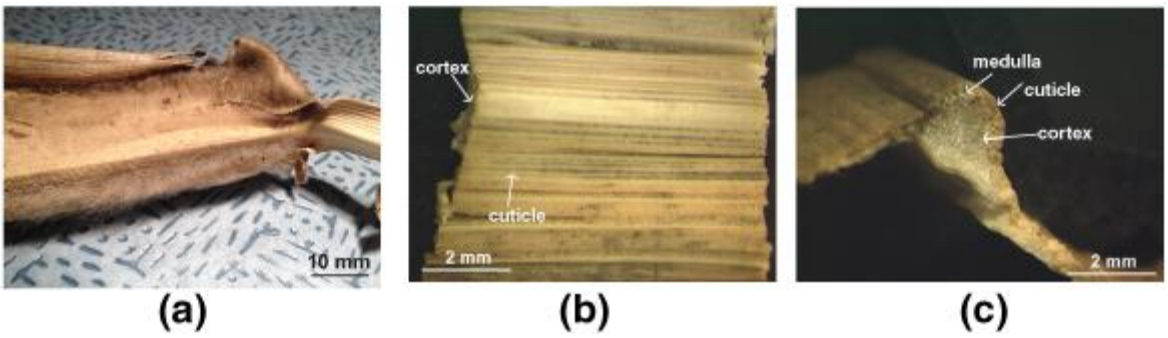

Figure 57 ASPROS (a) bast section, (b) longitudinal section macrograph 50x and (c) cross-section micrograph 50x

Moreover, the leaf tissue was found in both MH specimens, which were distinguished by the water and nutrients conducts (vascular tissue) size, since they change during the maize plant growth [107]. Though the similarities, MASH could not be paired against the machine-picked ones because of the sulphurated pre-treatment they were exposed, leaving only ASPROS husk for the microscopies showed in Figure 58. The textured surface (dermal tissue) shapes the husk, so it folds and protects the maize ears against bugs and plagues (Figure 58(a)), its length may vary 20-40 % depending on the maize landrace. Augusto et al. [196] highlighted MH's resistance to strain lengthwise, demonstrating MH’s length increases proportionally its strength. Both specimens showed fungi spots, some of them developed with ambience moisture, but after did not affect the extractions procedures.

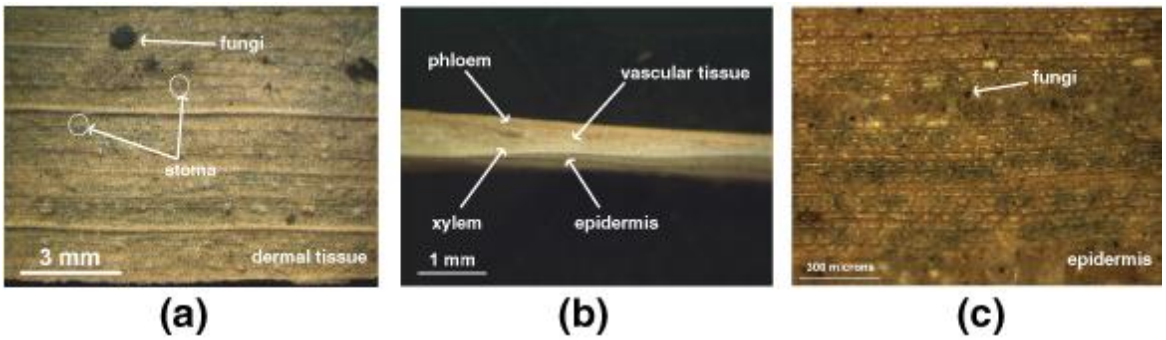

Figure 58 ASPROS husk tissue surface 50x (a). MH tissue cross-section 50x (b). epidermis close-up 200x (c)

The two husk types showed significant surface differences (Figure 59). ASPROS shows a more solid structure wood-like (a) and evident stomas (pores), what leads to

the assumption that the plant grew in a warmer climate than the MASH samples. On the other hand, MASH's almost uniform surface (b) presented slightly embedded aligned fibres with a linear pattern, resulting in a softer and mouldable layer. It also had a considerably higher presence of trichomes.

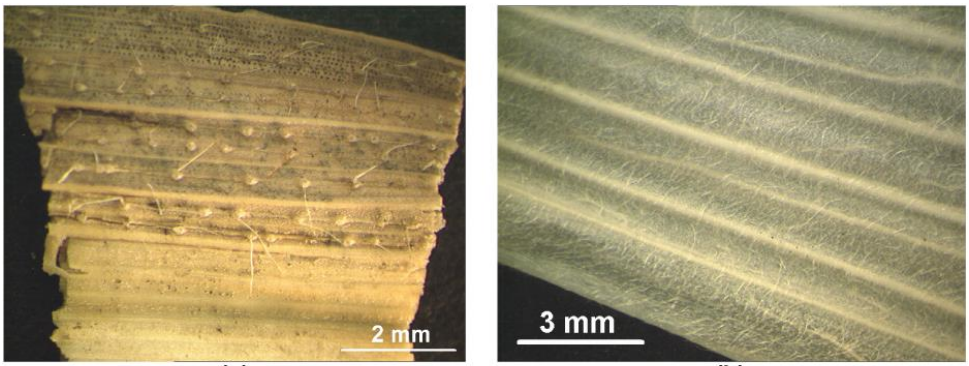

Figure 59 ASPROS (a) and MASH (b) husk vascular tissue, macro 50x

Furthermore, the MHF's morphological structure was also studied at a microscopic level so the differences between tissue and bast cell structures. ASPROS bast sample showed a uniform surface and a structure of aligned fibres. The elementary fibres were embedded into the cellulose interphase, that can be identified by the small white dash-shaped spots (Figure 60(a)). The bast in comparison with the leaf cellular arrangement has in both MH types visible aligned fibre bundles. Though the length of elementary fibres remained unknown as they were partially folded, in contrast to Figure 60(b) shows a rougher and sinuous surface remained.

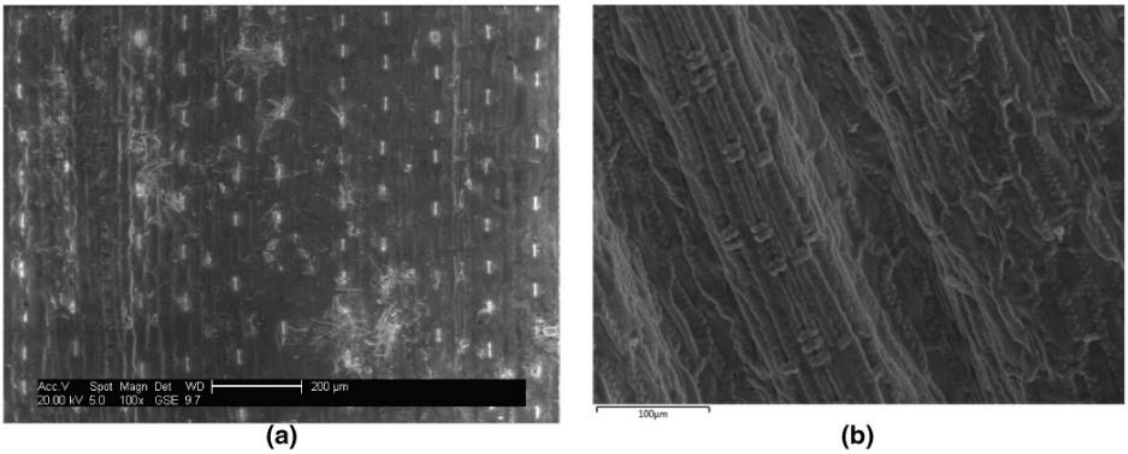

Figure 60 MHF's cell arrangement as per tissue type: (a) ASPROS AR bast tissue ESEM micrograph. (b) ASPROS AR leaf tissue ESEM micrograph

The morphological variation was observed along individual fibres, from both MH types. In the micrograph Figure 61(a) it is possible to identify the cellulose walls (B) and a section where the fibre bundles arrangement is perceptible (A). Figure 61(b) shows a very coarse and uneven surface (D), and the presence of several trichomes randomly distributed (C). This particular arrangement confirms that the ASPROS fibre bundle is made of many individual cells arranged in straight parallel lines, same that could benefit when mixed with a binder.

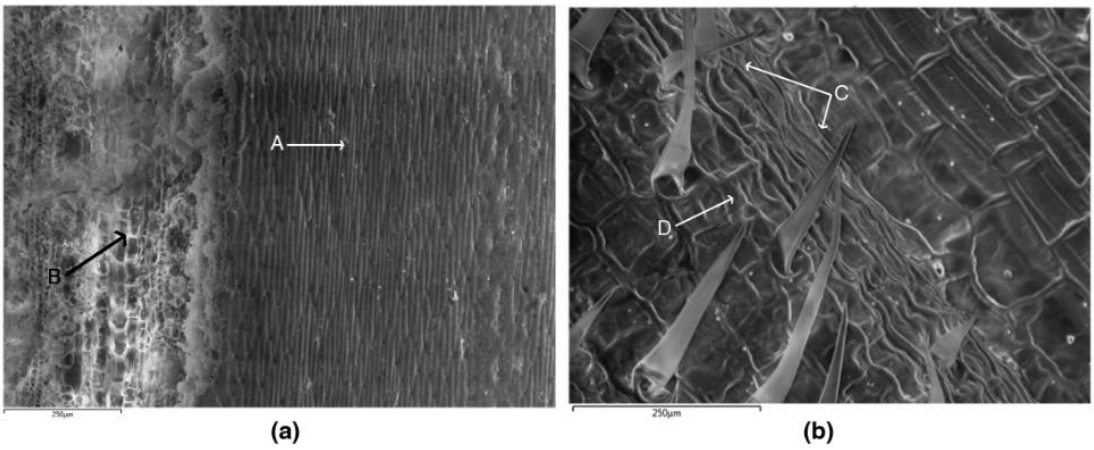

Figure 61 ASPROS husk AR morphology (a) detail husk edge and (b) surface detail

4.2.1 Maize husk chemical composition

The physical characteristics of both husk types are believed to be suitable as a composite reinforcement. Thomas et al. [195] stated that the mechanical performance of natural fibre is directly related to its cellulose content, microfibrillar angle and its polymerisation degree, where the latter is determined by the section of the plant where fibres are obtained. Therefore, to confirm and compare ASPROS and MASH proportions an elemental analysis was performed.

The element analysis results shown in Table 23 indicate a considerable increment of silicon (Si), especially in the ASPROS sample. Thus, Si presence may affect the future extraction treatments and even the matrix bonding [197].

Table 23 ESEM Element analysis of husks AR

		C	O	Mg	Si	P	K	Ca
A-AR	wt.%	24.23	53.62	-	21.71	-	0.45	-
M-AR	wt.%	37.41	49.03	0.35	9.79	0.48	2.05	0.88

4.2.2 Length

The ASPROS specimens were significantly more torn and damaged than the MASH batch as Figure 56 illustrates, a consequence of the harvesting processes, previously detailed in section 2.3.2.

Overall, Table 24 results indicate that MASH had a constant in length, whereas ASPROS batch variation was of 31 %. The husks width was found to be very irregular in both sources with a difference of 84%. Confirming the expected discrepancy in the ASPROS batch, but it also demonstrates that despite the different collection method, the MH size cannot be standardised as with any NF.

Table 24 Length and colour of studied husk batches

Sample	Colour		Mean (mm)	SD *	Min (mm)	Max (mm)
ASPROS	Greenish	Length	181.1	2.8	140.8	225.2
	- yellow	Width	67.4	1.9	40.4	99.8
MASH	Yellowish-	Length	238.8	1.5	214.1	267.4
	white	Width	123.2	2.8	76.8	160.1

* standard deviation

4.2.3 Maize husk fibre cross-sectional area

The study of natural fibres has helped to develop alternative techniques to measure their properties, this because of the wide range of variables characteristics when compared to their synthetic counterparts. Therefore, Thomason and Carruthers's [174] methodology was followed so the MH cross-section variation could be reduced, thus the following calculations (UTS, elongation % and *E*).

Figure 62 shows cross-section images obtained from both MH types, where the expected irregular cross-section area (CSA) is visible. Thereby, fibre shape was outlined as a visual aid to understand better its complex morphology [174]. During fibre assessment, some structural similarities between both husk types were spotted, i.e. the presence of lumen, microfibrils, bonding materials (A) (Figure 62), external impurities (soil), and in both cases signs of fungal attack. ASPROS husk flat-broad shape is similar to the cotton fibres [93]; whereas MASH fibre has a trilobal shaped bundle, closer to the polyester fibres [198]. Even though both MH types were

obtained in the same region, their physical inconsistency was proven and analysed, so its interference on the mechanical properties could be detected.

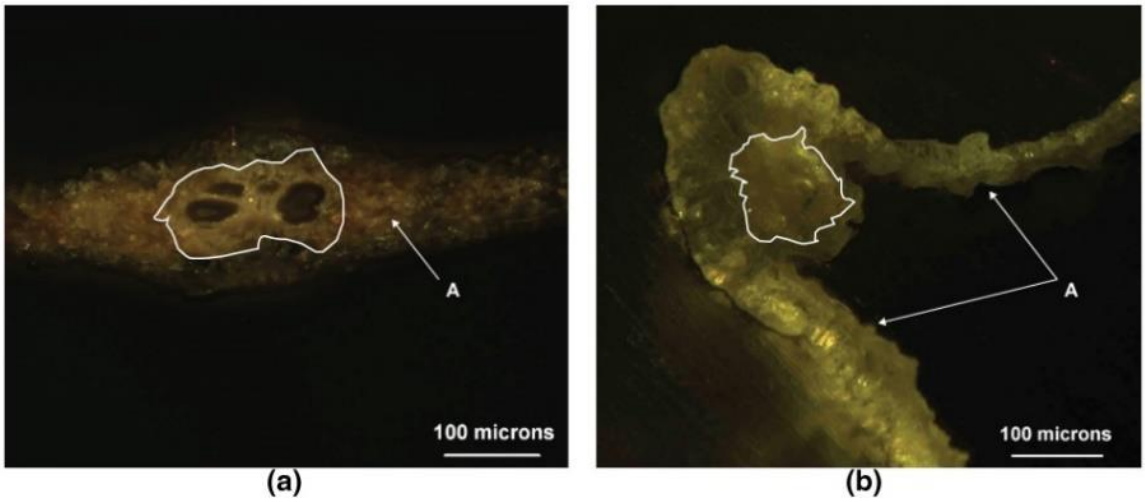

Figure 62 Micrographs of MHF CSA area. (a) ASPROS husk and (b) MASH outlined calculated CSA area of the fibre bundle

Both MHF types showed an irregular cross-section all along of the fibre' length and with a much greater fibre thickness variation. Thus, elliptical and circular models were used and compared to pinpoint the most suitable geometry for the CSA calculations in the studied specimens (Figure 63).

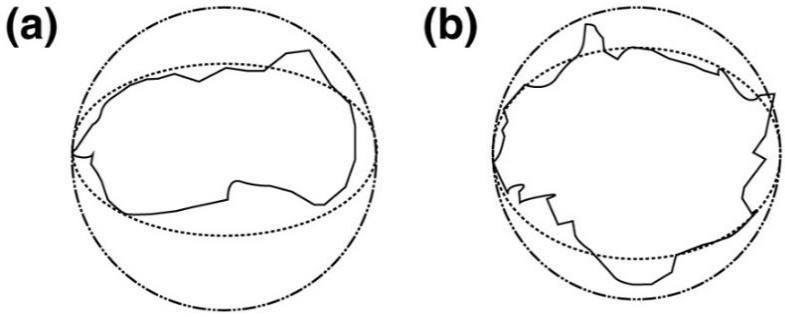

Figure 63 MHF CSA comparison of the ellipse and circular models. (a) ASPROS fibre and (b) MASH fibre

Table 25 displays the results from each fibre measured by both husk types. Based on methods applied to natural fibres [139,174], both geometries were calculated under the assumption that fibre's cross-section is either circular or elliptical, then compared to each other.

Table 25 Results of MHF CSA average from elliptical and circular systems

Specimen	Elliptical model	Average (mm^2)	SD	Circular model	Average (mm^2)	SD
A-AR		0.047	0.043		0.054	0.045
M-AR		0.937	0.594		1.291	1.428

Figure 64 ASPROS samples show a scattered distribution; however, even though both models have almost same statistical accuracy measuring the CSA. Whereas MASH-AR husk (Figure 56) presented a more uniform trend, pointing out the elliptical model as the best fit for these MHF type.

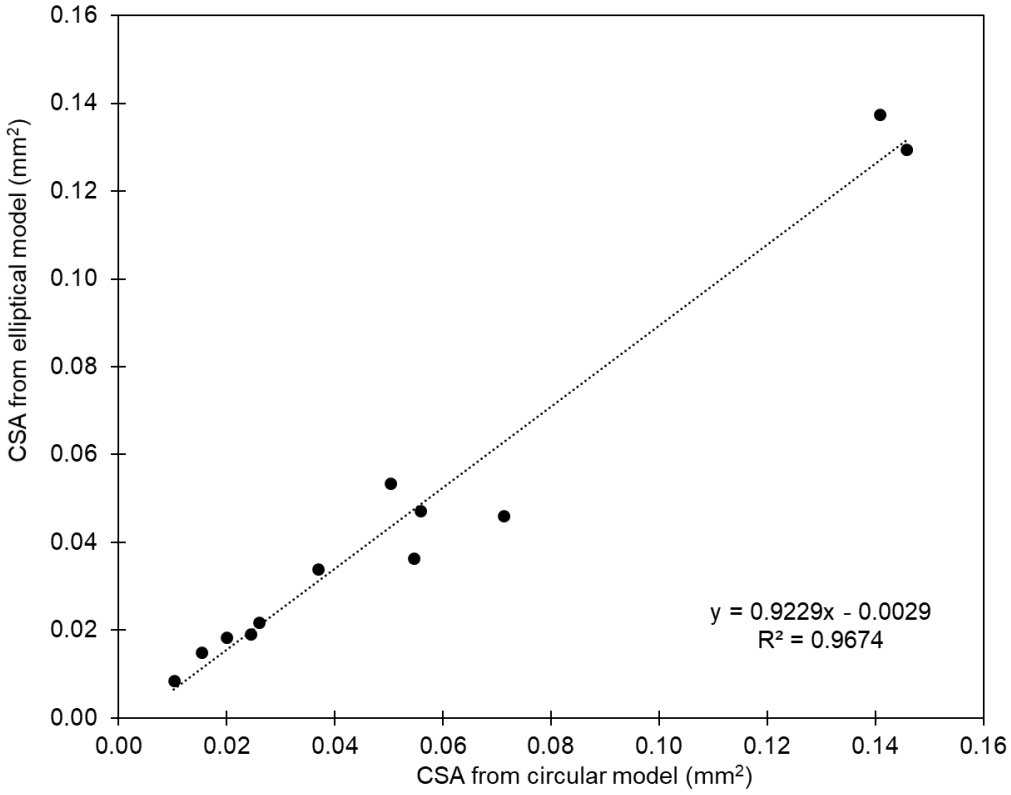

Figure 64 A-AR CSA from elliptical versus circular model

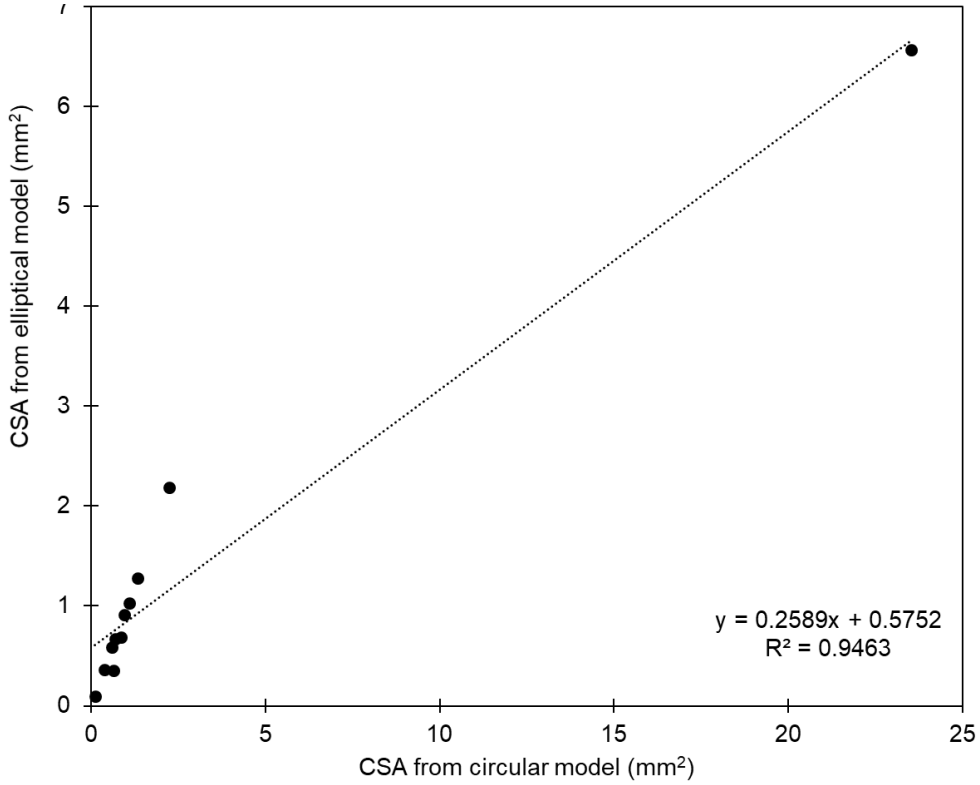

Figure 65 M-AR CSA from elliptical versus circular model

4.2.4 Maize husk moisture content

The MH moisture content in both ASPROS and MASH samples fell into the average ranges expected for an NF. For instance, the most commonly found in the literature were maize 9 wt.%, bamboo 9.16-10.16 wt.% and banana 10.71wt.% [110,124]. As shown in Figure 66, ASPROS husks with 10.3 wt.% reached its moisture equilibrium of water loss after six hours; whereas, MASH husks with an initial 8.6 wt.%, reaching equilibrium one hour faster than the other MH samples tested.

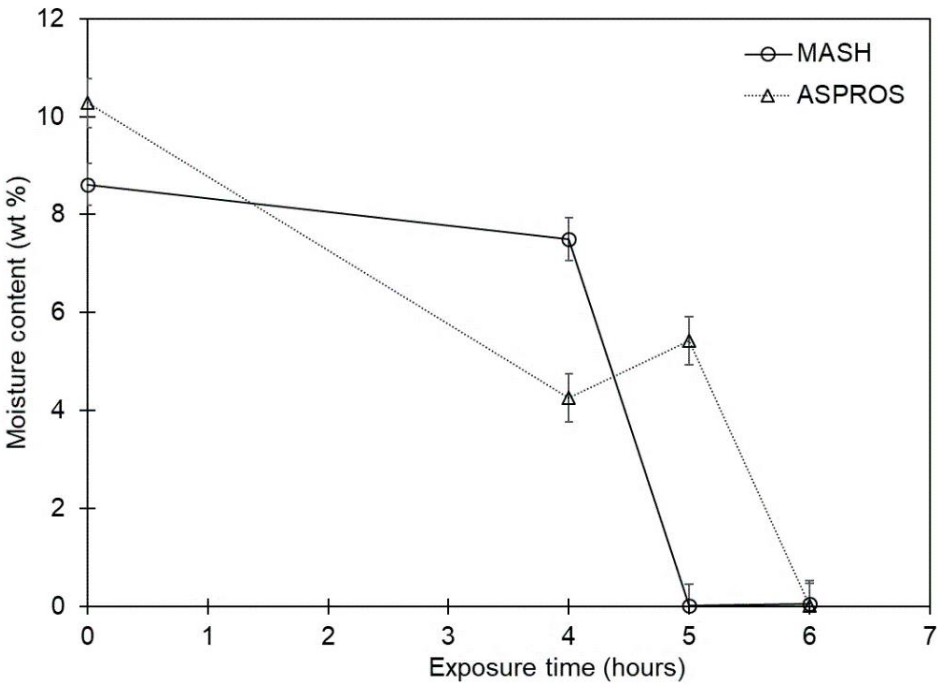

Figure 66 ASPROS and MASH husks wt.% of moisture content loss

4.3 Maize husk size reduction

MH as all natural fibres present significant variations; e.g. composition, length, and surface. However, the fibre quality and yield will still vary depending on the extraction method adopted. The MHF were obtained following three routes: chopped, milled and alkali (section 3.2.6); same that from now on will be assessed and compared to analyse and understand the implications of each method. It is important that before proceeding to an examination of the extracted fibres, the MHF morphology is fully understood, thence, any transformation can be spotted in the obtained results.

Therefore, the first micrographs were taken from raw specimens. Figure 67 shows a medulla of a 1/5 of the fibre' thickness (43µm). Corroborating the presence of xylem and phloem; thus, based on its shape a warm and dry environment of growth can be assumed [107]. Since these conducts manage plants' water and nutrient absorption, the levels of moisture content must be closely monitored during the fibre extraction processes to avoid the spread of fungi and fibre swelling.

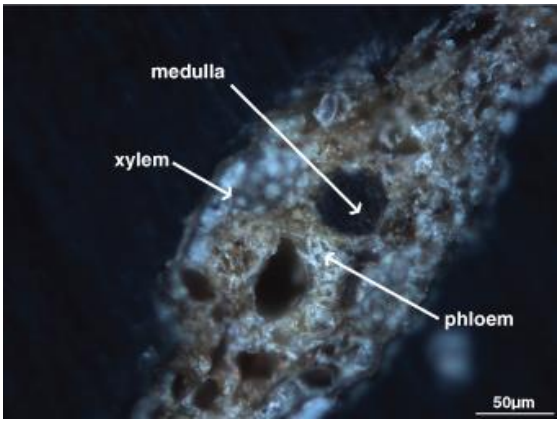

Figure 67 ASPROS-MHF AR cross-section optical micrograph, showing fibre' morphology

Moreover, the untreated MHF conductive tissue is held together by individual cells of cellulose, lignin, hemicellulose, pectin and waxes. Faruk et al. [110] among other authors contrasted the NF's chemical composition, proving NF' variability, however, MH was not considered. Carvalho et al. [196] have highlighted MH relevance and focussed on its possible scope within the NF. Thus, to place both MH types studied within the NF spectrum, both were analysed in the ESEM. Table 23 shows the elements found in the MH, same that can be observed as husk conjunctive layer (shaded area in Figure 68).

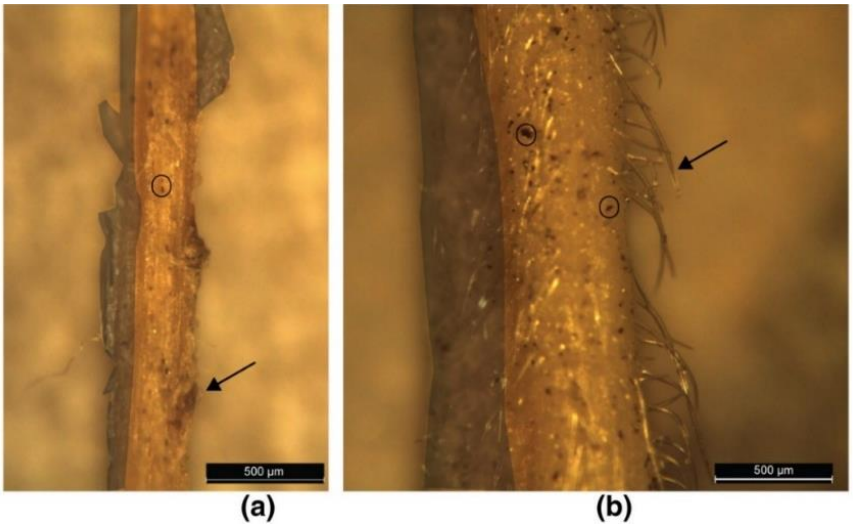

Figure 68 MHF optical micrographs (a) A-AR and (b) M-AR single fibre surface. The conjunctive tissue is the shaded area, the external elements circled (soil) and the arrows point out fibre's trichomes

4.3.1 Chopped

MH was trimmed to homogenise its size so that the composite compounding process could be more efficient as shown in Figure 69. Both husks types were cut into 30 x 30 mm, with a production rate of 2 kg/h approximately. Subsequently, the chopped MH was washed to reduce the presence of soil and other particles that might interfere with the bonding process between husk and matrix (section 3.2.4.)

Figure 69 Chopped MH (a) ASPROS, and (b) MASH after washing; still shows a pronounced ripple shape

4.3.2 Ball mill

The ball mill was used as an alternative method for the mechanical extraction; the aim was to obtain less rough fibres and ease the matrix/fibre blend. The trial was run only with MASH specimens, to measure its efficiency time and energy and certainly the fibre quality.

Figure 70 shows the MH before and after, where it can be noticed that the obtained powder surpassed the expected 0.4 mm fibre length, resulting in a 0.074 mm fibre length. This extreme reduction in the size of the raw material into dust and lack of a homogenous cellulosic material, as referred by Halvarsson [153], the MHF will require a considerable increment of binder presence needed to meet the basic fibreboard strength properties. In comparison to the other two mechanical methods tested (chopped and milled), the ball mill was discarded due to the elevated energy consumption.

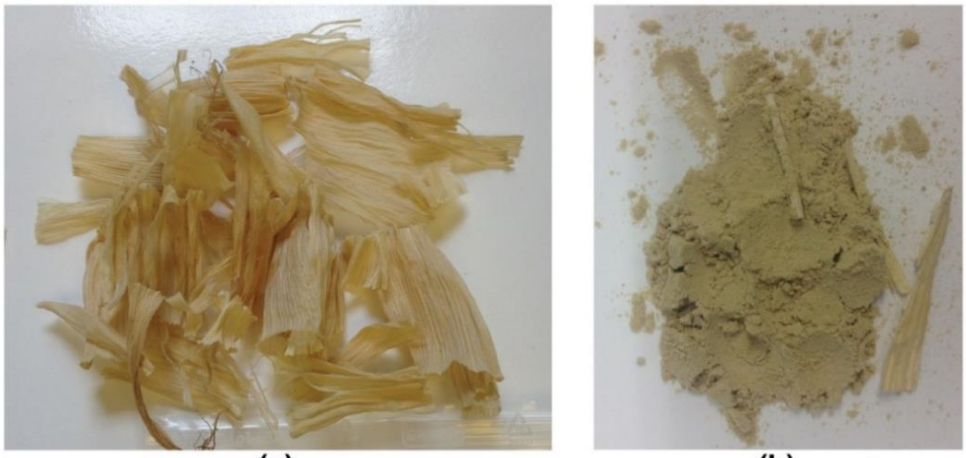

Figure 70 MH before and after ball mill. (a) MASH husk trimmed, washed and dried before going into the ball mill. (b) Pulverised husk after three hours in the ball mill

4.3.3 Milled

Mechanical extraction methods are considered to be the cheapest, mainly because is a straightforward technology and availability in comparison to the chemical counterparts [105]. Both MH types were processed in a conventional hammer-mill, in this way any differences such as fibre size, tensile properties and water content could be identified. From Figure 71 both husks seem very similar in size and physical appearance, though some effects of excessive mechanical stress were observed and will be detailed further ahead.

Figure 71 Milled MH batches (a) ASPROS, and (b) MASH after going through the milling process for 10 minutes at medium speed (25,000 RPM)

Figure 72(a) shows a clean and even extracted MH fibre bundle, nevertheless if the extraction process is too abrasive or not performed appropriately it will result in uneven surfaces and residues of cementing materials (hemicellulose and lignin) as it is shown in Figure 72(b) and (c). Similarly, curved bands split ends and fibre bundles spliced were also observed in the milled husks (Figure 72(d) and (e)). The presence of these defects represent a detriment in the fibres' overall mechanical properties, hence they will affect the final CM [199].

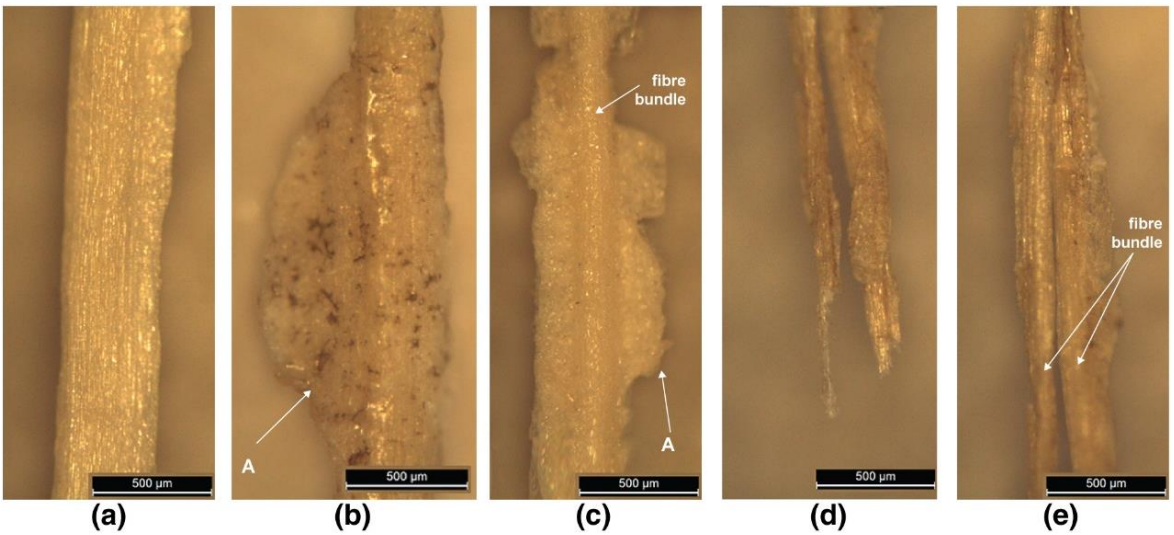

Figure 72 MHF milled optical micrographs showing diverse physical features: (a) shows clearly a fibre bundle, (b) and (c) are fibre bundles with some irregular non-cellulose material deposits, (d) split end frequently observed in both husk types ASPROS and MASH after going under the milling process; and (e) example of fibre bundles spliced due to excess of non-cellulose material

4.3.4 MH alkali extraction

The alkali extraction showed a slight effect on the MH breaks down into single fibre bundles when using NaOH the 5 % concentration. ASPROS samples demonstrated higher resistance to the alkalinisation as shown in Figure 73(a) and (b). However, as the caustic soda concentration and exposure time were increased as Reddy and Yang [96] did, the loss of the natural adhesive elements (pectin, hemicellulose and waxes) succeeded (Figure 73(d) and (h). It is worth to mention that MASH husks had a faster response to the alkalinisation, this is believed to be related to the previous treatment to they were subjected.

Figure 73 Visual guide of MH' physical changes after the alkalinisation process in both husk types, ASPROS top row and MASH second row, the samples code can be consulted in Table 13. The samples exposed to the lowest NaOH concentration were (a) A-AK01, (b)A-AK02, (e) M-AK01 and (f) M-AK02 A-AK03 for 60 min and 120 respectively. Husks exposed to a recommended concentration of 10g/l as follows: (c) A-AK03, (d) A-AK04, (g) M-AK03 and (h) M-AK04, for the same amount of time as the previous samples

The MHF extracted were observed in the ESEM to compare and assess their physical structure and overall conditions as a composite reinforcement according to the literature reviewed. Other authors (Reddy and Yang [96]) have taken a different approach by focussing on MHF's viability in automatic processes, however, they were found to be too small (2-20 cm fibre length) to be employed in textile-related. On the other hand, MHF size and structure be closer to those wood-sourced fibres used the manufacture of fibreboards.

Moreover, as it can be observed in the micrographs series bellow (Figure 74) MHF' surface morphology had significant changes after the alkalisation. Both husk types

extracted fibres had a consistent presence of trichomes (1) along the fibre before the NaOH exposure as shown in Figure 74(a) and (c). Albeit the alkalinisation was performed to make smoother and more uniform the MHF surface, MASH fibres (Figure 74(b)) lost most of its trichomes (1), yet its surface remained irregular in some areas. In Figure 74(d) ASPROS fibres show a more dramatic transformation, loss of all trichomes (1), a uniform surface smoothing (3) and even an unexpected fibre bleaching. Moreover, both husk types showed a unit cells reorganisation, thus a high delignification and foreign elements (soil residues and fungi) wash off can be assumed.

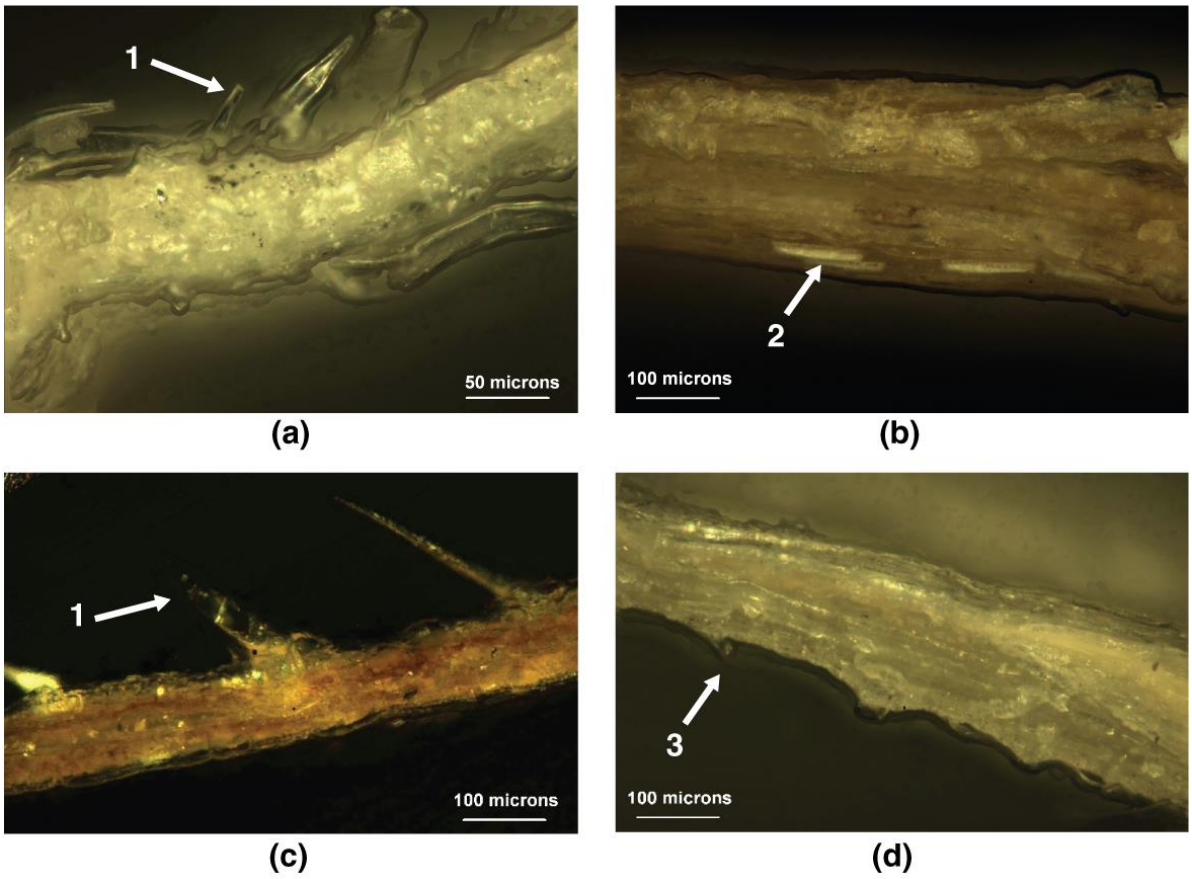

Figure 74 MHF optical micrographs of fibre surface before alkalinisation (a) MASH and (c) ASPROS, where it can be seen the natural fibre morphology with the presence of trichomes and other non-cellulosic elements. (b) A-AK04 and (d) M-AK04 fibres after a 120 min 10 g/l of alkali treatment, showing significant structural changes and loss rearrangement of individual elements

Taking a closer look at Figure 75(a) shows an ASPROS MHF that preserves its vascular tissue (xylem) and a strong bundle of fibres ; in comparison to sample A-AK04 (Figure 75(b)) that exhibits substantial variations in the cell arrangement after being exposed to a higher alkali concentration, leaving MHF's exposed, degummed and hollow.

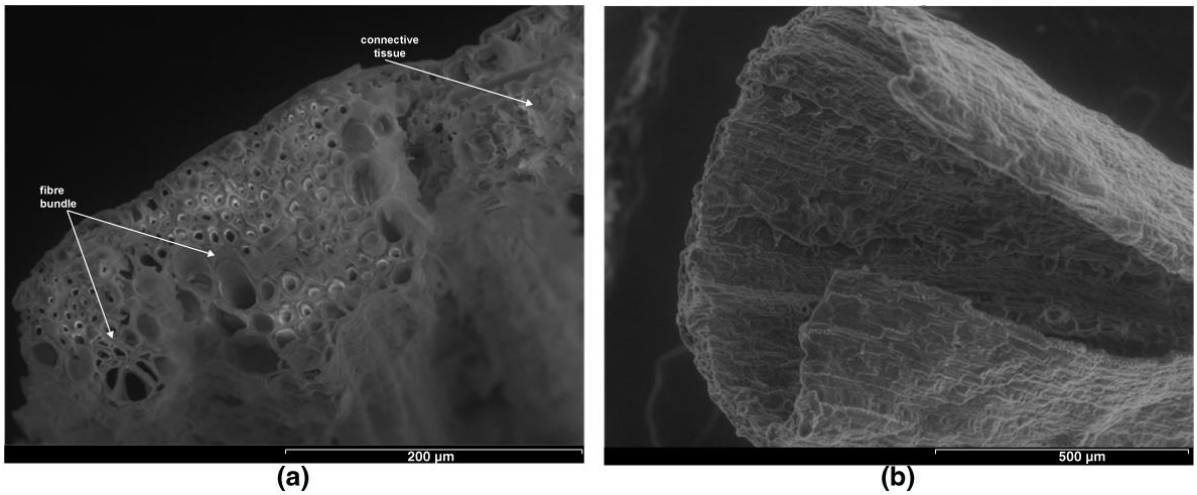

Figure 75 ESEM micrograph comparison of CSA' ASPROS fibres alkali extracted bundles at different concentrations, (a) sample A-AK02 (5 g/l NaOH/ 120 min), and (b) sample A-AK04 (10 g/l NaOH/ 120 min)

4.3.5 Enzymatic extraction

Previous studies of MH fibre extraction have demonstrated that the enzymatic treatment on its own is not capable of penetrating MHF surface; Therefore, an alkali extraction process had to be performed previously to the enzymatic exposure (section 3.2.6.5). The enzymes mainly helped in the removal of the coarser and smaller fibrous parts left after the alkalinization; just they did in Reddy and Yang's [96] tests. As a result, the bast pieces were softened, yet some sections were found to be more resistant to the NaOH as shown in Figure 76.

Another characteristic to be taken into account in the enzymatic extraction, besides the manufacturing costs, is the feasibility, in the case is to be used on a bigger scale. Especially because of the supplies and machinery scarce availability in some areas.

Figure 76 ASPROS husk slurry obtained from alkalinisation, showing remnants of bast structure and some fibre bundles still attached

Figure 77 contrasts MASH AR fibres (a) to one after the enzymatic extraction (b). Where MHF has a smoother surface, yet it does not show clear signs of fibrillation despite being exposed to both extraction methods (alkali and enzymatic).Thus, it can be deduced that the enzymatic concentration was not enough for these maize fibres.

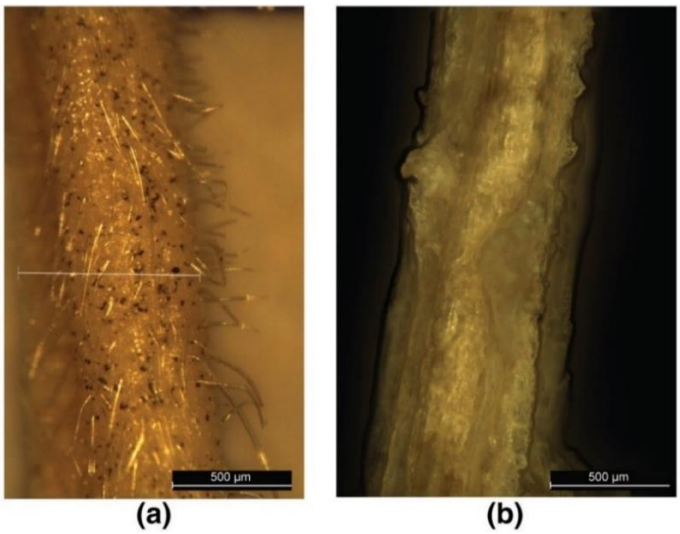

Figure 77 MHF optical micrograph fibre morphology in a longitudinal view: (a) A-AR displays a fair amount of trichomes, external residues, i.e. soil (black dots) and reinforcing elements. (b) M-AZ01 fibre showing visible changes on the surface (trichomes, waxes and non-fibrous tissue subtraction); the fibre structure is now visible; some non-cellulose deposits are still present

Moreover, the purpose of the enzymatic extraction was to remove the bonding elements, allowing the release of hemicellulose and lignin that naturally occur in MH. As discussed by Baillie [106] such components can interfere in the matrix/fibre linking during the composite manufacturing trials. Thence, to make this clearer the grade of de-lignification in the MHF was not uniform, confirming Yilmaz et al. [158] results that in the MHF mechanical and strength properties will be reflected in the final MHC material.

Therefore, as evidence of MHF' surface topography after going through the enzymatic extraction, is Figure 78(a), where the MHF bundle has at least three single fibres clustered and twisted. Whereas, the MHF surface in Figure 78(b) does not show the same level of cellulose degradation as the previous one, even though they went through the same process.

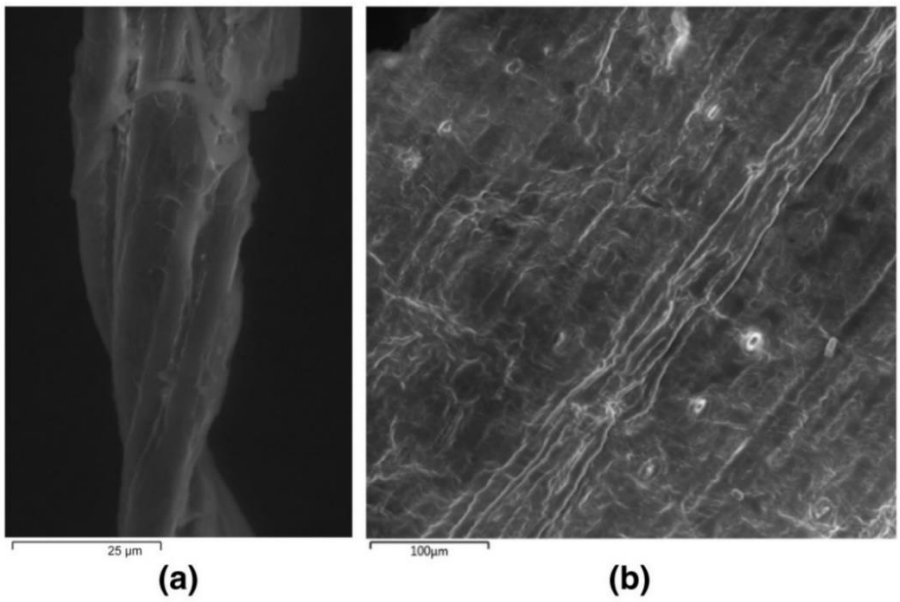

Figure 78 MASH husk ESEM micrographs (a) fibre bundle structure and (b) surface after enzymatic extraction

4.4 Tensile properties of maize husk

The tensile strength is one of the characteristics to take into consideration when working with NF, especially if it is going to be combined with other materials, e.g. oil-based resins, plastics or synthetic fibres. Henceforth, for the propose of this research

complete MH's tensile strength was tested, lest a thorough comparison with NF already applied in composite materials could be carried out.

Figure 79 shows ASPROS samples transversal breaking strength represents only 5 % of the longitudinal. Whereas MASH samples showed similar behaviour, yet the difference is not as significant as it was in ASPROS husks. Moreover, the apparent elongation percentage difference between both husks was not significative, therefore they are considered equal.

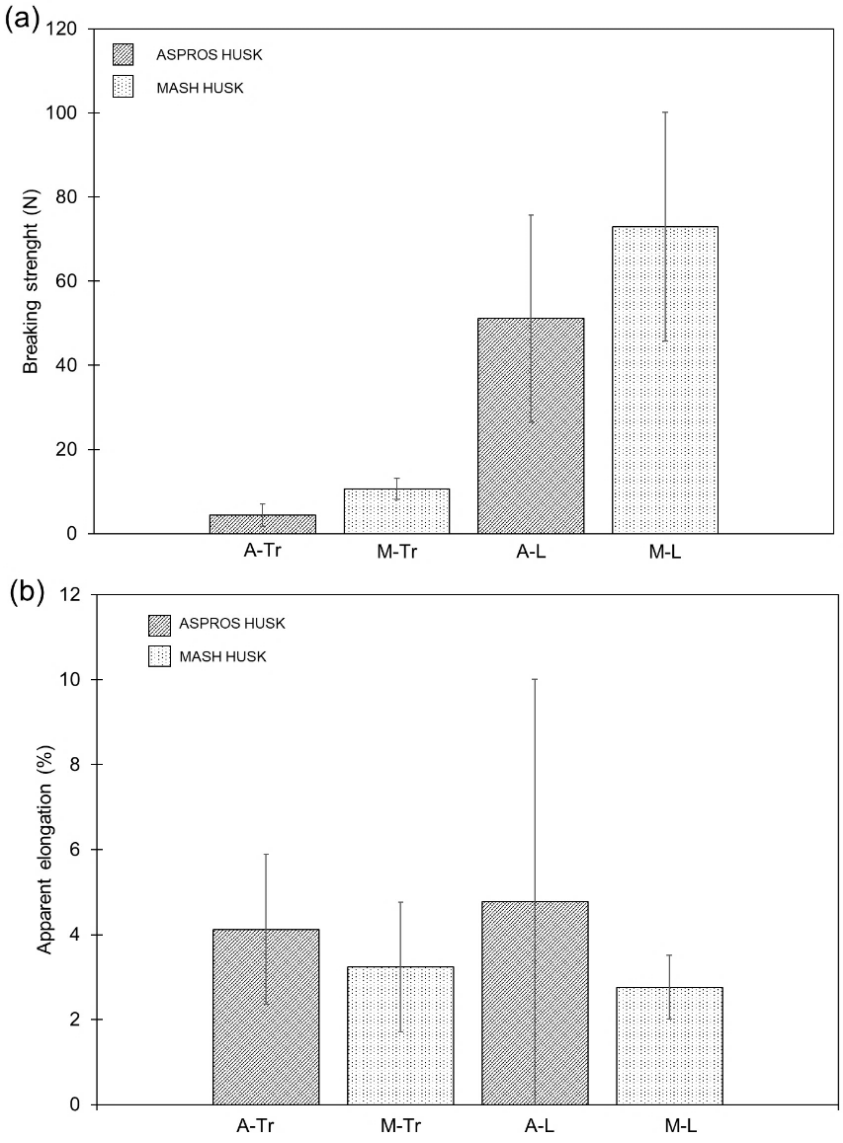

Figure 79 Results of MHF tensile test. (a) breaking strength and (b) apparent elongation percentage from both MH's types (ASPROS and MASH) in longitudinal and transversal directions

Table 26 shows the descriptive statistics for the breaking strength at the rupture of the MH samples. It can be highlighted, that both husks types showed a similar SD in both directions; whereas the longitudinal elongation percentage on ASPROS husk is considerably higher than those in the MASH samples.

Table 26 MH mechanical properties

	A-L		A-Tr		M-L		M-Tr	
	Mean	SD	Mean	SD	Mean	SD	Mean	SD
Breaking strength (N)	51.1	24.6	4.3	2.6	72.9	27.2	10.7	2.5
Apparent elongation (%)	4.7	5.2	4.1	1.7	2.8	0.75	3.2	1.5
Tensile strength (MPa)	/	/	5.7	7.6	/	/	2.7	1.5

4.5 Maize husk fibre mechanical properties

NF' mechanical properties can be identified according to their origin, the climate they grew in, plant age, and even the extraction method. Therefore, with all those variables present, it was necessary to run mechanical tests so MHF's features and capabilities could be clarified and compared.

Changes in thickness and mechanical properties per extraction method were compared using fibre samples from the first batch. Figure 80 shows an overview of 97 % variation on CSA between husk types and its changes according to the reduction process carried out. The MASH husk reported a significantly higher CSA (70 %) reduction than the ASPROS (48 %) samples; yet, ASPROS samples showed a greater SD throughout all the performed tests, especially in the milled husk.

Table 27 shows mean intervals of CSA, UTS, elongation at break percentage and Young's modulus (*E*) of both MH types used in this study. The 95 % confidence interval (CI) from the mean was calculated due to the significant variability observed in the results. Due to the lack of data on MHF in the literature review, it was essential to this study to carry out a single fibre test considering the obtained CSA approximations from both MH types (Figure 81, Figure 82 and Figure 83). Thus the mechanical properties were calculated with more accurately MHF's quality. The SD was considered too high in some samples from the same batch, highlighting MHF's expected in any NF.

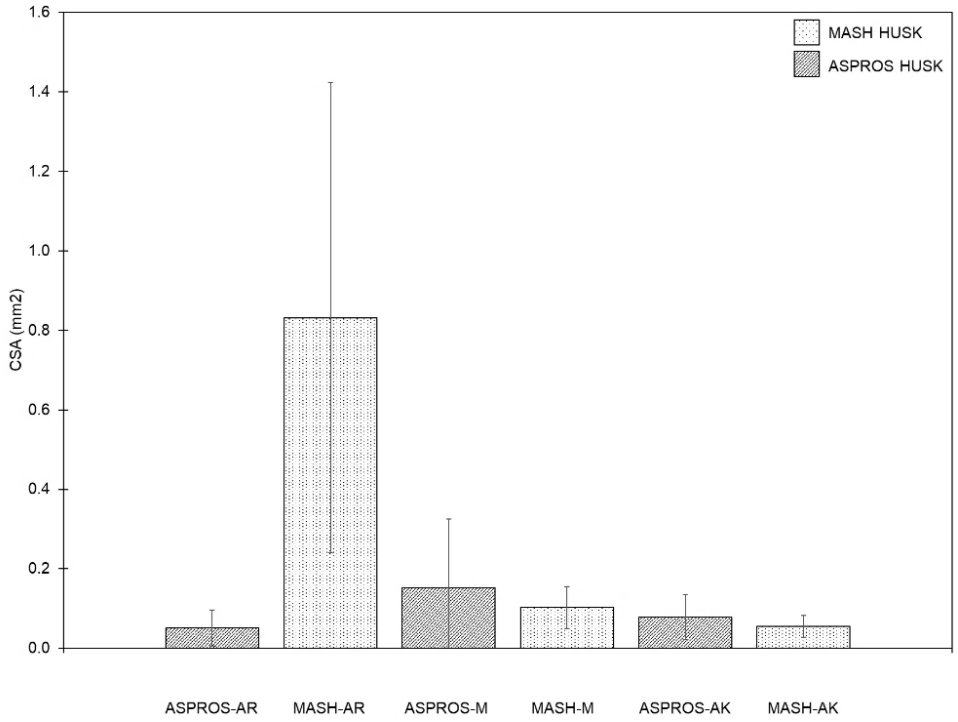

Figure 80 MHF calculated CSA per extraction process SD bars are given to show the variation range per each extraction process

Table 27 MHF obtained properties at a 95% CI

Type		**ASPROS**			**MASH**		
Size		As received	Milled	Alkali	As received	Milled	Alkali
CSA (mm^2)	Mean	0.04	0.14	0.08	1.30	0.101	0.050
	SD	0.04	0.16	0.05	1.80	0.062	0.020
	CI	0.017-0.072	0.033-0.237	0.047-0.112	0.139-2.376	0.068-0.138	0.036-0.067
UTS (MPa)	Mean	45.75	42.89	50.45	7.130	46.630	77.870
	SD	35.90	29.22	18.09	6.920	24.206	99.780
	CI	20.060-71.430	21.990-63.790	37.520-3.390	2.180-12.081	29.320-63.940	6.490-149.250
Elong. (%)	Mean	3.730	7.650	3.732	2.750	4.350	5.176
	SD	3.750	2.820	1.465	0.910	1.810	2.887
	CI	1.045-6.415	5.632-9.660	2.685-4.781	2.095-3.390	3.051-5.645	3.110-7.241
***E* (MPa)**	Mean	2.780	1.950	2.990	0.380	4.470	3.702
	SD	3.130	2.205	1.00	0.270	8.490	5.110
	CI	0.549-5.030	0.378-3.521	2.277-3.701	0.190-0.573	-1.598-10.547	0.047-7.359

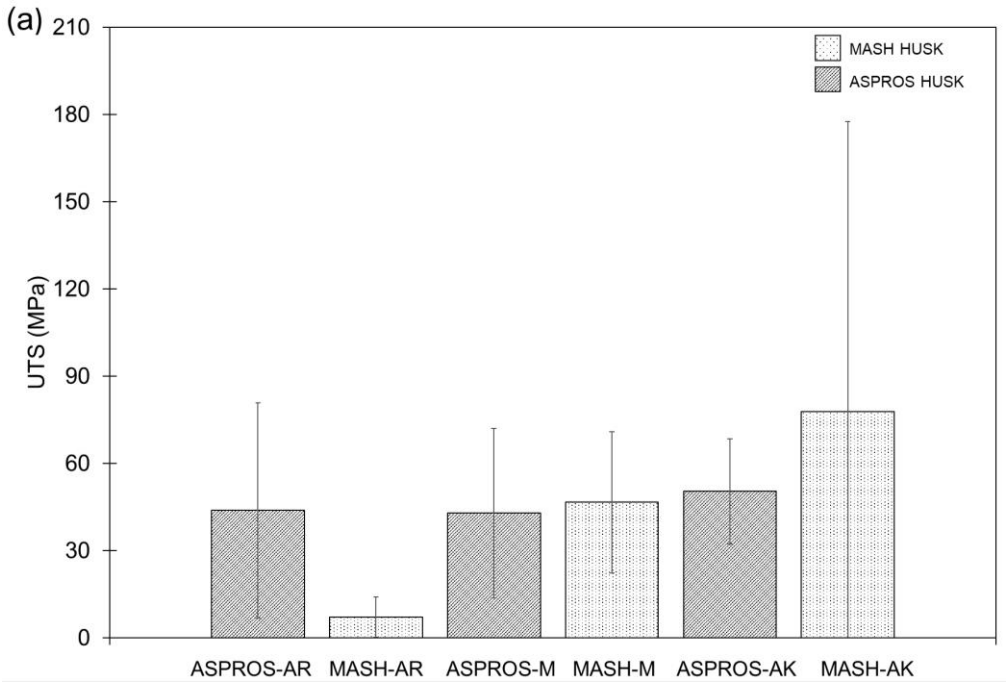

Figure 81 MHF tensile properties ultimate tensile strength. Error bars are given to show how properties may vary from each process

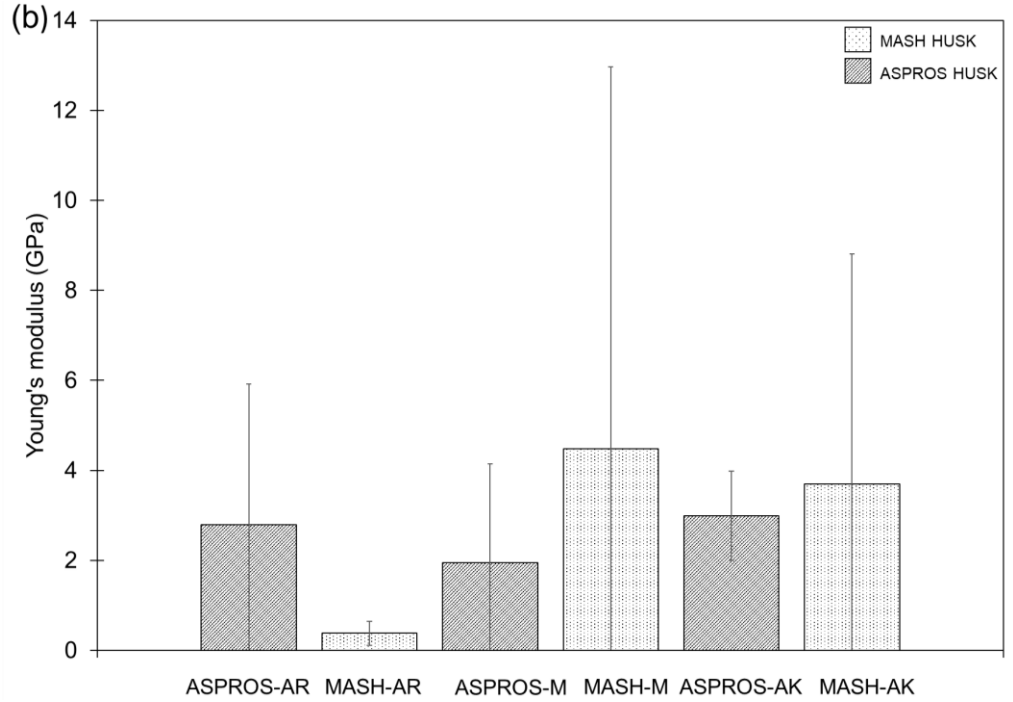

Figure 82 MHF tensile properties *E* modulus. Error bars are given to show how properties may vary from each process

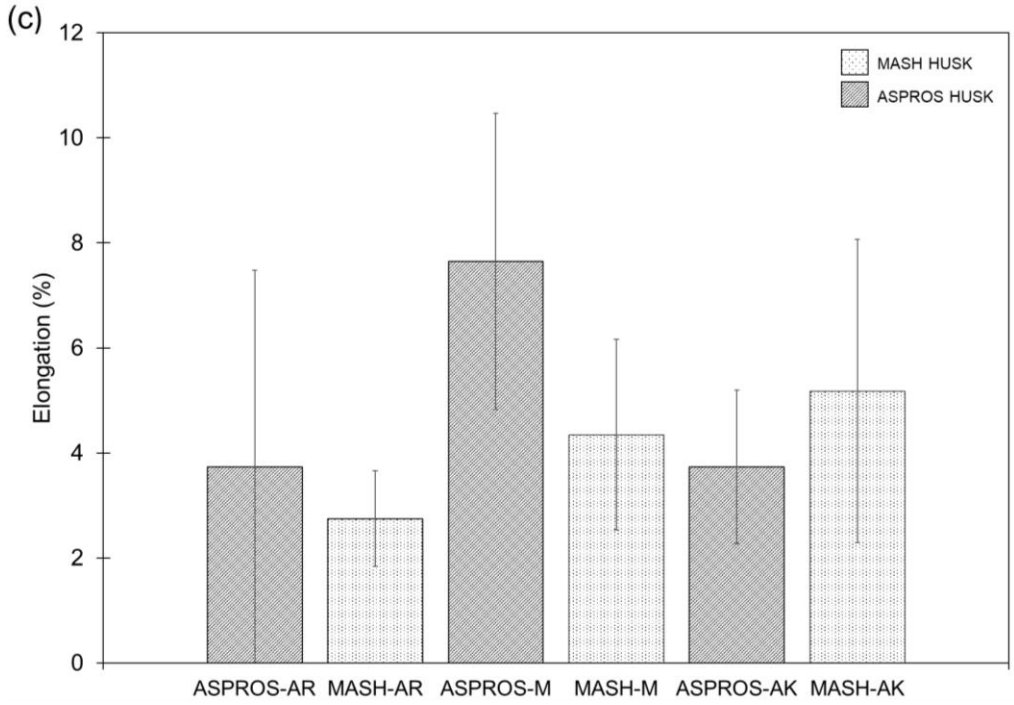

Figure 83 MHF tensile properties elongation percentage as per extraction process. Error bars are given to show how properties may vary from each process

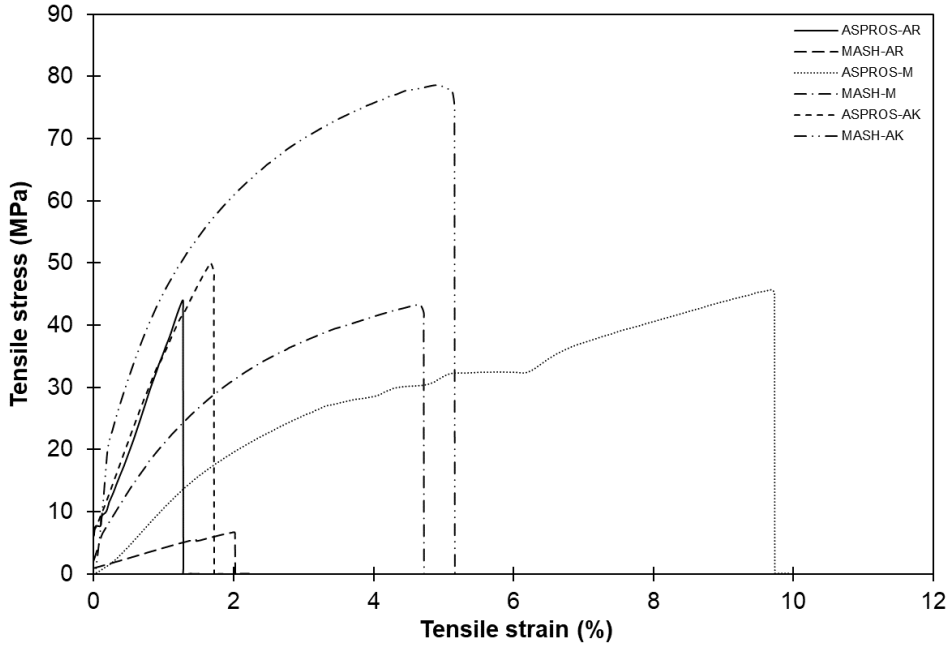

Figure 84 Tensile stress vs tensile strain for tested MHF from different extraction processes

From the conducted tensile test MHF the mean of the strain/strength behaviour in each size reduction method (AR, M and AK) were used as the graph below shows (Figure 84). From which, MASH-AR samples showed an exponential increment in both tensile strength and strain, while the alkali extracted samples showed the highest tensile strength. As to ASPROS fibres, tensile strength remained steady, however, the highest elasticity percentage was presented in the sample ASPROS-M.

4.6 Maize husk-based composite boards manufacturing

Fibreboard manufacturing process was examined from a broader perspective, this to ensure that the whole productive cycle falls within SD guidelines and fibreboards standards as mentioned before. The process phases have been fully described in section 3.2.9 and depicted in Figure 85.

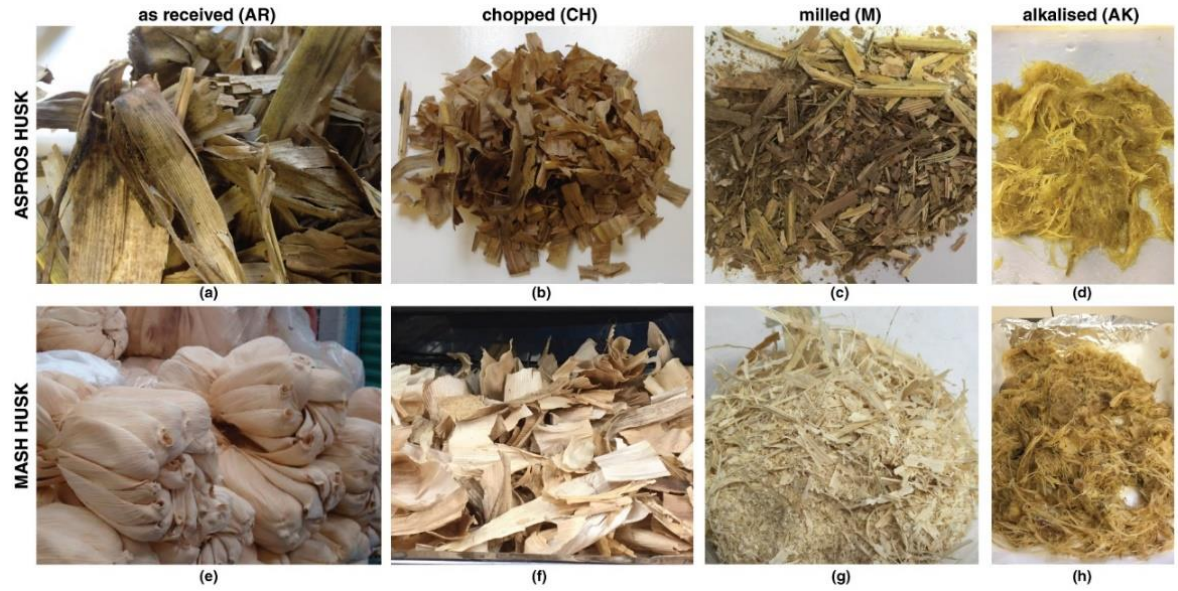

Figure 85 Husk sizes used in the MHC production, ASPROS samples are shown in the first row (a), (b), (c) and (d); and MASH samples in the row below (e), (f), (g) and (h)

Figure 86 shows the MHC manufacturing that begins with the raw material collection from freshly harvested fields (1) and its transportation to the transforming plant (2). Then, MH was reduced (3) within a length range of 0.5-30 mm to ease MHF handling, mixing and mainly to obtain the properties required for the board's production. Following the manufacturing process proposed in section 3.2.6, the reduced MH was soaked in water (4) to get rid of unwanted elements (soil, dirt, silicon residues, etc.). Though, in the case of a chemical extraction is at this point

where the NaOH is added to wash off cement compounds to get them ready for the subsequent steps. Next, all MHF was dried (5) before binder mixing (6) and composite compounding so that MHF could blend correctly with the three binders proposed. The mix was hot-pressed (7) to activate the natural MHF elements to react along with the binder and consolidate the MHC boards. Finally, the MHC boards were left to cool-down (8) to be later unmoulded and refined for the assessments and eventually select the most promising mix (MHF size, binder and manufacture settings).

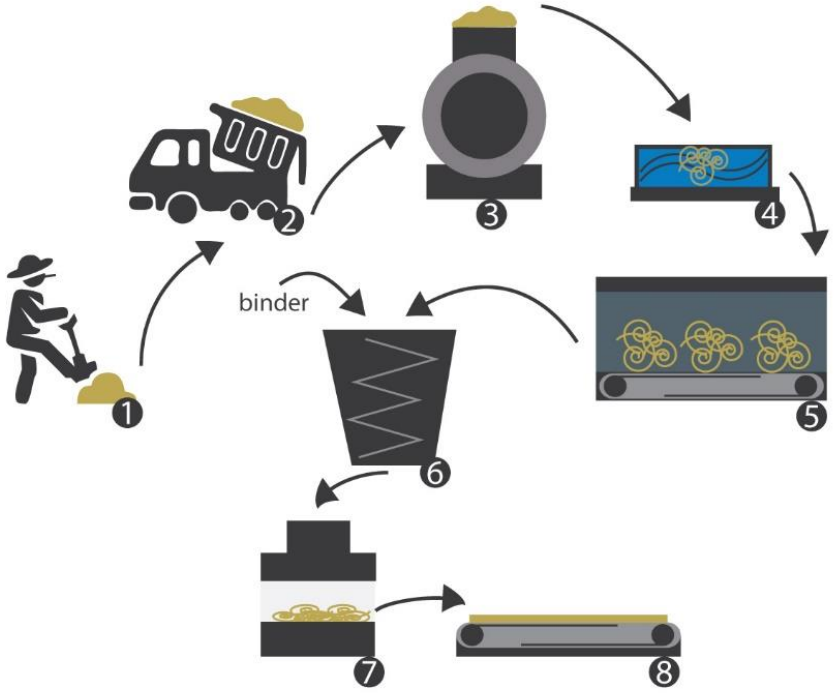

Figure 86 Lab scale MH composite board manufacturing process; (1) harvesting, (2) shipping, (3) size reduction (mechanical or chemical), (4) washing and (5) drying, (6) fibre/ binder impregnation, (7) mat-forming and hot pressing, (8) cooling and trimming

The MHF manufacturing process took the majority of the process from the wood-based fibreboard industry since it is one of the oldest CM mass-produced according to the Wood Handbook [165]. Thus, the hot-press has been the most recurred bonding method to produce composite boards; it was chosen as the main method to make the MH-based ones. However, binder preparation and fibre wetting had to be adapted to a lab scale and the various MH types and sizes (AR, CH, M and AK).

4.7 Maize husk composite characterisation

The data gathered from the selected samples were following standardised methods applied to commercial fibreboards as described in Table 28, mainly wood-based, e.g. light MDF and MDP. The MHC sample labels tested in this section can be found in Table 19.

Table 28 MHC first batch obtained features and selection tool

	MHC semi-static 3-point bend	**MHC wt.%**	**Selection tool**
Reference	ASTM D 1037-12 [176]	ASTM D1348-94 [173]	Pugh selection matrix [189]
Outcome	Density (kg/m3) FM (GPa) MOR (MPa) Stress-strain curve	Moisture content (%)	Quantitative and qualitative data
Sample size	123x51 mm	123x51 mm	19 blends and 2 commercial fibreboards
# per blend	3	3	/

Figure 87 shows Bs specimens' density and thickness comparison, where CHB-A samples were discarded on the basis of poor the structural conditions of the board, which showed a very brittle and uneven configuration. Moreover, the lignin bound boards (Figure 88) and the SSE-based boards (Figure 89) were also measured and compared.

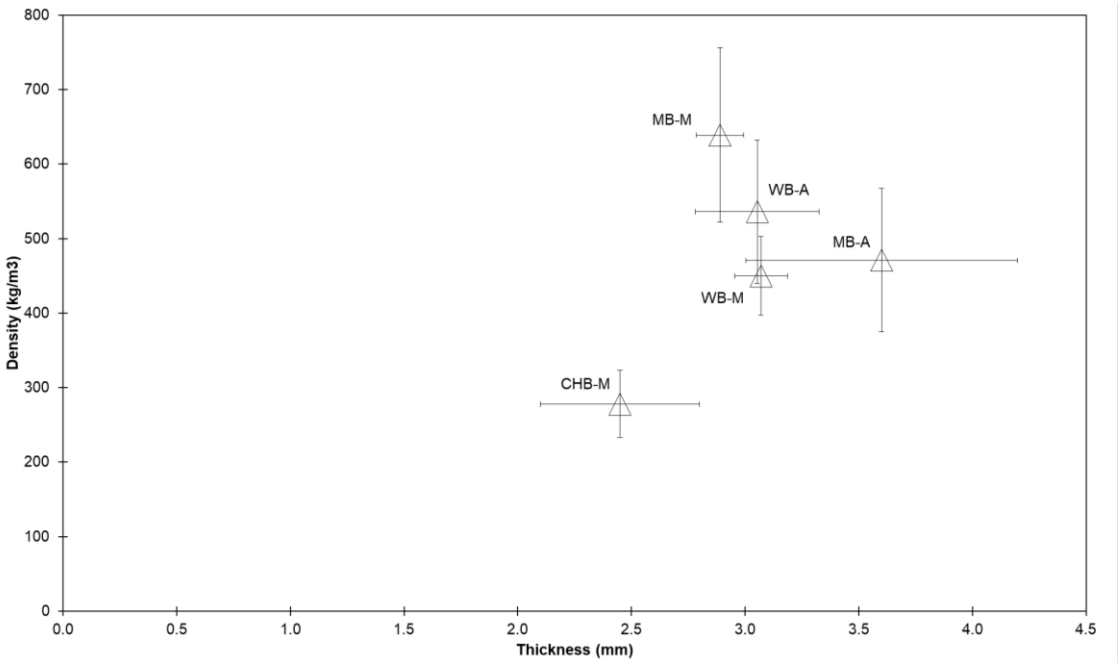

Figure 87 Binderless MHC boards density vs obtained thickness

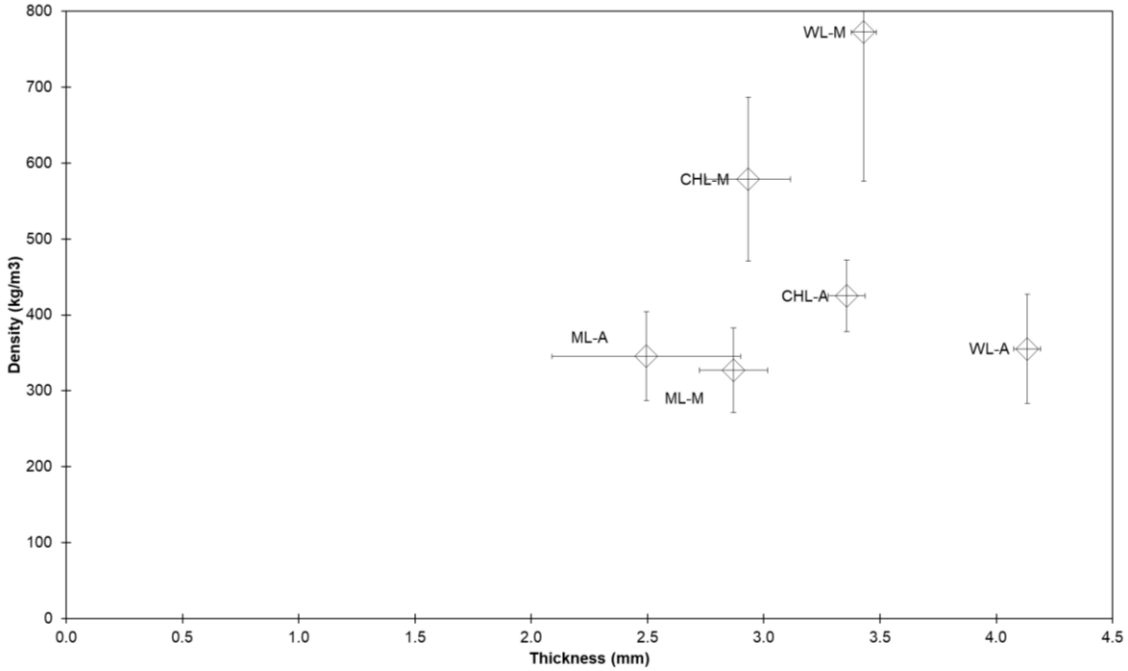

Figure 88 Lignin MHC boards density vs obtained thickness. SD is smaller than the markers

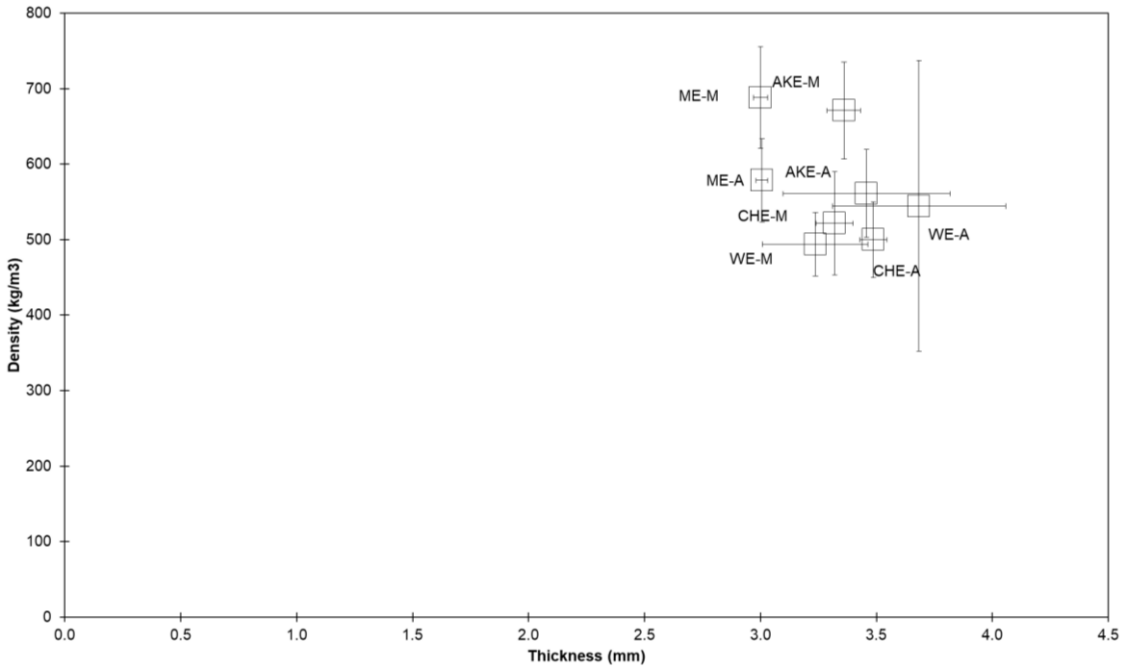

Figure 89 SSE resin MHC boards density vs obtained thickness. SD is smaller than the markers

The MH size affected the MHC boards features as discussed in section 3.2.9. Looking at Figure 90 it is evident that the ASPROS boards showed to be less dense than their pairs made with MASH husk, when attaining to some of the most commercial boards PB and light MDF with a density of 650 and 720 kg/m^3 respectively [200,201].

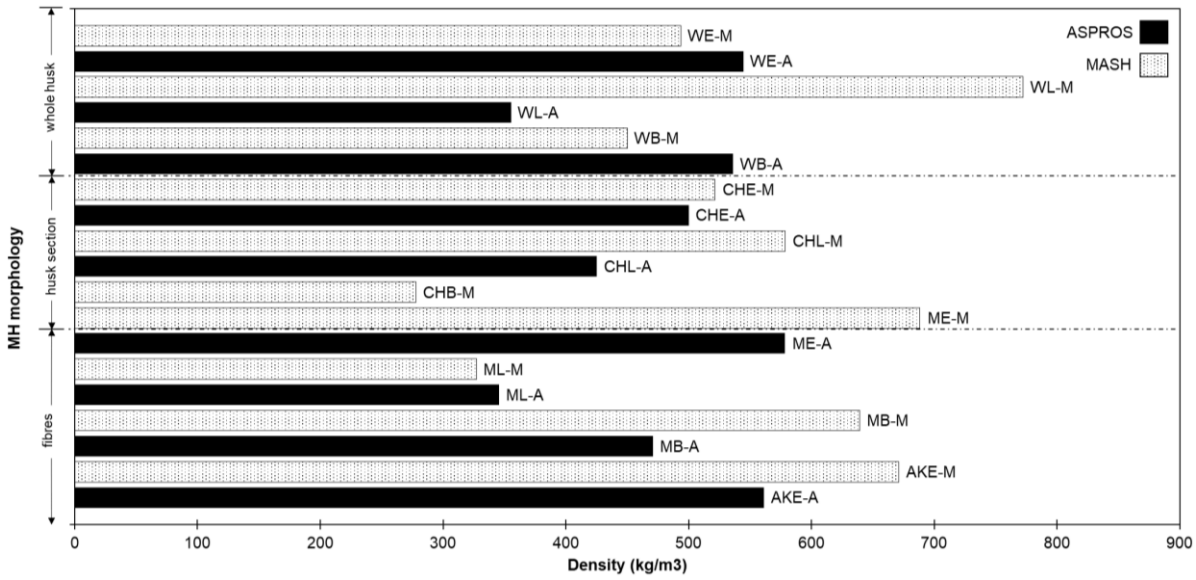

Figure 90 Classification of MHC boards by husk size, density and binder

4.7.1 Maize husk composite moisture content

Extraction methods and chemical surface modification of natural fibres, i.e. alkalinization [133], may affect their environmental moisture uptake. Hence, in Table 29, CHB-M, WE-A and AKE-M samples turned out to be the ones with a higher wt.% when left at ambient temperature conditions. On the other hand, CHL-A samples showed a 40 % less wt.% in comparison to WB-A, demonstrating the hydrophilic nature of the added lignin as Mathiasson and Kubát [188] reported. The table below shows the MHC boards divided per binder and husk type used; demonstrating a reduction of 34.5 % of moisture absorption in WB-A when the lignin was used (WL-A), whereas in MASH husk this percentage had a decrease of only 3.2 % from WB-M to WL-M. However, a rather interesting wt.% reduction was observed in the milled SSE-based specimens, specifically ME-A samples.

Table 29 Moisture content of the first batch MHC specimens manufactured

	ASPROS		MASH	
Binder	**Sample**	**Moisture (%)**	**Sample**	**Moisture (%)**
BS	WB-A	5.8	WB-M	6.1
	CHB-A	/	CHB-M	7.5
	MB-A	5.5	MB-M	6.0
L	WL-A	3.8	WL-M	5.9
	CHL-A	3.5	CHL-M	5.1
	ML-A	5.6	ML-M	4.9
SSE	WE-A	7.7	WE-M	5.5
	CHE-A	5.1	CHE-M	5.8
	ME-A	3.0	ME-M	5.8
	AKE-A	5.6	AKE-M	7.6

Moreover, in Figure 91, Figure 92, Figure 93, Figure 94, Figure 95 and Figure 96 provide a summary of the results for the wt.% in all the MHC specimens, apart from the alkali treated samples, these AKE-A and AKE-M boards reached their moisture equilibrium within 2 to 4 hours. Moreover, graph Figure 93 the sample CHB-A was not considered due to its lack of structural integrity to perform the test.

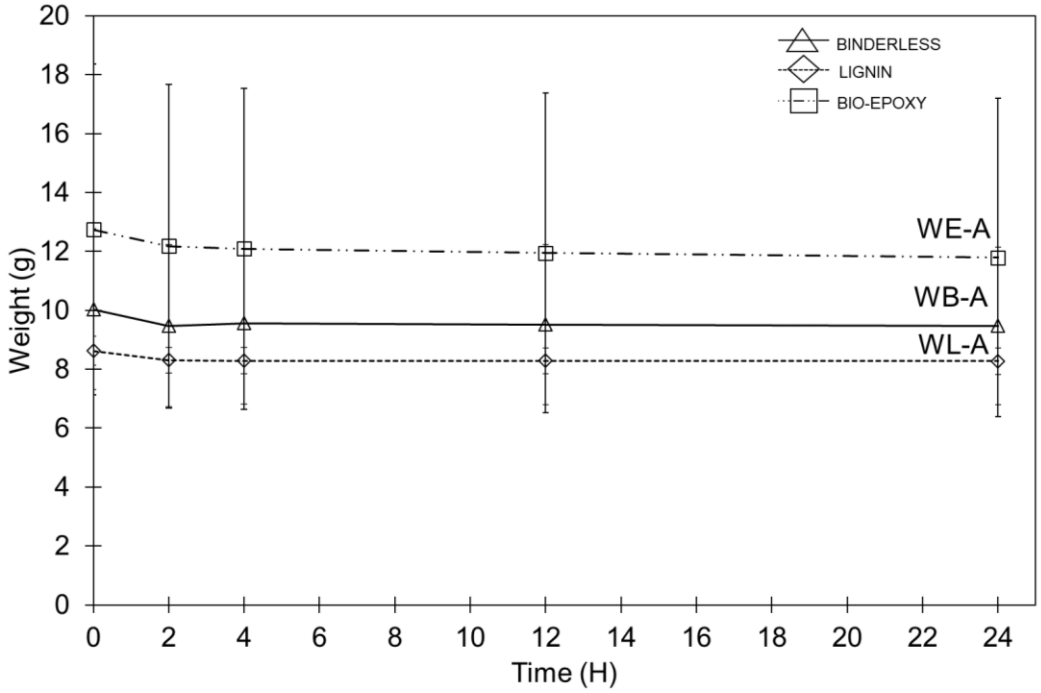

Figure 91 ASPROS whole husk comparison of wt.% loss in the different MHC, MH type and size, along with the three binders used in the specimen manufacturing

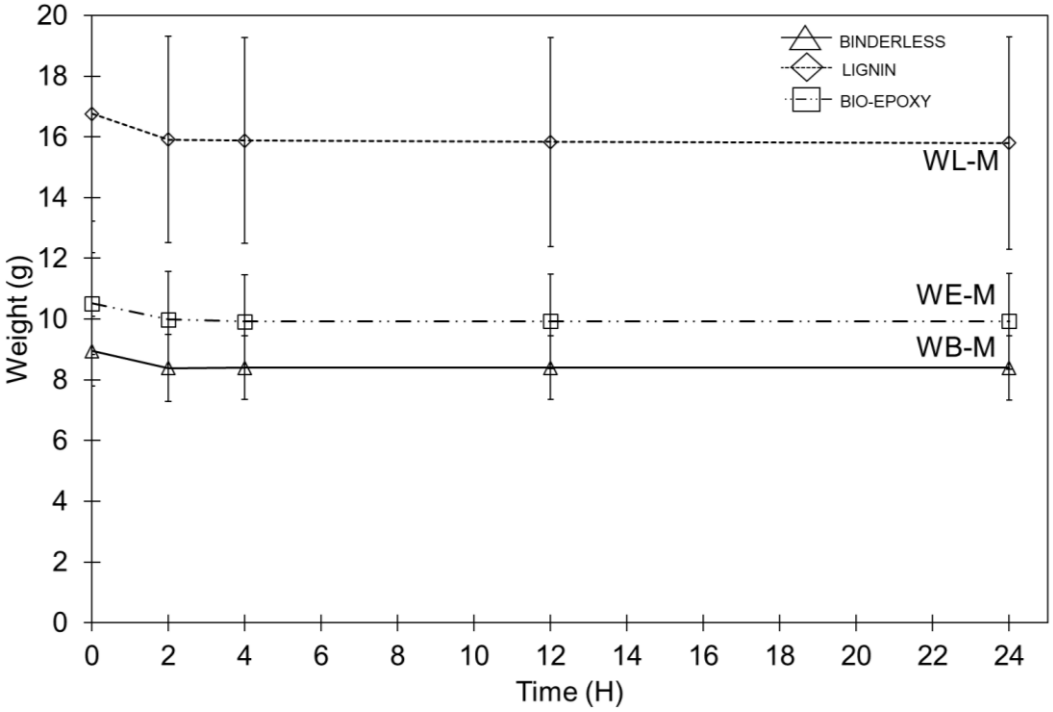

Figure 92 MASH whole husk comparison of wt.% loss in the different MHC, MH type and size, along with the three binders used in the specimen manufacturing

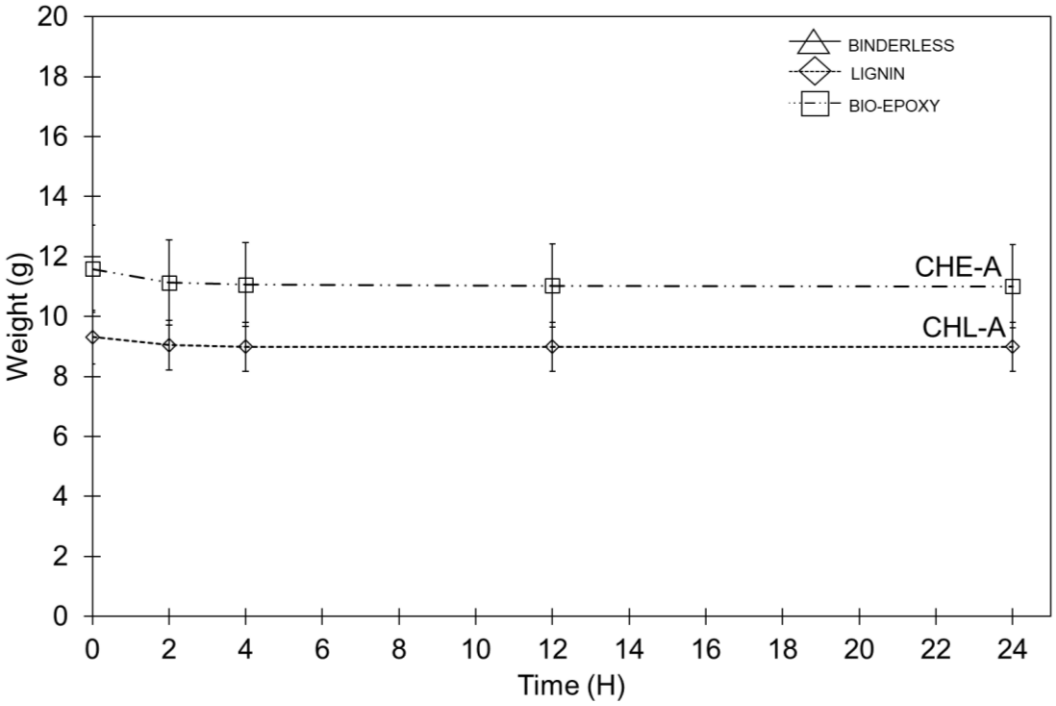

Figure 93 ASPROS chopped comparison of wt.% loss in the different MHC, MH type and size, along with the three binders used in the specimen manufacturing

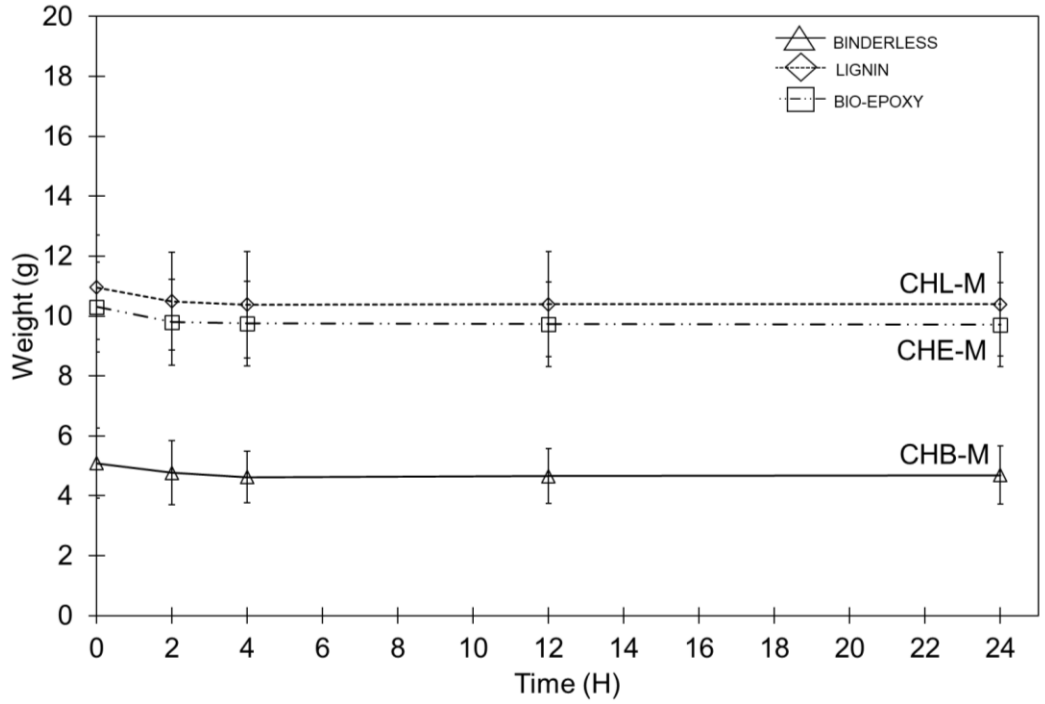

Figure 94 MASH chopped comparison of wt.% loss in the different MHC, MH type and size, along with the three binders used in the specimen manufacturing

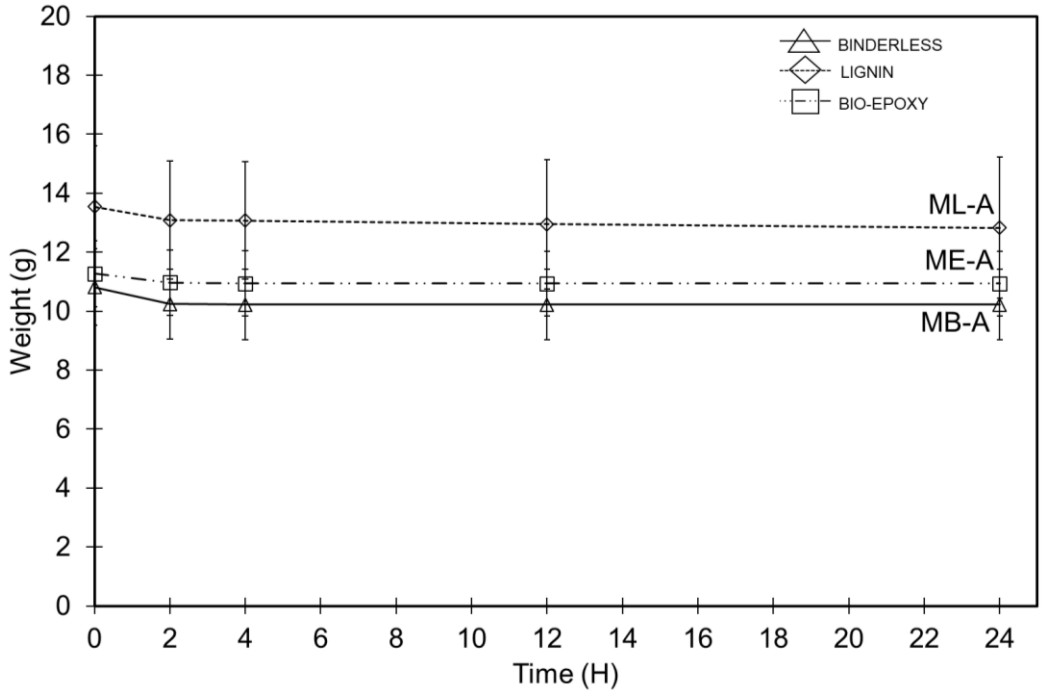

Figure 95 ASPROS milled comparison of wt.% loss in the different MHC, MH type and size, along with the three binders used in the specimen manufacturing

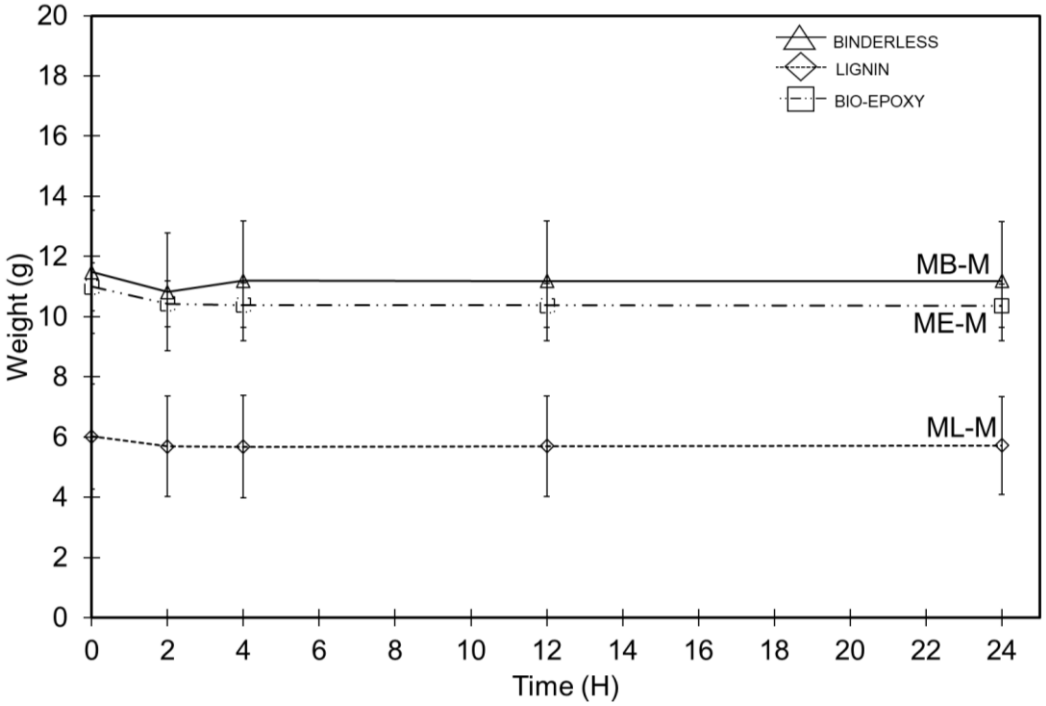

Figure 96 MASH milled comparison of wt.% loss in the different MHC, MH type and size, along with the three binders used in the specimen manufacturing

4.7.2 Flexural testing

Moreover, to be able to compare and select the MHC samples from the first batch the specimens were tested through a semi-static 3-point bend test; In this way, trial stiffness and dimensional stability of all 19 MHC blends could be determined. Then, they could be classified with similar natural fibre-based composite materials (fibreboards). The material was subjected to central maximum tension stress, the applied force transited through the board's thickness making the sample bend until its maximum flexural stress. Hence, indicating MHC's structural strength and flexibility.

Table 30 summarises the flexural properties found in the MHC blends. According to the results, the ME-M specimens had a MOR and FM 120 % higher than the closest specimen CHE-A. Based on the data and the issues encountered during the tests, it was also demonstrated that the MH' size modifications carried out previous to the MHC compounding had been responsible for the substantial differences in the results obtained, apart from the expected strength given by the binder.

Table 30 Summary of MHC boards flexural properties, FM and MOR

	ASPROS-based MHC			MASH-based MHC		
Binder	**Specimen**	**MOR (MPa)**	**FM (GPa)**	**Specimen**	**MOR (MPa)**	**FM (GPa)**
Bs	WB-A	0.865	10.2	WB-M	0.886	5.3
	CHB-A	/	/	CHB-M	0.207	3.0
L	MB-A	0.616	4.8	MB-M	1.5	10.4
	WL-A	0.940	7.2	WL-M	3.9	21.4
	CHL-A	1.3	11.6	CHL-M	1.1	13.5
	ML-A	0.127	3.4	ML-M	0.327	4.4
SSE	WE-A	7.8	70.6	WE-M	4.4	26.4
	CHE-A	11.2	176.7	CHE-M	11.5	68.4
	ME-A	7.9	181.4	ME-M	18.1	714.3
	AKE-A	3.9	45.1	AKE-M	8.4	64.8

Looking at Figure 97 the SSE group reported a significantly higher FM and average density than the BS and L groups. Most of the specimens' flexural properties and density expected fell below the levels accepted for non-wood fibreboards (wheat

straw-based fibreboard density 750-1100 kg/m^3 [182], hazelnut shell-based fibreboard density 800 kg/m^3 and FS 13.9-34.9 N/mm^2 [202]). Whereas the ME-M, ME-A and CHE-A specimens showed features closer to the ones expected in the wood-based standard fibreboards before mentioned.

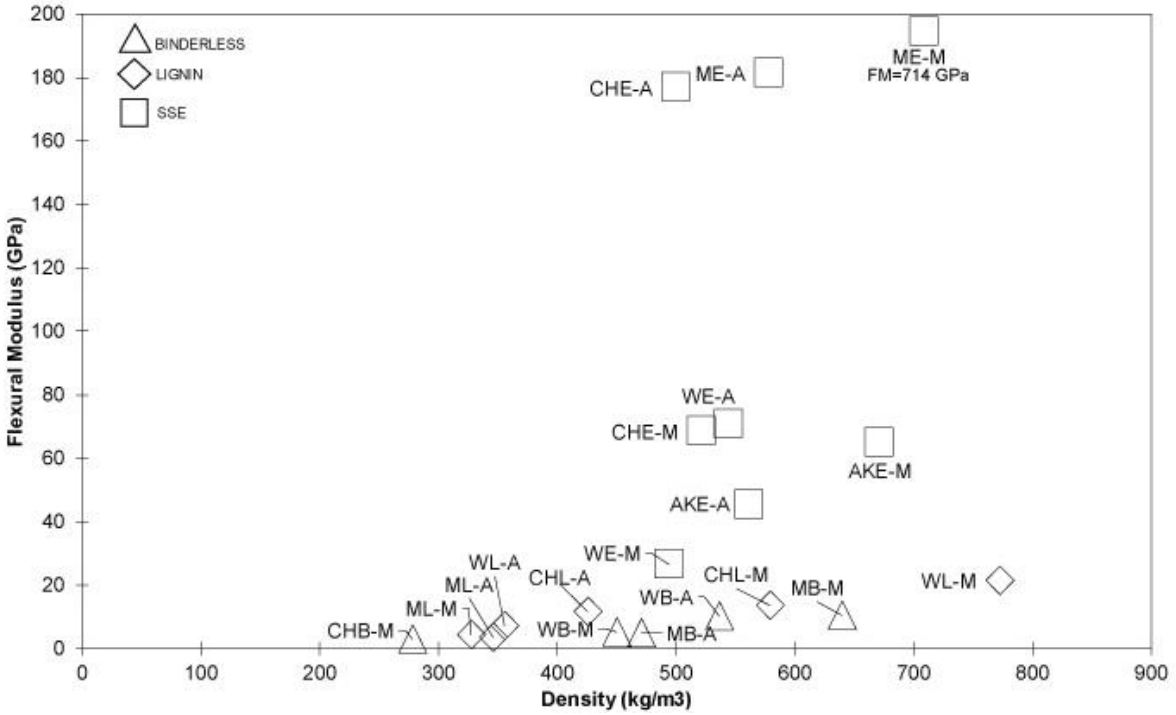

Figure 97 Flexural modulus vs density of the MHC boards according to the matrix used

4.7.3 Maize husk composite selection

The next section sets out the parameters to critically assess the MHC samples to gain a better understating of their limitations and capabilities. The results from the first filter evaluation are displayed in Table 31, where the twenty MHC blends were paired from the criteria discussed (section 3.2.17) against a known material used as a baseline (light MDF). Only 35% of the specimens covered the criteria, from which over half of them performed poorly in comparison to the selected baseline material characteristics.

In the second filter, chosen blends were set by eliminating the deficient ones (Table 32), in this case, the baseline was replaced by the ME-A specimen, as it was the

best-scored material from the first batch. After this filter, over 50% of the specimens met the characteristics needed, yet only four showed a higher or equivalent score.

Finally, Table 33 shows the third and the last filter carried out, contrasting the most promising screened blends against a commercial MDP board. This selection was focused on more abstract criteria, this to enable us to take forward the chosen specimens into deeper studies, i.e. the food chain supply competition, market analysis, price determination, to mention some.

Furthermore, it is important to emphasise the Pugh matrix usefulness at this stage of the project, because it does not require a high amount of quantitative data on the compared materials. The data used and considered for this decision tool can be found in Appendix F.

Table 31 Pugh selection matrix first filter

	Sample	Weight	Light MDF	WB-M	CHB-M	MB-M	WL-M	CHL-M	ML-M	WE-M	CHE-M	ME-M	AKE-M	WB-A	CHB-A	MB-A	WL-A	CHL-A	ML-A	WE-A	CHE-A	ME-A	AKE-A
	Criteria																						
Fibre	source	3	S	+	+	+	+	+	+	+	+	+	+	++	++	++	++	++	++	++	++	++	++
	availability (2015)	5	S	+	+	+	+	+	+	+	+	+	+	++	++	++	++	++	++	++	++	++	++
	size	2	S	- -	-	S	- -	-	S	- -	-	S	+	- -	-	S	- -	-	S	- -	-	S	+
	length	3	S	+ +	+	S	+	+	S	+	+	S	-	+	+	S	+	+	S	+	+	S	S
	UTS	4	S	S	S	S	S	S	S	S	S	S	S	S	--	S	S	--	S	S	--	S	S
	elongation	3	S	- -	- -	- -	- -	- -	- -	- -	- -	- -	-	- -	- -	S	- -	+	S	+	+	S	-
	Young's modulus	2	S	-	-	S	-	-	S	-	-	S	-	-	-	S	-	-	S	-	-	S	-
	extraction method	4	S	++	+	+	++	+	+	++	+	+	S	++	+	+	++	+	+	++	+	+	S
	cost	5	S	+	+	+	+	+	+	+	+	+	+	++	++	++	++	++	++	++	++	++	++
Matrix	type	4	S	++	++	++	+	+	+	+	+	+	+	++	++	++	+	+	+	+	+	+	+
	toxic emissions	5	S	++	++	++	++	++	++	+	+	+	+	++	++	++	++	++	++	+	+	+	+
	biodegradability	4	S	++	++	++	++	++	++	S	S	S	S	++	++	++	++	++	++	S	S	S	S
	availability	5	S	++	++	++	+	+	+	S	S	S	S	++	++	++	+	+	+	S	S	S	S
	price	4	S	++	++	++	- -	- -	- -	-	-	-	-	++	++	++	- -	- -	- -	-	-	-	-
MHC board	density	4	S	--	- -	S	+	S	-	-	- -	S	S	-	- -	- -	- -	- -	- -	-	-	-	-
	thickness	2	S	S	S	S	-	S	S	S	-	-	S	-	S	- -	- -	-	S	-	-	S	S
	MOR	3	S	- -	- -	- -	- -	- -	- -	- -	-	-	- -	- -	- -	- -	- -	- -	- -	- -	-	- -	- -
	flexural modulus	3	S	- -	- -	-	++	-	- -	+	++	++	++	-	- -	- -	- -	-	- -	++	++	++	++
	moisture content	4	S	S	S	S	S	S	S	S	S	S	S	S	- -	S	-	-	S	S	S	-	S
	thickness swell	4	S	+	+	+	++	++	++	+	S	S	- -	+	+	+	++	++	++	+	S	S	-
Qualitative	fibre wetting	4	S	- -	- -	-	- -	S	S	- -	-	-	S	- -	-	-	- -	-	S	-	S	S	S
	mixing	4	S	- -	-	-	- -	S	S	-	-	-	-	S	- -	- -	S	S	S	- -	-	S	S
	surface appearance	3	S	S	+	- -	S	- -	- -	S	+	+	-	-	- -	- -	-	-	S	S	S	+	-
	structural appearance	3	S	-	- -	- -	-	-	-	-	-	S	+	- -	- -	-	- -	- -	S	-	S	S	+
	voids	4	S	- -	- -	S	- -	- -	-	-	+	S	+	- -	- -	-	- -	-	S	-	S	S	+
	delamination	3	S	++	+	S	++	+	S	+	S	S	-	++	+	S	++	+	S	+	S	S	-
	retail price	5	S	++	++	++	-	-	-	++	+	S	+	++	++	++	-	-	-	++	+	+	S
	Total+		**0**	**22**	**20**	**17**	**21**	**16**	**12**	**13**	**12**	**9**	**11**	**23**	**21**	**19**	**17**	**17**	**14**	**17**	**13**	**12**	**12**
	Total-		**0**	**18**	**17**	**11**	**18**	**15**	**14**	**14**	**12**	**7**	**11**	**17**	**23**	**15**	**24**	**19**	**9**	**13**	**9**	**5**	**9**
	Total score		**0**	**4**	**3**	**6**	**3**	**1**	**-2**	**-1**	**0**	**2**	**0**	**6**	**-2**	**4**	**-7**	**-2**	**5**	**4**	**4**	**7**	**3**
	Weighted total +		**0**	**54**	**57**	**48**	**52**	**45**	**39**	**44**	**44**	**32**	**39**	**54**	**81**	**48**	**45**	**48**	**39**	**47**	**40**	**37**	**34**
	Weighted total -		**0**	**32**	**32**	**23**	**36**	**32**	**32**	**33**	**31**	**20**	**29**	**33**	**43**	**30**	**46**	**47**	**19**	**32**	**25**	**15**	**26**
	Weighted score		**0**	**22**	**25**	**25**	**16**	**13**	**7**	**11**	**13**	**12**	**10**	**21**	**38**	**18**	**-1**	**1**	**20**	**15**	**15**	**22**	**8**

S same
+ better
- worse
++ much better
- - much worse

Weighting:
1 = minor importance to the material development
2 = moderate importance to the material development
3 = important to the material development
4 = very important to the material development
5 = extremely important to the material development

boards selection code: good (green), acceptable (yellow), deficient (red)

Table 32 Pugh selection matrix second filter

	Sample		ME-A	CHB-M	MB-M	WL-M	CHL-M	CHE-M	ME-M	AKE-M	WB-A	MB-A	ML-A	WE-A	CHE-A	AKE-A
	Criteria	WEIGTH														
Fibre	husk	3	S	-	-	-	-	-	-	-	S	S	S	S	S	S
	availability (2015)	5	S	- -	- -	- -	- -	- -	- -	- -	S	S	S	S	S	S
	size	2	S	+	S	++	+	+	S	-	++	S	S	++	+	-
	length	3	S	++	+	++	+	+	+	+	+	S	S	++	+	S
	UTS	4	S	- -	+	+	- -	- -	+	+	+	S	S	+	- -	+
	elongation	3	S	-	-	- -	- -	-	-	-	-	S	S	- -	-	- -
	Young's modulus	2	S	S	++	S	S	S	++	++	++	S	S	++	S	+
	extraction method	4	S	+	S	++	+	+	S	-	++	S	S	++	+	-
	cost	5	S	- -	- -	- -	- -	- -	- -	- -	S	S	S	S	S	S
Matrix	type	4	S	++	++	+	+	S	S	S	++	++	+	S	S	S
	toxic emissions	5	S	++	++	+	+	S	S	S	++	++	+	S	S	S
	biodegradability	4	S	+	+	+	+	S	S	S	+	+	+	S	S	S
	availability	5	S	S	S	S	S	S	S	S	S	S	S	S	S	S
	price	4	S	++	+	- -	- -	S	S	S	++	++	-	S	S	S
MHC board	density	4	S	-	+	+	S	S	++	+	S	-	-	- -	- -	-
	thickness	2	S	-	S	+	S	S	S	+	S	+	-	+	+	+
	MOR	3	S	- -	- -	-	- -	+	++	+	- -	- -	- -	+	+	-
	flexural modulus	3	S	- -	- -	- -	- -	-	++	- -	- -	- -	- -	-	-	- -
	moisture content	4	S	- -	- -	- -	-	++	+	- -	- -	++	- -	-	-	-
	thickness swell	4	S	+	+	+	+	+	+	-	+	+	+	+	+	- -
Qualitative	fibre wetting	4	S	-	-	- -	- -	- -	S	S	-	-	- -	- -	- -	S
	mixing	4	S	- -	-	- -	-	-	S	S	- -	- -	-	-	-	-
	surface appearance	3	S	-	- -	-	- -	S	S	-	- -	- -	-	-	-	S
	structural appearance	3	S	- -	+	-	S	S	S	-	- -	-	-	-	-	S
	voids	4	S	- -	- -	-	- -	-	S	S	- -	- -	-	- -	- -	-
	delamination	3	S	- -	S	- -	- -	-	S	S	- -	S	S	- -	- -	S
	retail price	5	S	+	+	-	- -	+	-	-	+	+	-	++	++	-
	Total+		**0**	**13**	**14**	**13**	**7**	**8**	**12**	**7**	**17**	**12**	**4**	**13**	**8**	**3**
	Total-		**0**	**26**	**18**	**24**	**27**	**14**	**7**	**16**	**18**	**13**	**16**	**18**	**16**	**14**
	Total score		**0**	**-13**	**-4**	**-11**	**-20**	**-6**	**5**	**-9**	**-1**	**-1**	**-12**	**-5**	**-8**	**-11**
	Weighted total +		**0**	**35**	**41**	**35**	**26**	**25**	**27**	**17**	**40**	**32**	**17**	**25**	**23**	**7**
	Weighted total -		**0**	**54**	**38**	**53**	**54**	**39**	**21**	**44**	**34**	**28**	**39**	**35**	**39**	**40**
	Weighted score		**0**	**-19**	**3**	**-18**	**-28**	**-14**	**6**	**-27**	**6**	**4**	**-22**	**-10**	**-16**	**-33**

S	same	Weighting:	1 = minor importance to the material development
+	better		2 = moderate importance to the material development
-	worse		3 = important to the material development
++	much better		4 = very important to the material development
- -	much worse		5 = extremely important to the material development

boards selection code: good; acceptable; deficient

Table 33 Pugh selection matrix third filter

	Sample		MDP	ME-A	MB-M	ME-M	AKE-M	MB-A	WB-A	AKE-A
	Criteria	WEIGTH		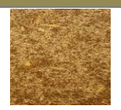	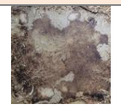	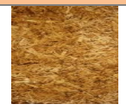	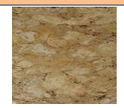			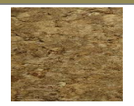
MHC board	source	3	S	++	+	+	+	++	++	++
	extraction method	2	S	S	S	S	S	S	++	S
	extraction cost	4	S	S	S	S	-	S	++	-
	matrix availability	3	S	-	++	-	-	++	++	-
	matrix price	4	S	-	++	-	-	++	++	-
	density	3	S	-	S	S	S	- -	-	-
	MOR	3	S	- -	- -	-	- -	- -	- -	- -
	thickness swell	3	S	S	+	S	-	+	-	-
MHC manufacturing	efficiency	3	S	S	-	S	+	-	- -	S
	precision	3	S	S	- -	S	S	- -	- -	S
	processes adaptability	4	S	++	+	++	+	+	- -	+
	training needed	5	S	S	S	S	-	S	-	S
	energy consumption	4	S	S	+	S	S	+	+	S
Qualitative	appearance	3	S	+	- -	S	+	- -	- -	+
	food supply chain competition	5	S	S	- -	- -	- -	S	S	S
	possible substitute of known fibreboards	4	S	+	- -	+	+	- -	- -	+
	market demand	5	S	S	-	S	S	- -	- -	S
	retail price	3	S	+	+	+	+	+	++	+
	Total+		**0**	**7**	**9**	**5**	**6**	**10**	**12**	**6**
	Total-		**0**	**5**	**12**	**5**	**9**	**13**	**17**	**7**
	Total score		**0**	**2**	**-3**	**0**	**-3**	**-3**	**-5**	**-1**
	Weighted total +		**0**	**17**	**24**	**14**	**20**	**30**	**23**	**17**
	Weighted total -		**0**	**13**	**26**	**15**	**27**	**24**	**36**	**20**
	Weighted score		**0**	**4**	**-2**	**-1**	**-7**	**6**	**-13**	**-3**

S	same	Weighting:	1 = minor importance to the material development
+	better		2 = moderate importance to the material development
-	worse		3 = important to the material development
++	much better		4 = very important to the material development
	much worse		5 = extremely important to the material development

boards selection code: good; acceptable; deficient

4.8 Maize husk composite optimisation

From the obtained results and selection of the first batch of MHC produced exhibited a very wide range of properties as detailed in Table 31. Thence, the specimens were filtered in Table 33 and compared to reformulate and enhance the selected MHC samples (ME-M and AKE-M). Some of the manufacturing steps had to be reassessed and narrowed down for the following MHC boards batch, i.e. the use of only milled and alkali extracted ASPROS husk, a decrease of resin content and reduced heat exposure during the hot-pressing. During this phase, some of the manufacturing flaws and issues spotted before were addressed as well, bringing the production process closer to a more precise and realistic solution. To accomplishing a competitive price for the MHC in the Mexican market, a blend with less resin content was also manufactured and tested.

Once the new batch was produced, further tests were to be performed on the selected blends detailed below in Table 34 to obtain more accurate data. From now on only ASPROS husks were used for the MHC manufacture.

Table 34 Second batch of MHC bends and percentage of fibre/binder (w/w)

Sample		MH (%)	Extraction method	SSE (%)
M-EM	M30	70	Milled	30
AKE-M	AK30	70	Alkalinized	30
M-EM	M20	80	Milled	20

A variety of studies have been carried out on natural fibres-based composite materials, demonstrating their properties and possible applications. For this reason, more tests on MHC were adapted to improve their manufacturing, and consequently the board's properties. Thus, the experiments carried out were used to establish an MHC boards general overview including density, moisture content, impact, tensile and elastic properties, and moisture and environmental resistance as shown in Table 35.

Table 35 MHC tests and obtained features

	MH Tensile	Accelerated ageing (AA)	Thickness swell	Impact test
Standard		ASTM ASTM D1037-12 [176]		ASTM D256-10 [190]
Outcome	UTS Young's Modulus Elongation at break (%)	Environmental exposure to extreme climates UTS Young's Modulus Elongation at break (%)	Percentage of thickens swelling	Impact resistance
Sample size	Dog-bone shaped	Dog-bone shaped	50 x 50 mm	65.5 x 127 mm
#	7	7	5	5

4.8.1 Maize husk composite mechanical and physical properties

The final batch of MHC boards doubled in some properties the first batch, the variation of *E*, elongation at break, UTS, density and IR are detailed in Table 36. Overall, MHC boards tensile properties were considered acceptable concerning the literature obtained from wood-based fibreboards [203] as Figure 98 shows. The thickness swelling presented considerable distension in the AK30 samples (Figure 99), as a consequence of the MH delignification process during the alkali extraction. None of the manufactured MH fibreboards reached the ASTM wood-based standard for MDF.

Table 36 Summary of MHC mechanical and physical properties compared with light MDF

Specimen	Density (kg/m3)	UTS (MPa)	EB (%)	*E* modulus (GPa)	IR (J/m)
M30*	889.7	15.3	2.2	1.2	8.3
AK30**	1014.3	14.7	1.5	1.6	12.6
M20*	864.8	14.0	1.9	0.9	6.6

The nomenclature used for the first batch * ME-A ** AKE-A

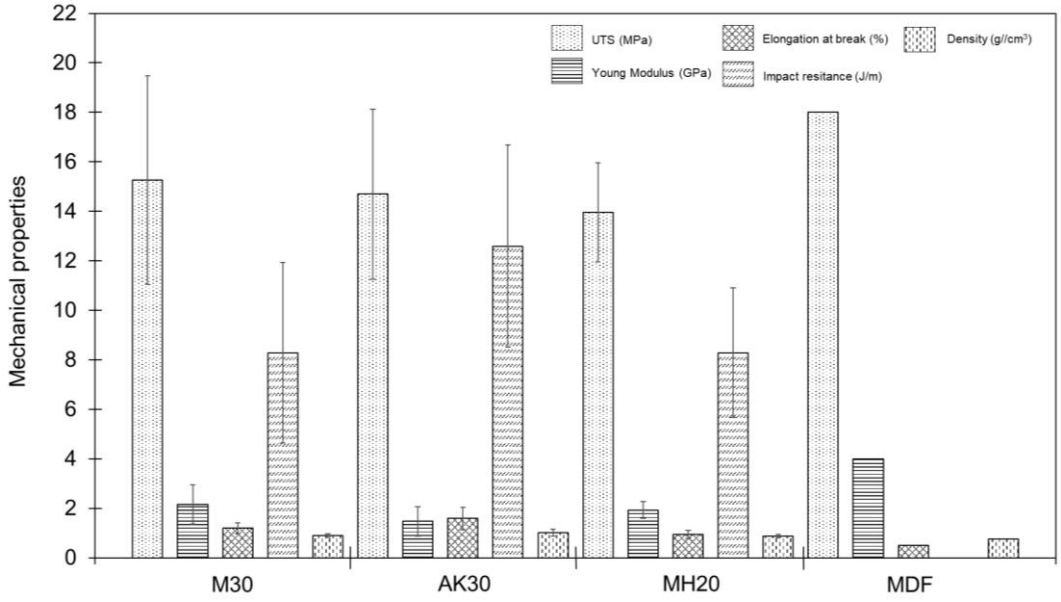

Figure 98 Mechanical properties of optimised MHC specimens and WBF [200]

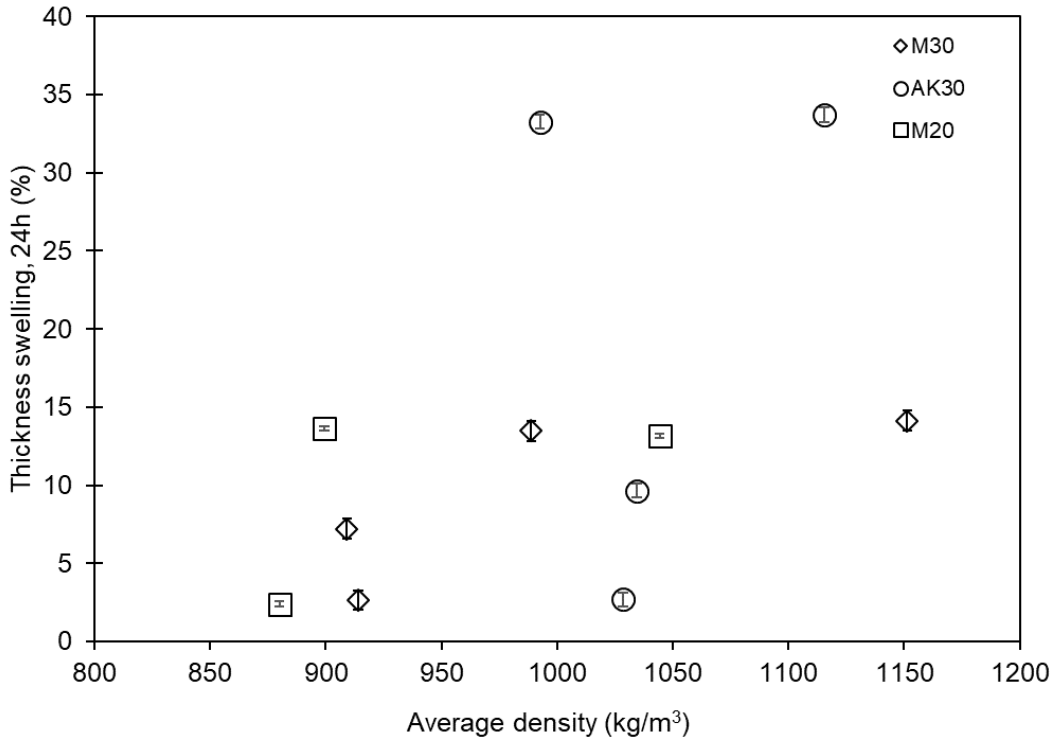

Figure 99 MHC boards thickness swelling in relation to its average density. SD bars are smaller than markers

The deterioration of tensile properties after the completion of the AA cycle (Figure 100). The UTS, Young's Modulus and Elongation at break percentage for the untreated control samples are shown in Table 37. Moreover, the properties preservation are detailed so they can be compared with the ones displayed in Table 36.

Table 37 Tensile properties of MHC boards after ageing cycle

Specimen	Density (kg/m^3)	UTS (MPa)	Elongation at break (%)	Young's modulus (GPa)	Thickness swell (%)
M30	889.7	16.3	1.6	1.6	3.3
AK30	1014.3	11.2	3.8	1.3	3.9
M20	864.8	12.9	1.7	1.3	4.8

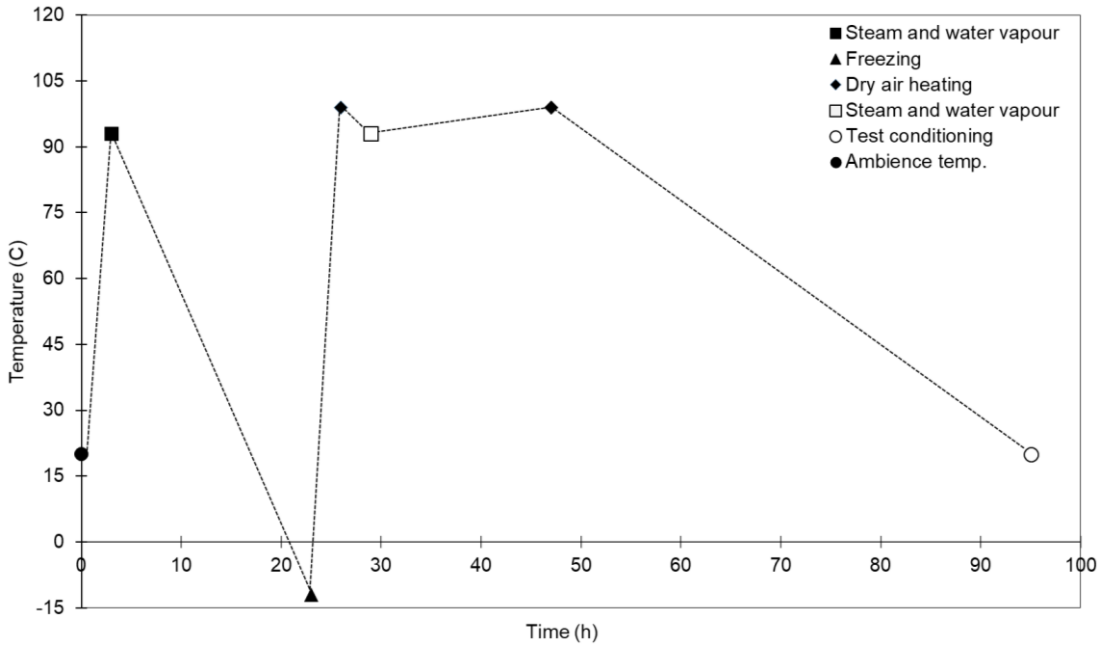

Figure 100 AA cycle of approximately 95 hours

5 MAIZE HUSK-BASED COMPOSITE MANUFACTURING DISCUSSION

This section presents a broad analysis of the significant results from the application of MH waste to developing a new CM. Followed by a detailed review of the significant results from the tests performed on the two types of MH waste, as well as the MHF extraction methods, followed by the MHC boards manufacturing and possible end-use application requirements.

5.1 Factors affecting maize husk feasibility as reinforcement for a composite material

As discussed in section 2.4.1 AW application as reinforcement has shown a considerable increment recently, and a number of research has concentrated on how to increase green composites mechanical performance to extend their application range among CM. In this section, a review of the most significant factors that have affected the MHC performance has been carried out, complemented by MH and material's improvements reached.

5.2.1 Characterisation and comparison of ASPROS and MASH maize husks

Prior to the analysis of the MHF extracted, the two MH types used ASPROS and MASH were assessed to identify the husk features and contrast their chemical composition, CSA, length, tensile strength and moisture content with some of the NF already utilised in the composite industry. The purpose of these experiments was to set a reference point with both MH types as free from any extra processes as possible. Hence, any variation during and after the size reduction procedures could be detected and if necessary avoided. Most of the studies found on MH have focussed on the fibre extraction, therefore a lack of research on the complete husk characterisation was identified. The exception was Guimarães et al. [204] study, in which MH was devised for handcrafts and cigars production.

The two husk types were tested in order to obtain enough information to decide whether the extraction processes were necessary and how they will be performed. ASPROS and MASH first impressions showed variances in colour, structure and size according to the harvesting method used. Thence, a deeper inspection carried out in both husks types tissues showed that ASPROS samples had 30 % more presence of bast sections than MASH samples, which are mostly formed of vascular tissue (section 4.24.1). These results are consistent with those obtained by Baillie [106] and De Carvalho Mendes et al. [196] who took advantage of the NF structure and resistance to produce more competitive CM. The differences found in the chemical composition between the two MH types are believed to have been influenced by MASH's sulphuretted process, where the majority of the bast tissue is removed. Thence, the presence of additional elements in MASH specimens increased (Table 23), besides significant fibre and tissue variations than the observed in wood-based fibres [96].

Figure 101 shows A-AR and A-M had the maximum levels of silicon, though both husks surpassed the percentage of incorporated silica in wood-based fibreboards reported by Halvarsson [153]. According to this data three mean differences between ASPROS and MASH can be inferred, ASPROS silicon content variation was very low. However, MASH samples showed the lowest levels overall. Finally, chopped MH watches had a minor silicon ratio (35-57 %) in comparison to the other two sizes tested. A feature that may help to get a stronger MH/binder linkage when manufacturing the MHC, as shown in previous studies.

Moreover, MH epidermis is coated by a waxy film compounded by inorganic substances among which Si is responsible for the hydrophilic properties of the fibres. Due to MH's chemical content variation a chemical extraction was carried out, so the overall levels could be more balanced, therefore MHC compounding

could improve the material performance, as other researchers did when working with NF (Ferreira et al., and, Gassan and Bledzki [114]).

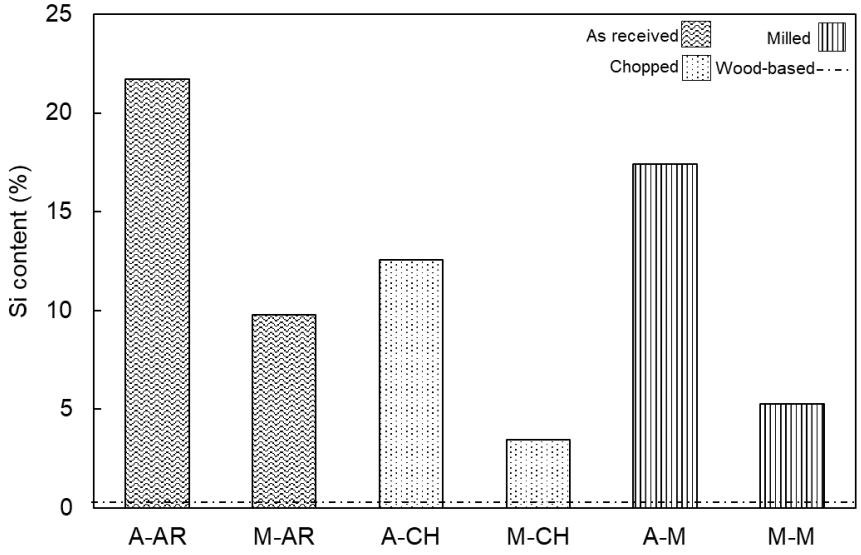

Figure 101 ASPROS (A) and MASH (M) husks silicon content (%) after mechanical size-reduction compared with wood-based fibreboard silicon percentage [153]

Furthermore, the tensile test results obtained by Guimarães [204] when compared with those obtained in this research show a 50 % variation between ASPROS and MASH transversal and longitudinal strength. The difference amidst both directions is not comparable because of the substantial strength gap. The variability in strain in transversal samples resulted from fibre misalignment and conjunctive tissue detachment, behaviour that will be discussed further ahead.

Moreover, both MH's longitudinal TS in Figure 103 was more consistent and reliable that transversal TS as shown in Figure 102. M-L samples showed a TS 56 % higher than A-L husks. However, ASPROS samples had a more uniform SD. ASPROS and MASH samples in neither of the directions tested reached Guimarães's [204] results and fibre stability. It is worth to mention that in both

graphs the data reached negative numbers. However, those are not shown because of its nullity in the overall results.

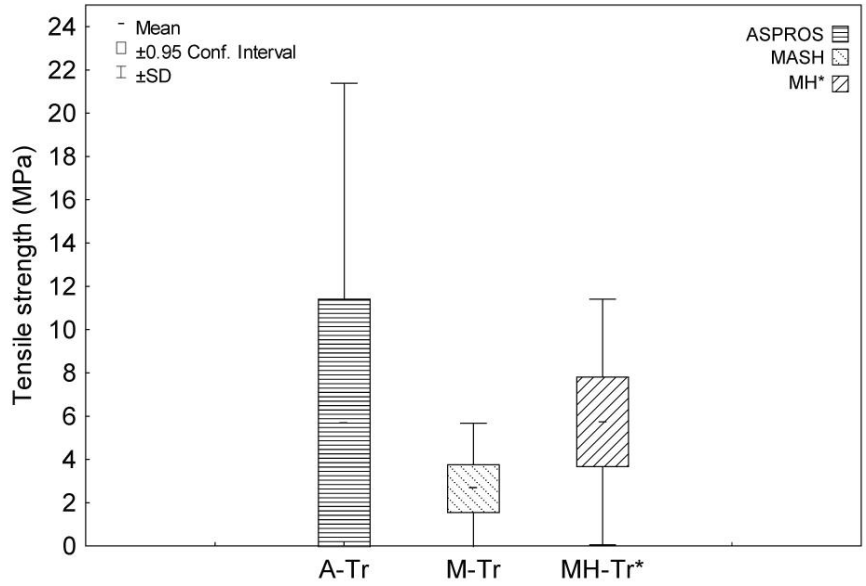

Figure 102 MH transversal tensile strength statistical comparison paired up with MH (*) tested by Guimarães et al. [204]

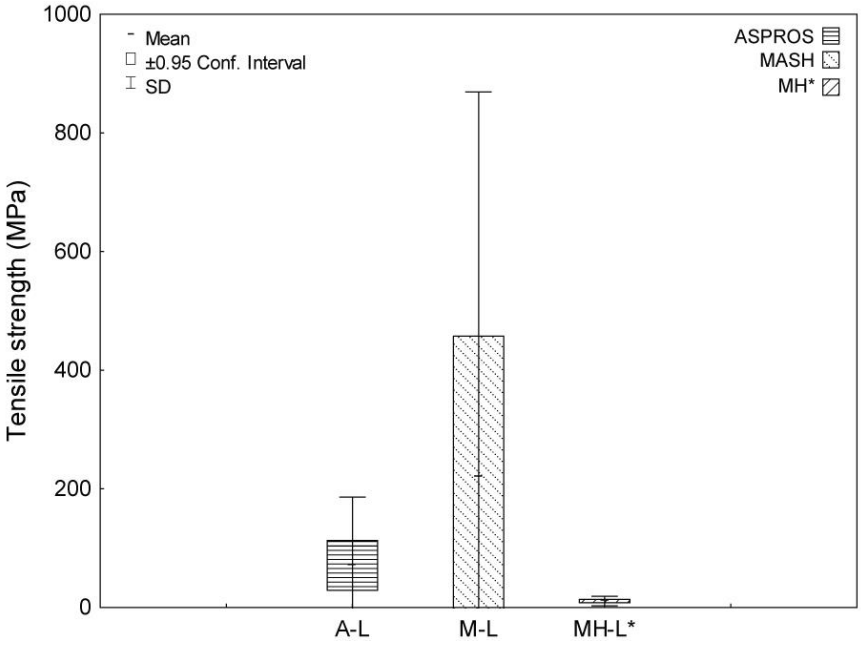

Figure 103 MH longitudinal tensile strength statistical comparison paired up with MH (*) tested by Guimarães et al. [204]

Zhu [144] carried out a tensile test on flax fabrics (woven and non-woven) with the idea of producing more efficient unidirectional (UD) composites. However, the flax fibre uneven thickness could not be used without previous chemical treatments; still, the UD fabric had around 20 % than the non-woven. Therefore, in order to demonstrate MH's resistance and viability to be used without any further treatments for fibre extraction and utilise its natural structure as an advantage for a possible laminar composite.

Correspondingly, the difference between MH's transversal and longitudinal was studied and found some similitudes with the Guimarães et al. [204]; hence the image analysis showed below. The MH topography and crack propagation reflected relevant data from both MH types. MASH samples were less able to follow a straight cut according to the photographs taken during the tensile testing in, besides they were the samples most difficult to align vertically. Although both husks showed fibre stacking (A) in different sections as shown in Figure 104(b) and(c), this due to the natural husk waviness. Moreover, as observed in Figure 104 (a) and (c) the fracture trail (B) in both husk types had significant differences due to the uneven strength distribution across the MH sample's width. However, MASH husk showed 43 % increment in the breaking force in comparison to ASPROS husk (Table 26). On the other hand, MH's apparent elongation the highest value was held by ASPROS husk of 4.7 % against MASH's 2.8 %. Whereas, MASH samples stiffness stood out with 2.8 %, nearly half of ASPROS result.

These differences can be explained in part by the damage caused by the mechanical harvesting, previously mentioned in section 4.4; hence, ASPROS husk lower breaking force in both directions transversal and longitudinal. This rather disappointing finding underpins Halvarsson [153] and De Carvalho Mendes et al. [196] premise on the need of breaking down the NF for a better compounding.

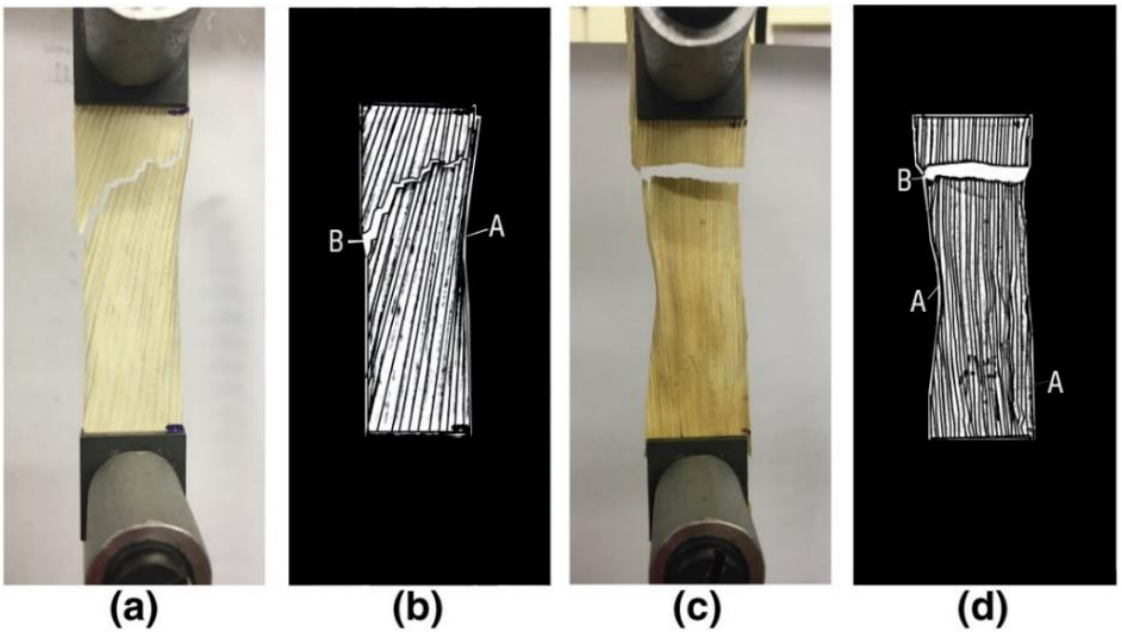

Figure 104 MH tensile test photographs, fibre direction and post-breaking analysis: (a) and (b) MASH-ARL husk; (c) and (d) ASPROS-ARL husk

Therefore, based on the obtained results each MH type may be utilised in diverse industries, e.g. to exploit ASPROS husk elasticity to enhance thermoset-based materials. This finding is consistent with that of Baillie [106] who listed the required properties of an NF when using a thermoset matrix; those were long, straight fibres and fibre optimisation (chemical treatments).

Figure 105 depicts the difference between ASPROS and MASH transversally from which it can be concluded that the samples differ at the 0.05 level of significance when tested transversally. In contrast, Figure 106 shows a considerable difference between samples when tested longitudinally. Thus, MASH husks almost doubled ASPROS P value, besides it had a more homogenous distribution; Then it can be concluded that both husks types are longitudinally stronger (ARL) and its overall performance was not affected even despite the damage suffered when collected. These results are in agreement with those obtained by Guimarães et al. [204].

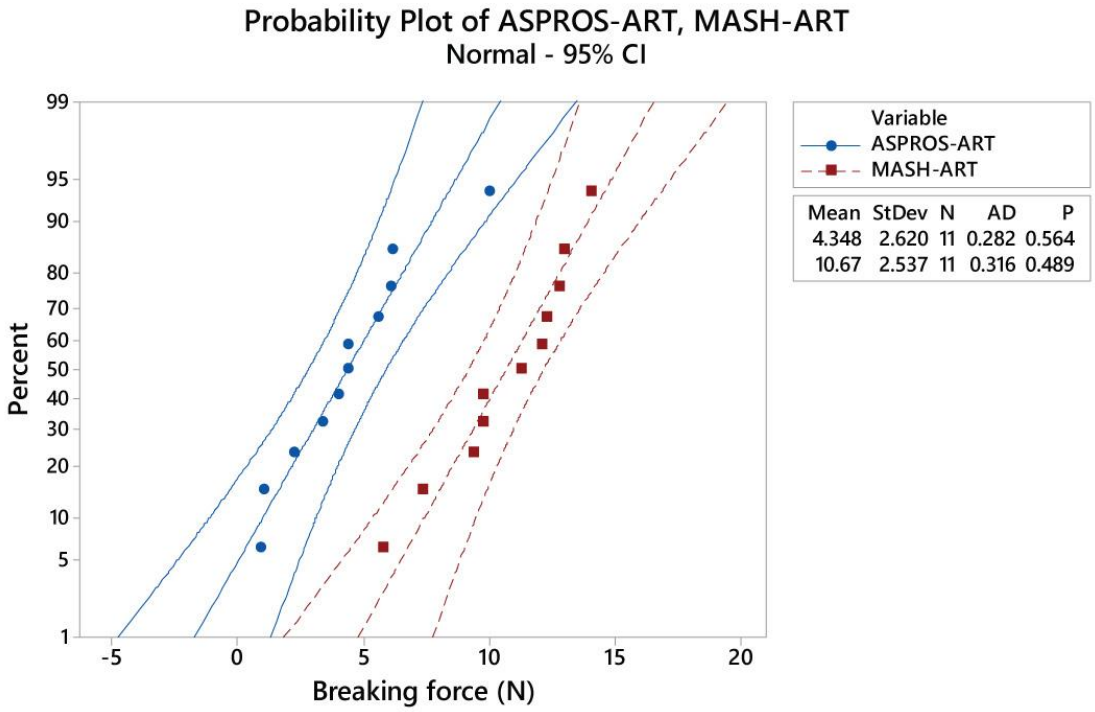

Figure 105 Probability plot normal 95 % CI of husk transversal breaking force

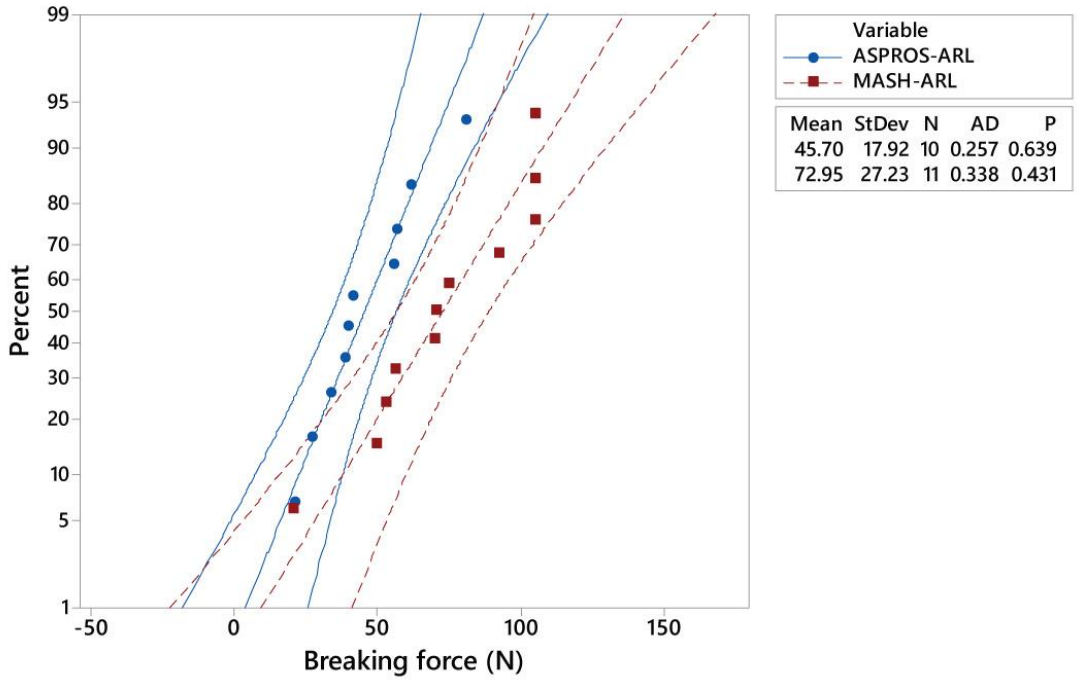

Figure 106 Probability plot normal 95 % CI of husk longitudinal breaking force

5.2.3 Effects of treatments on maize husk fibres tensile properties

The exposure of AW to a suitable surface treatment objective was to improve fibre's compatibility with the matrix. Therefore, the four MHF sizes obtained were tested and analysed to understand better the influence of fibre configurations and effects of the chemical surface treatments. This research will consider Youssef's et al. [95] MH chemical composition report to avoid confusing data: cellulose 43 %, hemicellulose 31 %, lignin 22 %, and ash 1.9 %. Thus, MH's mechanical properties can be observed more clearly, and so the transformation fibres may have suffered according to the size and extraction methods.

The rearrangement of hydrogen bonds between cellulose molecules determines the MHF stiffness, as experienced by Aziz and Ansell [108] and, Huda and Yang [92]. Moreover, mechanical stability in CM appears to be determined by fibre reinforcement thickness, length and elasticity according to Ashby and Johnson [205], who conducted several experiments where he was able to determine 10 μm as the optimal fibre thickness for a competitive material, however the study was based on synthetic fibres. Therefore, the same assumption cannot be held when working with NF, especially if we consider Yilmaz et al.[127] study on MHF's non-uniformity in the thickness of the fibre. Both can be taken as reference and make a double measured of both MHF types, in this way the approximations may draw closer to the exact cross-section dimension.

Table 38 compares the principal features of the MHF extracted for the present research to those similar NF found in the literature. Reddy and Yang's [96] obtained fibres had a considerable higher difference between CSA's, which is believed to occur due to the overexposure to acidic chemicals such as NaO_2. Therefore, when compared the obtained MHF against other NF it can be observed that despite their origin the chemical extraction processes (alkali and enzymatic treatment) yielded enough fibre to make the time and cost-effective

[96,127]. The mechanically extracted methods generated around 80-85 % of fibre, whereas the alkali produced nearly 70 %. In the case of the ball milled and enzymatic extractions, the yield obtained was less than 50 %, thereby these methods were not taken further in this investigation.

Table 38 Comparison of MHF characteristics produced in the present study with comparable cellulosic fibres

Fibre type	Diameter (µm)	Tensile strength (MPa)	Elongation at break (%)	Moisture content (%)
ASPROS-AR	0.9-13.7	7.9-127	1.1-13.2	10.3
MASH-AR	9.7-218.6	0.88-23.6	1-3.8	8.6
ASPROS-M	1.5-61.8	7.1-105	3.3-13.7	10.3
MASH-M	3-7.6	17.3-98.4	1.9-6.9	8.6
ASPROS-AK	1.2-20.8	17.1-69.2	1.8-6.7	6
MASH-AK	1.1-9.5	3.5-352	1.3-10.7	8
MHF Yilmaz [127]	41-72	5.96-13.6**	8.4 -16.8	7.7-10
MHF R&Y [96]	1.3-13.3	23.8**	15.3	8.7
Cotton*	12-45	19-45**	3-10	8.5
Flax *	15-25	343-1035	2.5-3.3	12
Hemp *	18-50	534-900	2.2	12
Jute *	15-25	400-800	1.8	12
Ramie *	15-40	32-44**	4-5	12

*** natural fibres data from [106,127] ** Breaking tenacity (cN/tex)**

The mechanically extracted fibres ASPROS-AR, MASH-AR, ASPROS-M and MASH-M which have considerably lower production costs had a tensile performance comparable to the other maize fibres; cotton and ramie. Despite MHF's higher elongation rates, their tensile strength is slightly less competitive than the registered in another NF. These findings helped us to understand the MHF properties and morphology better after the extraction processes; thereby more appropriate compounding techniques may be used, i.e. blowline and high-pressure fibre resination.

Aziz and Ansell [108] stated that not only the fibre thickness has significant implications in the final fibreboards manufactured. The fibre strength, stiffness

and density are considered as the characteristics commonly analysed in the synthetic fibre-based composites, so their performance can be predicted. Nevertheless, this type of forecast is still very far to be accurate when working with NF due to their non-uniformity structure and chemical composition.

Below are the MHF's CSA QQ plots (Figure 107, Figure 108 and Figure 109) from the two MH types tested, divided as per extraction method. All the samples had a normal distribution, from which ASPROS milled, and both alkalinised fibres had a P value of 0.05. Hence there is not a significant statistical difference between them. It is worth to mention that some of the data points are outliers (marked in red), these points that do not appear to belong with the rest of the data may be removed, but since the sample size is too small to avoid bigger differences they were not deleted. MASH AR, M and ASPROS-M showed a lightly tailed distribution, yet they are not enough to be discarded. Overall ASPROS fibre's CSA consistency was confirmed regardless of the extraction method used.

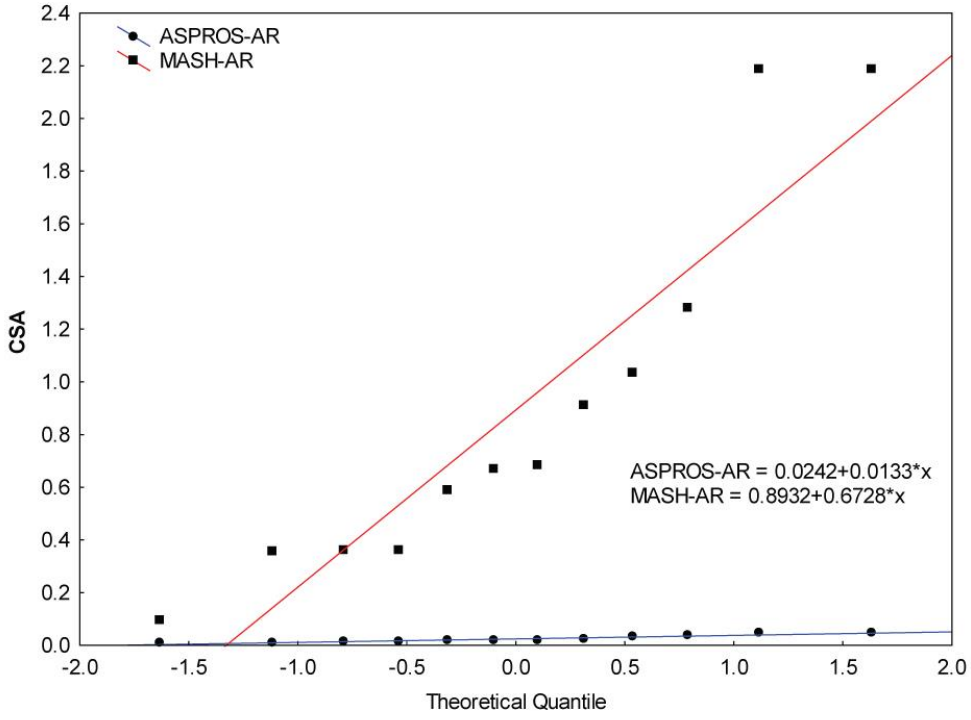

Figure 107 AR ASPROS and MASH husks MHF cross-section area QQ plot

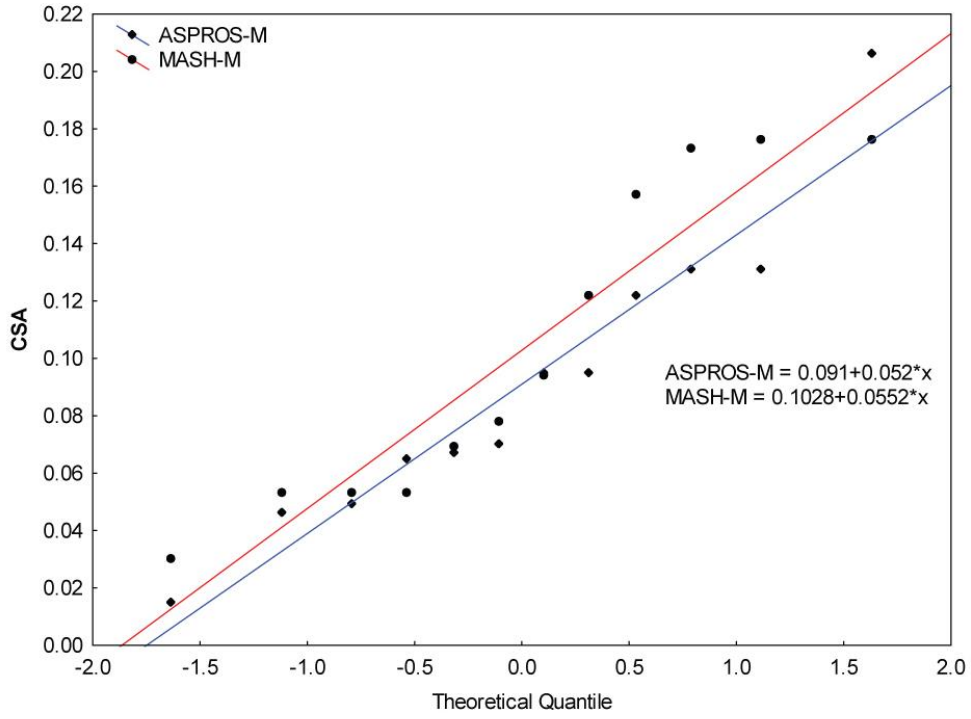

Figure 108 Milled ASPROS and MASH husks MHF cross-section area QQ plot

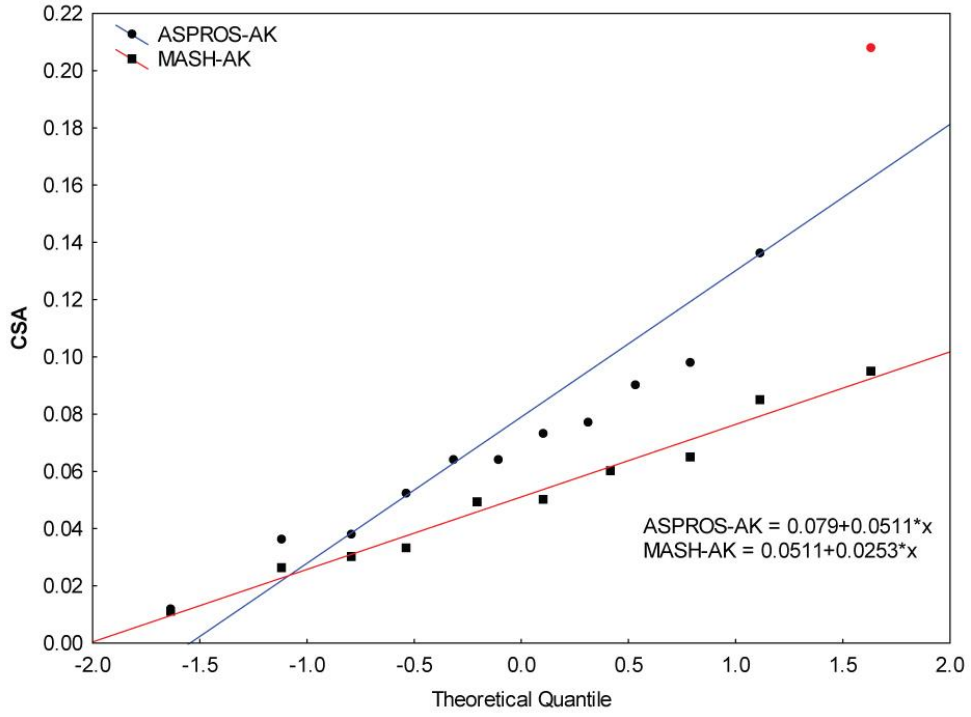

Figure 109 Alkali ASPROS and MASH husks MHF cross-section area QQ plot

Figure 110, Figure 111 and Figure 112 depict the typical stress-strain behaviour curve from a tensile test, in this case, the graphs are divided per extracted MHF's reduction size method used. All samples had a variation on the initial strain attributed to the fibre's natural waviness and twisting of the fibre bundles similar to those reported by Zhu [144] in flax fibres. The linear load curve is shown for ASPROS-AR, ASPROS-AK and MASH-AR specimens reflect MH's stiffness, a behaviour observed for Symington et al. [192] in flax, abaca and kenaf fibres.

Figure 110 shows MASH-AR fibres as the weakest of all the samples, fibre's elasticity and strength were considerably improved. Although after the fibre extraction they presented an exponential increment in both tensile strength and strain, especially the alkalinised fibres since they had the highest tensile strength. Whereas, ASPROS samples fell closer to the values found in the literature reported by Symington et al. [192], showing a steadier tensile strength regardless of the extraction method. As it can be seen in Figure 111, ASPROS-M had the highest elasticity percentage with a regular strain strength. Overall, relevant evidence has been offered to recommend milled MHF's as suitable to be tested as a green composite precursor, whereas AR fibres may work best as rough composite filler due to its thickness and surface roughness.

In Figure 112 the 95 % CI obtained from the MHF failure strength was plotted and compared to NF already used in green composite manufacturing. The ASPROS-AK was the only group that had a closer approximation to a normal curve (shape value: 3.5), presenting reproducibility and reliability of strength values in a range of fibre bundles. Shape values below or closer to 2 represent a right-skewed distribution, in other words, a lower consistency of the samples. The shape value for most of the tests carried out were below 3, which is typical of single fibre failure strength measurement. The MHF behaviour has been proven to be similar to cotton and ramie, besides extracted MHF; hence, these

somewhat reassuring results show MHF possibility to be transformed into a fibreboard.

Figure 111 MASH-M displays the largest Young's modulus with 4.5 GPa and an SD of ±8.5, evidencing MHF's unevenness and fibre stiffness. The AK extracted MASH specimens, displayed results of 3.0 GPa (±5.1). The testing of the ASPROS-AR fibres gave Young's modulus to be of 2.8 GPa (±3.1), and 1.9 GPa (±2.2) and 3.0 GPa (±1.0) for M and AK respectively. The MASH-AR fibre had a much lower average Young's modulus of 0.4 GPa (±0.3), although their SD was lower than most of the other tested fibres. Surprisingly, the evidence showed that the fibres that had a constant performance were the ones extracted from the ASPROS husk, predominantly the alkalinised husk.

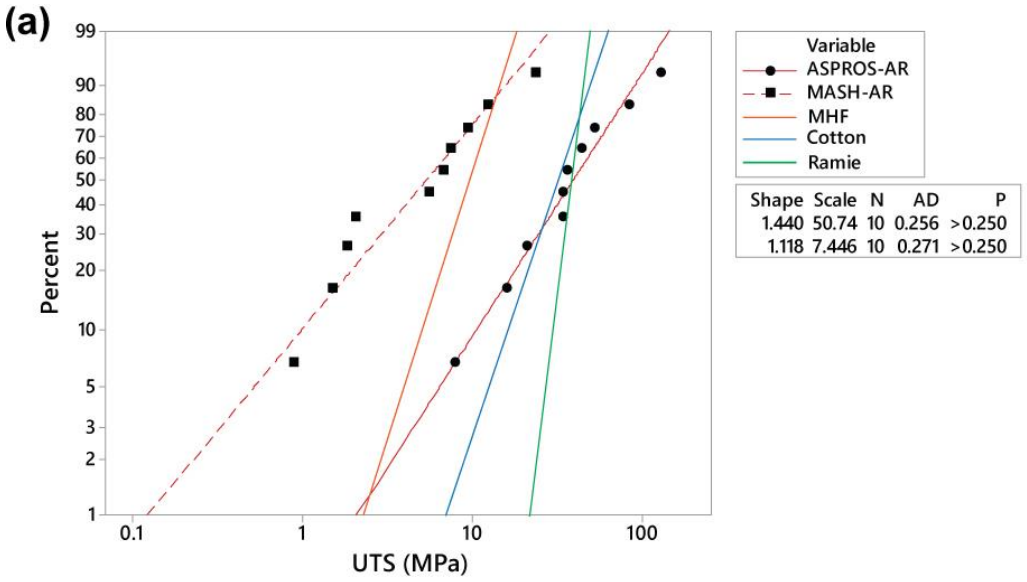

Figure 110 Weibull probability plots of AR MHF's tensile strength compared with other natural fibres from [192]

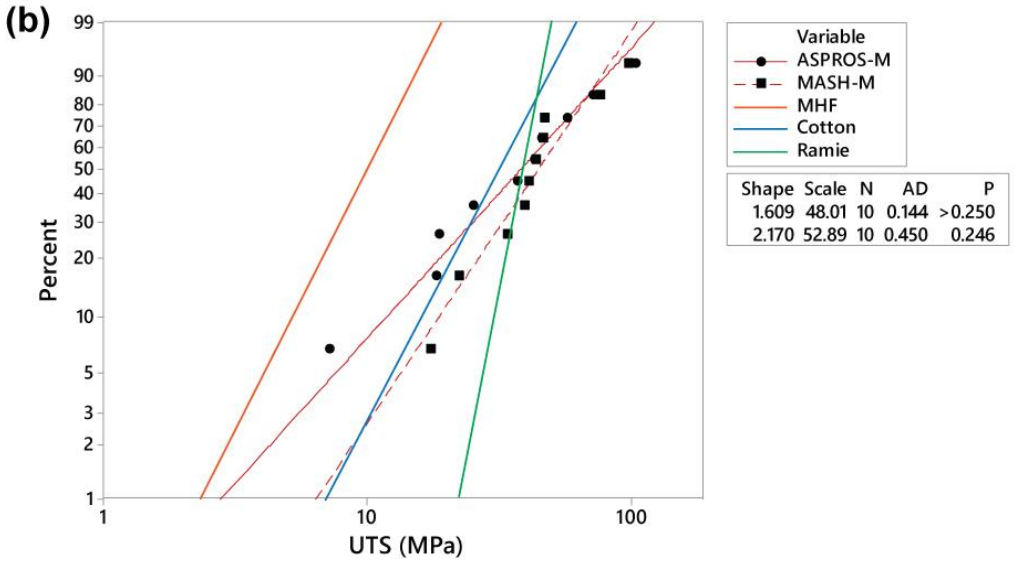

Figure 111 Weibull probability plots of milled MHF's tensile strength compared with other natural fibres from [192]

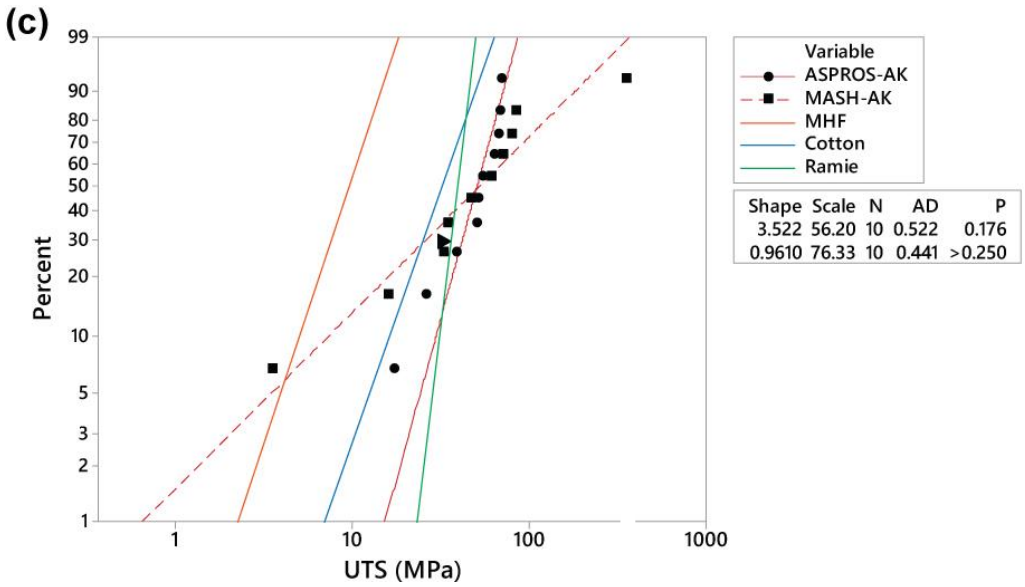

Figure 112 Weibull probability plots of alkali MHF's tensile strength compared with other natural fibres from [192]

5.3 Implications of the manufacture of a maize husk-based composite

5.3.1 Manufacture of maize husk-based composite

The MH composite manufacturing process is based on the standard wood-based fibreboard one, this to assure MH favourable reception into a fully developed and proven manufacturing system. Some attempts to integrate non-wood fibres and alternative adhesives have been studied [123,126,153,178,182], yet, to date, only Çöpür et al. [202] and García Martínez et al. [32] have been successfully commercialised and remained in the market.

Furthermore, several studies have already demonstrated MHF's capability as composite filler [92,95,206,207]; as many other natural fibres currently used in the materials manufacturing industry, however, only a few have studied a maize husk based-fibreboard. For the manufacture of MHC boards, each step was analysed and approached with a strong emphasis in the four extraction methods and three bonding systems tested. Moreover, MHC boards were critically assessed by measuring their overall features throughout ASTM standards for fibreboards.

One of the aims of the present research not only demonstrated MH suitability, hence both manufacturing steps of WBF and MHC were analysed and compared in Figure 113. The differences that can be observed from the original WBF manufacturing diagram are a few steps simplifications, resulting in three steps reduction driven by the four diverse size reduction methods tested in third step (section 3.2.6). The MH mechanical extractions (milling and chopping) were conducted based on current practices from the wood board manufacturing industry, the aim was to reduce costs and the risk of corrosion in the equipment [165], whereas the alkali and enzymatic methods were select to improve MHC chemical structure as suggested by Reddy and Yang [96] and Yılmaz et al. [158]. Therefore, the final manufacturing layout was be adapted according to

the results obtained from the nineteen types of MHC boards manufactured, taking into consideration husk type, size and matrix.

El-Haggar [47] remarked the significance of achieving a cleaner production without forfeit efficient manufacturing processes. Consequently, in order to address these focal points, this research focused on optimising MHC's manufacture as well as developing a competitive fibreboard for the local market. It is important to mention that the raw material diversification might as well be considered a big improvement for the fibreboard industry adaptability. Thus, the available agricultural residues will become a very valuable resource for the farmers.

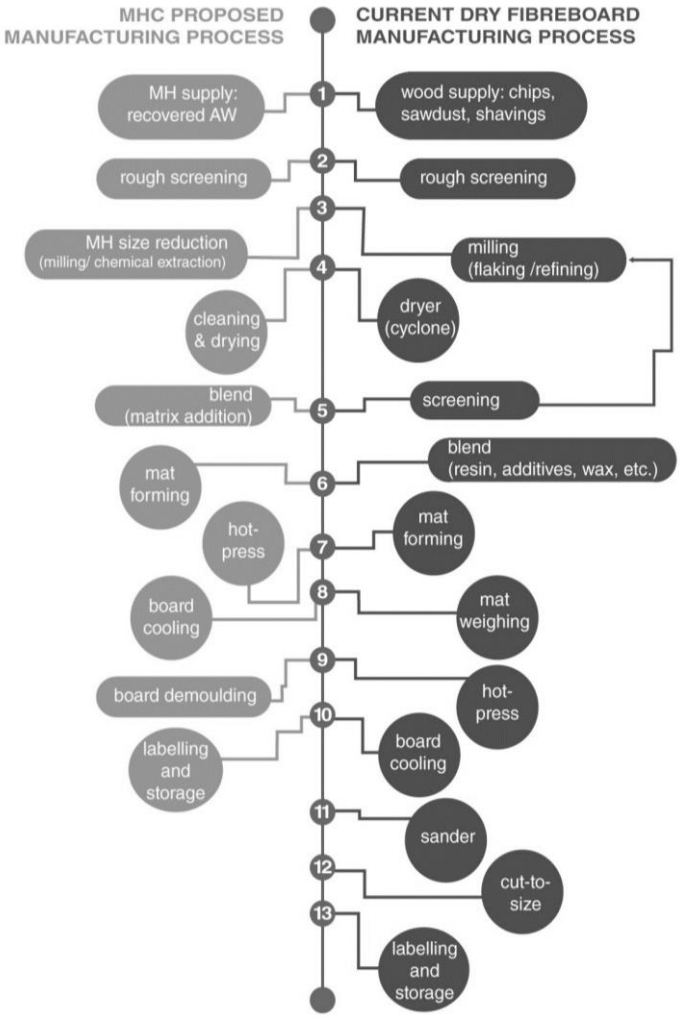

Figure 113 MHC and WBF manufacturing stages comparison

5.4 Effects of flexural properties on the maize husk-based composites produced

The results of the semi-static 3-point bend test helped to discard some of the MHC alternatives, based on the data obtained from the 19 pre-selected boards. The targeted properties were set taking as a baseline a 3 mm wood-based light MDF and MDP as detailed in the data matrix (Figure_Apx 7-12). The MHC board labelling found through this section remains the same as in section 3.2.9.

MB-M, ME-M, MB-M and AKE-M specimens density fell within the expected levels, yet only ME-M compared the bending strength control valves as shown below in Figure 114 and Figure 115. Moreover, WL-M presented higher density values than similar AW-based fibreboards found in the literature [171,202], its resistance remained significantly lower (Figure 116). The MOR analysis showed significant differences between Bs and L boards to the SSE group. Taking a closer look to the Bs group, it can be concluded that only CHB-M and MB-M samples differ 60 % from each other, while the rest of the Bs samples did not show significant differences amongst them. The lignin bonded boards had no apparent differences between them, yet they were not comparable to the control sample either, even though the samples with bigger MH segments showed a slightly higher resistance. On the other hand, the green epoxy resin group did not show significant differences, in comparison to the other blends. Therefore, at this point, only ME-M samples showed the possibility to reach light MDF strength.

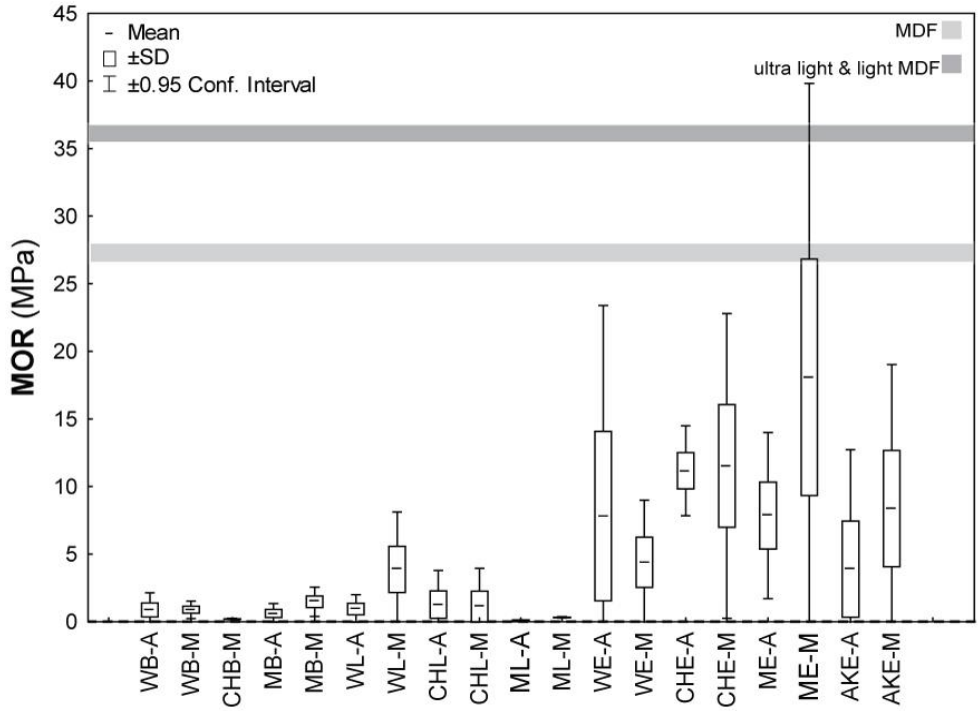

Figure 114 MHC's produced boards MOR statistical comparison to WBF [200,201]

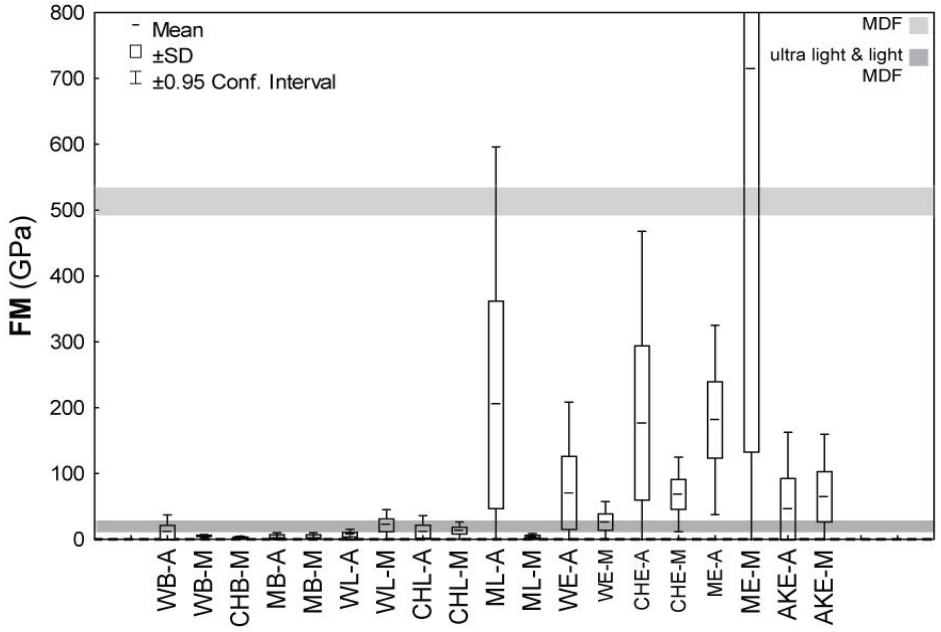

Figure 115 MHC's produced boards FM statistical comparison to WBF [200,201]

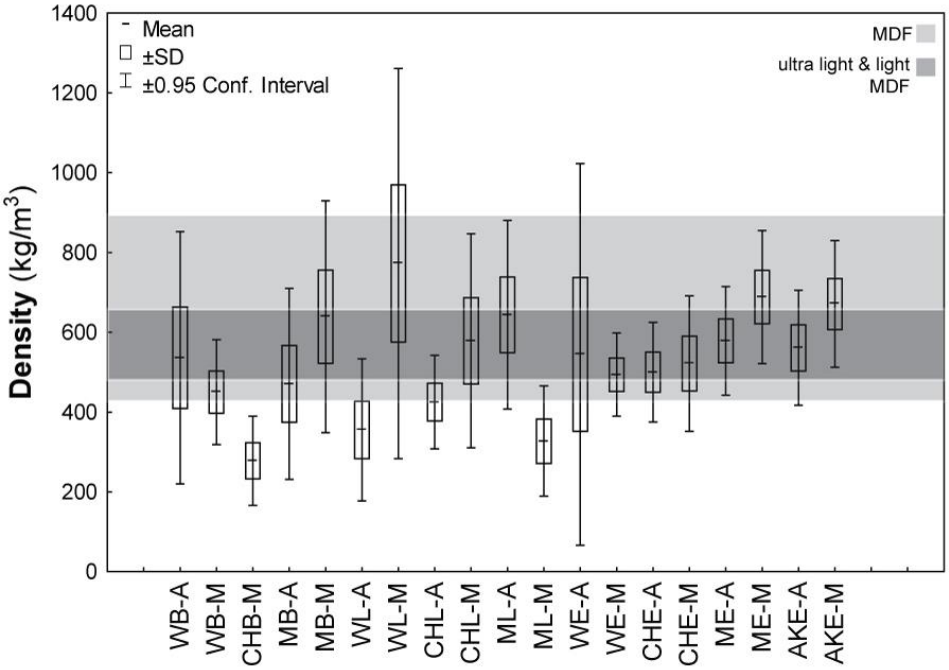

Figure 116 MHC's produced boards density statistical comparison to WBF [200,201]

Moreover, the flexural strength was found to vary according to MH size and matrix combination. During testing severe interlaminar shear was observed on MHC boards, the fractures observed were not constant, in contrast to the typical failure in CM observed by Purslow [129] in synthetic fibre reinforced composites. Therefore, it is assumed that this behaviour change was because of the use of NF.

Moreover, delamination was recurrent within MHC lignin group samples as shown in Figure 117 (a) and (d); however, these specimens demonstrated a higher flexural strain than the Bs and SSE samples. On the other hand, a rather interesting result was observed in WB-M specimens as the board delamination did not occur, this is attributed to MH's natural structure which improved MHC' flexibility considerably.

Now turning to the failures shown in Figure 117(c) and (d), these were identified based on Purslow's [129] work as a surface peel. Notwithstanding that WB-M

sample did not break during the test, only CHE-M specimens did not show a complete de-bonding; albeit they did show fibre shear in addition to the delamination (Figure 117(b)).

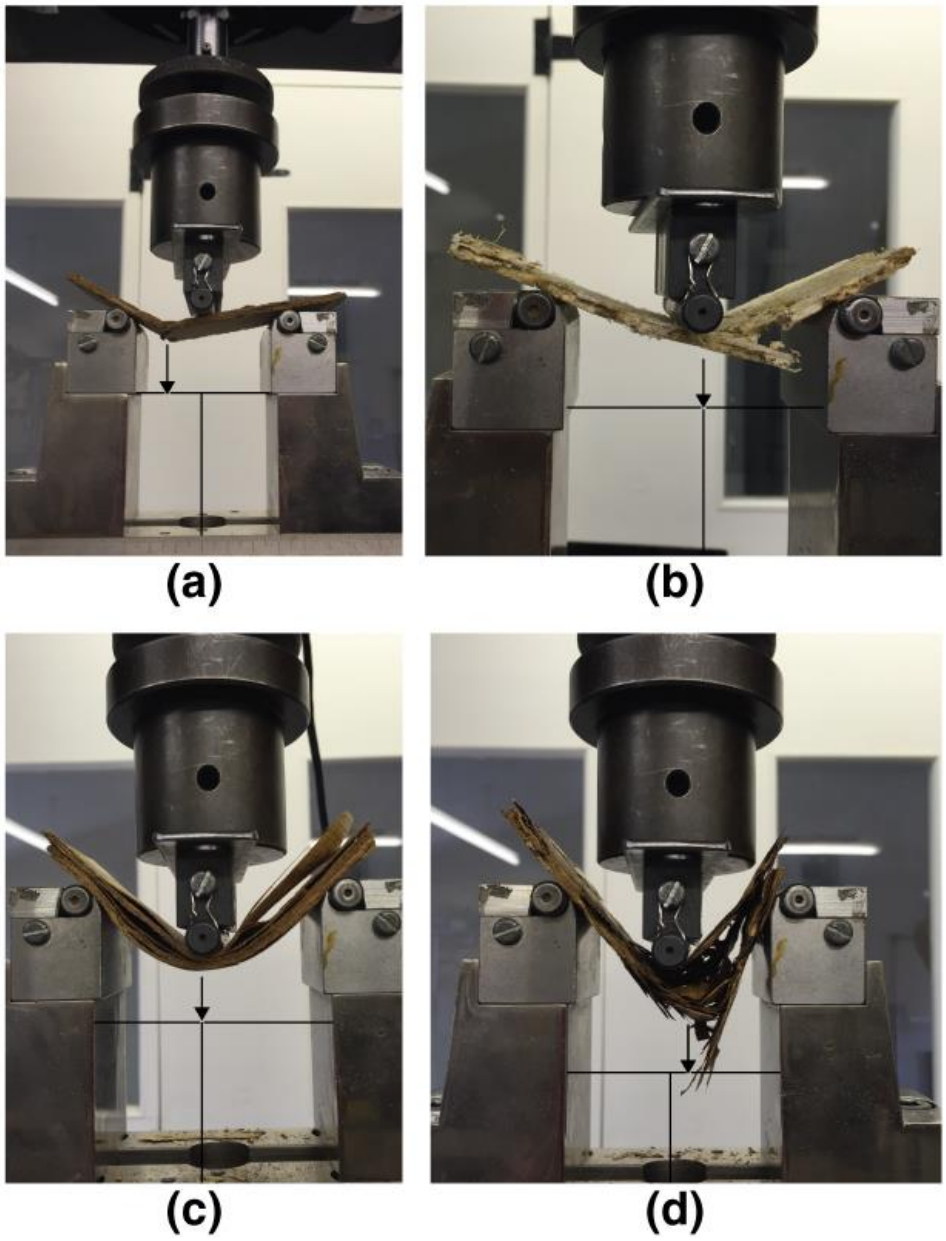

Figure 117 3-point bending test samples during tension, (a) ML-A breakpoint displaced from the centre, (b) AKE-M sheared breakpoint and delamination, (c) specimen WB-M and (d) CHL-A showed an interlaminar peel failure

For the first batch, the pressure settings were based on Pizzi's [121] report on bio-based adhesives resistance to heat and detailed in section 3.2.9.6. The trials with raw MH took more than planned because the heat resistance in MASH and ASPROS husks presented a variation of ± 50°C. Thus the MHC manufacturing process had to be dived to maintain the adequate temperature for the fibres and binder, so the obtained boards were not structurally damaged from the beginning. Once the temperatures were standardised the MHF bonding with the binders (Bs, L and SSE) resulted into a wide range of MHC, as the manufacturing parameters differed the thickness and densities of the MHC boards did too as shown in Figure 118.

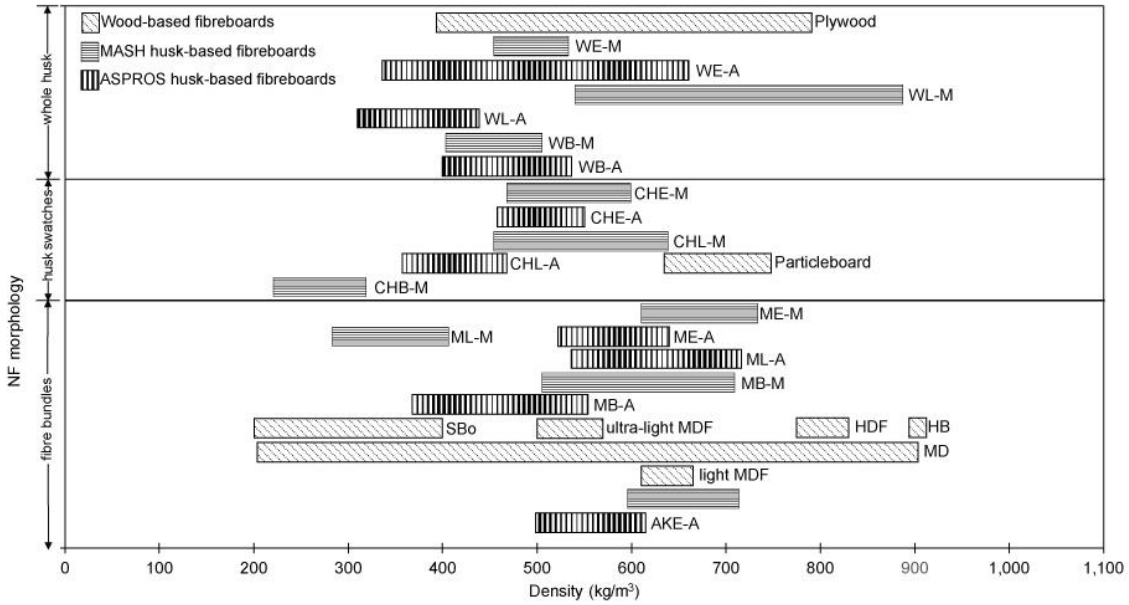

Figure 118 Classification of MHC boards and most common WBF by size and density

Previous studies (Halvarsson [153] and Faruk et al. [110]) evaluated AW-based fibreboards reported uneven results on average density; though, they confirmed that the mechanical properties of the materials with a higher density were positively affected. Density echoes the efficacy during the hot-pressing by re-arranging MHF atoms to form a compact and reliable MHF/binder coupling. However, Ashby and Jones [208] reckon that an NF-based composite density

cannot be higher than 2500 kg/m^3, this is because of the large presence of C and O atoms in NF.

Perhaps the most compelling finding at this stage was to demonstrate MH's wide range of possible materials despite the fibre low strength properties observed. As it has been already discussed MH size reduction significant effect on the mechanical performance of the MHC material, yet from the two MH types and four extraction methods only one of each were selected to manufacture the last MHC batch.

5.5.1 Influence of different fibre/matrix configurations on maize husk-based composites manufacturing

As previously outlined in the literature review, neither the addition of NF to the composite manufacturing nor the reduction of oil-based resins would represent significant progress towards more sustainable development. Instead, the rethinking of the whole production system may give us that opportunity. Thus, aspects such as responsible consumption, re-use, recycle, smart disposal and recuperation to the productive cycle were considered into the MHC (Figure 143).

Sampathrajan et al. [209] provided important insights into NF's advantages when employed as CM reinforcement due to their specific properties, i.e. wool and coir thermal isolation and flexural resistance. Moreover, Reddy and Yang [96] reported that the obtained fibres from the MH showed a tendency to be coarser after being exposed to lower levels of alkalinisation. MHF's natural structure has been compared with cotton fibres; both are ribbon-like with entwined fibre bundles, expected characteristics of fibres used in the textile industry [157].

Given the breadth of possible fibre changes when they are chemically modified, observations in NF of Gassan and Bledzki [114] served as an indicator to deduce MHF' transformations. Thus, Figure 119 shows potential hydroxyl

groups (-OH) rearrangement after MHF alkalinisation, which helped to increase fibres hydrophobicity. Another common outcome reported in NF when exposed to NaOH is the fibre shrinkage, which is likely to affect MHF' strength because of the accelerated loss of hemicellulose [114]; though such modifications resulted in a more homogenous fibre surface ready for binder coupling as shown in Figure 75.

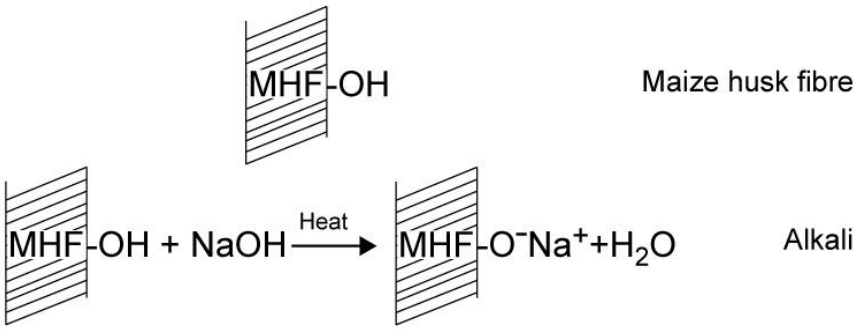

Figure 119 Hypothetical reaction of MHF with sodium hydroxide (NaOH)

Rowell et al. [210] remark fibre size, humidity uptake and fibre dispersion as the common drawbacks when working with agro-fibres. Figure 120 shows the most relevant faults in MHC boards surface topography, displaying (a) and (c) lignin crystallisation and uneven surface due to MH chunks overlapping. Process conditions and processing aids were needed to obtain efficient boards, based on the early findings provided some support for the MHC selection, optimisation and further testing, to eventually obtain an MHC board that rendered appropriate strength and performance levels. In the same fashion, uniform fibre dispersion was compromised during processing techniques as shown in Figure 120(b) and (d), by modifying initial MHF lengths. Several compounding methods had to be tested to improve lignocellulosic fibre/thermosetting matrices blending, so a continuous surface and structural stable boards could be obtained. Another challenge faced during the MHC boards manufacturing was to decrease voids incidence (Figure 121); this accords with the earlier observations on fibre clumping compromising MHC mechanical performance.

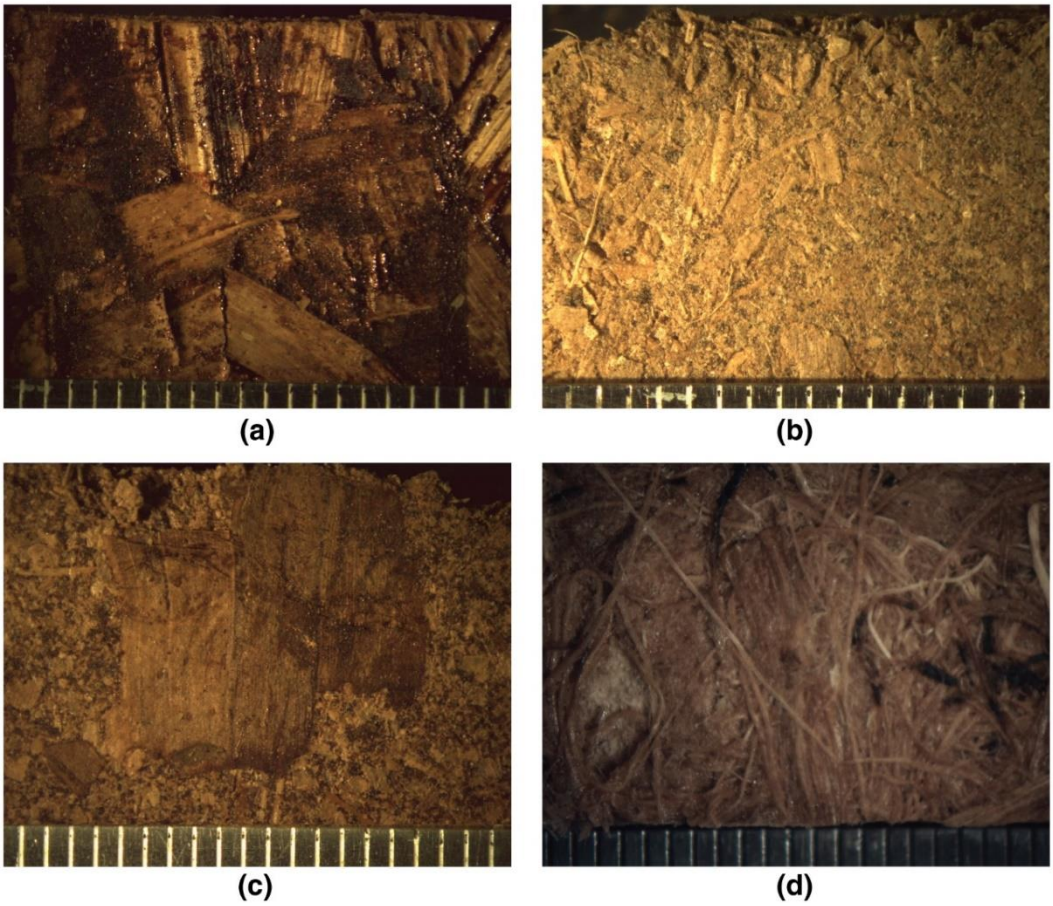

Figure 120 MHC boards micrographs of surface topography: (a) chopped/lignin, (b) milled/SSE, (c) complete MH/binderless and (d) alkali MHF/SSE

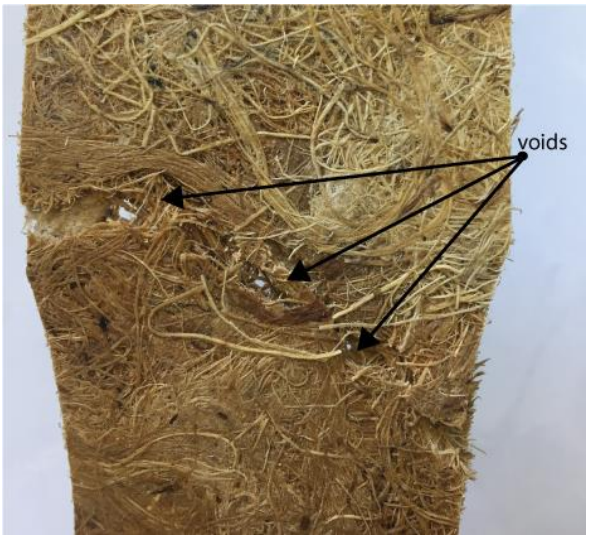

Figure 121 AK30 sample showing voids and uneven surface

The issues encountered during the initial MHC production and the appropriate adjustments required for each blend increasing the number of trials considerably. However, the knowledge gained from MHF increased and facilitated the production of nineteen acceptable boards to be tested and analysed further. Therefore, as depicted in Figure 122 MHC board' dimension stability was successfully improved, by leaving a perfectly angled and clean edge.

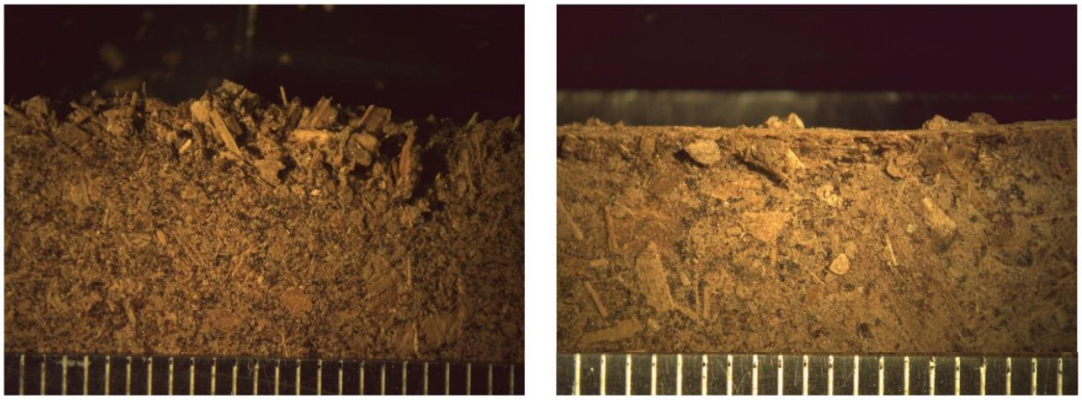

Figure 122 Milled husk/SSE resin boards edge stability comparison after demoulding. M30 (a) first batch board and (b) second batch

Moreover, initial MHC compounding was based on the limited literature found on MHF' heat resistance and cellulose degradation levels [159,188,196]; thence, compounding trials had to be carried out to obtain the correct temperature and press time per blend, resulting in a different matrix/fibre interfacial strength. Given these facts, a number of drawbacks and manufacturing issues were faced during this phase, such as a dramatical volume reduction and fibre stalking during the board's production, resulting in voids (V) across the surface (Figure 123(a) and (b)). Contrary to expectations, this study did not find a significant difference between MHF and other NF's used in fibreboards'. However, it was surprising that the different binders did not represent a significant factor in the hot-pressing issues, though they were more frequent as the MH' size changed as shown in Figure 123(d).

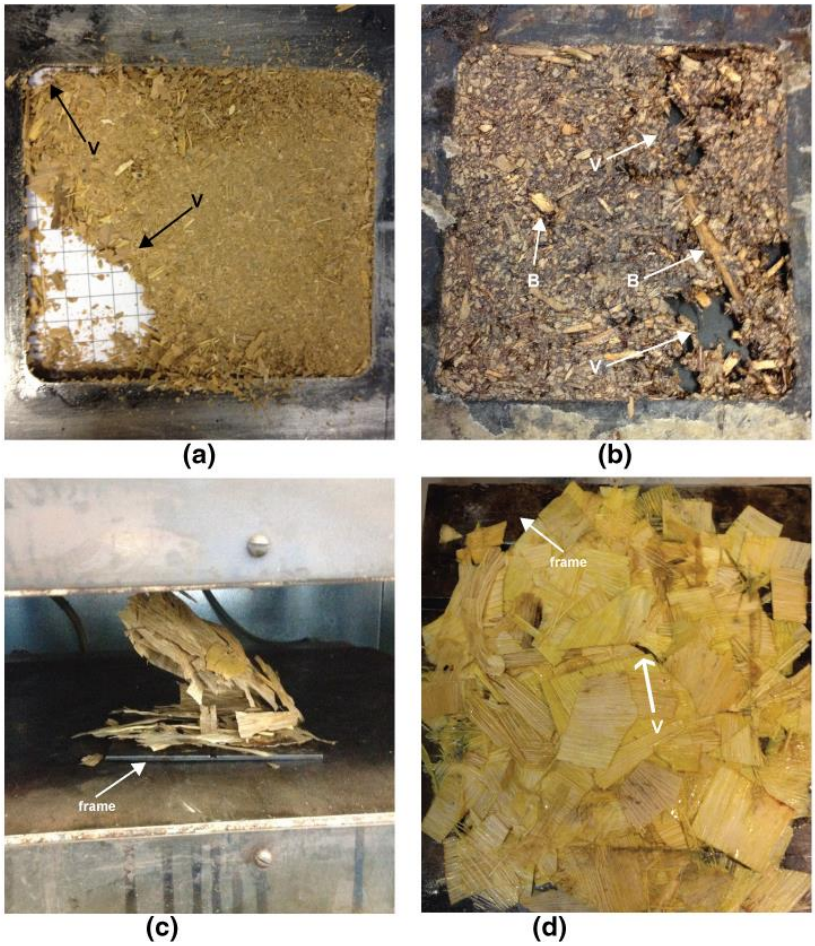

Figure 123 MHC manufacturing failures: (a) MB-A showed a high number of voids (V) due to the lack of MHF. (b) ML-A had the presence of big bast pieces (B) affecting boards' integrity, hence generating voids (V). (c) WB-M showed severe delamination after hot-pressing. (d) CHE-M the MH swatches exceeded the frame leaving empty areas (V) and the edge with material surplus

Although some MHC boards had a severe presence of fibre stacking and some sections (Figure 123(d) and (b)), it is believed that the weak fibre/matrix bond caused MASH-W delamination observed in Figure 123(c). These results observed in the MHC are consistent with that of Ye et al. [126] who persistently found these manufacturing issues in the wood-based board's production. Responding to an incorrect resin/ fibre proportion that restricted the linkage between both agents. Thus, the MHF and binder proportions had to be

reconsidered for further samples, besides the temperature variations before mentioned.

5.6 Selection and optimisation of the manufactured maize husk-based composites

MHC boards were subject to thorough scrutiny supported by Pugh matrices (Table 31, Table 32 and Table 33); yet, to assure an objective board selection Ashby and Jones's [208] scheme of how engineered materials force manufacturing industries to adapt to them (7.1Appendix G) was revised. Resulting in substantial and more comprehensive manufacturing system (SDA) in which the designed material would not be exempted from meeting the standardised criteria for cellulosic fibreboards (attributive and intrinsic properties). Following this exploratory research MHC boards were produced with the help of simple adaptations to the current WBF production line, making more affordable the shift towards alternative cellulosic materials. A total of 72 trials were manufactured. However, only 19 had the structural strength and steadiness to be tested and studied more in detail. Figure 124 illustrates the heterogeneity of the press parameters used, that resulted in different thicknesses and densities of the compounded boards. The MHC's aimed thickness was of 3 mm, yet considerable anomalies were observed during the manufacturing process, e.g. faster heat degradation, binder maturing, which affected the density/thickness synergy greatly.

Moreover, the optimised MHC boards were produced at two different resin levels: 20 % and 30 %, and only two fibre extraction methods were used (milling and alkalinisation). Although a more long-lasting solution should be considered for adequate full-scale production of MHC boards, waxed paper sheets during pressing were used, so the use of a release agent was not necessary and minimised MHF stacking, voids presence and MHC fibreboards adhesion of to the press plates.

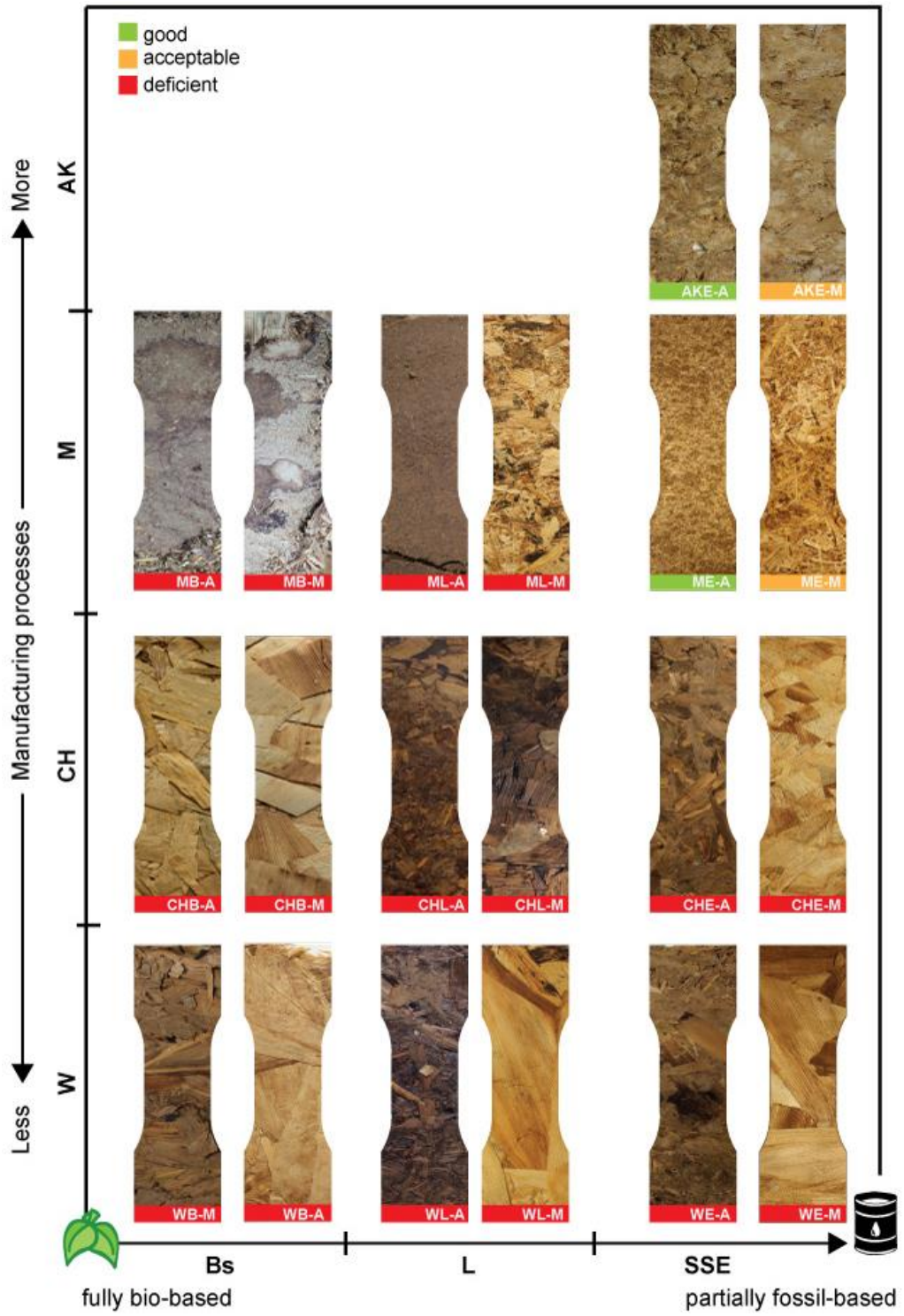

Figure 124 MHC boards manufactured and tested. The boards are classified by MH size, binder nature and number of manufacturing processes involved in the boards manufacturing

Even though most of the ASPROS-based specimens showed limited flexural properties and water uptake (wt.%); AKE-A and ME-A had a competitive and promising performance. These results are likely to be related what Mohanty et al. [109] mentioned on board's strength that can be attributable to the physical and mechanical properties of the MHF, binder type and the way these two are linked.

On the other hand, despite MASH composites showed very competitive results, and in some cases superior to those obtained by ASPROS-based composites. However, its close relation to the traditional Mexican cuisine and high demand led us to dismiss MASH-based samples. Therefore, from now on all the specimens tested were made using only ASPROS husks.

Table 39 summarises MHC flexural results and compares them to similar AW-composites found in the literature. These results further support the idea of AW' high-density levels, showing that ME-A, hazelnut husk and laccase boards density average fell within MDF's one by ± 5.4, 5.9 and 13.6 % respectively. However, no evidence of higher MOR outcomes from the three MH blends was found; Thus, leaving the extremes to Lacasse-based board with the highest modulus and hazelnut-based with the lowest. Moreover, the reduced FM in AKE-A samples can be explained by the high presence of voids in the boards. A possible explanation for this condition might be uneven fibre wetting during the manufacturing process as suggested by Sellers et al. [211].

Table 39 Properties of produced MHC first batch and similar AW- based boards

NF-based boards	Binder	Thickness (mm)	Density (kg/m^3)	MOR (MPa)	FM (GPa)	Wt.%
ME-A	SS	3.0	579	7.9	181.4	3
ME-M	SS	3.0	714	18.1	714.3	5.8
AKE-A	SS	3.5	561	3.9	45.1	5.6
Light MDF	UF	3.1	755	36	501.4	5.1
Hazelnut husk 30% MDF [202]	UF	10	800	1.4	n/a	12
Laccase fibreboard [171]	Lignin	8	858	40.1	/	/

Moreover, AL-Oqla et al. [163] extensive studies on NF-based composite materials development have proven that the most significant challenge is the insufficiency of data due to the large variety of NF, matrices (binders), and manufacturing processes. Therefore, when designing a novel composite material, there are specific variables to consider [208,212], some of the most important are summarised in the following scheme in Figure 125. In which MHC boards can be tailored to the market/client needs since this approach allows to revisit material's assessment and selection as many times as required to continue improving its properties and manufacturing processes. Thus, the most obvious finding to emerge from this approach is that even in the most elemental processes used, the DT and SDA principles carry the most weight.

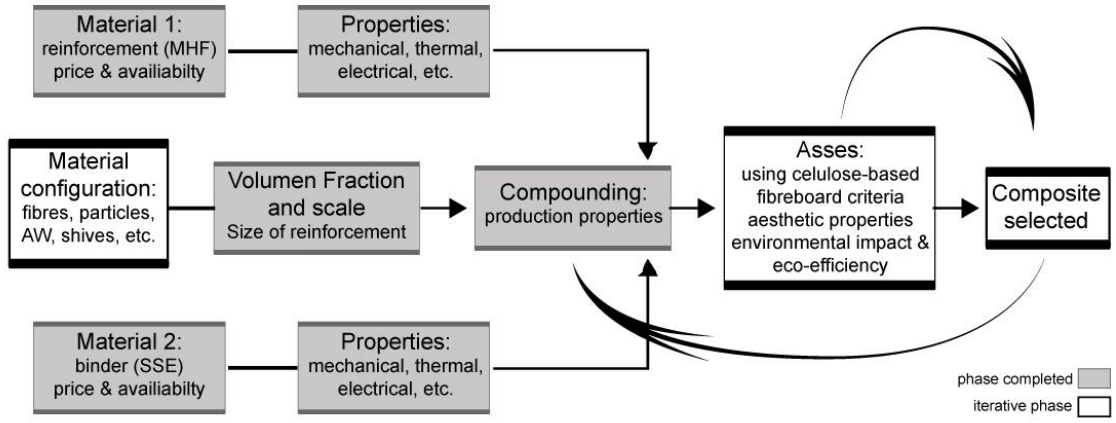

Figure 125 Design variables in composites by Ashby and Johnson [212], adapted to the MHC development process

In the first batch of MHC samples, vast differences were observed on the physical properties due to the wide blend selection (MH size, binder and husk type), that resulted in various chemical microstructures. Although this diversity provided interesting insights, the variables had to be reduced to get a more in-depth assessment of the second MHC batch; thence, based on BS-EN 312-2010 requirements, standard mechanical tests were performed. As Table 40 shows, the best results were found in the alkali extracted fibreboards with a

density greater than 1000 kg/m^3. Result that surpassed commercial MDF's density, therefore AK30 boards can be considered a potential HDF. These results demonstrate MH's capability of producing moderate mechanical properties compared to the reference fibreboards, glued with thermosetting resins.

Table 40 MHC mechanical and physical properties compared with light MDF [200]

Specimen	Density (kg/m^3)	UTS (MPa)	Elongation at break (%)	*E* modulus (GPa)	Swell in water, 24 H (%)	Impact resistance (J/m)
Light MDF	720-735	18	0.5	4	15	/
M30*	889.7	15.3	2.2	1.2	22	8.3
AK30**	1014.3	14.7	1.5	1.6	47.6	12.6
M20*	864.8	14.0	1.9	0.9	28.6	6.6

The nomenclature used for the first batch * ME-A ** AKE-A

The wood-based materials *E* modulus variation (0.8-25 GPa) reported by The Engineered Wood Association [203] showed a significative lower gap between those obtained in MHC boards. Figure 126 graphs depict 0.95 CI of *E* modulus values from M30 specimens that fell within MDP and light MDF ranges. As for the alkali treatment samples (AK30), they produced a significant reduction of 30 % overall performance; whereas M20 samples had a more discrete reduction of only 13.6 %. Comparison of the findings with those of the first MHC batch confirms that the use of MHF could be greatly improved by adjusting manufacturing settings and fibre's natural moisture uptake. Thus, demonstrating that MHF/SSE interaction is more efficient than the wood fibres/UFM since the UFM's strength declined by half when mixed; Even though SSE Young's modulus remains slightly higher than all the MHC specimens. In conclusion, it is evident that the tensile strengths of MHC boards decreased slightly as the MHF loading increased in the same fashion as the coir fibre/polyester composites evaluated by Monteiro et al. [38].

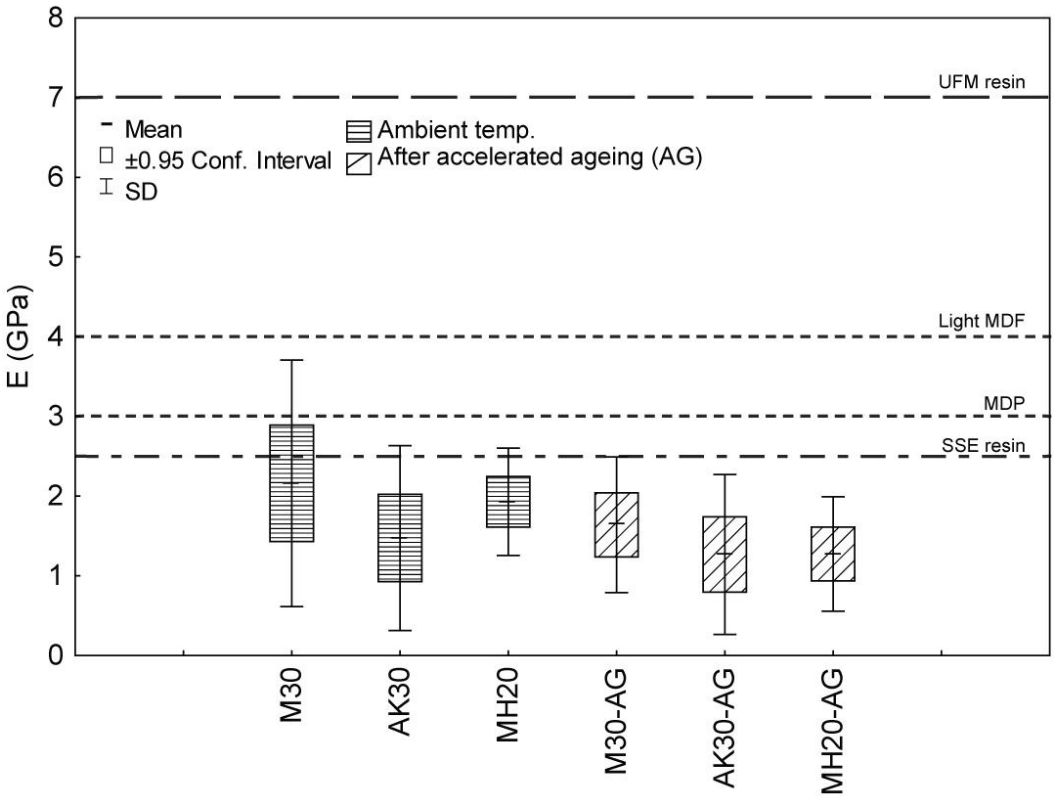

Figure 126 Young's modulus performance MHC boards before and after AA, resins used for fibreboards and wood-based boards (fibreboard and light MDF)

Figure 127 displays MHC's board UTS, where the highest was showed by M30 at 15.3 MPa; however, the difference between AK30 and M20 was of 4.5 %. Therefore, there is not enough evidence to conclude that there are significative differences between the three blends, since a $p<0.05$ was recorded. What is more, even after the environmental exposure the MHC' means did not differ significantly. Interestingly, M30 specimens reported an increment of 6.5 % on the UTS after the AG exposure. Meanwhile, AK30 and M20 had a strength reduction of 23.8 % and 7.8 % respectively.

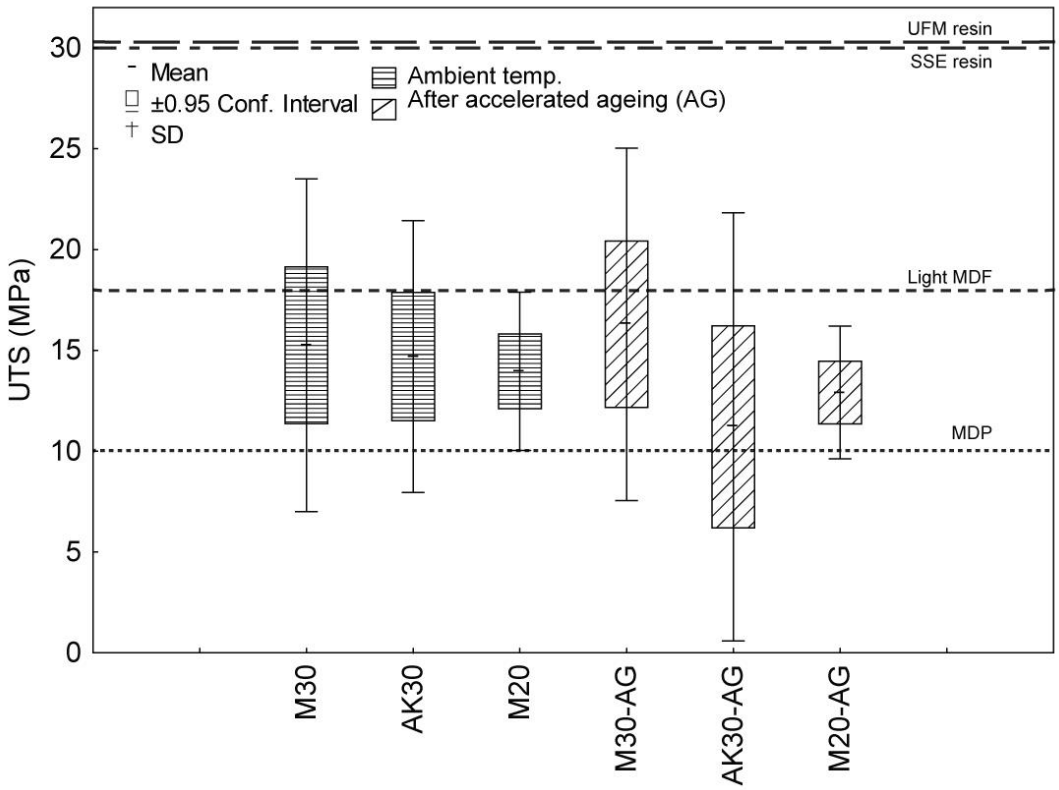

Figure 127 UTS performance of MHC boards, resins used for fibreboards and wood-based boards (MDP and light MDF)

These results suggest that the MHF's size and extraction methods applied did not influence UTS and *E* modulus, as much as they did in density and elongation levels. Alkali-treated fibres boards (AK30) increased 2.5 times their elongation levels (from 1.5 to 3.8 %), whereas the milled specimens (M30 and M20) showed a reduction of 27.2 % and 10.5 % respectively, after the AG exposure as shown in Figure 128. These results confirm Guimarães et al. [204] and Yilmaz et al. [127] suggestions on the effects of chemical extraction on MHC material performance. Based on the literature, these enhancements are believed to be related to MH fibre CSA reduction and the given elasticity of the SSE resin [133,179,206]; Even though the MHC boards showed rather low elongation levels, they did not show a reliable performance as their CI is higher than before the AG.

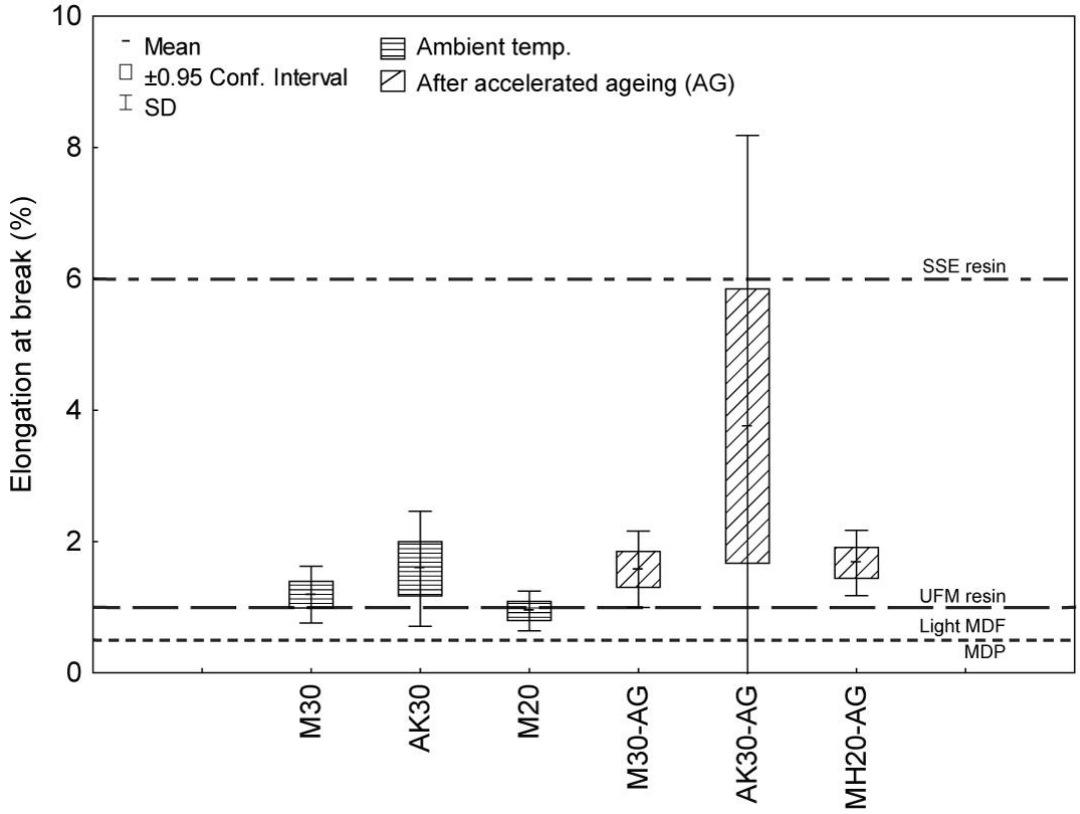

Figure 128 Elongation at break comparison between MHC boards manufactured, resins and wood-based boards (fibreboard and light MDF)

Huda and Yang [92] and Reddy and Yang [96] reported similar investigations but using thermoplastic matrices in which they confirmed that the decrease in UTS is indeed due to the reduction in fibre diameter; thus, a consequence of the loss of the non-cellulosic elements which were removed by the alkaline treatment. On the other hand, Pickering et al. [146] stated that alkali treatments not only modify cellulose structure but increase surface coarseness, thereby creating a stronger interfacial bonding. Figure 129 describes the hypothetical chemical reactions of milled and alkalise MHF with bisphenol A/F type epoxy resin (BA/F) as one of the main elements of the SSE. During the alkalinisation of MH, a realignment of the hydroxyl groups (-OH) occurred, resulting in a strong linkage to the SSE (Figure 129(3)). Though, if the reaction takes place in an acid solution, it would be as shown in Figure 129(2). Finally, it is important to

highlight that BA/F was used as SSE's exact chemical identity is protected under trade secret [213].

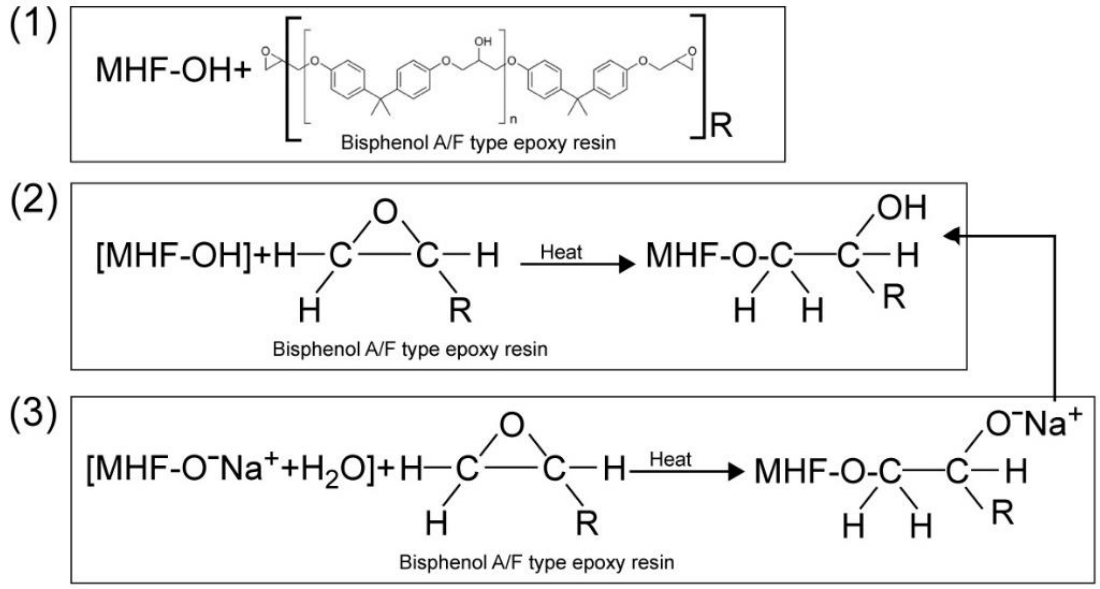

Figure 129 Hypothetical maize husk composite chemical reaction. (1) MHF, AR plus BA/F resin, (2) BA/F resin with milled maize husk fibre, and (3) alkalise maize husk fibre. R represents BA/F organic group

Figure 130 can be SSEn the load-elongation curves obtained in the tensile test. M30 and M20 curves indicate that both milled samples had a linear elastic behaviour. Hence they are more brittle than the other blends. As for the alkali extracted samples (AK30) those resulted in being more ductile, as consequence of MHF/SSE stronger cross-link reached. Even though AK30' first section of the curve is very similar to the milled specimens; these specimens did not break immediately. Thus, such behaviour might be due to MH fibre' entanglement, that consequently increased interlaminar strength of the composite.

Moreover, these improvements seen on MHC's mechanical properties are directly related to MHF alkali extraction. However, the changes observed were not far from results obtained in the samples with resin reduction (M20) (Figure 131 and Figure 132). Further improvements were observed in the alkalised MHF boards that showed a good interfacial bonding and less presence of voids.

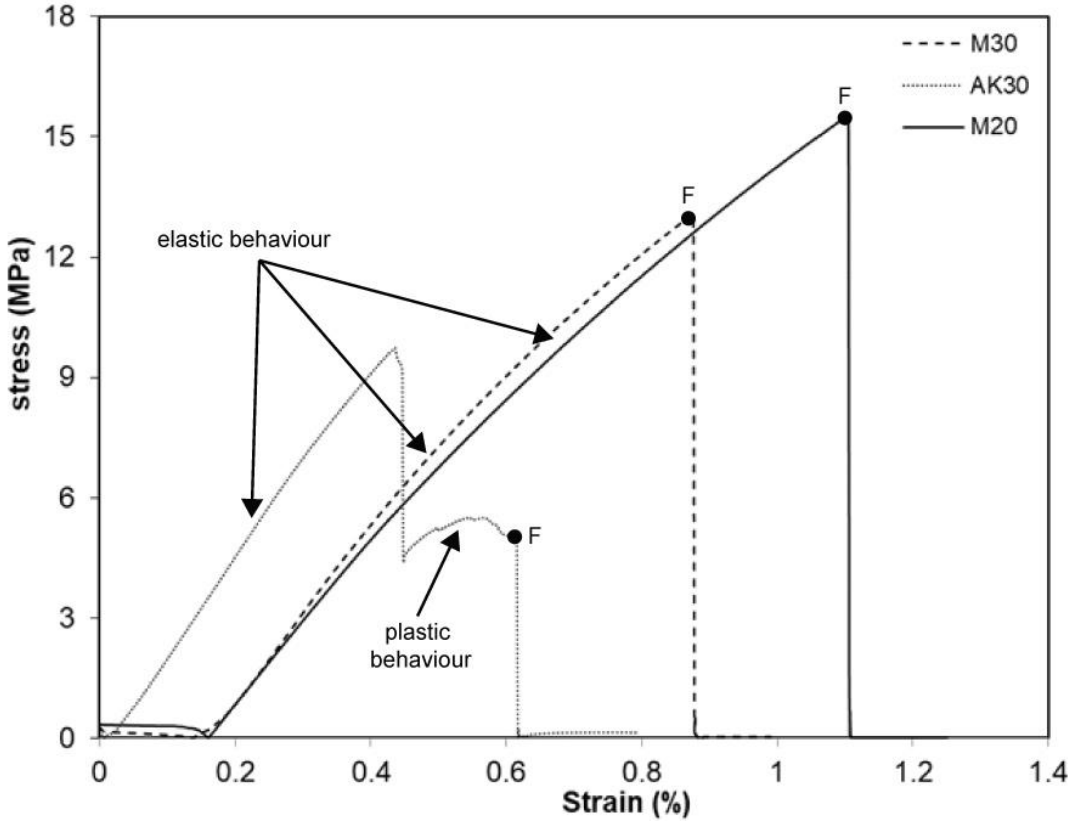

Figure 130 A typical stress-strain curve for MHC specimens indicating fracture point (F), elastic and plastic regions

Figure 131 AK30 control samples fractures after tensile test

Figure 132 Aged AK30 samples fractures after tensile test

One unexpected finding was the extent to which MHC's mechanical properties investigated (Figure 126, Figure 127, Figure 128 and Figure 130) demonstrated that tested boards could be used under more challenging environmental conditions than only as interior panels. Moisture resistance and thickness swelling remain as the principal drawbacks for AW-based composites when compared with synthetic fibres-based [110,122]. Results obtained from the AA conditions, they had evident surface attrition shown in Figure 133, aside from its mechanical detraction before reported. All three MH blends showed surface darkening. However, AK30 specimen exhibited more evident signs of structural decay (delamination, swellings and uneven surface).

Furthermore, the tensile test proved in accordance to Reddy and Yang's [72] data on AW-fibres, that milled specimens' clean fracture places them within stiffer material' behaviour. On the other hand, AK30's lower *E* modulus and UTS concord with consistent plastic response in both tensile tests (before and after AA). Even though M20 resin ratio has considerably lowered its mechanical performance after the ageing, it did not represent considerable attritions in the

material's surface. This outcome is similar to that of Cysne Barbosa et al. [214] who reported signs of cracks and delamination in carbon fibre/epoxy composites after AA. Regardless that MH fibres' strength is noticeably more limited than carbon fibre's, the resin wearing and general deterioration proved to be very similar. Therefore, AA provided enough evidence supported by the mechanical tests, to hypothesise that MHC boards comply with the international standards as a non-structural wood-based fibreboards (MDF and MDP) substitute. Although, it is worth to mention that the environmental conditions in which the MHC boards were tested are not likely to occur when used in interiors. Therefore it may be assumed that under mild conditions they can perform well in outdoor environments.

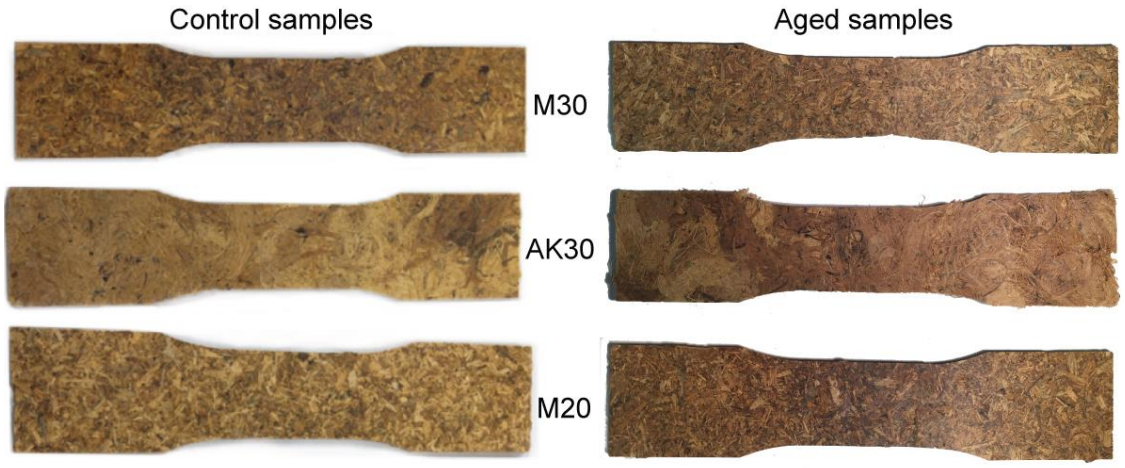

Figure 133 MHC boards visual comparison after AA exposure

Further analysis on the aged surface showed a dramatic thickness swelling in the AK30 specimens (47.6 %), whereas the milled specimens only had 20 % distension. The mass variation was higher in M20 (4.8 %) in contrast with M30 and AK30 that only showed an increment of 3.3 % and 3.9 % respectively. These findings are presented in Figure 134 reflect the SSE content in the boards, though the alkalinised fibres also exhibited a slightly higher mass difference as it has been observed in Rathke et al. [181] and Ku et al. [215] work. The weight gain did not occur progressively, the reason for this behaviour

is that the environmental chamber did not have constant conditions such as temperature, humidity and exposure time as ASTM D1037-12 [176] suggests.

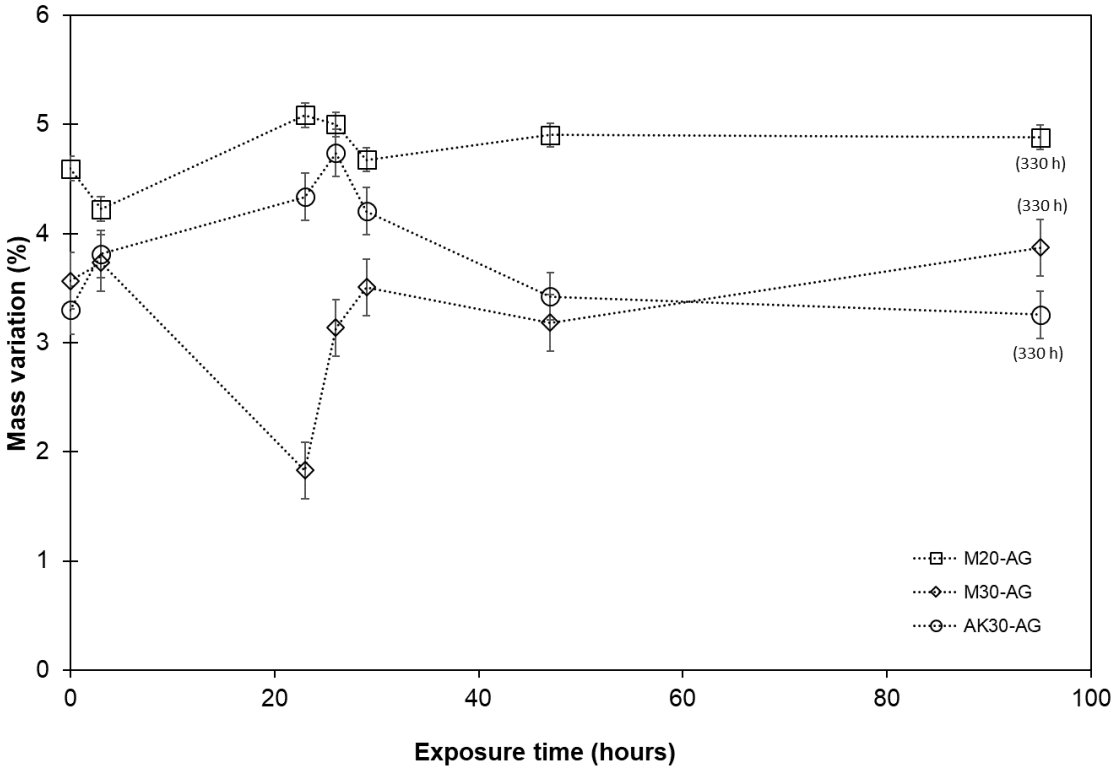

Figure 134 MHC boards mass variation during AA, the final conditioning step was carried out 48 hours after completing six cycles so that the boards will settle after all the stress. SD bars are smaller than the markers in some cases

Microscopic analysis of the samples allowed to observe the fibre/binder dispersion, compression and other physical changes on the MHC boards along the cross-sectional area. Figure 135 shows the surface and edge of all control samples, from which it can be noticed that the milled samples had a better fibre distribution (b) and (d), in contrast to the alkali that kept air bubbles (circles) between the fibres and the resin (c). All the specimens had, in different proportions, gaps between MHF and SSE resin pointed out with arrows, a signal that a better fibre impregnation might be helpful to diminish this voids (a), (e) and (f).

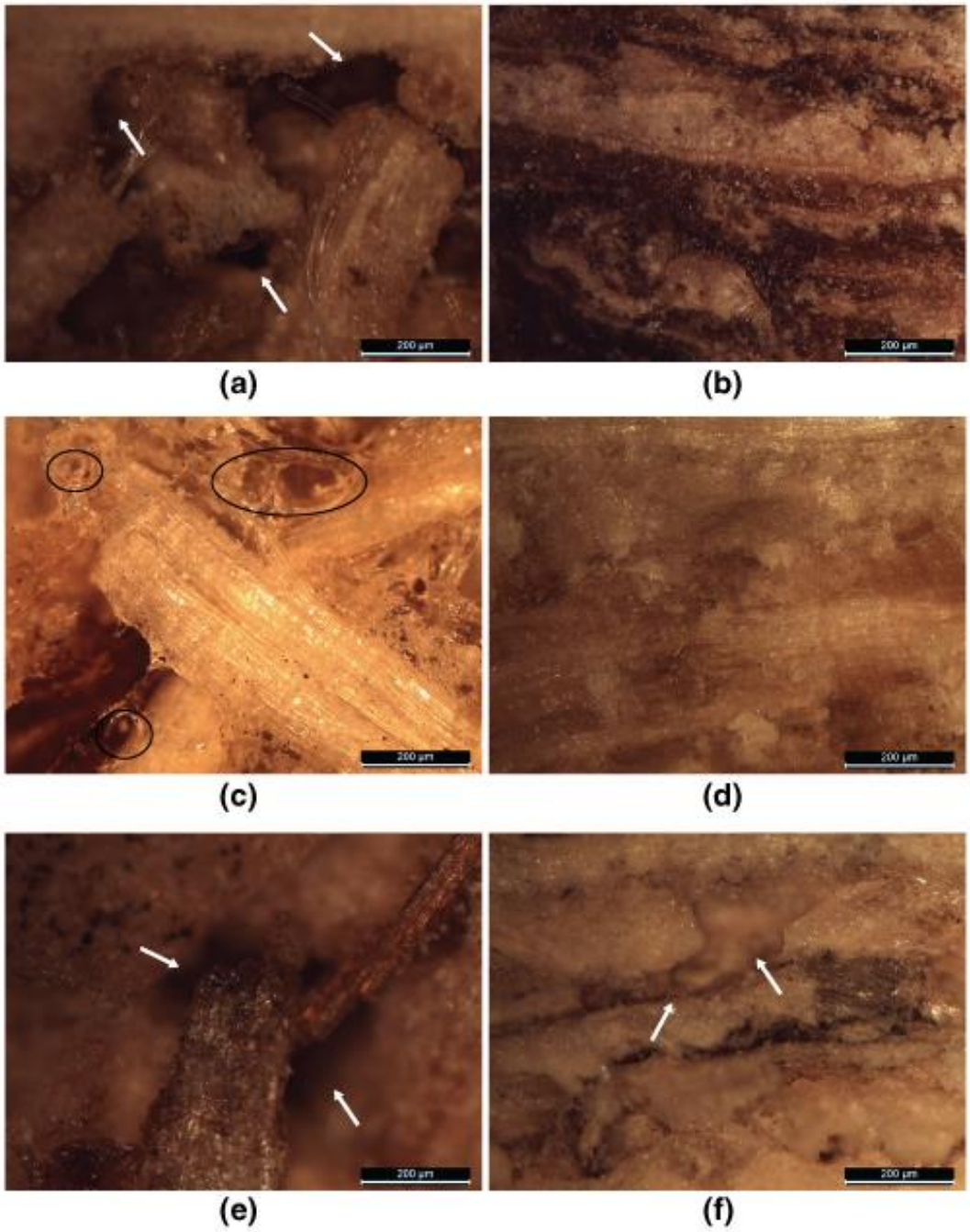

Figure 135 MHC control samples micrographs of MH/SSE bonding. (a) M30 surface and (b) board edge; (c) AK30 and (d) board edge; (e) M20 surface and (f) board edge. Air bubbles trapped between binder and fibre are circled, whereas the mass gaps (voids) are pointed with white arrows

The second MH-based fibreboard batch had a better appearance and surpassed the first batch's quality after pressing, as discussed before (Figure 122). The highest density was found on the alkali extracted specimens (AK30), with an average density above 1000 kg/m^3 doubling first batch specimens'. Even though the milled board's range had a slightly lower density of 800-900 kg/m^3, values that fall within those found in standard MDF and even HDF boards; Therefore, all three MHC boards can be paired up with WBF's typical density as shown in Figure 136.

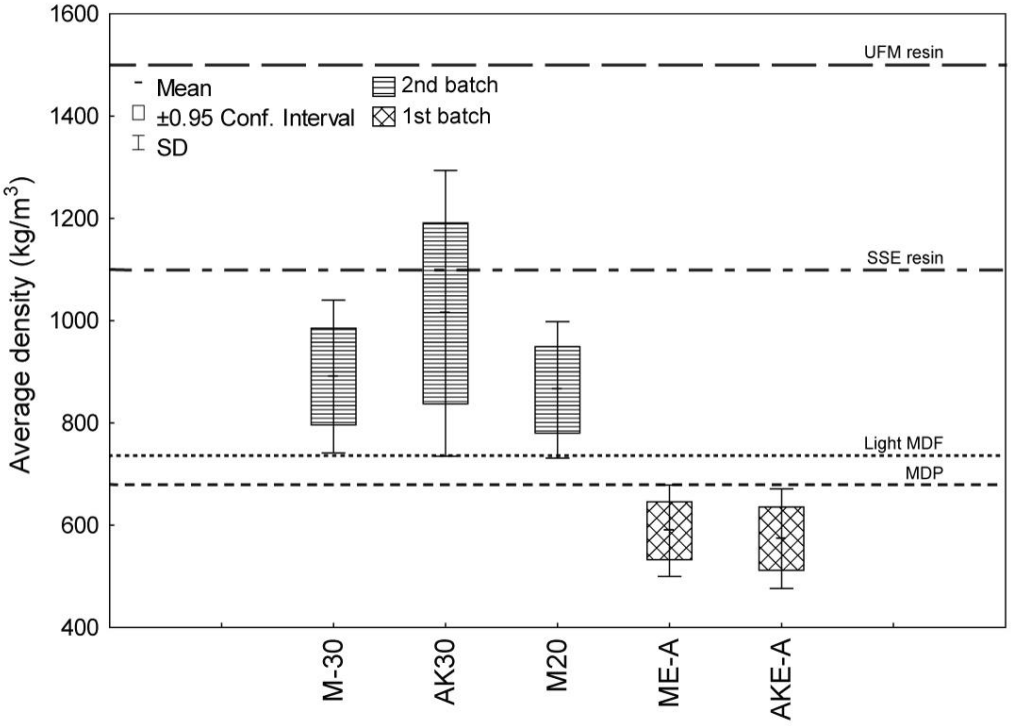

Figure 136 Average density comparison between the two batches of MHC boards, resins and WBF (fibreboard and light MDF)

Figure 137 shows MHC fibreboard IR, same that had a significant increment in AK30 specimens; yet remains 20 % below WBF levels. What is more important to recognise here, is that even though the IR is not as expected, the MHF ductility coupled with SSE strength can produce a viable CM. Maybe the

applications initially though (decorative or wall panels) for the MHC will not work, however this does not mean it is not a valuable material.

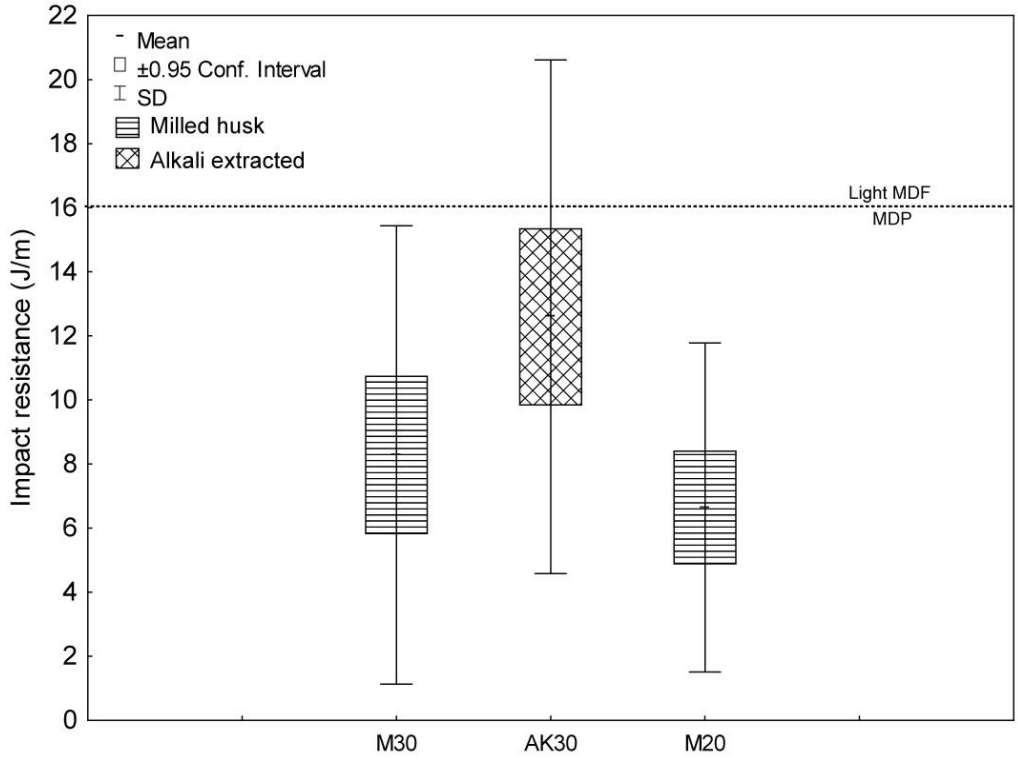

Figure 137 Impact strength plot of MHC compared to WBF

Results showed that the breaking point in the M30 remained consistent in all the samples tested, contrary to the other two blends, M20 and AK30, this behaviour might be related to a more uniform fibre wetting during manufacturing. All the samples made with milled MHF detached completely after the impact (Figure 138(a) and (c)), whereas half of the AK30 samples did not (Figure 138(b)). Several factors are known to influence such reduced IR and can be attributed to MH's natural wavy shape, MHF length and the elasticity gained through the alkalisation. In the case of the milled specimens (M30 and M20) it has been suggested by Adams [102] the shorter the MHF the stress and strength of the boards are determined by the fibre/matrix bond; thus these specimens exhibited a 20.5 % IR reduction. Although the resin reduction influenced the IR results too, it was not the principal cause. Overall, the impact levels observed fall far

below those in light MDF and MDP boards. However, the findings in the MHC resulted comparable to the obtained in the jute/PP composites (6.04-9.18 J/m) reported by Bakar and Hassan [216].

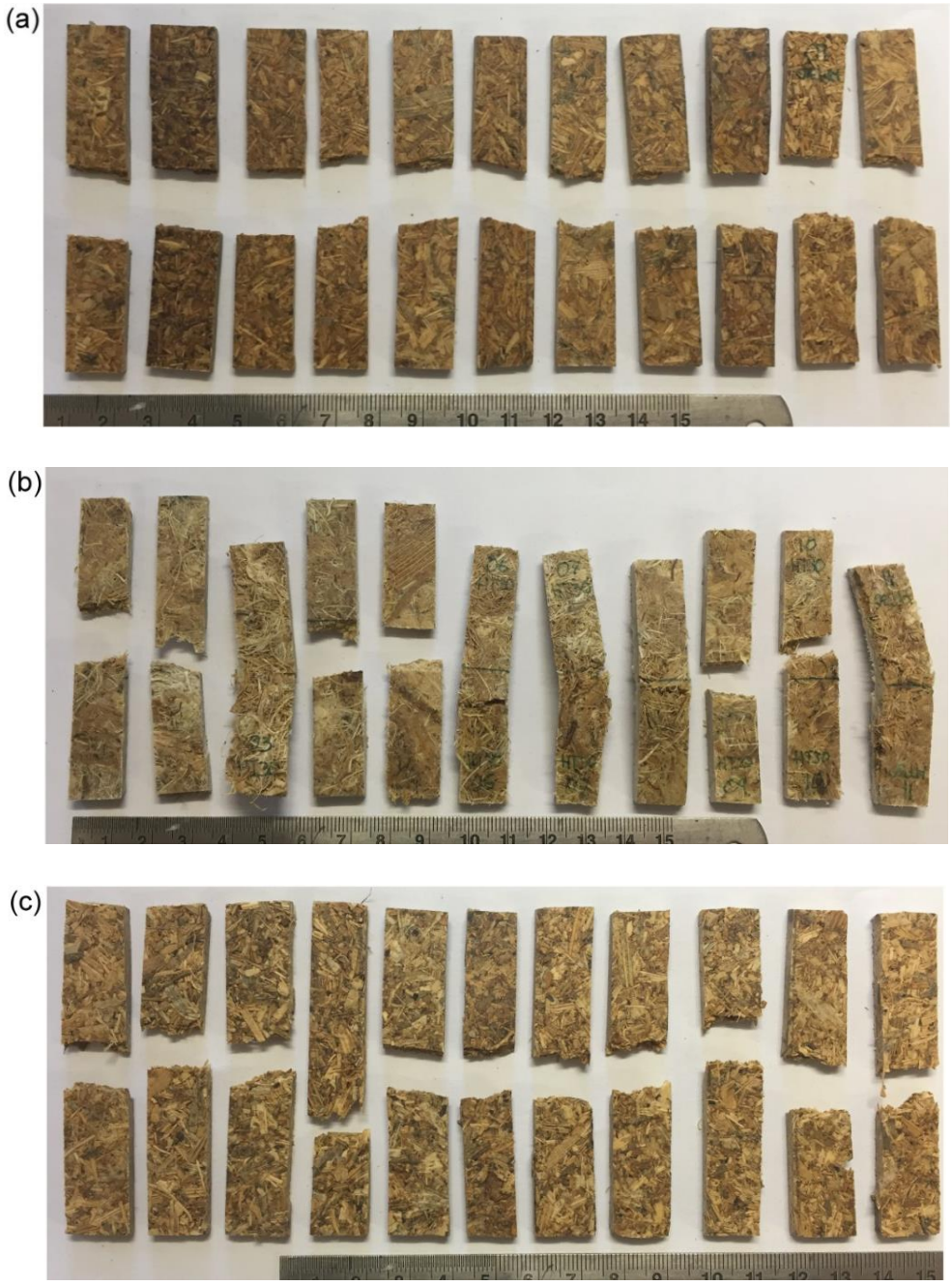

Figure 138 Fracture in MHC samples after the impact test. Samples (a) M30, (b) AK30 and (c) M20

So far MHC' properties studied had the purpose of demonstrating MH' feasibility to make a competitive CM; interestingly, the manufactured boards achieved, and in some cases surpass WBF. However, AA findings were rather encouraging on the possibility of MHC boards to reach wood-based fibreboard's environmental resistance [217], known as one of the most difficult characteristics to get without chemical additives.

Prior to this study, it was difficult to make predictions about MHC' performance when exposed to atmospheric moisture and while immersed in water, due to the scarcity of literature on MH. The reports on AW-based composites indicated its sensitivity to water uptake, that results in elevated percentages of thickness swelling [92,110,194,218], and the MHC boards were not the exception as shown in Figure 139.

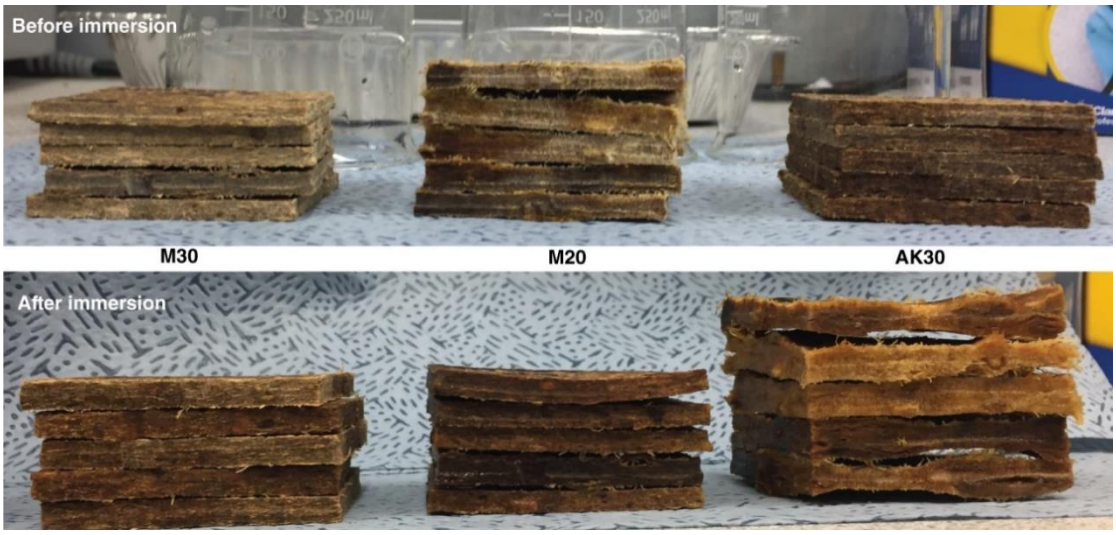

Figure 139 MHC samples before and after 24 hours water immersion cycle

Water uptake variations encountered in MHC are summarised in Figure 140, where it can be observed an increment of 31.3 % in the AK30 boards in comparison to M30 specimens. This percentage is greater when they are compared to WBF. This behaviour is attributed to the physical and chemical alterations made to the MHF; however, these findings might not be definitive.

Although, they did confirm the AW-based composites absorption ratio that oscillates between 3-12 wt.% according to Sreekumar and Thomas [194].

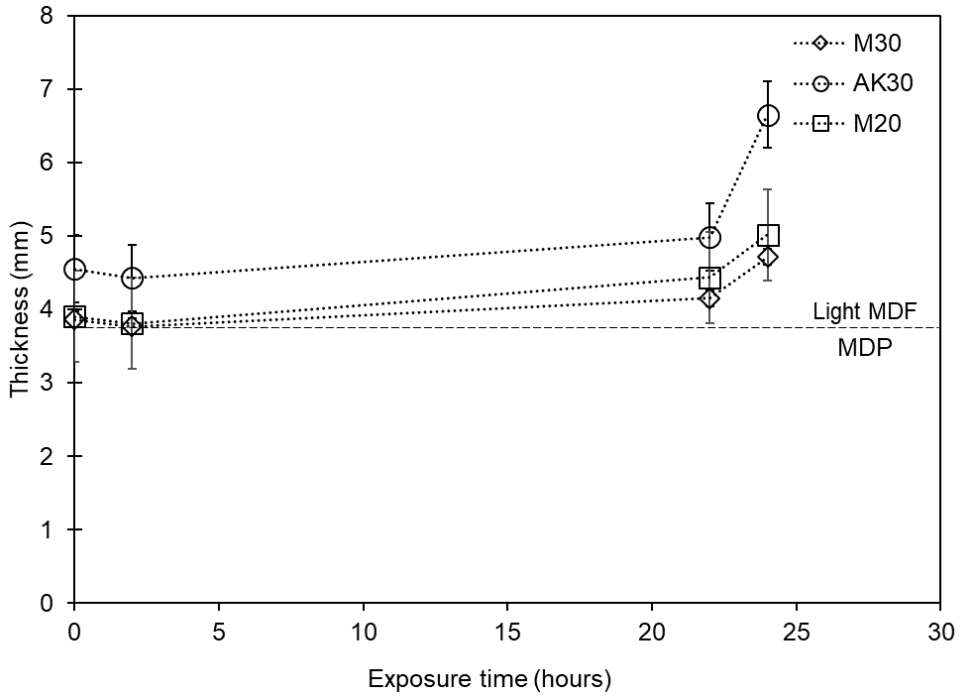

Figure 140 MHC boards water uptake. Measurements of dried samples at 2, 22 and 24 hours

Moreover, both milled MH boards met the expected water uptake levels, contrary to the data found in the literature that raw MH fibres were more prone to have a slight increment in the moisture content. Therefore, AK30 hygroscopicity can be attributed to the hydroxyl groups attached to the MHF walls (Figure 119) after the alkali treatment. The discrepancies between MHC' blends to reach their moisture uptake limit as shown in Figure 139; due to the fibres' natural structure and composition. Resulting in the board's delamination, since the moisture absorbed acts as a separating agent because of fibre saturation levels (A) as shown in Figure 141.

Figure 141 AK30 sample cross-section area after 2 hours of water immersion at 20 °C, delamination and fibre swelling can be observed (A)

The results in this chapter indicate the likelihood of manufacturing a CM with MHF and three different binding systems (binderless, lignin and bio-epoxy resin), by adapting conventional WBF manufacturing processes. These composites were prepared using different sizes (whole, chopped, milled and alkali) of MH at two concentrations (30 and 20 % w/w). The mechanical (UTS and *E* moduli) and density properties were measured and, in some cases, enhanced by using only milled and alkali MHF, while MHC hardness remained considerably low. Furthermore, MHC boards endurance to extreme environmental conditions was rather surprising. In general, regardless of the MHC mechanical properties achieved, these findings on MH and MHF have significant implications for the understanding of how AW materials can be reintegrated into the manufacturing system.

6 SYSTEMIC DESIGN APPROACH DISCUSSION

This chapter discusses the insights from the application of a multidisciplinary SDA framework, and as such, it is discussed separately. It is worth to mention that MR&D represents the main core of this work, hence it has been discussed separately in section 5. Therefore, the corresponding SDA's sections will be discussed and analysed followed by a detailed review of the MHC material properties appraisal used to determine its feasibility (technical) and viability (business) to be taken into full-scale production.

6.1 Implications of the systemic design approach

The materials industry still employs linear methods for the development of novel materials regardless of its nature (oil-based, metals or natural fibres). In reviewing the literature, some data was found on the association between material development and DT application. Thus it was hypothesised the conception of a multidisciplinary SDA to enable sustainable innovation for a new AW-based material.

The proposed SDA framework (Figure 55) draws upon the merge of four methodologies (DBoP, DfSI, MR&D and TES), all with the same objective of enabling the MHC board manufacture. Therefore, the smooth integration of the four categories was essential to ensure that the innovation drivers, based on Brown's [1] *human-centered* approach and Ceschin and Gaziulusoy [29] studies, were met throughout a comprehensive and realistic methodology. The SDA theoretical and methodological principles have a flexible two-way connection, and thus, the stakeholders can take part in the solution search and establish a direct dialogue.

Transdisciplinarity in MD is possible; therefore, a more complex understanding of the problem and its context was accomplished. The attainment of a feasible MHC board from MH waste supports the premise of transdisciplinary research that focuses on solving the "main issue" by means of shared knowledge and

expertise. Thus, as Leavy [219] suggested, a problem such as the excessive production of MH could be approached through a transdisciplinary methodology (SDA). Though for this research, the linkage to a restorative economic system (circular economy) was of paramount importance and extended the initial research' scope, considering not only the AW but all the actors involved in it.

Consequently, the strongest characteristics of each SDA methodology were adopted and tailored for the Mexican context, resulting in the schematic presented in Figure 142. Showing complete incorporation of the McArthur Foundation [44] circular economy approach with the MHC manufacturing process, in which the recovery and study of existing AW materials in Mexico were the main drivers. Thus, it is likely that such connection between the circular economy and SDA allowed the study of the implications of taking away this copious amount of lignocellulosic material from the fields, and analyse whether this will represent a positive impact in the community.

The implementation of DfS approaches has been more concentrated in the technological side rather than the specific cultural context. As stated by Manzini and Vezzoli, to reach a significative innovation for sustainability a comprehensive intervention is required [220]. Thus, by substituting old systems to promote new consumption systems only covers the life cycle design, but if both technical and socio-cultural changes are brought together, integral product development can be achieved.

Similarly, Castillo's et al. DBoP main design drivers [31] (Figure 7) were crucial for reaching the SDA objective to develop an MHC material. Thus, the involvement of the main stakeholders in the project, maize producers, farmers, local people, researchers and investors, enriched the project greatly. However, due to the length of the research, a specific social study will be necessary during and after the pilot plant set up. The other three design drivers mentioned are merged in the TES.

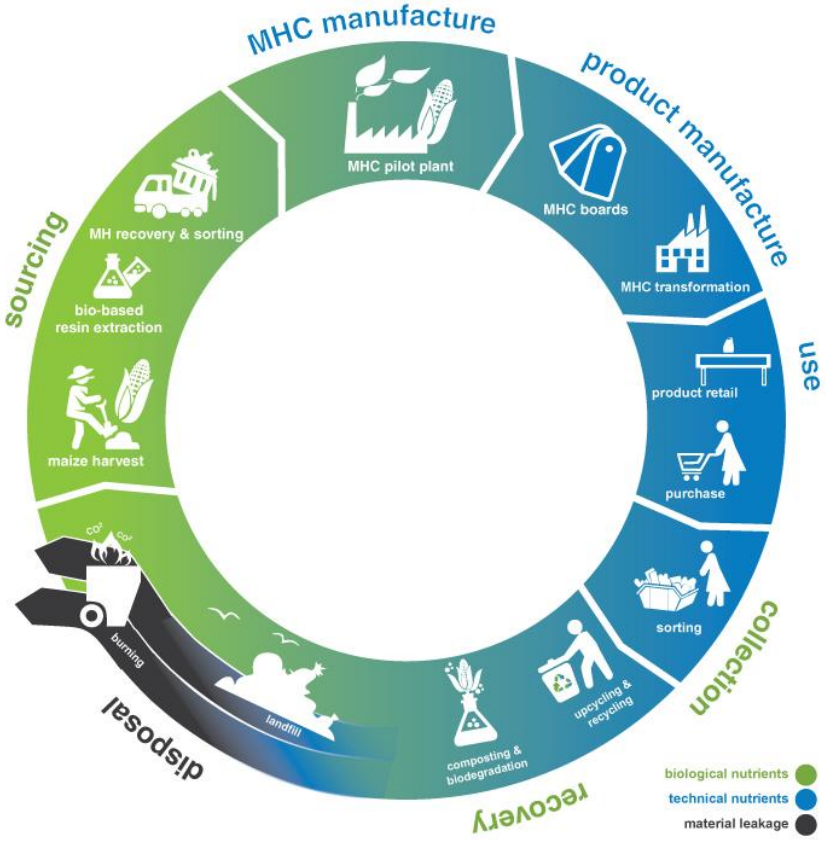

Figure 142 MHC manufacturing and product life-cycle

The MHC circular manufacturing cycle may help us understand the raw material flow if it is structured in a way that each category feeds from the others, thus, the AW could be kept in the loop to continue the cycle with a low rate of material loss. Furthermore, Raworth's [221] latest findings complement this research hypothesis (design for the base of the pyramid) on the importance of the society' involvement in ecological matters, also including an alien matter such as a productive circular system to recover AW. Her approach "A Doughnut for the Anthropocene: compass in the 21st century" displays the possibility of a well-balanced lifestyle within the planetary boundaries and the social foundation (based on the UN 2015 Sustainable Development Goals [58]). Although the SDA approach did not consider such a wider context, it is consistent with Raworth's doughnut (Figure_Apx 7-7) analysis on the raw material's overexploitation and lack of social participation. This rather unexpected

similarity might be explained by the fact that both approaches are aiming towards feasible and sustainable development. However, a note of caution is due here because according to Raworth, the ecologic/social balance will be achieved through a “human thrive”, concept that can be interpreted as *unlimited growth*; although this view has led to the current raw materials global depletion and social detachment from the industrial processes.

Moreover, inconsistencies in the SDA application along the MHC productive cycle could be argued, mainly due to the small-scale tests and the little literature found on MH waste exploitation. However, the extent of these results only reflects the present research objectives, despite the great scope pictured. From there a diagram showing SDA’s ability to work across disciplines and applied to the MHC productive cycle is depicted in Figure 143. Going from the centre out there are three main layers that shape the SDA’s framework implementation. First are the stakeholders: farmers, researchers, manufacturers and policymakers; the outer layer emphasises MHC’s material manufacturing feasibleness, and economic and social impact; and finally, the middle layer concentrates on the general outcomes, e.g. new waste management in the area, alternative jobs creation, community involvement, etc. While a novel material is being developed, the impact wave in the locality is evident. That at the same time shows freedom of the combined action between each section; thus, proving SDA’s transdisciplinarity and information flow effectiveness.

Overall, the development of an AW-based material is considered to have a positive impact regarding CO^2 emissions and energy consumption throughout each manufacturing stage, as well as it efficiently integrated diverse disciplines, objectives and outcomes with the help of the design-driven framework.

Figure 143 SDA framework application in the MHC manufacturing cycle. The colour coding is corresponding to the one in Figure 55

6.2 Preliminary techno-economic study of maize husk-based composite manufacture

This study has examined and weighted the different factors included in the SDA framework (Figure 55); which are thought to contribute to the obtention of an MHC material. Therefore, a preliminary technical and economic assessment was carried out to get a comprehensive view of an MHC's pilot plant, and a better understanding of its impact in the region (State of Mexico), maize fields and air pollution levels. Although the DBoP innovation drivers are meant to integrate the MHC development towards a more sustainable model, these

results should be interpreted with caution because it is possible that they might not apply to similar contexts. However, this research findings will provide support for the conceptualisation of a novel material, considering Raworth's [221] social and planetary boundaries.

Previous studies evaluating AW (i.e. rice [72], banana [37], coffee [24]) as alternative raw material for composite materials have highlighted its potential and possible low environmental impact. Thence, MH's potential and viability to become more than just a pile of rubbish is a true statement; however, does not assures its success or the local's acceptance. Moreover, a point often overlooked is the importance of quantifying the impact that this approach could bring to the people involved in maize harvest and waste management in the area. A task that is considerably restricted if it is based only in general assumptions and lab-size experiments, thus the pilot plant set up in situ will give more realistic inputs and aid to enhance the whole SDA approach. Even though some of these aspects fall outside the scope of this research, a general overview of wood-based composites market in Mexico and how an MHC would fit in this scenario is also presented.

6.2.1 Mexican wood-based fibreboard market overview

The natural fibre-based composites market 2017-2021 forecast shows a steady global growth rate of 11.33 % according to Lucintel's report [222]. However, only a few novel materials similar to WBF have transcended the lab boundaries in the last decade. Table 41 shows a material selection that may compete directly or substitute conventional WBF, along with some of the *green* WBF present in the Mexican market. Mechanical properties, popularity, applications, and availability are the similarities between these materials and the MHC produced, yet the retail price is still to be determined. Contrary to expectations, the lack of competitive sale prices and a weak raw material supply chain are some of the main difficulties that those promising composites have encountered, despite the growing demand for WBF.

It is well known that WBF's are produced using pine or eucalyptus wood and thermosetting adhesive resins, e.g. UFM [169]. Therefore, the imminent oil and wood shortage has forced the WBF industry to look up for more sustainable and cost-effective alternatives. Tough WBF main use has been under dry environmental conditions, e.g. cladding boards, furniture, wall panels, etc. The diverse uses of WBF boards reduce the chances to other NF-based boards to undertake such a challenge. In the view of the growth of *greener materials* market, the companies have started marketing WBF with sustainable certifications, i.e. FSC ®, CARB phase 2 and ECC as shown in Table 41.

The previous indicates that the local market is not only consuming alternative materials but claiming to broaden the fibreboards offer. However, from the data obtained by SEMARNAT [70] and FAO (2017) [12] on Mexico's timber and MDF production, a steady decrease of -17.8 % and -14.7 % correspondingly has prevailed since 2012. Despite this trend, in 2015 the principal WBF producers together with the Mexican government invested nearly £4.3 million to upgrade their machinery and equipment according to SAGARPA [70]. This apparent inconsistency corresponds more to the market's demand since MDF' import percentage is 15.9 times greater (460,656 m^3) than the national production (29,000m^3) [12]; reviling a substantial market opportunity for local manufacturers, besides the change to introduce analogous materials.

On the other hand, AW's usage in composite materials has been embraced for different manufacturing industries: automotive applications have been under the spotlight for the implications on the mass market production as presented by Koronis et al. [218]. Nevertheless, some concerns have been raised regarding AW's demand, e.g. shortage, supply chain. Thereby other smaller industries such as construction, packaging and consumer products, have not been able to foresee the added value in the application of composites from available lignocellulosic materials [109].

Table 41 Material benchmarking for agro-waste based composites [9,200,201,223]

	Analogous materials				Substitute materials			
	Çurface Re-worked	Curran Cellucomp	Coco dust Kokoboard	Agricola Studio Atupertu	Supremo Carb Duraplay	Tecnotabla Proteak	Light MDF Masisa	WBF EMMAN
								
	Coffee waste	Carrot fibres	Coconut fibres	Seasonal food-waste	Wood fibres	Wood fibres	Wood fibres	Wood fibres
Applications								
Decorative	yes	no	yes	yes	yes	yes	yes	no
Structural	yes	yes	yes	no	no	yes	no	no
Food-related	yes	no	no	no	no	no	no	no
Characteristics								
Natural colour	revealed	revealed	revealed	revealed	revealed	revealed	revealed	revealed
Roughness	medium	no	high	high	medium	medium	medium	high
Scent	low	neutral	medium	low	medium	medium	medium	medium
Visible fibres	high	no	high	high	high	high	high	high
Certification	yes	no	yes	yes	CARB phase 2 ECC*	FSC®**	CARB phase 2	Euro MDF board
Naturalness	high	no	high	high	medium	medium	medium	medium
Time-worn	medium	no	yes	10 years	yes	yes	yes	high
Local resources	yes	no	yes	yes	no	yes	no	yes
Currently available	no	yes	yes	no	yes	no	yes	yes

* Eco-Certified Composite ** Responsible management of the world's forests

6.2.2 Technical Feasibility

In order to complement the SDA framework objectives, and to understand and deliver an innovative solution to the excessive MH waste, a technical assessment of the machinery and processes proposed was carried out. Therefore, the equipment chosen to produce MHC' samples was the same or similar to that used for the WBF industry. From there and considering the modifications needed to switch from wood shavings to MHFs, the proposed MHC production line accomplished the reduction of three steps (screening, mat weighting and board trimming) as shown in Figure 113.

It is well known that clean, innovative technologies are not yet capable of matching conventional technologies cost-effectiveness, industry openness, and operational ease. Considering DBoP's principle of co-creation [31], it made more sense, to begin with, an incremental innovation in the manufacturing line rather than a disruptive. Thus, the transition to a novel raw material would be smothered by all the stakeholders involved (farmers, machinery operators, manufacturer and final users) as part of a first stage towards a new production-consumption system.

As mentioned in the literature, back in the 1930's the best solution to the unused wood residues was the fabrication of WBF. This process has been enhanced a lot since its creation, but up to date, only a few reports have shown the interest in replacing the woody fibres with any other cellulosic material [160]. Though the main drawback the WBF industry is facing nowadays is the intense global deforestation, that not only makes more difficult to obtain the raw material but also increases their production costs [224].

A specialised perspective on socio-technical shift has been adopted by Nakamura et al. [225] who assures that rooted systems rethinking may trigger an evolutionary process of innovation. Thereby, this section will review the MHC manufacturing technical details to guarantee its viability as a small-sized

enterprise (SME). This preliminary assessment is a preview of the SME needs, and possible constraints to adapt the existent technology from the WBF industry to an AW-fibre. This phase can be very challenging when working in rural areas, especially because of the limited infrastructure available. However, since it will be an “upgrade”, an adjustment to the current technology, it would not require tailored industrial systems.

Moreover, any manufacturing project needs to track the processes and procedures with the purpose of optimising results and assure a fluid implementation. Thence, manufacturing readiness level (MRL) [225] allows getting a more precise view of MHC’s maturity for production and further commercialisation. MRL assessment for the proposed manufacturing process is depicted in Figure 144; it gives a glimpse of the progress made up to this point. An MRL 4-5 evaluates the following points: (1) the capabilities of production exist, either at lab scale or for a prototype, (2) the manufacturing technology has been identified in the region, (3) manufacturability trials are in place, and able to provide samples, (4) manufacturing constraints have been identified during the trials, (5) MHC samples have been optimised for production, and finally, (6) production costs have been confirmed.

Interestingly, the MRL allocation for the three MHC blends (AK30, M20 and M30) showed a 4-5 level, a stage not very common for novel material research as it usually takes around 9-13 years to reach the same MRL level (Figure 8) where a linear MD approach is used. Thereby, the MRL results obtained demonstrate SDA’s effectiveness in this case study. Even though the research still requires further development and investment for commercialisation, the progress achieved pinpoints the remaining levels to be reached once the pilot plant is in place; therefore, it is suggested to interpret MRL results with caution, as they do not represent a final assessment of the MHC manufacturing. Bearing in mind that the improvements and innovations in manufacturing processes are not isolated events, nor, unidimensional.

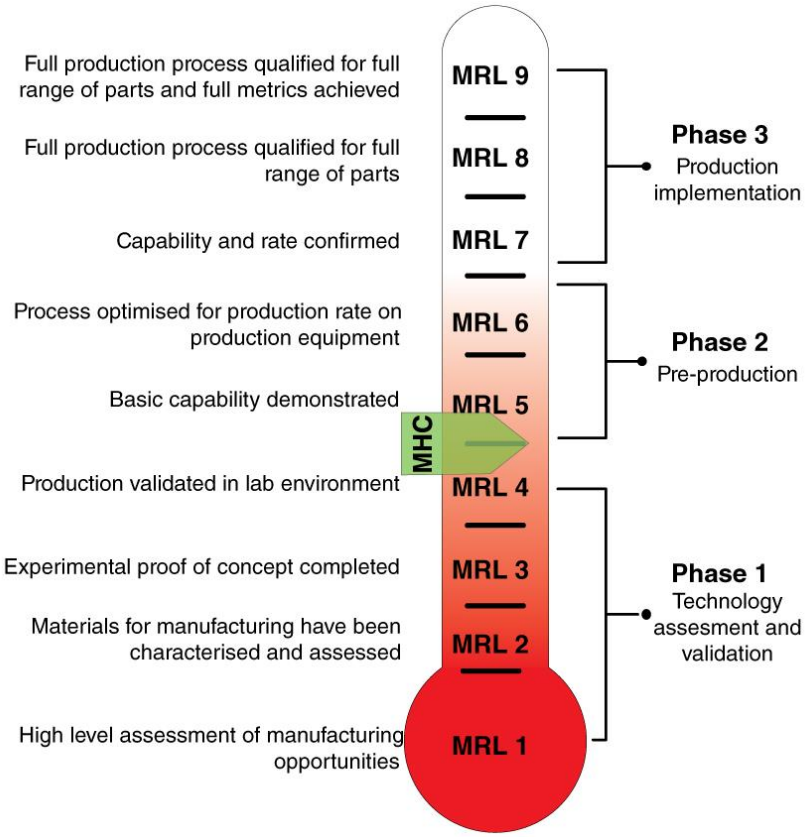

Figure 144 MRL assessment of MHC' production

6.2.3 Commercial Viability

Diverse factors are known to define the survival of a new CM in the market, as the product concept, manufacture, retail price, potential markup, product range, durability, regulations, to mention the most important. Thence, MHC boards have covered the first two as shown by the MRL level achieved, which demonstrates its technical capabilities to be deployed. Thus, to have a comprehensive perspective on MHC commercial potential this section will focus on obtaining MHC manufacture cost and potential retail price, local market demand and regulations.

Based on the data previously discussed in section 2.3, MH's supply can be confirmed with around 990,00 MT available per year, and its considered sufficient material to feed a small MHC production line to cover the pilot plant

demand. Despite the annual growth of £122.7 M of the largest WBF producers in Mexico (Proteak, Masisa, Duraplay and EMMAN) reported by SEMARNAT (2013) [70], in 2013 Masisa imported most of their raw material from Chile and Brazil to keep its production line going [226], corroborating the inefficiency and unreliability of mature wood fibres within the local supply chain. The latter situation resulted in a drop of 8.9 % in the MDF sales in 2017 and of 8.9 % of the annual production [226].

The introduction of novel cellulosic materials could become a key enabler for the WBF industry, aside from contributing to the sustainable development of the country from its rural communities; and correspondingly providing additional evidence of the MHC manufacturing competitiveness within the local WBF producers from an early stage point of view (Figure 145). However, even with the MHC boards, the national production of fibreboards remains far from covering the existent commercial deficit of 47 % [168].

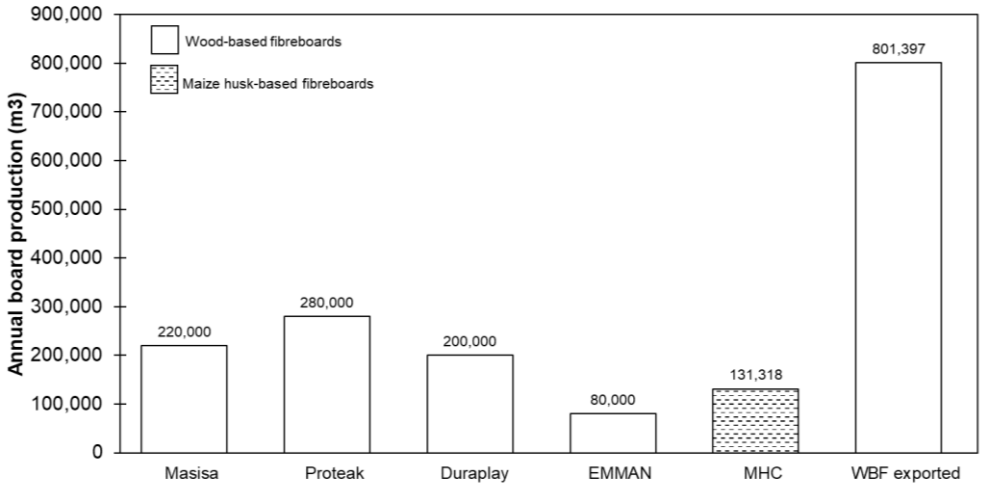

Figure 145 WBF annual production and exports in 2016 in Mexico [168] compared with MHC boards production forecasted for pilot plant

The price of MDF in Mexico in 2015 was 80 % higher than PB, this because of the dependence on plywood price. Plywood is the engineered wood more popular in the Mexican market [70]. That means for the furniture makers there

are neither economical nor technical incentives to shift from traditional timber to WBF. Leaving a gap for a competitive wood substitute material, to which MHC boards may cover.

To set up an MHC pilot plant with an approximate production of 517 m^3, and with the properties stipulated for fibreboards on international standards (ASTM D 1037-12 [176], ASTM D 1348-94 [173] and ASTM D 256-10 [190]) as summarised in Table 42; the equipment, raw material and workforce costs were estimated by the local market values and the Mexican national minimum wage rate for 2017 [227].

Table 42 MHC boards general properties for manufacturing

MHC type	MH (wt.%)	Extraction method	SSE (%)	Board size (m)	Thickness (mm)	Density (kg/m^3)
M30	70	milled	30			890
AK30	70	alkalinised	30	1.22x2.44	3	1014
M20	80	milled	20			865

The initial capital investment costs (CIC) and expenses were calculated in Table 43, where the model and amount of each piece of equipment were considered for the three MHC blends, in this way a broader range of price and applications will be covered. The equipment was selected calculating a progressive production starting at a 50 % of its capacity and expecting to reach its full capacity by the 4^{th} year [228]. 301 working days, divided into two 8-hour shifts, with an estimate board production rate of 116 units per day were considered for the CIC.

MHC production cost (PC) is estimated with prices from the Mexican market during 2017. Each MHC' blend cost is detailed in Table 44. SSE resin contributes to 75.5-84.5 % of the total PC, whereas MHF only represents 12.6-15 %. The elevated price indicates that SSE resin has a significant effect on the material's competitiveness, especially when compared with WBF materials retail prices.

Table 43 Capital investment cost (CIC) and monthly operational expenses

Item	Description		Qty	Supplier	Unit price (£)	Total cost (£) per blend		
						MH30	AK30	MH20
Operational expenses	Warehouse rent, 2 offices, 5 parking spaces and workshop		970 m^2	/	2,987	2,987	2,987	2,987
	Office furniture	/	/	/	1,200	1,200	1,200	1,200
	Maintenance and operational costs (M&O) (water, telephone, internet, stationary, etc.)		/	/	1,122	1,122	1,122	1,122
	Electricity	55/60 kW/h	/	CFE	1.93	107.43	122	107.43
	Machinery maintenance	10 % of TEC	/	/	/	1,177.1	1,199.6	1,177.1
	Water	from 1 to 250 m^3		/	/	359.10	430.92	359.10
	MH transportation	3 ½ tons per trip	/	world freights rates	1.60	1,920	1,920	1,920
					Subtotal	8,873	8,982	8,873
Total Equipment Cost (TEC)	Metal container (silo)	1 ton	3	Sn Juan Tepeuxila, Mexico	214.86	429.72	644.58	10,073
	Hammer mil W2-500	200-300 kg/ h	1	Henai Richi	759.54	759.54	759.54	429.72
	Vertical feeder	1.5 m^2	1	Sinopes, China	379.77	379.77	379.77	759.54
	Resin applicator		1	Yuyang	1,139.3	1,139.3	1,139.3	379.77
	Convection oven	50L / 10 – 300 ℃	1	JKI	216.47	216.47	216.47	1,139.3
	Hot press AY214 with platen 2.5 x 1.3 x .42 m	3 layers /120 T	1	Kingiso	7,595.42	7,595.42	7,595.42	216.47
	Dust collector LD2304	76x45x45.5 cm	1	Mengmat	63.71	63.71	63.71	7,595.42
	Trolley cart and small hand tools	as required	2	Various	160.76	160.76	160.76	63.71
	Work tables steel cover	2.44x.90 m	2	Uline	427.70	427.70	427.70	160.76
	Storage racks	3x1.2x4 m 1-4 layers	2	Mecalux	37.98	37.98	37.98	427.70
Misc.	Delivery cost	/	/	/	**/**	224.20	228.50	37.98
	Installation	/	/	/	**/**	336.31	342.75	224.20
					Subtotal	11,343.18	11,568.78	11,343.18
					Total	20,215.81	20,550.30	20,215.81

Table 44 MHC boards production cost (PC)

	Category	Description	Qty	Unit price (£)	Total cost (£) per blend		
					M30	AK30	MH20
Raw materials	Maize husk	split husk	M30 = 580 kg AK30 = 870 kg M20 = 522 kg	.54p / kg	313.2	469.8	281.88
	Sodium phosphate, monobasic monohydrate, 99%	pellets	6.7 kg	35.32	0	236.64	0
	Acetic acid	liquid	14 L	16	0	224.8	0
	Two phases epoxy bio-resin	liquid	M30 = 174 L AK30 = 261 L M20 = 156.6 L	11.97/ L	2,082.78	3,124.17	1,874.5
				Subtotal	2,395.98	4,055.41	2,156.38
Labour	Machine operator	Technician	2	6.45	6.45	12.90	6.45
	Semi-skilled labourers	Production line	2-3	4.30	8.60	12.90	8.60
	Administrative staff	Secretary	1	8.20	8.20	8.20	8.20
	Insurance	Worker insurance	5-6	58.01	9.66	11.60	9.66
				Subtotal	32.91	45.60	32.91
Others	General expenses	25 % of labour and M&O			17.57	20.75	17.57
	Property insurance cost	5 % of TEC			18.90	19.28	18.90
				Subtotal	36.47	40.03	36.47
				Total production cost per 8h shift	2,465.36	4,141.04	2,225.76
				# boards per shift	58	58	58
				Production cost per cubic metre	4.6	7.8	4.2
				Net price per board	41.31	69.92	37.72
				Retail price per board	49.57	83.89	45.26

These results appear to be linked to the extensive research of more eco-friendly adhesives and alternative NF, presented by Akaranta [111], Li et al. [229], Halvarsson [182] and Zhang, Zhang and Xue [147] to mention a few.

Several factors are known to play a role in determining MHC prices, from which the most evident are the raw materials elevated prices (SSE resin), and the low-risk projected profit (-16 %), which is the minimum percentage recommended by Karmee at al. (2015) [228] for a new product investment in an established market. As shown in Figure 146 M30 boards were found to be the most competitive and less expensive blend (£41.4), albeit its UTS performance was not the highest. Results place AK30 as the less marketable blend with an extremely high net price (£70.1).

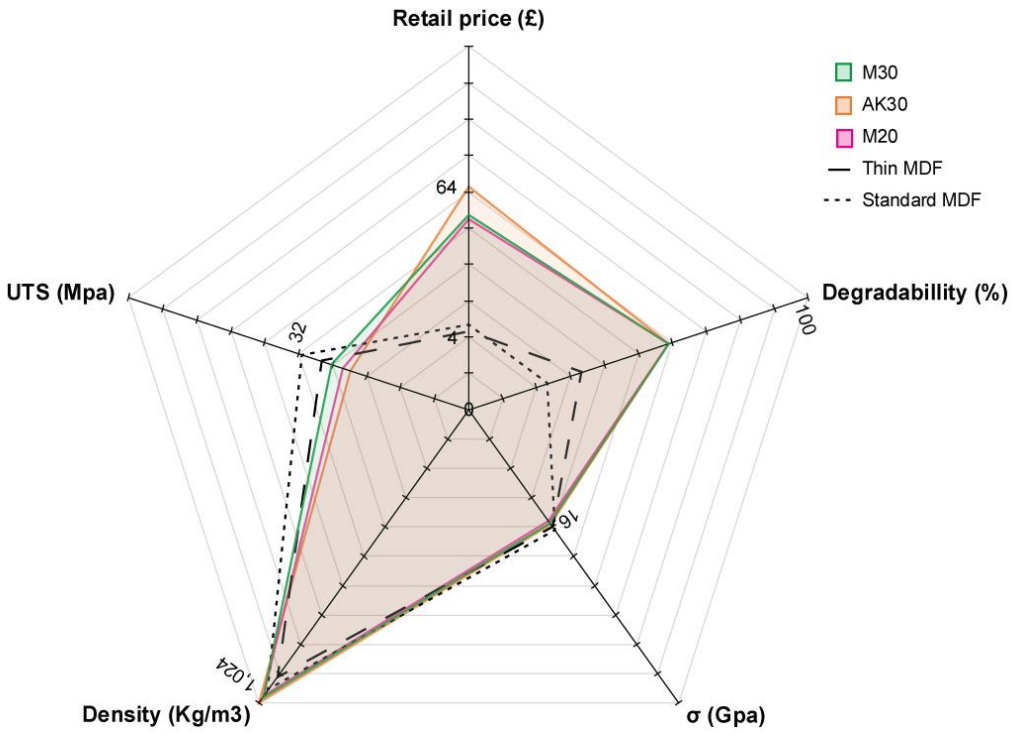

Figure 146 Calculated net price and more feature properties of M30, AK30 and M20 boards against most popular WBF (Table_Apx 7-1)

Overall, the MHC board's properties fell within the ranges allowed and outperformed WBF's degradability percentage. Altogether these results prove

the cost-effectiveness struggle that most of the GC face in the market. However, these results also shed light for novel materials to get some more realistic and competitive prices in the long term as the breakeven point projection for the MHC will allow the boards to reduce its price by 74 to 89 %, placing MHC in similar circumstances as the WBF.

Despite its exploratory and preliminary nature, this study intended to give a general insight into MHC cost-effectiveness, as well as understand its potential if other binders were used to manufacture the boards. Figure 147 describes positive results for the *greener* binders considered (greenpoxy 56 and tannin) regarding its carbon content levels. However, its cost position in comparison to its oil-based counterparts is far to be favourable. The SSE, cashew oil and greenproxy 56 cost overlap within the bounds of a reasonable price range, yet, despite SSE has the lowest carbon content it remains as the most suitable option when compared with UF and PP. A price rising tendency was observed in all the bio-based binders contrary to their oil-based counterparts (UF and PP) as a correlation to carbon content and biodegradability. Such trend resulted in a price difference of up to 10 times. As the market gets mature and industry embraces widely these materials a shit in this trend could benefit this type of materials.

The circular economy is a key factor in energising well-established companies within their business approach. The Ellen MacArthur Foundation [44]) highlights the importance of the application of the circular economy model to boost companies by adding value to their products, coupled with a two-way interaction with customers and suppliers. Thus, a change in the paradigm of waste production can be achieved by shifting the consumer’ and producer' responsibility and getting them involved in the product lifecycle.

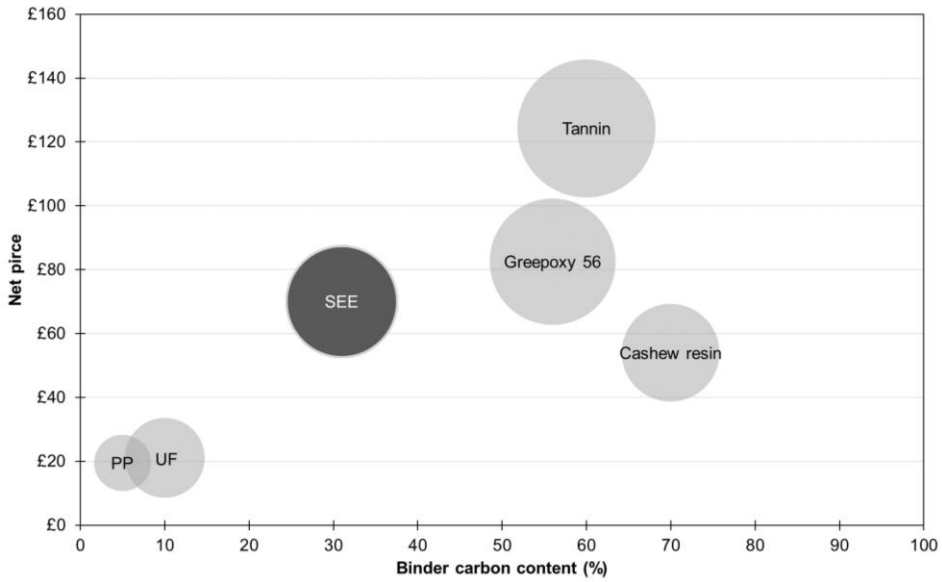

Figure 147 Retail price approximation of MHC boards manufactured vs percentage of binder carbon content of the most common binders used in fibreboards. SSE boards represent the MHC manufactured; the rest are hypothetical blends

Although the findings on MHC prices and market opportunities should be interpreted with caution, this study was able to spot some strong points for a potential pilot plant and an eventual SME. Figure 148 depicts the theoretical business model for the MHC pilot plant proposed; it intends to add value to MH waste by transforming it into a CM. It is important to bear in mind Chesbrough's [230] business model type 5 framework; where these companies experiment directly with the business model. Hence, the MHC manufacturing partners, suppliers and customers could have a deeper understanding of the supply chain and after-use, as they look for major technology shifts and CO^2 emission reduction opportunities. The target markets are SME and industrial furniture companies, construction companies, designers, architects, and amateur and professional woodworkers. Design, performance and sustainability are the MHC differentiators. Taken all this together, the assumptions suggest that MHC pilot plant can have a positive effect on the Mexican market; moreover, deeper analysis on the business model is suggested.

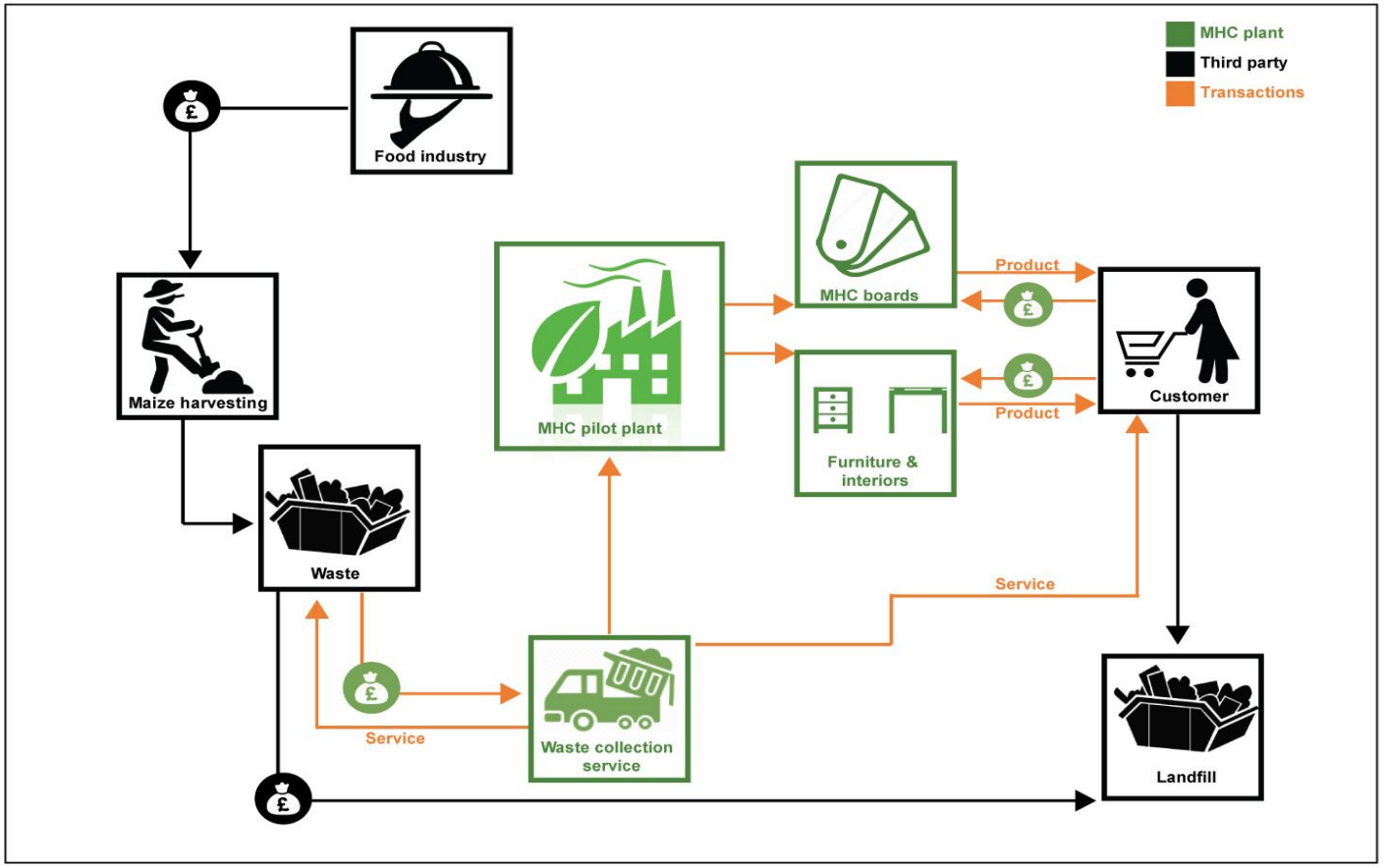

Figure 148 Theoretical business model for the MHC pilot plant

7 GENERAL CONCLUSIONS

- SDA application contributed to collect relevant data throughout the four methodologies selected:
    - DBoP provided the background information for the study case and the approach to the AW surplus issue in the region.
    - DfSI, pinpoint design and sustainability strategies to tackle the social and environmental consequences of the MH waste overproduction.
    - MR&D focussed on the MH characterisation and transformation into a maize husk-based fibreboard
    - TES gave a general overview of the economic and technical viability to set up a pilot plant in Mexico; in addition to the potential retail price and market allocation of the MHC boards.
- The data collected on MH' morphology and mechanical properties allowed both a qualitative and quantitative assessment of the whole husk and fibres. Thence, demonstrating their potential as a composite reinforcement.
- ASPROS milled fibres and husk had a steadier mechanical performance than the as received and alkali extracted fibres.
- Both husk types exhibited an increment of 4-67 % on their tensile properties after the alkali treatment.
- Binderless boards showed poor mechanical properties, thus, they were not select for optimisation. The MH/lignin boards were brittle and unstable, making them unsuitable for further optimisation.
- The improvement of fibre wetting and dispersion through extraction methods (milled and alkali) MHC enhanced physical and mechanical properties.
- The M30 boards met the requirements as general-purpose fibreboards for use in humid conditions according to BS EN622-5:2009. M20 boards

were classified as general propose for use in humid conditions boards according to British standard for fibreboards for interior applications (BS EN 622-5:2009). AK30 met the requirements of general-purpose fibreboards for use in dry conditions according to BS EN622-5:2009.

- Milling was the most cost-effective size-reduction method of MH. However, MHF alkalinisation was beneficial for the MHC panels, thereby improving fibre/binder cross-linking.
- The mechanical strength and physical properties of the MHC panels, UTS, MOR, elongation, E modulus, swell percentage, and IR are strongly correlated to the board's density and resin content.
- After accelerated ageing, UTS, MOR, E modulus and swell percentage were found to decrease in the three MHC blends (M30, AK30 and M20), whereas the elongation percentage was found to increase only in AK30 boards. M30 and M20 boards were found to be more resistant to moisture and shape distortion than AK30 boards.
- This study confirmed that MH production in the State of Mexico area could feed an MHC pilot plant. However, the calculated MHC prices were considerably higher than the WBF in the market by a factor of 6-8 times.
- MRL assessment of the MHC manufacture gave a promising result for the level obtained in research. Even though, the sample production and testing were made in a lab scale.

7.1 FUTURE RESEARCH SUGGESTIONS

- The SDA transferability should be investigated with a different case study.
- The addition and change of SDA's methodologies should be studied and equalled with the present research.
- The MHF enzymatic extraction method could be studied further to compare the surface modifications effect on MHF/binder cross-linking strength.
- Study the physical and mechanical implications of binder reduction at 85/15, 90/10 and 95/5 % fibre/ matrix ratio in MHC boards.
- Different adhesion systems for MHC production, e.g. tannin, natural oils, UF, could be investigated. Not only to increase the knowledge on MHF/binder but to obtain more affordable MHC boards.
- To carry out an exhaustive life cycle assessment to confront MHC boards manufacture environmental impact whit the current MH waste management practices.
- Study more in-depth the social implications of establishing an MHC pilot plant in the State of Mexico.
- Further research could also be conducted to determine the MHC's commercial effectiveness, building up from the observed opportunities in the present research.
- To prove MHC' capability to be transferred into a full-scale manufacturing

REFERENCES

1. Brown T. (2009). Change by Design. Available at: DOI:10.1017/CBO9781107415324.004

2. Keeble, B. R. (1988). The Brundtland report:'Our common future'. Available at: http://www.un-documents.net/our-common-future.pdf (Accessed: 16 May 2018)

3. Lawrence RJ., Després C. Futures of Transdisciplinarity. Futures. 2004; 36(4): 397–405. Available at: DOI:10.1016/j.futures.2003.10.005

4. Barbero, S. (2010). Systemic Design In The Energy Sector: Theory And Case Studies. In Management of Technology Step to Sustainability Production, Conference article (Rovinj, 2-4 giugno 2010). Available at: http://0-search.proquest.com.pugwash.lib.warwick.ac.uk/docview/879347230?accountid=14888%5Cnhttp://webcat.warwick.ac.uk:4550/resserv??genre=article&issn=&title=Acta+Technica+Corviniensis+-+Bulletin+of+Engineering&volume=4&issue=2&date=2011-04-01&atitle=SY

5. The Food and Agriculture Organization (FAO). (2006). Estudio de tendencias y perspectivas del sector forestal en América Latina al año 2020. Available at: http://www.fao.org/docrep/006/j2215s/j2215s08.htm

6. Secretaría de Agricultura, Ganadería, Desarrollo Rural, Pesca y Alimentación de México (SAGARPA). 2012. Sustainable Modernization of Traditional Agriculture, MasAgro. Available at: http://masagro.mx/index.php/en/ (Accessed: 26 October 2015)

7. Secretaría de Medio Ambiente y Recursos Naturales (SEMARNAT). Residuos Urbanos. 2016. Informe de la Situación del Medio Ambiente en México.

8. Food and Agriculture Organization of the United Nations (FAO).

Emissions of nitrous oxide from the decomposition of crop residues on cultivated soils. Annual report. 2013. Available at: http://faostat3.fao.org/browse/G1/GA/E (Accessed: 9 June 2015)

9. Karana E., Barati B., Rognoli V., Van Der Laan AZ. Material driven design (MDD): A method to design for material experiences. International Journal of Design. 2015; 9(2): 35–54.

10. Muratovski, G. (2015). Research for designers: A guide to methods and practice. Sage

11. Schmaltz, J. NASA. Agricultural Fires Dot Mexico. May 02,2013. Available at: https://www.nasa.gov/mission_pages/fires/main/world/20130503-mexico.html (Accessed: 28 September 2017)

12. Food and Agriculture Organization of the United Nations (FAO). Statistics Division; Production quantities by country. 2014. Available at: http://faostat3.fao.org/browse/Q/QC/E (Accessed: 14 October 2015)

13. Youngquist, J. A., English, B. E., Scharmer, R. C., Chow, P., & Shook, S. R. (1994). Literature review on use of nonwood plant fibers for building materials and panels. Gen. Tech. Rep. FPL-GTR-80. Madison, WI: US Department of Agriculture, Forest Service, Forest Products Laboratory.

14. Design Council. The design economy report. October 2009. Available at: https://www.designcouncil.org.uk/resources/report/design-economy-report

15. Brown, T., & Wyatt, J. (2010). Design thinking for social innovation. Development Outreach, 12(1), 29-43.

16. Luchs, M. G., Griffin, A., & Swan, S. (Eds.). (2015). Design thinking: new product development essentials from the PDMA. John Wiley & Sons.

17. Peters, T. (2005). Leadership: Essentials. Reprinted. DK Adult Publication.

18. IDEO. Design Thinking - IDEO U. 2017. Available at: http://www.ideou.com/pages/design-thinking (Accessed: 6 March 2017)

19. Roos, G. (2016). Design-based innovation for manufacturing firm success in high-cost operating environments. She Ji: The Journal of Design, Economics, and Innovation, 2(1), 5-28. Available at: DOI:10.1016/j.sheji.2016.03.001

20. Friedman, K. (2012). Models of design: Envisioning a future design education. Visible language, 46(1/2), 133-153.

21. IDEO.org. Clean Team. Available at: http://www.designkit.org/case-studies/1#spotlight (Accessed: 6 March 2017)

22. Brown, T. (2009). Change by design.

23. Roos G. The role of Design in the industrial innovation process. (2012). Available at: https://www.researchgate.net/publication/274387660_The_role_of_Design_in_the_industrial_innovation_process

24. Barbero, S., & Toso, D. (2010). Systemic Design of a Productive Chain: reusing coffee waste as an input to agricultural production. Environmental Quality Management, 19(3), 67-77. Available at: DOI:10.1002/tqem

25. Bistagnino L. Design sistemico : progettare la sostenibilità produttiva e ambientale. (2009). Publications Open Repository Torino. Available at: http://porto.polito.it/1956267/ (Accessed: 14 September 2017)

26. Chick, A., & Micklethwaite, P. (2011). Design for sustainable change: how design and designers can drive the sustainability agenda (Vol. 38). AVA publishing. Available at: http://unicorn.dmz.cranfield.ac.uk//uhtbin/cgisirsi/CRANFIELD/LIBPOL/0/5?user_id=&search_type=KEYWORD&srchfield1=GENERAL%5ESUBJECT%5EGENERAL%5E%5Ewords+or+phrase&library=ALL&language=ANY&format=ANY&item_type=ANY&location=ANY&match_on=KEYWORD&sort_by=ANY&s (Accessed: 2 March 2017)

27. De Pauw, I. C. (2015). Nature-Inspired Design: Strategies for Sustainable Product Development.

28. Papanek, V., & Fuller, R. B. (1972). Design for the real world (p. 22). London: Thames and Hudson.

29. Ceschin, F., & Gaziulusoy, I. (2016). Evolution of design for sustainability: From product design to design for system innovations and transitions. Design Studies, 47, 118-163. Available at: DOI:10.1016/j.destud.2016.09.002

30. Thorpe, A. (2007). The designer's atlas of sustainability. Island Press.

31. Castillo, L. G., Diehl, J. C., & Brezet, J. C. (2012, May). Design considerations for base of the pyramid (BoP) projects. In Proceedings of the Nothern World Mandate: Culumus Helsinki Conference (pp. 24-26). Available at: http://cumulushelsinki2012.org/cumulushelsinki2012.org/wp-content/uploads/2012/05/Design-Considerations-for-Base-of-the-Pyramid.pdf

32. García, A. M., García, A. I., Cabezas, M. Á. L., & Reche, A. S. (2015). Study of the influence of the almond variety in the properties of injected parts with biodegradable almond shell based masterbatches. Waste and Biomass Valorization, 6(3), 363-370. Available at: DOI:10.1007/s12649-015-9351-x

33. Madurwar, M. V., Ralegaonkar, R. V., & Mandavgane, S. A. (2013). Application of agro-waste for sustainable construction materials: A review. Construction and Building Materials, 38, 872-878. Available at: DOI:10.1016/j.conbuildmat.2012.09.011

34. Cooper, R. G. (1990). Stage-gate systems: a new tool for managing new products. Business horizons, 33(3), 44-54. Available at: DOI:10.1016/0007-6813(90)90040-I (Accessed: 11 April 2017)

35. National Research Council. (2011). Materials Needs and R&D Strategy for Future Military Aerospace Propulsion Systems. National Academies Press. Available at: DOI:10.17226/13144 (Accessed: 11 April 2017)

36. Roos G. The role of design in the innovation process. Journal of Engineering Design. 2012; 1(3): 269–278. Available at: DOI:10.1080/09544829008901657

37. Quintana, G., Velasquez, J., Betancourt, S., & Ganan, P. (2009). Binderless fiberboard from steam exploded banana bunch. Industrial crops and products, 29(1), 60-66. Available at: DOI:http://dx.doi.org/10.1016/j.indcrop.2008.04.007

38. Monteiro, S. N., Terrones, L. A. H., & D'almeida, J. R. M. (2008). Mechanical performance of coir fiber/polyester composites. Polymer testing, 27(5), 591-595. Available at: DOI:10.1016/j.polymertesting.2008.03.003

39. Goswami, P., & O'Haire, T. (2016). Developments in the use of green (biodegradable), recycled and biopolymer materials in technical nonwovens. In Advances in Technical Nonwovens (pp. 97-114). Available at: DOI:10.1016/B978-0-08-100575-0.00003-6 (Accessed: 23 May 2018)

40. Huerta Cardoso, O.I. Feasability study of a novel bio-based material through a design thinking approach. PhD thesis. Cranfield University. 2017.

41. Quintero García, S. L., & González Salcedo, L. O. (2011). Uso de fibra de estopa de coco para mejorar las propiedades mecánicas del concreto. Revista Científica Ingeniería y Desarrollo, 20(20), 134-150.

42. Manzini, E., Vezzoli, C., & Clark, G. (2001). Product-service systems: using an existing concept as a new approach to sustainability. Journal of Design Research, 1(2), 27-40.

43. Vezzoli, C. (2014). The “material” side of design for sustainability. In Materials Experience (pp. 105-121). Available at: DOI:10.1016/B978-0-08-099359-1.00008-4 (Accessed: 29 February 2016)

44. MacArthur, E. (2013). Towards the circular economy. J. Ind. Ecol, 23-44. Available at: DOI:2012-04-03

45. Braungart, M., McDonough, W., & Bollinger, A. (2007). Cradle-to-cradle design: creating healthy emissions–a strategy for eco-effective product and system design. Journal of cleaner production, 15(13-14), 1337-1348..

46. Method. Our business. Available at: https://methodhome.com/beyond-the-bottle/our-business/ (Accessed: 28 May 2018)

47. El Haggar, S. (2010). Sustainable industrial design and waste management: cradle-to-cradle for sustainable development. Academic Press.

48. The World Bank. Let’s Talk Development. [Blog] The 2017 global poverty update from the World Bank. 16 October 2017. Available at: http://blogs.worldbank.org/developmenttalk/2017-global-poverty-update-world-bank (Accessed: 29 May 2018)

49. Consejo Nacional de Evaluacion de la Politica de Desarrolo Social (CONEVAL). Pobreza en México. 2016. Available at: https://www.coneval.org.mx/Medicion/Paginas/PobrezaInicio.aspx (Accessed: 29 May 2018)

50. Jacintos Nieves, A. Diagnóstico del manejo de residuos de actividades agropecuarias y su gestión en México. Tesis en Ingeniería Civil. Universidad Autonoma de México; 2012. Available at: http://132.248.9.195/ptb2011/julio/0670961/Index.html

51. Hoornweg, D., & Bhada-Tata, P. (2012). What a waste: a global review of solid waste management. Available at: DOI:10.1111/febs.13058

52. United Nations (UN). Sustainable consumption and production. 2015. Available at: https://www.un.org/sustainabledevelopment/sustainable-consumption-production/ (Accessed: 2 June 2018)

53. Secretaría del Medio Ambiente y Recursos Naturales (SEMARNAT). Programa Nacional para la Prevención y Gestión Integral de los Residuos 2009-2012. 2009.

54. The World Bank. CO^2 emissions (kt) table. 2015. Available at: http://data.worldbank.org/indicator/EN.ATM.CO2E.KT/countries/1W?order=wbapi_data_value_2010 wbapi_data_value wbapi_data_value-first&sort=desc&display=default (Accessed: 26 October 2015)

55. Yevich, R., & Logan, J. A. (2003). An assessment of biofuel use and burning of agricultural waste in the developing world. Global biogeochemical cycles, 17(4). Available at: DOI:10.1029/2002GB001952

56. Nieto, M.E., Cuarenta, M.J., Tellez, S., Palos, I. Residuos agrícolas: su impacto en el cambio climático y su aprovechamiento en la generación de productos de alto valor agregado. [Lecture]. Universidad Autónoma de Tamaulipas. 20 October 2014.

57. Costner, P., & sobre Plaguicidas, R. D. A. (2006). Estimando las liberaciones y priorizando las fuentes de dioxinas en el Convenio de Estocolmo. Red de Acción sobre Plaguicidas y Alternativas en México (RAPAM).

58. Instituto Nacional de Estadística y Geografía (INEGI). Objetivos de Desarrollo Sostenible. Available at: http://143.137.108.139/acerca.html (Accessed: 1 June 2018)

59. FAOSTAT. 2006-2016 crops residues emissions of nitrous oxide from the decomposition of crop residues on cultivated soils. Available at: http://www.fao.org/faostat/en/#data/GA/visualize (Accessed: 4 June 2018)

60. FAOSTAT. Emissions CO^2eq burning crop residues in Mexico. Available at: http://www.fao.org/faostat/en/#data/GB/visualize (Accessed: 28 September 2017)

61. Quintero Núñez, M., & Moncada Aguilar, A. (2008). Contaminación y control de las quemas agrícolas en Imperial, California, y Mexicali, Baja California. Región y sociedad, 20(43), 3-24. Available at: -148.215.2.10/articulo.oa?id=10204301

62. FAOSTAT. CO^2 emissions per crop burning practices as per crop type in 2016. 2016. Available at: http://www.fao.org/faostat/en/#data/GA/visualize (Accessed: 4 June 2018)

63. Moreno, A. D., Rodríguez, M. G., Velasco, A. R., Enriquez, J. C. M., Lara, R. G., Gutiérrez, A. M., & Hernández, N. A. D. (2013). Características y análisis de composición de los residuos sólidos de la Ciudad de México. Revista Internacional de Contaminación Ambiental, 29(1), 39-46.

64. Secretaría del Medio Ambiente y Recursos Naturales (SEMARNAT). Ley general para la prevención y gestión integral de los residuos. 2015. Available at: http://www.diputados.gob.mx/LeyesBiblio/ref/lgpgir/LGPGIR_orig_08oct03.pdf (Accessed: 5 June 2018)

65. Tlaxcala E. Carreteros in the lanfill Bordo de Xochiaca, Nezahualcoyotl, Mexico. 2007.

66. Hoornweg, D., & Bhada-Tata, P. (2012). What a waste: a global review of solid waste management. Available at: http://web.worldbank.org/WBSITE/EXTERNAL/TOPICS/EXTURBANDEVELOPMENT/0,,contentMDK:23172887~pagePK:210058~piPK:210062~theSitePK:337178,00.html (Accessed: 27 April 2017)

67. The Organisation for Economic Co-operation and Development (OECD). Glossary of statistical terms - Agricultural waste definition. 2001. Available

at: https://stats.oecd.org/glossary/detail.asp?ID=77 (Accessed: 30 May 2018)

68. Secretaría de Agricultura, Ganadería, Desarrollo Rural, Pesca y Alimentación de México (SAGARPA). Mapa de proyectos de manejo de residuos. 2015. Available at: http://www.sagarpa.gob.mx/ProgramasSAGARPA/2015/Productividad_y_competitividad_agroalimentaria/Programa_regional_de_desarrollo_previsto_en_el_PND/36 incentivos/211PP064 NUEVA AMERICA S.P.R. DE R.L/5. PROYECTO/Manejo de residuos Detallado.pdf

69. Secretaría de Agricultura, Ganadería, Desarrollo Rural, Pesca y Alimentación de México (SAGARPA). SIAP Servicio de Información Agroalimentaria y Pesquera. 2014. Available at: http://www.siap.gob.mx/cierre-de-la-produccion-agricola-por-cultivo/

70. Secretaría del Medio Ambiente y Recursos Naturales (SEMARNAT). Anuario Estadístico de la Producción Forestal 2013. 2014. Available at: http://www.cnf.gob.mx:8090/snif/portal/economica/anuarios-estadisticos-de-la-produccion-forestal

71. Palomo Martínez, G. G., & Becerril, A. (1993). Atlas de ubicación de productos agropecuarios utilizables en la planificación y desarrollo de la agricultura en México (No. C/338.170972 P3).

72. Reddy, N., & Yang, Y. (2005). Biofibers from agricultural byproducts for industrial applications. Trends in Biotechnology, 23(1), 22-27. Available at: DOI:http://dx.doi.org/10.1016/j.tibtech.2004.11.002

73. Taborda, J. D. T. (2014). Propiedades mecánicas de una matriz de poliéster reforzada con fibra de coco comparadas con la misma matriz reforzada con fibra de vidrio. PhD thesis. Universidad Tecnológica de Pereira. Facultad de Ingeniería Mecánica. Ingeniería Mecánica.

74. Granados Sánchez, D., & López Ríos, G. F. (2002). Manejo de la palma de coco (Cocos nucifera L.) en México. Revista Chapingo. Serie ciencias forestales y del ambiente, 8(1). Available at: http://www.redalyc.org/html/629/62980105/ (Accessed: 24 September 2017)

75. Iqbal, H. M. N., Kyazze, G., & Keshavarz, T. (2013). Advances in the valorization of lignocellulosic materials by biotechnology: an overview. BioResources, 8(2), 3157-3176..

76. Valdez-Vazquez, I., Acevedo-Benítez, J. A., & Hernández-Santiago, C. (2010). Distribution and potential of bioenergy resources from agricultural activities in Mexico. Renewable and Sustainable Energy Reviews, 14(7), 2147-2153.. Available at: DOI:10.1016/j.rser.2010.03.034

77. Servicio de Información Agroalimentaria y Pesquera (SIAP). Anuario Estadístico de la Producción Agrícola 2017. 2018. Available at: http://nube.siap.gob.mx/cierreagricola/ (Accessed: 1 June 2018)

78. Index mundi. Corn Production by Country in 1000 MT - Country Rankings. Available at: http://www.indexmundi.com/agriculture/?commodity=corn (Accessed: 25 September 2017)

79. The Observatory of Economic Complexit. Countries that import Maize except seed corn. 2016.Available at: https://atlas.media.mit.edu/en/visualize/geo_map/hs92/import/show/all/100590/2016/ (Accessed: 7 June 2018)

80. Centro Internacional de Mejoramiento de Maíz y Trigo (CIMMYT). Annual Report. 2013. Available at: https://s3.amazonaws.com/ewbgeneral/EWB-USA 2013 Annual Report_High Res.pdf

81. Renard, G., & Storr, S. (2014). Maize CRP Annual Report 2013. Available at: DOI:10.1111/epp.12066

82. Centro Internacional de Mejoramiento de Maíz y Trigo (CIMMYT). MasAgro, How will Mexico feed a growing population in the face of

climate change and food insecurity ?. [Brochure]. 2014. Available at: http://masagro.cimmyt.org/

83. Fernández, A. T., Wise, T. A., & Garvey, E. (2012). Achieving Mexico's Maize Potential. Tufts University.

84. Fernández Suárez, R., Morales Chávez, L. A., & Gálvez Mariscal, A. (2013). Importancia de los maíces nativos de México en la dieta nacional: Una revisión indispensable. Revista fitotecnia mexicana, 36, 275-283.

85. Centro Internacional de Mejoramiento de Maíz y Trigo (CIMMYT). CGIAR Research Program on Maize. 2012. Available at: http://www.cimmyt.org/maize-crp/ (Accessed: 25 September 2017)

86. Ortega, R., Arias, L.M., Figueroa, J.D.D. Tabla descriptiva de razas de maíz en México. [Workshop] 17 and 18 March 2010. Comisión Nacional para el Conocimiento y Uso de la Biodiversidad.

87. Cruz, M.S., Gómez, M.M., Ortiz, M.E., Entzana, A.M., Suárez, C.Y., Santillán, V., et al. Situación actual y perspectivas del maíz en México 1996-2012. Secretaría de Agricultura, Ganadería, Desarrollo Rural, Pesca y Alimentación (SAGARPA) and Servicio de Información Agroalimentaria y Pesquera (SIAP). 2012.

88. Shen, L., Haufe, J., & Patel, M. K. (2009). Product overview and market projection of emerging bio-based plastics PRO-BIP 2009. Report for European polysaccharide network of excellence (EPNOE) and European bioplastics, 243. Available at: DOI:10.1002/9780470697474.ch1

89. Khan, M. A. (2010). Hydrolysis of hemicellulose by commercial enzyme mixtures. Available at: DOI:1402-1552 - ISRN: LTU-DUPP--10/040--SE

90. Tomerlin, L. (2003). Biofuel from corn stover. Agriculture Scientific and Professional Review, 9(2), 45-51.

91. Prado-Martínez, M., Anzaldo-Hernández, J., Becerra-Aguilar, B., Palacios-Juárez, H., Vargas-Radillo, J. D. J., & Rentería-Urquiza, M. (2012). Caracterización de hojas de mazorca de maíz y de bagazo de caña para la elaboración de una pulpa celulósica mixta. Madera y bosques, 18(3), 37-51. Available at: http://www.scielo.org.mx/scielo.php?script=sci_arttext&pid=S1405-04712012000300004&lng=es&nrm=iso&tlng=es (Accessed: 11 April 2016)

92. Huda, S., & Yang, Y. (2009). A novel approach of manufacturing light-weight composites with polypropylene web and mechanically split cornhusk. Industrial crops and products, 30(1), 17-23. Available at: DOI:10.1016/j.indcrop.2008.12.007

93. Reddy, N., Thillainayagam, V. A., & Yang, Y. (2011). Dyeing Natural Cellulose Fibers from Cornhusks: A Comparative Study with Cotton Fibers. Industrial & Engineering Chemistry Research, 50(9), 5642-5650.. Available at: DOI:10.1021/ie200217w

94. Wu, J., Zhang, X., Wan, J., Ma, F., Tang, Y., & Zhang, X. (2011). Production of fiberboard using corn stalk pretreated with white-rot fungus Trametes hirsute by hot pressing without adhesive. Bioresource technology, 102(24), 11258-11261. Available at: DOI:http://dx.doi.org/10.1016/j.biortech.2011.09.097

95. Youssef, A. M., El-Gendy, A., & Kamel, S. (2015). Evaluation of corn husk fibers reinforced recycled low density polyethylene composites. Materials Chemistry and Physics, 152, 26-33. Available at: DOI:10.1016/j.matchemphys.2014.12.004

96. Reddy, N., & Yang, Y. (2005). Properties and potential applications of natural cellulose fibers from cornhusks. Green Chemistry, 7(4), 190-195. Available at: http://pubs.rsc.org/en/content/articlehtml/2005/gc/b415102j

97. Rodríguez Chávez, J. J., Valtierra Pacheco, E., Hernández Romero, O., & López Reyna, M. D. C. (2009). Factores de éxito de las PYMES en el medio rural: el caso del procesamiento y comercialización de hoja de maíz para tamal en la localidad de Palomas, Mpio de Cd. del Maíz SLP México. Thesis. Colegio de Postgraduados, Campus Montecillo, Postgrado de Socioeconomía, Estadística e Informática, Desarrollo Rural. Available at: http://www.cm.colpos.mx/desarrollo/TRIPTICO/RESUMENES_TESIS/RODRIGUEZ_CHAVEZ_JUAN_JOSE.htm (Accessed: 26 October 2015)

98. SIFUPRO. Innovacion tecnológica en el proceso del blanqueado de la hoja de maiz para tamal. 2013. Available at: http://siproduce.sifupro.org.mx/seguimiento/archivero/30/2013/anuales/anu_1551-25-2014-05-5.pdf (Accessed: 1 October 2017)

99. Ontiveros G. Muñecas de hoja de maiz. 2016.

100. Aspros. Semillas de maiz, siembra aspros. Available at: http://www.asprossemillas.com/ (Accessed: 13 October 2015)

101. Hull, D., & Clyne, T. W. (1996). An introduction to composite materials. Cambridge university press. Available at: https://books.google.co.uk/books?id=BRcdDu4bUhMC

102. Harris, B. (1986). Engineering composite materials (pp. 81-105). London: Institute of metals. Available at: DOI:10.1016/0010-4361(87)90420-4

103. Ibrahim, I. D., Jamiru, T., Sadiku, R. E., Kupolati, W. K., Agwuncha, S. C., & Ekundayo, G. (2015). The use of polypropylene in bamboo fibre composites and their mechanical properties–A review. Journal of Reinforced Plastics and Composites, 34(16), 1347-1356. Available at: DOI:10.1177/0731684415591302

104. Zini, E., & Scandola, M. (2011). Green composites: an overview. Polymer

composites, 32(12), 1905-1915. Available at: DOI:10.1002/pc.21224

105. Fowler, P. A., Hughes, J. M., & Elias, R. M. (2006). Biocomposites: technology, environmental credentials and market forces. Journal of the Science of Food and Agriculture, 86(12), 1781-1789. Available at: DOI:10.1002/jsfa.2558 (Accessed: 14 October 2015)

106. Baillie, C. (Ed.). (2005). Green composites: polymer composites and the environment. CRC Press.

107. Kalia, S., Kaith, B. S., & Kaur, I. (Eds.). (2011). Cellulose fibers: bio-and nano-polymer composites: green chemistry and technology. Springer Science & Business Media. Available at: DOI:10.1007/978-3-642-17370-7 (Accessed: 29 September 2014)

108. Shaz, I., and Ansell, MP. (2004). Optimising the properties of green composites. Green Compos. Polym. Compos. Environ, 154. Available at: DOI:10.1016/B978-1-85573-739-6.50011-7 (Accessed: 1 October 2017)

109. Mohanty, A. K., Misra, M., & Drzal, L. T. (Eds.). (2005). Natural fibers, biopolymers, and biocomposites. CRC press. Available at: https://books.google.com/books?hl=en&lr=&id=AwXugfY2oc4C&pgis=1 (Accessed: 14 October 2015)

110. Faruk, O., Bledzki, A. K., Fink, H. P., & Sain, M. (2012). Biocomposites reinforced with natural fibers: 2000–2010. Progress in polymer science, 37(11), 1552-1596. Available at: DOI:http://dx.doi.org/10.1016/j.progpolymsci.2012.04.003

111. Akaranta, O. (2000). Production of particle boards from bioresources. Bioresource technology, 75(1), 87-89. Available at: DOI:http://dx.doi.org/10.1016/S0960-8524(00)00035-3 (Accessed: 2 September 2015)

112. Luna, H., Hernández-Vázquez, L., Reyo, A., Arias, L., Manjarrez, N., & Navarro-Ocaña, A. (2014). Banana and maize leaf wastes as a green

alternative for the preparation of benzyl alcohols used as starting materials for fragrances. Industrial Crops and Products, 59, 105-108. Available at: DOI:http://dx.doi.org/10.1016/j.indcrop.2014.04.023

113. Thakur, V. K. (2013). Green composites from natural resources. CRC Press. Available at: https://books.google.com/books?hl=en&lr=&id=gX76AQAAQBAJ&pgis=1 (Accessed: 26 October 2015)

114. Gassan, J., & Bledzki, A. K. (1999). Alkali treatment of jute fibers: relationship between structure and mechanical properties. Journal of Applied Polymer Science, 71(4), 623-629.

115. Yang, H. S., Kim, D. J., Lee, Y. K., Kim, H. J., Jeon, J. Y., & Kang, C. W. (2004). Possibility of using waste tire composites reinforced with rice straw as construction materials. Bioresource technology, 95(1), 61-65.

116. Johar, N., Ahmad, I., & Dufresne, A. (2012). Extraction, preparation and characterization of cellulose fibres and nanocrystals from rice husk. Industrial Crops and Products, 37(1), 93-99. Available at: DOI:10.1016/j.indcrop.2011.12.016

117. Padkho, N. (2012). A new design recycle agricultural waste materials for profitable use rice straw and maize husk in wall. Procedia Engineering, 32, 1113-1118. Available at: DOI:10.1016/j.proeng.2012.02.063

118. Zhu, J., Zhu, H., Immonen, K., Brighton, J., & Abhyankar, H. (2015). Improving mechanical properties of novel flax/tannin composites through different chemical treatments. Industrial Crops and Products, 67, 346-354. Available at: DOI:http://dx.doi.org/10.1016/j.indcrop.2015.01.052

119. Kinloch, A. J., Taylor, A. C., Techapaitoon, M., Teo, W. S., & Sprenger, S. (2015). Tough, natural-fibre composites based upon epoxy matrices. Journal of materials science, 50(21), 6947-6960. Available at: DOI:10.1007/s10853-015-9246-z (Accessed: 2 September 2015)

120. O'donnell, A., Dweib, M. A., & Wool, R. P. (2004). Natural fiber composites with plant oil-based resin. Composites science and technology, 64(9), 1135-1145. Available at: DOI:10.1016/j.compscitech.2003.09.024

121. Pizzi, A. (2006). Recent developments in eco-efficient bio-based adhesives for wood bonding: opportunities and issues. Journal of adhesion science and technology, 20(8), 829-846. Available at: DOI:10.1163/156856106777638635

122. Mohanty, A. K., Misra, M. A., & Hinrichsen, G. (2000). Biofibres, biodegradable polymers and biocomposites: An overview. Macromolecular materials and Engineering, 276(1), 1-24. Available at: DOI:10.1002/(SICI)1439-2054(20000301)276:1<1::AID-MAME1>3.0.CO;2-W

123. Nayeri, M. D., Tahir, P. M., Jawaid, M., Ashaari, Z., Abdullah, L. C., Bakar, E. S., & Namvar, F. (2014). Medium density fibreboard made from Kenaf (Hibiscus cannabinus L.) stem: effect of thermo-mechanical refining and resin content. BioResources, 9(2), 2372-2381. Available at: DOI:10.15376/biores.9.2.2372-2381

124. Mo, X., Cheng, E., Wang, D., & Sun, X. S. (2003). Physical properties of medium-density wheat straw particleboard using different adhesives. Industrial Crops and Products, 18(1), 47-53. Available at: DOI:10.1016/S0926-6690(03)00032-3

125. Halvarsson, S., Edlund, H., & Norgren, M. (2009). Manufacture of non-resin wheat straw fibreboards. industrial crops and products, 29(2-3), 437-445. Available at: DOI:10.1016/j.indcrop.2008.08.007

126. Ye, X. P., Julson, J., Kuo, M., Womac, A., & Myers, D. (2007). Properties of medium density fiberboards made from renewable biomass.

Bioresource Technology, 98(5), 1077-1084. Available at: DOI:http://dx.doi.org/10.1016/j.biortech.2006.04.022

127. Yilmaz, N. D., Sulak, M., Yilmaz, K., & Kalin, F. (2016). Physical and chemical properties of water-retted fibers extracted from different locations in corn husks. Journal of Natural Fibers, 13(4), 397-409. Available at: DOI:http://dx.doi.org/10.1080/15440478.2015.1029201

128. Slootmaker, T., & Müssig, J. (2010). SEM Catalogue for animal and plant fibres. Industrial Applications of Natural Fibres: Structure, Properties and Technical Applications, 311-336.

129. Purslow, D. (1986). Matrix fractography of fibre-reinforced epoxy composites. Composites, 17(4), 289-303. Available at: DOI:10.1016/0010-4361(86)90746-9 (Accessed: 29 March 2016)

130. Cantwell, W. J., & Morton, J. (1991). The impact resistance of composite materials—a review. composites, 22(5), 347-362. Available at: DOI:10.1016/0010-4361(91)90549-V

131. Nechwatal, A., Mieck, K. P., & Reußmann, T. (2003). Developments in the characterization of natural fibre properties and in the use of natural fibres for composites. Composites Science and Technology, 63(9), 1273-1279. Available at: DOI:10.1016/S0266-3538(03)00098-8

132. Larrauri, J. A., Rupérez, P., Borroto, B., & Saura-Calixto, F. (1996). Mango peels as a new tropical fibre: preparation and characterization. LWT-Food Science and Technology, 29(8), 729-733. Available at: DOI:http://dx.doi.org/10.1006/fstl.1996.0113

133. Ma, Z., Pan, G., Xu, H., Huang, Y., & Yang, Y. (2015). Cellulosic fibers with high aspect ratio from cornhusks via controlled swelling and alkaline penetration. Carbohydrate polymers, 124, 50-56. Available at: DOI:10.1016/j.carbpol.2015.02.008 (Accessed: 31 March 2016)

134. Reddy, N., & Yang, Y. (2011). Biocomposites developed using water-plasticized wheat gluten as matrix and jute fibers as reinforcement. Polymer International, 60(4), 711-716. Available at: DOI:10.1002/pi.3014

135. Bledzki, A. K., & Gassan, J. (1999). Composites reinforced with cellulose based fibres. Progress in polymer science, 24(2), 221-274. Available at: DOI:http://dx.doi.org/10.1016/S0079-6700(98)00018-5

136. Huda, S., & Yang, Y. (2008). Chemically extracted cornhusk fibers as reinforcement in light-weight poly (propylene) composites. Macromolecular Materials and Engineering, 293(3), 235-243. Available at: DOI:10.1002/mame.200700317

137. Ahmad, F., Choi, H. S., & Park, M. K. (2015). A review: natural fiber composites selection in view of mechanical, light weight, and economic properties. Macromolecular materials and engineering, 300(1), 10-24. Available at: DOI:10.1002/mame.201400089 (Accessed: 24 August 2015)

138. Kozłowski, R. M. (Ed.). (2012). Handbook of natural fibres: Types, properties and factors affecting breeding and cultivation. Elsevier. Available at: http://app.knovel.com/web/toc.v/cid:kpHNFVTPF1/viewerType:toc/root_slug:handbook-natural-fibres/url_slug:handbook-natural-fibres (Accessed: 14 October 2015)

139. Rao, K. M. M., Rao, K. M., & Prasad, A. R. (2010). Fabrication and testing of natural fibre composites: Vakka, sisal, bamboo and banana. Materials & Design, 31, 508-513. Available at: DOI:10.1016/j.matdes.2009.06.023

140. European Commission (EU). Regulation 605/2014. Regulation (EC) No 1272/2008 of the European Parliament and of the Council on classification, labelling and packaging of substances and mixtures. 2014. Available at: http://eur-lex.europa.eu/legal-content/EN/ALL/?uri=uriserv:OJ.L_.2014.167.01.0036.01.ENG (Accessed: 23 May 2017)

141. California Air Resources Board (CARB). Final regulation of the airborne toxic control measure to reduce formaldehyde. Emissions from composite wood products. 2007. Available at: https://www.arb.ca.gov/regact/2007/compwood07/fro-final.pdf (Accessed: 6 March 2017)

142. Salthammer, T., Mentese, S., & Marutzky, R. (2010). Formaldehyde in the indoor environment. Chemical reviews, 110(4), 2536-2572.

143. Satyanarayana, K. G., Arizaga, G. G., & Wypych, F. (2009). Biodegradable composites based on lignocellulosic fibers—An overview. Progress in polymer science, 34(9), 982-1021. Available at: DOI:10.1016/j.progpolymsci.2008.12.002 (Accessed: 28 August 2014)

144. Zhu, J. (2015). Development of novel flax bio-matrix composites for non-structural and structural vehicle applications.

145. Mwaikambo, L. Y., & Ansell, M. P. (2001). Cure characteristics of alkali catalysed cashew nut shell liquid-formaldehyde resin. Journal of Materials Science, 36(15), 3693-3698.

146. Pickering, K. L., Efendy, M. A., & Le, T. M. (2016). A review of recent developments in natural fibre composites and their mechanical performance. Composites Part A: Applied Science and Manufacturing, 83, 98-112. Available at: DOI:10.1016/j.compositesa.2015.08.038

147. Zhang, D., Zhang, A., & Xue, L. (2015). A review of preparation of binderless fiberboards and its self-bonding mechanism. Wood Science and Technology, 49(4), 661-679. Available at: DOI:10.1007/s00226-015-0728-6

148. Hüttermann, A., Mai, C., & Kharazipour, A. (2001). Modification of lignin for the production of new compounded materials. Applied microbiology and biotechnology, 55(4), 387-394. Available at: DOI:10.1007/s002530000590

149. Xie, L., Liu, J., & Du, A. (2012, October). Effect of hot-pressing factors on binderless fiberboard properties. In Biobase Material Science and Engineering (BMSE), 2012 International Conference on (pp. 8-11). IEEE. Available at: DOI:10.1109/BMSE.2012.6466168

150. Widyorini, R., Xu, J., Umemura, K., & Kawai, S. (2005). Manufacture and properties of binderless particleboard from bagasse I: effects of raw material type, storage methods, and manufacturing process. Journal of Wood Science, 51(6), 648. Available at: DOI:10.1007/s10086-005-0713-z (Accessed: 29 September 2015)

151. Hashim, R., Saari, N., Sulaiman, O., Sugimoto, T., Hiziroglu, S., Sato, M., & Tanaka, R. (2010). Effect of particle geometry on the properties of binderless particleboard manufactured from oil palm trunk. Materials & Design, 31(9), 4251-4257. Available at: DOI:10.1016/j.matdes.2010.04.012 (Accessed: 28 September 2015)

152. Shen, K.C. US 4627951. Process for manufacturing composite products from lignocellulosic materials. United States Patent and Trademark Office. December 1986.

153. Halvarsson, S. (2010). Manufacture of straw MDF and fibreboards PhD thesis. Kopieringen Mittuniversitetet.

154. Tupciauskas, R., Gravitis, J., Veveris, A., & Tuherm, H. (2009, October). Self-binding fibreboard made of steam exploded wood. In Proceedings of the 5th meeting of the Nordic Baltic Network in Wood Material Science & Engineering (WSE) (pp. 1-2). Copenhagen:: Forest & Landcape Working Papers.

155. Zhou, X., Tang, L., Zhang, W., Lv, C., Zheng, F., Zhang, R., & Liu, X. (2010). Enzymatic hydrolysis lignin derived from corn stover as an intrinstic binder for bio-composites manufacture: effect of fiber moisture

content and pressing temperature on boards' properties. BioResources, 6(1), 253-264.

156. Van Dam, J. E., van den Oever, M. J., Teunissen, W., Keijsers, E. R., & Peralta, A. G. (2004). Process for production of high density/high performance binderless boards from whole coconut husk: Part 1: Lignin as intrinsic thermosetting binder resin. Industrial Crops and Products, 19(3), 207-216. Available at: DOI:10.1016/j.indcrop.2003.10.003 (Accessed: 23 May 2017)

157. Csiszar, E., Urbánszki, K., & Szakacs, G. (2001). Biotreatment of desized cotton fabric by commercial cellulase and xylanase enzymes. Journal of Molecular Catalysis B: Enzymatic, 11(4-6), 1065-1072. Available at: DOI:10.1016/S1381-1177(00)00149-1 (Accessed: 13 October 2015)

158. Yılmaz, N. D., Çalışkan, E., & Yılmaz, K. (2014). Effect of xylanase enzyme on mechanical properties of fibres extracted from undried and dried corn husks. Available at: DOI:10.1080/00405000.2012.736707

159. Ghaffar, S. H., & Fan, M. (2014). Lignin in straw and its applications as an adhesive. International Journal of Adhesion and Adhesives, 48, 92-101. Available at: DOI:10.1016/j.ijadhadh.2013.09.001

160. Lehmann, W. F. (2000). Wood-Based Composites and Laminates. Kirk-Othmer Encyclopedia of Chemical Technology, 1-47.

161. Zhu, H., Li, Y., Pettersson, B., Zhang, L., Lindström, M., & Henriksson, G. (2014). Technical soda lignin dissolved in urea as an environmental friendly binder in wood fiberboard. Journal of Adhesion Science and Technology, 28(5), 490-498. Available at: DOI:10.1080/01694243.2013.843284

162. Anglès, M. N., Ferrando, F., Farriol, X., & Salvadó, J. (2001). Suitability of steam exploded residual softwood for the production of binderless panels.

Effect of the pre-treatment severity and lignin addition. Biomass and Bioenergy, 21(3), 211-224. Available at: DOI:10.1016/S0961-9534(01)00031-9

163. Jawaid, M., Salit, M. S., & Alothman, O. Y. (Eds.). (2017). Green Biocomposites: Design and Applications. Springer. Available at: DOI:10.1007/978-3-319-49382-4

164. Sealy, C., & Vaia, R. A. (2015). Composites come together. Reinforced Plastics, 59(1), 34-37. Available at: DOI:10.1016/S1369-7021(06)71564-4

165. Ross, R. J. (2010). Wood handbook: wood as an engineering material. USDA Forest Service, Forest Products Laboratory, General Technical Report FPL-GTR-190, 2010: 509 p. 1 v., 190.

166. Altenbach, H., Altenbach, J., Kissing, W., & Altenbach, H. (2004). Mechanics of composite structural elements (pp. 78-84). Berlin: Springer-Verlag. Available at: DOI:10.1007/978-3-662-08589-9

167. British International Standards (BSI). BS EN 622-5:2009. Fibreboards. Specifications. Requirements for dry process boards (MDF). 2010.

168. Secretaría del Medio Ambiente y Recursos Naturales (SEMARNAT). Economía forestal en México 2015. [Brochure]. 2015.

169. Sellers Jr, T. (2001). Wood adhesive innovations and applications in North America. Forest Products Journal, 51(6), 12.

170. British International Standards (BSI). BS ISO 16895:2013. Wood-based panels. Dry-process fibreboard. 2AD. 2013.

171. Felby, C., Hassingboe, J., & Lund, M. (2002). Pilot-scale production of fiberboards made by laccase oxidized wood fibers: board properties and evidence for cross-linking of lignin. Enzyme and microbial technology, 31(6), 736-741. Available at: DOI:http://dx.doi.org/10.1016/S0141-

0229(02)00111-4

172. American Society for Testing and Materials (ASTM). ASTM D5035-11(2015), Standard Test Method for Breaking Force and Elongation of Textile Fabrics (Strip Method). ASTM International. West Conshohocken, PA. 2015. Available at: DOI:10.1520/D5034-09.2

173. American Society for Testing and Materials (ASTM). ASTM D 1348-94 Standard Test Methods for Moisture in Cellulose, 94(Reapproved 2008). ASTM International. West Conshohocken, PA. 2008. Available at: DOI:10.1520/D1348-94R08.loose

174. Thomason, J. L., & Carruthers, J. (2012). Natural fibre cross sectional area, its variability and effects on the determination of fibre properties. Journal of Biobased Materials and Bioenergy, 6(4), 424-430. Available at: DOI:10.1166/jbmb.2012.1231

175. American Society for Testing and Materials (ASTM International). ASTM D3822 / D3822M-14, Standard Test Method for Tensile Properties of Single Textile Fibers. ASTM International. West Conshohocken, PA. 2014. Avalailable at: DOI: 10.1520/D3822_D3822M-14

176. American Society for Testing and Materials (ASTM International). ASTM D1037-12, Standard Test Methods for Evaluating Properties of Wood-Base Fiber and Particle Panel Materials. ASTM International. West Conshohocken, PA. 2012. Avalailable at: DOI: 10.1520/D1037-12

177. American Society for Testing and Materials (ASTM International). Standard test method for unnotched cantilever beam impact strength of plastics. 1993; 08: 1–12. Available at: DOI:10.1520/D4812-11.2

178. Akgül, M., & Çamlibel, O. (2008). Manufacture of medium density fiberboard (MDF) panels from rhododendron (R. ponticum L.) biomass. Building and Environment, 43(4), 438-443. Available at:

DOI:10.1016/j.buildenv.2007.01.003

179. Yılmaz, N. D., Çalışkan, E., & Yılmaz, K. (2014). Effect of xylanase enzyme on mechanical properties of fibres extracted from undried and dried corn husks.

180. Reddy, N., & Yang, Y. (2005). Structure and properties of high quality natural cellulose fibers from cornstalks. Polymer, 46(15), 5494-5500. Available at: DOI:http://dx.doi.org/10.1016/j.polymer.2005.04.073

181. Rathke, J., Sinn, G., Harm, M., Teischinger, A., Weigl, M., & Müller, U. (2012). Effects of alternative raw materials and varying resin content on mechanical and fracture mechanical properties of particle board. BioResources, 7(3), 2970-2985..

182. Halvarsson, S., Edlund, H., & Norgren, M. (2008). Properties of medium-density fibreboard (MDF) based on wheat straw and melamine modified urea formaldehyde (UMF) resin. Industrial crops and products, 28(1), 37-46. Available at: DOI:10.1016/j.indcrop.2008.01.005

183. Abbott, A. P., Conde, J. P., Davis, S. J., & Wise, W. R. (2012). Starch as a replacement for urea-formaldehyde in medium density fibreboard. Green Chemistry, 14(11), 3067-3070. Available at: DOI:10.1039/c2gc36194a

184. Nasir, M., Gupta, A., Beg, M. D. H., Chua, G. K., & Asim, M. (2014). Laccase application in medium density fibreboard to prepare a bio-composite. RSC advances, 4(22), 11520-11527. Available at: DOI:10.1039/c3ra40593a

185. Sicomin epoxy systems. GreenPoxy 56 clear epoxy resin, technical datasheet. 2015. Available at: http://www.sicomin.com/datasheets/product-pdf1152.pdf

186. Entropy resins, Inc. Super Sap® CPL technical data sheet. 2013.

Available at: https://europe.entropyresins.eu/store/supersap-cpm-cpf-cpl/

187. Roffael, E., Dix, B., & Okum, J. (2000). Use of spruce tannin as a binder in particleboards and medium density fiberboards (MDF). European Journal of Wood and Wood Products, 58(5), 301-305. Available at: DOI:10.1007/s001070050432

188. Mathiasson, A., & Kubat, D. G. (1994). Lignin as binder in particle boards using high frequency heating. Holz als Roh-und Werkstoff, 52(1), 9. Available at: DOI:10.1007/BF02615010

189. Pugh, S. (2009). The Systems Engineering Tool Box.

190. American Society for Testing and Materials (ASTM International). ASTM D256-10e1, Standard Test Methods for Determining the Izod Pendulum Impact Resistance of Plastics. ASTM International. West Conshohocken, PA. 2010. Available at: DOI:10.1520/D0256-10.

191. Fahmy, Y., Fahmy, T. Y., Mobarak, F., El-Sakhawy, M., & Fadl, M. H. (2017). Agricultural residues (wastes) for manufacture of paper, board, and miscellaneous products: background overview and future prospects. Available at: DOI:10.5281/zenodo.546735

192. Symington, M. C., Banks, W. M., West, O. D., & Pethrick, R. A. (2009). Tensile testing of cellulose based natural fibers for structural composite applications. Journal of composite materials, 43(9), 1083-1108. Available at: DOI:10.1177/0021998308097740

193. American Society for Testing and Materials (ASTM International). ASTM D3822 / D3822M-14, Standard Test Method for Tensile Properties of Single Textile Fibers. ASTM International. West Conshohocken, PA, 2014. Available at: DOI:10.1520/D3822

194. Sreekumar, P. A., & Thomas, S. (2008). Matrices for natural-fibre reinforced composites. In Properties and performance of natural-fibre

composites (pp. 67-126). Available at: DOI:10.1533/9781845694593.1.67

195. Kalia, S., Kaith, B. S., & Kaur, I. (Eds.). (2011). Cellulose fibers: bio-and nano-polymer composites: green chemistry and technology. Springer Science & Business Media. Available at: DOI:10.1007/978-3-642-17370-7 (Accessed: 29 September 2014)

196. Mendes, C. A. D. C., Adnet, F. A. D. O., Leite, M. C. A. M., Furtado, C. R. G., & Sousa, A. M. F. D. (2015). Chemical, physical, mechanical, thermal and morphological characterization of corn husk residue. Cellulose Chemistry and Technology, 49(9-10), 727-35. Available at: http://www.scopus.com/inward/record.url?eid=2-s2.0-84961256771&partnerID=tZOtx3y1

197. Lü, H., Zhang, X., & Yu, B. (2015). Optimization of corn-stalk skin flake-wood shaving composite technology. Journal of forestry research, 26(3), 759-763. Available at: DOI:10.1007/s11676-015-0054-8

198. Tyagi, G. K., & Madhusoodhanan, P. (2006). Effect of fibre cross-sectional shape on handle characteristics of polyester-viscose and polyester-cotton ring and MJS yarn fabrics. Available at: http://nopr.niscair.res.in/bitstream/123456789/24581/1/IJFTR 31%284%29 496-500.pdf (Accessed: 20 November 2017)

199. Baillie, C., & Feinblatt, E. (2014). Ethical practices in the processing of green composites. In Natural Fibre Composites (pp. 161-175). Available at: DOI:10.1533/9780857099228.2.161 (Accessed: 13 October 2015)

200. PROTEAK. Tecnotabla technical datasheet. Available at: http://www.tecnotabla.com/wp-content/uploads/materiales/fichas-tecnicas/FichaB%C3%A1sicas_digital_ESP.pdf

201. MASISA. Medium density panel (MDP) technical datasheet. Available at: http://www.masisa.com/mex/productos/

202. Çöpür, Y., Güler, C., Taşçıoğlu, C., & Tozluoğlu, A. (2008). Incorporation of hazelnut shell and husk in MDF production. Bioresource Technology, 99(15), 7402-7406. Available at: DOI:10.1016/j.biortech.2008.01.021

203. The Engineered Wood Association. History of APA, plywood, and engineered wood. 2014. Available at: http://www.apawood.org/apas-history (Accessed: 13 October 2015)

204. Guimarães, G. M., Paes, M. C. D., França, F., & Marconcini, J. M. (2008). Corn husks mechanical characterization. In: Encontro da sociedade brasileira de pesquisa em materiais-SBPMat. 7., 2008, Guarujá, Rio de Janeiro.

205. Elvin, K., Owain, P., & Valentina, R. (2014). Introduction to Materials Experience. Available at: DOI:10.1016/B978-0-08-099359-1.15001-5 (Accessed: 17 February 2016)

206. Sari, N. H., Wardana, I. N. G., Irawan, Y. S., & Siswanto, E. (2016). Physical and acoustical properties of corn husk fiber panels. Advances in Acoustics and Vibration, 2016. Available at: DOI:10.1155/2016/5971814

207. Barl, B., Biliaderis, C. G., Murray, E. D., & Macgregor, A. W. (1991). Combined chemical and enzymic treatments of corn husk lignocellulosics. Journal of the Science of Food and Agriculture, 56(2), 195-214. Available at: DOI:10.1002/jsfa.2740560209

208. Jones, D. R., & Ashby, M. F. (2011). Engineering materials 1: An introduction to properties, applications and design. Elsevier. Available at: https://app.knovel.com/web/toc.v/cid:kpEMAIPADI (Accessed: 15 October 2017)

209. Sampathrajan, A., Vijayaraghavan, N. C., & Swaminathan, K. R. (1992). Mechanical and thermal properties of particle boards made from farm residues. Bioresource technology, 40(3), 249-251. Available at:

DOI:10.1016/0960-8524(92)90151-M (Accessed: 23 June 2016)

210. Rowell, R. M., Sanadi, A. R., Caulfield, D. F., & Jacobson, R. E. (1997). Utilization of natural fibers in plastic composites: problems and opportunities. Lignocellulosic-plastic composites, 23-51. Available at: http://www.fpl.fs.fed.us/documnts/pdf1997/rowel97d.pdf

211. Da Silva, L. F., Öchsner, A., & Adams, R. D. (Eds.). (2011). Handbook of adhesion technology. Springer Science & Business Media. Available at: DOI:10.1007/978-3-642-01169-6

212. Ashby, M. F., & Johnson, K. (2013). Materials and design: the art and science of material selection in product design. Butterworth-Heinemann..

213. Entropy resins, Inc. Super Sap® CPL Material Safety Data Sheet. 2007. Available at: https://europe.entropyresins.eu/store/supersap-cpm-cpf-

214. Barbosa, A. P. C., Fulco, A. P. P., Guerra, E. S., Arakaki, F. K., Tosatto, M., Costa, M. C. B., & Melo, J. D. D. (2017). Accelerated aging effects on carbon fiber/epoxy composites. Composites Part B: Engineering, 110, 298-306. Available at: DOI:10.1016/j.compositesb.2016.11.004

215. Ku, H., Wang, H., Pattarachaiyakoop, N., & Trada, M. (2011). A review on the tensile properties of natural fiber reinforced polymer composites. Composites Part B: Engineering, 42(4), 856-873. Available at: DOI:10.1016/j.compositesb.2011.01.010

216. Bakar, A. A., & Hassan, A. (2003). Impact properties of oil palm empty fruit bunch filled impact modified unplasticised poly (vinyl chloride) composites. Jurnal Teknologi, 39(A), 73-82.

217. British International Standards (BSI). BS EN 322:1993 Wood-based panels. Determination of moisture conten. 1993.

218. Koronis, G., Silva, A., & Fontul, M. (2013). Green composites: a review of

adequate materials for automotive applications. Composites Part B: Engineering, 44(1), 120-127. Available at: DOI:10.1016/j.compositesb.2012.07.004

219. Leavy, P. (2011). Essentials of Transdisciplinary Research. New York: Routledge.

220. Vezzoli, C., & Manzini, E. (2008). Design for environmental sustainability (p. 4). London: Springer. Available at: DOI:10.1007/978-1-84800-163-3 (Accessed: 18 April 2017)

221. Raworth, K. (2017). A Doughnut for the Anthropocene: humanity's compass in the 21st century. The Lancet Planetary Health, 1(2), e48-e49. Available at: DOI:10.1016/S2542-5196(17)30028-1

222. Brief, L. (2011). Opportunities in natural fiber composites. Lucintel LLC, Irving (TX). Available at: http://www.lucintel.com/LucintelBrief/PotentialofNaturalfibercomposites-Final.pdf

223. Duraplay. MDF supremo carb technical sheet. Available at: http://www.duraplay.com.mx/index.php/menu-tableros/menu-duraplay (Accessed: 6 March 2017)

224. Food and Agriculture Organization of the United Nations (FAO). Global Forest Resources Assessment 2005, Main report. FAO Forestry Paper 147. Forestry Paper. 2006; 147: 350 pp. Available at: DOI:ISBN 978-92-5-106654-6

225. Nakamura, H., Kajikawa, Y., & Suzuki, S. (2013). Multi-level perspectives with technology readiness measures for aviation innovation. Sustainability science, 8(1), 87-101. Available at: DOI:10.1007/s11625-012-0187-z

226. MASISA. Informe integrado. Financiero. Social. Ambiental. 2017.

227. Comisión Nacional de los Salarios Mínimos. Secretaría del Trabajo y

Previsión Social (STPS). Tabla de Salarios Mínimos Generales y Profesionales por Áreas Geográficas. 2017. Available at: https://www.gob.mx/cms/uploads/attachment/file/273917/Tabla_de_salarios_minimos_vigentes_a_partir_de_01_dic_2017.pdf (Accessed: 8 December 2017)

228. Karmee, S. K., Patria, R. D., & Lin, C. S. K. (2015). Techno-economic evaluation of biodiesel production from waste cooking oil—a case study of Hong Kong. International journal of molecular sciences, 16(3), 4362-4371. Available at: DOI:10.3390/ijms16034362

229. Li, R., Lan, C., Wu, Z., Huang, T., Chen, X., Liao, Y., ... & Xie, Y. (2017). A novel particleboard using unsaturated polyester resin as a formaldehyde-free adhesive. Construction and Building Materials, 148, 781-788. Available at: DOI:10.1016/j.conbuildmat.2017.04.203

230. Chesbrough, H. (2007). Business model innovation: it's not just about technology anymore. Strategy & leadership, 35(6), 12-17. Available at: DOI:10.1108/10878570710833714

231. MASISA. Medium Density Panel (MDF) technical sheet. 2015. Available at: http://www.masisa.com/mex/productos/

APPENDICES

Appendix A Samples code keys

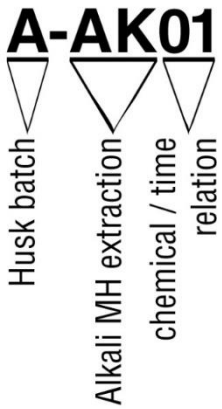

Figure_Apx 7-1 Alkali and enzymatic extractions key code. Husk batch from Table 1. MH size reduction method from Table 12. NaOH / time relation from Table 13. NaOH – enzymes / time relation from Table 14

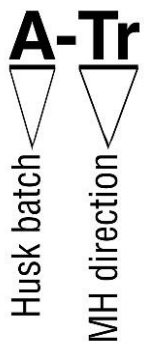

Figure_Apx 7-2 MH swatches tensile test key code. Husk batch from Table 1. MH fibre direction from Table 15

Appendix B CNC cutting programme

ASCII Text Information for Toolpaths
NOTE: ALL sizes, positions etc. are in mm
Material:
X Min:0.000 Y Min:0.000 Z Min:-3.000
X Max:250.000 Y Max:250.000 Z Max:-3.000
X Size:250.000 Y Size:250.000 Z Size:0.000
Thickness:3.000
Home Position:
X:0.00000 Y:0.00000 Z:15.00000 R:0.00000
Safe Z: 15.000
Rotary A Index:
AH:0.00000
Default Feed Rates (in mm/second)
Cutting Feed Rate:4560
Plunge Feed Rate :3000
Rapid Feed Rate :98765
Spindle Speed :19700 r.p.m
First Tool Information
Tool Number:1
Description:3.000 mm dia. ball nose
Description (uppercase):3.000 MM DIA. BALL NOSE
Feed Rate Change - 98765

Rapid (1st) X 37.00000 Y 9.11003 Z 15.00000 R 13.11844 FeedRate:98765

Plunge (1st) X 37.00000 Y 9.11003 Z -1.60000 R 13.11844 FeedRate:3000

Feed Rate Change - 4560

Feed (1st) X 88.00000 Y 9.11003 Z -1.60000 R 13.11844

CCW Arc (1st) Start:88.000,9.110 Mid:89.061,9.549 End:X 89.50000,Y 10.61003,Z -1.60000 Centre:88.000,10.610 Centre Inc:-0.000,1.500 Radius:1.500

Feed (1st) X 89.50000 Y 70.61003 Z -1.60000 R 101.67840

CCW Arc (1st) Start:89.500,70.610 Mid:89.470,70.909 End:X 89.38088,Y 71.19584,Z -1.60000 Centre:88.000,70.610 Centre Inc:-1.500,-0.000 Radius:1.500

CW Arc (1st) Start:89.381,71.196 Mid:84.741,86.561 End:X 83.49930,Y 102.56426,Z -1.60000 Centre:157.965,100.291 Centre Inc:68.584,29.095 Radius:74.500

Feed (1st) X 83.49930 Y 153.65580 Z -1.60000 R 221.26427

CW Arc (1st) Start:83.499,153.656 Mid:84.741,169.659 End:X 89.38088,Y 185.02422,Z -1.60000 Centre:157.965,155.929 Centre Inc:74.465,2.273 Radius:74.500

CCW Arc (1st) Start:89.381,185.024 Mid:89.470,185.311 End:X 89.50000,Y 185.61003,Z -1.60000 Centre:88.000,185.610 Centre Inc:-1.381,0.586 Radius:1.500

Feed (1st) X 89.50000 Y 245.61003 Z -1.60000 R 353.67831

CCW Arc (1st) Start:89.500,245.610 Mid:89.061,246.671 End:X 88.00000,Y 247.11003,Z -1.60000 Centre:88.000,245.610 Centre Inc:-1.500,0.000 Radius:1.500

Feed (1st) X 37.00000 Y 247.11003 Z -1.60000 R 355.83831

CCW Arc (1st) Start:37.000,247.110 Mid:35.939,246.671 End:X 35.50000,Y 245.61003,Z -1.60000 Centre:37.000,245.610 Centre Inc:-0.000,-1.500 Radius:1.500

Feed (1st) X 35.50000 Y 185.61003 Z -1.60000 R 267.27835

CCW Arc (1st) Start:35.500,185.610 Mid:35.530,185.311 End:X 35.61912,Y 185.02422,Z -1.60000 Centre:37.000,185.610 Centre Inc:1.500,0.000 Radius:1.500

CW Arc (1st) Start:35.619,185.024 Mid:40.259,169.659 End:X 41.50070,Y 153.65580,Z -1.60000 Centre:-32.965,155.929 Centre Inc:-68.584,-29.095 Radius:74.500

Feed (1st) X 41.50070 Y 102.56426 Z -1.60000 R 147.69248

CW Arc (1st) Start:41.501,102.564 Mid:40.259,86.561 End:X 35.61912,Y 71.19584,Z -1.60000 Centre:-32.965,100.291 Centre Inc:-74.465,-2.273 Radius:74.500

CCW Arc (1st) Start:35.619,71.196 Mid:35.530,70.909 End:X 35.50000,Y 70.61003,Z -1.60000 Centre:37.000,70.610 Centre Inc:1.381,-0.586 Radius:1.500

Feed (1st) X 35.50000 Y 10.61003 Z -1.60000 R 15.27844

CCW Arc (1st) Start:35.500,10.610 Mid:35.939,9.549 End:X 37.00000,Y 9.11003,Z -1.60000 Centre:37.000,10.610 Centre

Inc:1.500,0.000 Radius:1.500

Plunge X 37.00000 Y 9.11003 Z -3.20000 R 13.11844 FeedRate:3000

Feed Rate Change - 4560

Feed (1st) X 88.00000 Y 9.11003 Z -3.20000 R 13.11844

CCW Arc (1st) Start:88.000,9.110 Mid:89.061,9.549 End:X 89.50000,Y 10.61003,Z -3.20000 Centre:88.000,10.610 Centre Inc:-0.000,1.500 Radius:1.500

Feed (1st) X 89.50000 Y 70.61003 Z -3.20000 R 101.67840

CCW Arc (1st) Start:89.500,70.610 Mid:89.470,70.909 End:X 89.38088,Y 71.19584,Z -3.20000 Centre:88.000,70.610 Centre Inc:-1.500,-0.000 Radius:1.500

CW Arc (1st) Start:89.381,71.196 Mid:84.741,86.561 End:X 83.49930,Y 102.56426,Z -3.20000 Centre:157.965,100.291 Centre Inc:68.584,29.095 Radius:74.500

Feed (1st) X 83.49930 Y 153.65580 Z -3.20000 R 221.26427

CW Arc (1st) Start:83.499,153.656 Mid:84.741,169.659 End:X 89.38088,Y 185.02422,Z -3.20000 Centre:157.965,155.929 Centre Inc:74.465,2.273 Radius:74.500

CCW Arc (1st) Start:89.381,185.024 Mid:89.470,185.311 End:X 89.50000,Y 185.61003,Z -3.20000 Centre:88.000,185.610 Centre Inc:-1.381,0.586 Radius:1.500

Feed (1st) X 89.50000 Y 245.61003 Z -3.20000 R 353.67831

CCW Arc (1st) Start:89.500,245.610 Mid:89.061,246.671 End:X 88.00000,Y 247.11003,Z -3.20000 Centre:88.000,245.610 Centre Inc:-1.500,0.000 Radius:1.500

Feed (1st) X 37.00000 Y 247.11003 Z -3.20000 R 355.83831

CCW Arc (1st) Start:37.000,247.110 Mid:35.939,246.671 End:X 35.50000,Y 245.61003,Z -3.20000 Centre:37.000,245.610 Centre Inc:-0.000,-1.500 Radius:1.500

Feed (1st) X 35.50000 Y 185.61003 Z -3.20000 R 267.27835

CCW Arc (1st) Start:35.500,185.610 Mid:35.530,185.311 End:X 35.61912,Y 185.02422,Z -3.20000 Centre:37.000,185.610 Centre Inc:1.500,0.000 Radius:1.500

CW Arc (1st) Start:35.619,185.024 Mid:40.259,169.659 End:X 41.50070,Y 153.65580,Z -3.20000 Centre:-32.965,155.929 Centre Inc:-68.584,-29.095 Radius:74.500

Feed (1st) X 41.50070 Y 102.56426 Z -3.20000 R 147.69248

CW Arc (1st) Start:41.501,102.564 Mid:40.259,86.561 End:X 35.61912,Y 71.19584,Z -3.20000 Centre:-32.965,100.291 Centre Inc:-74.465,-2.273 Radius:74.500

CCW Arc (1st) Start:35.619,71.196 Mid:35.530,70.909 End:X 35.50000,Y 70.61003,Z -3.20000 Centre:37.000,70.610 Centre Inc:1.381,-0.586 Radius:1.500

Feed (1st) X 35.50000 Y 10.61003 Z -3.20000 R 15.27844

CCW Arc (1st) Start:35.500,10.610 Mid:35.939,9.549 End:X 37.00000,Y 9.11003,Z -3.20000 Centre:37.000,10.610 Centre Inc:1.500,0.000 Radius:1.500

Feed Rate Change - 98765

Retract X 37.00000 Y 9.11003 Z 15.00000 R 13.11844

Feed Rate Change - 98765

Rapid (1st) X 100.00000 Y 9.11003 Z 15.00000 R 13.11844 FeedRate:98765

Plunge X 100.00000 Y 9.11003 Z -1.60000 R 13.11844 FeedRate:3000

Feed Rate Change - 4560

Feed (1st) X 151.00000 Y 9.11003 Z -1.60000 R 13.11844

CCW Arc (1st) Start:151.000,9.110 Mid:152.061,9.549 End:X 152.50000,Y 10.61003,Z -1.60000 Centre:151.000,10.610 Centre Inc:0.000,1.500 Radius:1.500

Feed (1st) X 152.50000 Y 70.61003 Z -1.60000 R 101.67840

CCW Arc (1st) Start:152.500,70.610 Mid:152.470,70.909 End:X 152.38088,Y 71.19584,Z -1.60000 Centre:151.000,70.610 Centre Inc:-1.500,0.000 Radius:1.500

CW Arc (1st) Start:152.381,71.196 Mid:147.741,86.561 End:X 146.49930,Y 102.56426,Z -1.60000 Centre:220.965,100.291 Centre Inc:68.584,29.095 Radius:74.500

Feed (1st) X 146.49930 Y 153.65580 Z -1.60000 R 221.26427

CW Arc (1st) Start:146.499,153.656 Mid:147.741,169.659 End:X 152.38088,Y 185.02422,Z -1.60000 Centre:220.965,155.929

Centre Inc:74.465,2.273 Radius:74.500

CCW Arc (1st) Start:152.381,185.024 Mid:152.470,185.311 End:X 152.50000,Y 185.61003,Z -1.60000 Centre:151.000,185.610 Centre Inc:-1.381,0.586 Radius:1.500

Feed (1st) X 152.50000 Y 245.61003 Z -1.60000 R 353.67831

CCW Arc (1st) Start:152.500,245.610 Mid:152.061,246.671 End:X 151.00000,Y 247.11003,Z -1.60000 Centre:151.000,245.610 Centre Inc:-1.500,0.000 Radius:1.500

Feed (1st) X 100.00000 Y 247.11003 Z -1.60000 R 355.83831

CCW Arc (1st) Start:100.000,247.110 Mid:98.939,246.671 End:X 98.50000,Y 245.61003,Z -1.60000 Centre:100.000,245.610 Centre Inc:0.000,-1.500 Radius:1.500

Feed (1st) X 98.50000 Y 185.61003 Z -1.60000 R 267.27835

CCW Arc (1st) Start:98.500,185.610 Mid:98.530,185.311 End:X 98.61912,Y 185.02422,Z -1.60000 Centre:100.000,185.610 Centre Inc:1.500,-0.000 Radius:1.500

CW Arc (1st) Start:98.619,185.024 Mid:103.259,169.659 End:X 104.50070,Y 153.65580,Z -1.60000 Centre:30.035,155.929 Centre Inc:-68.584,-29.095 Radius:74.500

Feed (1st) X 104.50070 Y 102.56426 Z -1.60000 R 147.69248

CW Arc (1st) Start:104.501,102.564 Mid:103.259,86.561 End:X 98.61912,Y 71.19584,Z -1.60000 Centre:30.035,100.291 Centre Inc:-74.465,-2.273 Radius:74.500

CCW Arc (1st) Start:98.619,71.196 Mid:98.530,70.909 End:X 98.50000,Y 70.61003,Z -1.60000 Centre:100.000,70.610 Centre Inc:1.381,-0.586 Radius:1.500

Feed (1st) X 98.50000 Y 10.61003 Z -1.60000 R 15.27844

CCW Arc (1st) Start:98.500,10.610 Mid:98.939,9.549 End:X 100.00000,Y 9.11003,Z -1.60000 Centre:100.000,10.610 Centre Inc:1.500,0.000 Radius:1.500

Plunge X 100.00000 Y 9.11003 Z -3.20000 R 13.11844 FeedRate:3000

Feed Rate Change - 4560

Feed (1st) X 151.00000 Y 9.11003 Z -3.20000 R 13.11844

CCW Arc (1st) Start:151.000,9.110 Mid:152.061,9.549 End:X 152.50000,Y 10.61003,Z -3.20000 Centre:151.000,10.610 Centre Inc:0.000,1.500 Radius:1.500

Feed (1st) X 152.50000 Y 70.61003 Z -3.20000 R 101.67840

CCW Arc (1st) Start:152.500,70.610 Mid:152.470,70.909 End:X 152.38088,Y 71.19584,Z -3.20000 Centre:151.000,70.610 Centre Inc:-1.500,0.000 Radius:1.500

CW Arc (1st) Start:152.381,71.196 Mid:147.741,86.561 End:X 146.49930,Y 102.56426,Z -3.20000 Centre:220.965,100.291 Centre Inc:68.584,29.095 Radius:74.500

Feed (1st) X 146.49930 Y 153.65580 Z -3.20000 R 221.26427

CW Arc (1st) Start:146.499,153.656 Mid:147.741,169.659 End:X 152.38088,Y 185.02422,Z -3.20000 Centre:220.965,155.929 Centre Inc:74.465,2.273 Radius:74.500

CCW Arc (1st) Start:152.381,185.024 Mid:152.470,185.311 End:X 152.50000,Y 185.61003,Z -3.20000 Centre:151.000,185.610 Centre Inc:-1.381,0.586 Radius:1.500

Feed (1st) X 152.50000 Y 245.61003 Z -3.20000 R 353.67831

CCW Arc (1st) Start:152.500,245.610 Mid:152.061,246.671 End:X 151.00000,Y 247.11003,Z -3.20000 Centre:151.000,245.610 Centre Inc:-1.500,0.000 Radius:1.500

Feed (1st) X 100.00000 Y 247.11003 Z -3.20000 R 355.83831

CCW Arc (1st) Start:100.000,247.110 Mid:98.939,246.671 End:X 98.50000,Y 245.61003,Z -3.20000 Centre:100.000,245.610 Centre Inc:0.000,-1.500 Radius:1.500

Feed (1st) X 98.50000 Y 185.61003 Z -3.20000 R 267.27835

CCW Arc (1st) Start:98.500,185.610 Mid:98.530,185.311 End:X 98.61912,Y 185.02422,Z -3.20000 Centre:100.000,185.610 Centre Inc:1.500,-0.000 Radius:1.500

CW Arc (1st) Start:98.619,185.024 Mid:103.259,169.659 End:X 104.50070,Y 153.65580,Z -3.20000 Centre:30.035,155.929 Centre Inc:-68.584,-29.095 Radius:74.500

Feed (1st) X 104.50070 Y 102.56426 Z -3.20000 R 147.69248

CW Arc (1st) Start:104.501,102.564 Mid:103.259,86.561 End:X 98.61912,Y 71.19584,Z -3.20000 Centre:30.035,100.291

Centre Inc:-74.465,-2.273 Radius:74.500

CCW Arc (1st) Start:98.619,71.196 Mid:98.530,70.909 End:X 98.50000,Y 70.61003,Z -3.20000 Centre:100.000,70.610 Centre Inc:1.381,-0.586 Radius:1.500

Feed (1st) X 98.50000 Y 10.61003 Z -3.20000 R 15.27844

CCW Arc (1st) Start:98.500,10.610 Mid:98.939,9.549 End:X 100.00000,Y 9.11003,Z -3.20000 Centre:100.000,10.610 Centre Inc:1.500,0.000 Radius:1.500

Feed Rate Change - 98765

Retract X 100.00000 Y 9.11003 Z 15.00000 R 13.11844

Feed Rate Change - 98765

Rapid (1st) X 161.50000 Y 54.38997 Z 15.00000 R 78.32153 FeedRate:98765

Plunge X 161.50000 Y 54.38997 Z -1.60000 R 78.32153 FeedRate:3000

Feed Rate Change - 4560

Feed (1st) X 161.50000 Y 4.38997 Z -1.60000 R 6.32156

CCW Arc (1st) Start:161.500,4.390 Mid:161.939,3.329 End:X 163.00000,Y 2.88997,Z -1.60000 Centre:163.000,4.390 Centre Inc:1.500,-0.000 Radius:1.500

Feed (1st) X 213.00000 Y 2.88997 Z -1.60000 R 4.16156

CCW Arc (1st) Start:213.000,2.890 Mid:214.061,3.329 End:X 214.50000,Y 4.38997,Z -1.60000 Centre:213.000,4.390 Centre Inc:0.000,1.500 Radius:1.500

Feed (1st) X 214.50000 Y 54.38997 Z -1.60000 R 78.32153

CCW Arc (1st) Start:214.500,54.390 Mid:214.061,55.451 End:X 213.00000,Y 55.88997,Z -1.60000 Centre:213.000,54.390 Centre Inc:-1.500,0.000 Radius:1.500

Feed (1st) X 163.00000 Y 55.88997 Z -1.60000 R 80.48153

CCW Arc (1st) Start:163.000,55.890 Mid:161.939,55.451 End:X 161.50000,Y 54.38997,Z -1.60000 Centre:163.000,54.390 Centre Inc:-0.000,-1.500 Radius:1.500

Plunge X 161.50000 Y 54.38997 Z -3.20000 R 78.32153 FeedRate:3000

Feed Rate Change - 4560

Feed (1st) X 161.50000 Y 4.38997 Z -3.20000 R 6.32156

CCW Arc (1st) Start:161.500,4.390 Mid:161.939,3.329 End:X 163.00000,Y 2.88997,Z -3.20000 Centre:163.000,4.390 Centre Inc:1.500,-0.000 Radius:1.500

Feed (1st) X 213.00000 Y 2.88997 Z -3.20000 R 4.16156

CCW Arc (1st) Start:213.000,2.890 Mid:214.061,3.329 End:X 214.50000,Y 4.38997,Z -3.20000 Centre:213.000,4.390 Centre Inc:0.000,1.500 Radius:1.500

Feed (1st) X 214.50000 Y 54.38997 Z -3.20000 R 78.32153

CCW Arc (1st) Start:214.500,54.390 Mid:214.061,55.451 End:X 213.00000,Y 55.88997,Z -3.20000 Centre:213.000,54.390 Centre Inc:-1.500,0.000 Radius:1.500

Feed (1st) X 163.00000 Y 55.88997 Z -3.20000 R 80.48153

CCW Arc (1st) Start:163.000,55.890 Mid:161.939,55.451 End:X 161.50000,Y 54.38997,Z -3.20000 Centre:163.000,54.390 Centre Inc:-0.000,-1.500 Radius:1.500

Feed Rate Change - 98765

Retract X 161.50000 Y 54.38997 Z 15.00000 R 78.32153

Feed Rate Change - 98765

Rapid (1st) X 161.93934 Y 117.45063 Z 15.00000 R 169.12885 FeedRate:98765

Plunge X 161.93934 Y 117.45063 Z -1.60000 R 169.12885 FeedRate:3000

Feed Rate Change - 4560

CCW Arc (1st) Start:161.939,117.451 Mid:161.614,116.964 End:X 161.50000,Y 116.38997,Z -1.60000 Centre:163.000,116.390 Centre Inc:1.061,-1.061 Radius:1.500

Feed (1st) X 161.50000 Y 66.38997 Z -1.60000 R 95.60152

CCW Arc (1st) Start:161.500,66.390 Mid:161.939,65.329 End:X 163.00000,Y 64.88997,Z -1.60000 Centre:163.000,66.390 Centre Inc:1.500,-0.000 Radius:1.500

Feed (1st) X 213.00000 Y 64.88997 Z -1.60000 R 93.44153

CCW Arc (1st) Start:213.000,64.890 Mid:214.061,65.329 End:X 214.50000,Y 66.38997,Z -1.60000 Centre:213.000,66.390 Centre Inc:0.000,1.500 Radius:1.500

Feed (1st) X 214.50000 Y 116.38997 Z -

1.60000 R 167.60150

CCW Arc (1st) Start:214.500,116.390 Mid:214.061,117.451 End:X 213.00000,Y 117.88997,Z -1.60000 Centre:213.000,116.390 Centre Inc:-1.500,0.000 Radius:1.500

Feed (1st) X 163.00000 Y 117.88997 Z -1.60000 R 169.76150

CCW Arc (1st) Start:163.000,117.890 Mid:162.426,117.776 End:X 161.93934,Y 117.45063,Z -1.60000 Centre:163.000,116.390 Centre Inc:0.000,-1.500 Radius:1.500

Plunge X 161.93934 Y 117.45063 Z -3.20000 R 169.12885 FeedRate:3000

Feed Rate Change - 4560

CCW Arc (1st) Start:161.939,117.451 Mid:161.614,116.964 End:X 161.50000,Y 116.38997,Z -3.20000 Centre:163.000,116.390 Centre Inc:1.061,-1.061 Radius:1.500

Feed (1st) X 161.50000 Y 66.38997 Z -3.20000 R 95.60152

CCW Arc (1st) Start:161.500,66.390 Mid:161.939,65.329 End:X 163.00000,Y 64.88997,Z -3.20000 Centre:163.000,66.390 Centre Inc:1.500,-0.000 Radius:1.500

Feed (1st) X 213.00000 Y 64.88997 Z -3.20000 R 93.44153

CCW Arc (1st) Start:213.000,64.890 Mid:214.061,65.329 End:X 214.50000,Y 66.38997,Z -3.20000 Centre:213.000,66.390 Centre Inc:0.000,1.500 Radius:1.500

Feed (1st) X 214.50000 Y 116.38997 Z -3.20000 R 167.60150

CCW Arc (1st) Start:214.500,116.390 Mid:214.061,117.451 End:X 213.00000,Y 117.88997,Z -3.20000 Centre:213.000,116.390 Centre Inc:-1.500,0.000 Radius:1.500

Feed (1st) X 163.00000 Y 117.88997 Z -3.20000 R 169.76150

CCW Arc (1st) Start:163.000,117.890 Mid:162.426,117.776 End:X 161.93934,Y 117.45063,Z -3.20000 Centre:163.000,116.390 Centre Inc:0.000,-1.500 Radius:1.500

Feed Rate Change - 98765

Retract X 161.93934 Y 117.45063 Z 15.00000 R 169.12885

Feed Rate Change - 98765

Rapid (1st) X 161.50000 Y 178.38997 Z 15.00000 R 256.88147 FeedRate:98765

Plunge X 161.50000 Y 178.38997 Z -1.60000 R 256.88147 FeedRate:3000

Feed Rate Change - 4560

Feed (1st) X 161.50000 Y 128.38997 Z -1.60000 R 184.88149

CCW Arc (1st) Start:161.500,128.390 Mid:161.939,127.329 End:X 163.00000,Y 126.88997,Z -1.60000 Centre:163.000,128.390 Centre Inc:1.500,-0.000 Radius:1.500

Feed (1st) X 213.00000 Y 126.88997 Z -1.60000 R 182.72149

CCW Arc (1st) Start:213.000,126.890 Mid:214.061,127.329 End:X 214.50000,Y 128.38997,Z -1.60000 Centre:213.000,128.390 Centre Inc:0.000,1.500 Radius:1.500

Feed (1st) X 214.50000 Y 178.38997 Z -1.60000 R 256.88147

CCW Arc (1st) Start:214.500,178.390 Mid:214.061,179.451 End:X 213.00000,Y 179.88997,Z -1.60000 Centre:213.000,178.390 Centre Inc:-1.500,0.000 Radius:1.500

Feed (1st) X 163.00000 Y 179.88997 Z -1.60000 R 259.04147

CCW Arc (1st) Start:163.000,179.890 Mid:161.939,179.451 End:X 161.50000,Y 178.38997,Z -1.60000 Centre:163.000,178.390 Centre Inc:0.000,-1.500 Radius:1.500

Plunge X 161.50000 Y 178.38997 Z -3.20000 R 256.88147 FeedRate:3000

Feed Rate Change - 4560

Feed (1st) X 161.50000 Y 128.38997 Z -3.20000 R 184.88149

CCW Arc (1st) Start:161.500,128.390 Mid:161.939,127.329 End:X 163.00000,Y 126.88997,Z -3.20000 Centre:163.000,128.390 Centre Inc:1.500,-0.000 Radius:1.500

Feed (1st) X 213.00000 Y 126.88997 Z -3.20000 R 182.72149

CCW Arc (1st) Start:213.000,126.890 Mid:214.061,127.329 End:X 214.50000,Y 128.38997,Z -3.20000 Centre:213.000,128.390 Centre Inc:0.000,1.500 Radius:1.500

Feed (1st) X 214.50000 Y 178.38997 Z -3.20000 R 256.88147

CCW Arc (1st) Start:214.500,178.390 Mid:214.061,179.451 End:X 213.00000,Y 179.88997,Z -3.20000 Centre:213.000,178.390 Centre Inc:-1.500,0.000 Radius:1.500

Feed (1st) X 163.00000 Y 179.88997 Z -3.20000 R 259.04147

CCW Arc (1st) Start:163.000,179.890 Mid:161.939,179.451 End:X 161.50000,Y 178.38997,Z -3.20000 Centre:163.000,178.390 Centre Inc:0.000,-1.500 Radius:1.500

Feed Rate Change - 98765

Retract X 161.50000 Y 178.38997 Z 15.00000 R 256.88147

Feed Rate Change - 98765

Rapid (1st) X 161.93934 Y 241.36717 Z 15.00000 R 347.56861 FeedRate:98765

Plunge X 161.93934 Y 241.36717 Z -1.60000 R 347.56861 FeedRate:3000

Feed Rate Change - 4560

CCW Arc (1st) Start:161.939,241.367 Mid:161.614,240.881 End:X 161.50000,Y 240.30651,Z -1.60000 Centre:163.000,240.307 Centre Inc:1.061,-1.061 Radius:1.500

Feed (1st) X 161.50000 Y 190.30651 Z -1.60000 R 274.04128

CCW Arc (1st) Start:161.500,190.307 Mid:161.939,189.246 End:X 163.00000,Y 188.80651,Z -1.60000 Centre:163.000,190.307 Centre Inc:1.500,-0.000 Radius:1.500

Feed (1st) X 213.00000 Y 188.80651 Z -1.60000 R 271.88128

CCW Arc (1st) Start:213.000,188.807 Mid:214.061,189.246 End:X 214.50000,Y 190.30651,Z -1.60000 Centre:213.000,190.307 Centre Inc:0.000,1.500 Radius:1.500

Feed (1st) X 214.50000 Y 240.30651 Z -1.60000 R 346.04126

CCW Arc (1st) Start:214.500,240.307 Mid:214.061,241.367 End:X 213.00000,Y 241.80651,Z -1.60000 Centre:213.000,240.307 Centre Inc:-1.500,0.000 Radius:1.500

Feed (1st) X 163.00000 Y 241.80651 Z -1.60000 R 348.20125

CCW Arc (1st) Start:163.000,241.807 Mid:162.426,241.692 End:X 161.93934,Y 241.36717,Z -1.60000 Centre:163.000,240.307 Centre Inc:-0.000,-1.500 Radius:1.500

Plunge X 161.93934 Y 241.36717 Z -3.20000 R 347.56861 FeedRate:3000

Feed Rate Change - 4560

CCW Arc (1st) Start:161.939,241.367 Mid:161.614,240.881 End:X 161.50000,Y 240.30651,Z -3.20000 Centre:163.000,240.307 Centre Inc:1.061,-1.061 Radius:1.500

Feed (1st) X 161.50000 Y 190.30651 Z -3.20000 R 274.04128

CCW Arc (1st) Start:161.500,190.307 Mid:161.939,189.246 End:X 163.00000,Y 188.80651,Z -3.20000 Centre:163.000,190.307 Centre Inc:1.500,-0.000 Radius:1.500

Feed (1st) X 213.00000 Y 188.80651 Z -3.20000 R 271.88128

CCW Arc (1st) Start:213.000,188.807 Mid:214.061,189.246 End:X 214.50000,Y 190.30651,Z -3.20000 Centre:213.000,190.307 Centre Inc:0.000,1.500 Radius:1.500

Feed (1st) X 214.50000 Y 240.30651 Z -3.20000 R 346.04126

CCW Arc (1st) Start:214.500,240.307 Mid:214.061,241.367 End:X 213.00000,Y 241.80651,Z -3.20000 Centre:213.000,240.307 Centre Inc:-1.500,0.000 Radius:1.500

Feed (1st) X 163.00000 Y 241.80651 Z -3.20000 R 348.20125

CCW Arc (1st) Start:163.000,241.807 Mid:162.426,241.692 End:X 161.93934,Y 241.36717,Z -3.20000 Centre:163.000,240.307 Centre Inc:-0.000,-1.500 Radius:1.500

Feed Rate Change - 98765

Retract X 161.93934 Y 241.36717 Z 15.00000 R 347.56861

Feed Rate Change - 98765

Rapid (1st) X 0.00000 Y 0.00000 Z 15.00000 R 0.00000 FeedRate:98765

End Of File

Final Tool Position: X 0.00000 Y 0.00000 Z 15.00000 R 0.00000

Home Position: 0.00000 0.00000 15.00000 0.00000

Appendix C Designed adapter for 100N load cell

Due to the novelty of MH reinforced BC, it is also very important to select the best technology to test accurately MHF.

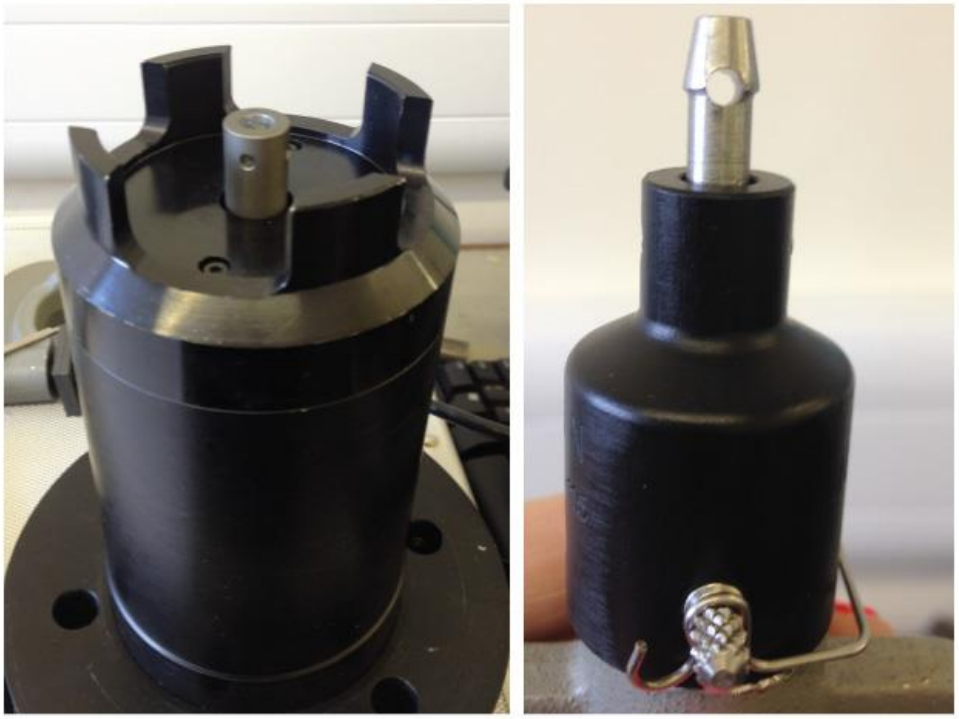

Figure_Apx 7-3 Adaptor designed for 100N load cell

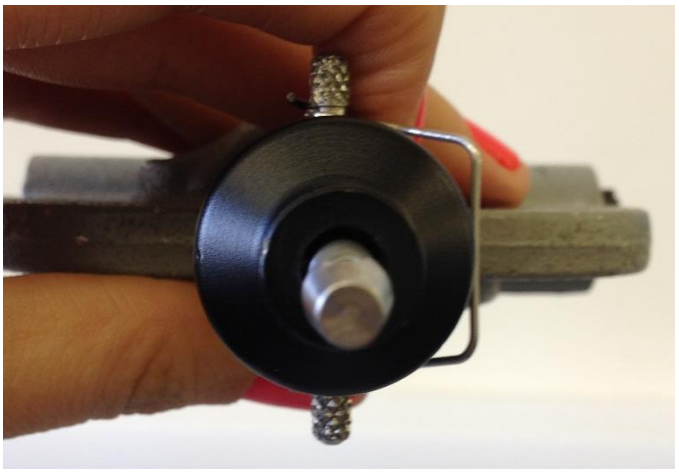

Figure_Apx 7-4 Adaptor designed for 100N load cell

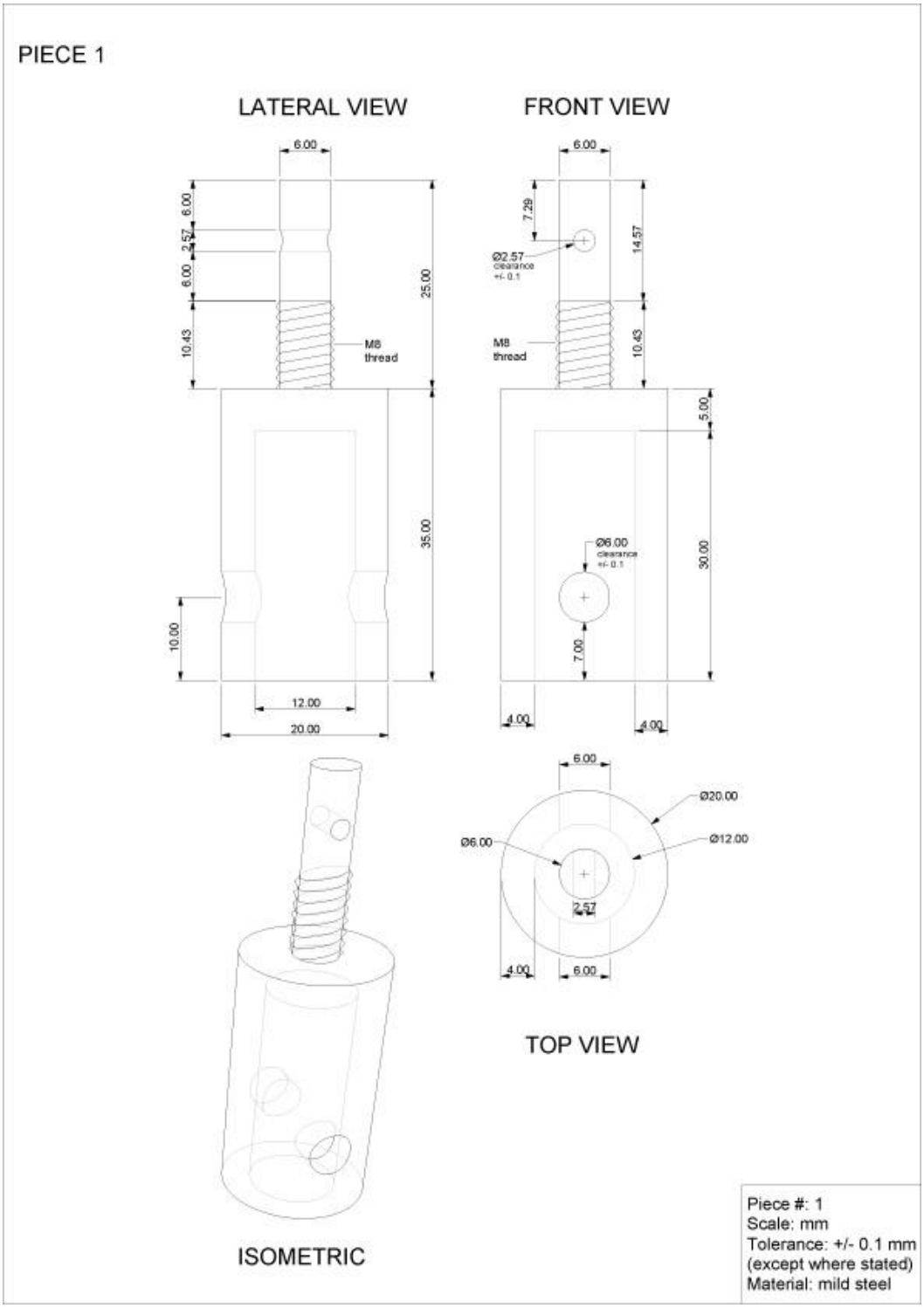

Figure_Apx 7-5 Adaptor manufacturing blueprints

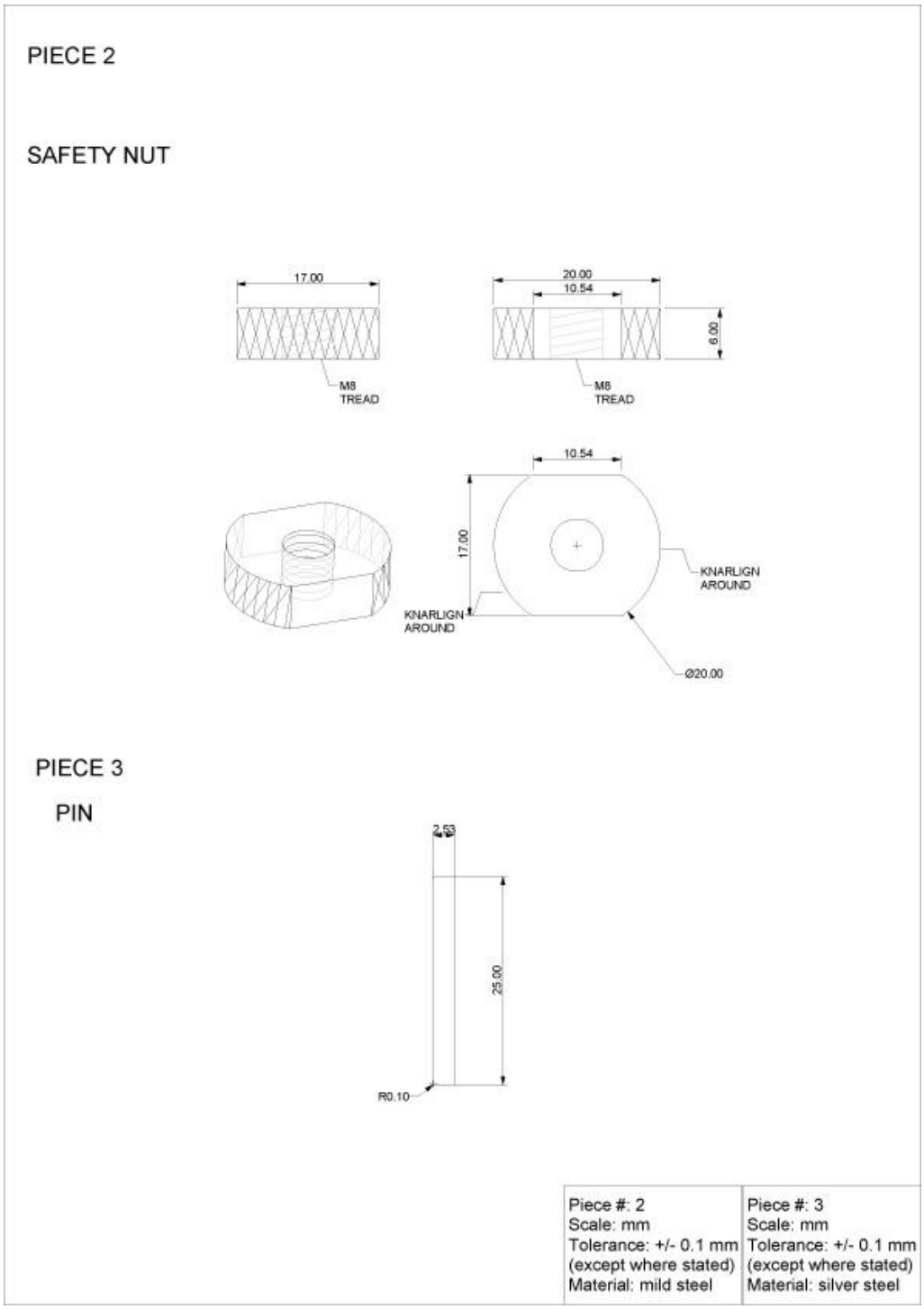

Figure 7-6 Adaptor safety nut manufacturing blueprints

Appendix D Shortfalls and overshoot in the Raworth's Doughnut

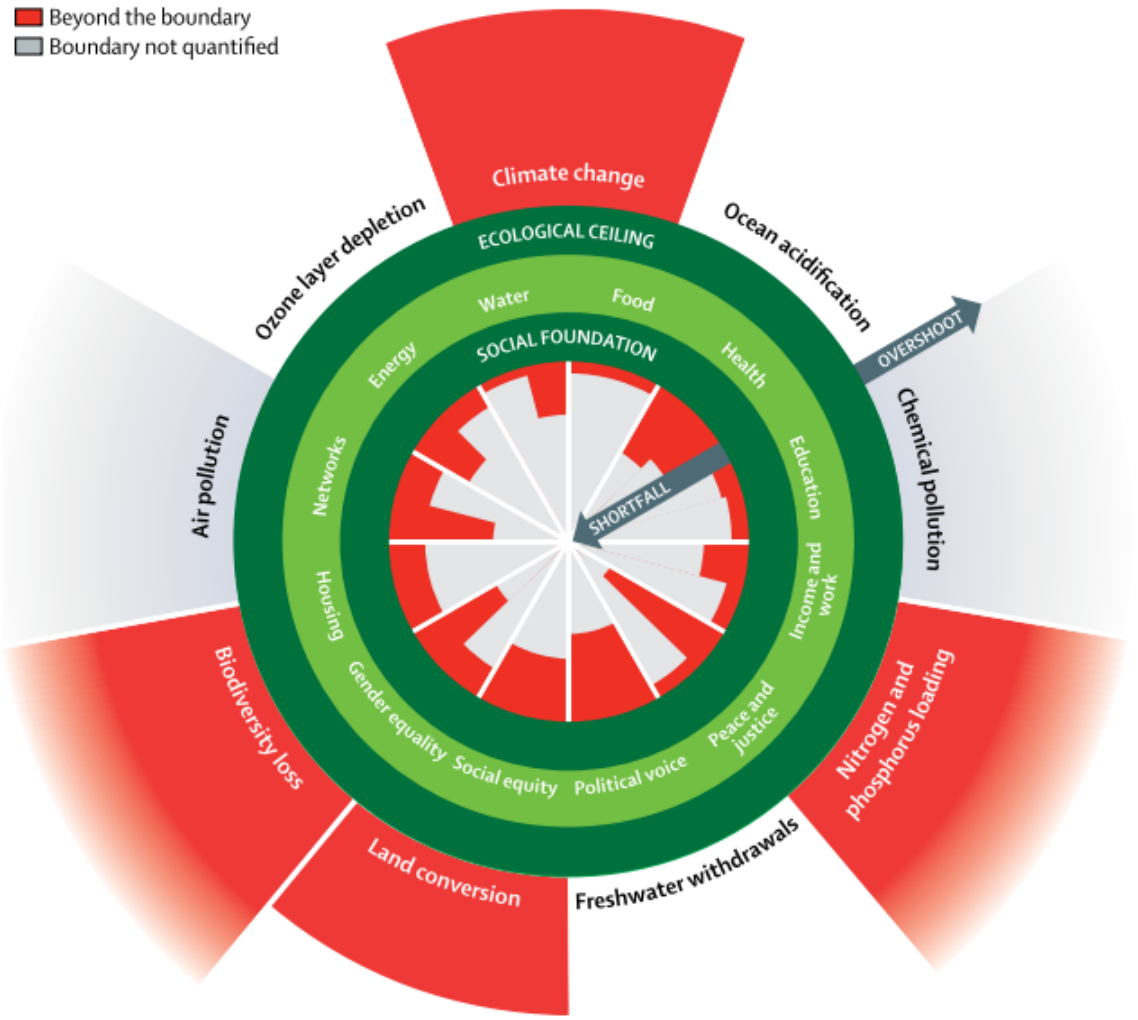

Figure_Apx 7-7 Shortfalls and overshoot in the Doughnut. Dark green circles show the social foundation and ecological ceiling, encompassing a safe and just space for humanity. Red wedges show shortfalls in the social foundation or overshoot of the ecological ceiling

Appendix E Tensile test fractures

Figure_Apx 7-8 M30 control samples fractures after tensile test

Figure_Apx 7-9 M30 aged samples fractures after tensile test

Figure_Apx 7-10 M20 control samples fractures after tensile test

Figure_Apx 7-11 M30 aged samples fractures after tensile test

Appendix F Pugh selection data matrix

	Sample		MDP [1]	light MDF[2]	WB-M	CHB-M	MB-M	WL-M	CHL-M	ML-M	WE-M	CHE-M	ME-M	AKE-M	WB-A	CHB-A	MB-A	WL-A	CHL-A	ML-A	WE-A	CHE-A	ME-A	AKE-A
	Criteria																							
fibre	source	units	Pine wood	Eucalyptus wood	MASH	MASH	MASH	MASH	MASH	MASH	MASH	MASH	MASH	MASH	ASPROS	ASPROS	ASPROS	ASPROS	ASPROS	ASPROS	ASPROS	ASPROS	ASPROS	ASPROS
fibre	availability (2015)	MT	64,000$^{(1)}$	29,000$^{(1)}$	.63	.63	.63	.63	.63	.63	.63	.63	.63	.63	1.6	1.6	1.6	1.6	1.6	1.6	1.6	1.6	1.6	1.6
fibre	size	/	particles	fibres	hull	swatches	particles & fibres	hull	swatches	particles & fibres	hull	swatches	particles & fibres	fibres	hull	swatches	particles & fibres	hull	swatches	particles & fibres	hull	swatches	particles & fibres	fibre
fibre	length	mm	2.15	2.15	239 x 67	30x30	.0937$^{(2)}$	239 x 67	30x30	.0937$^{(2)}$	239 x 67	30x30	.0937$^{(2)}$	.0937$^{(2)}$	181 x 67	30x30	.047$^{(2)}$	181 x 67	30x30	.047$^{(2)}$	181 x 67	30x30	.047$^{(2)}$	.047$^{(2)}$
fibre	UTS	MPa	10-80	10-80	72.9$^{(3)}$	10.7$^{(3)}$	46.6	72.9$^{(3)}$	10.7$^{(3)}$	46.6	72.9$^{(3)}$	10.7$^{(3)}$	46.6	77.9	51.1$^{(3)}$	4.3$^{(3)}$	42.9	51.1$^{(3)}$	4.3$^{(3)}$	42.9	51.1$^{(3)}$	4.3$^{(3)}$	42.9	50.5
fibre	elongation	%	10	10	2.8	3.2	4.3	2.8	3.2	4.3	2.8	3.2	4.3	5.2	3.7	4.1	7.6	3.7	4.1	7.6	3.7	4.1	7.6	3.7
fibre	Young's Modulus	GPa	n/a	n/a	n/a	n/a	4.5	n/a	n/a	4.5	n/a	n/a	4.5	3.7	4.8	n/a	1.9	4.8	n/a	1.9	4.8	n/a	1.9	3.0
fibre	extraction method	/	Chipped & defibrillated	Chipped & defibrillated	/	manually trimmed	milled	/	manually trimmed	milled	/	manually trimmed	milled	chemical	/	manually trimmed	milled	/	manually trimmed	milled	/	manually trimmed	milled	chemical
fibre	cost $^{(4)}$	£/ton	689,53	239,51	32.50	32.50	32.50	32.50	32.50	32.50	32.50	32.50	32.50	32.50	0-.65p	0-.65p	0-.65p	0-.65p	0-.65p	0-.65p	0-.65p	0-.65p	0-.65p	0-.65p
matrix	type		UF resin	UF resin	n/a	n/a	n/a	lignin	lignin	lignin	Bio-epoxy	Bio-epoxy	Bio-epoxy	Bio-epoxy	n/a	n/a	n/a	lignin	lignin	lignin	Bio-epoxy	Bio-epoxy	Bio-epoxy	Bio-epoxy
matrix	toxic emissions	mg/100g	0.7-1	10	0	0	0	0	0	0	n/a	n/a	n/a	n/a	0	0	0	0	0	0	n/a	n/a	n/a	n/a
matrix	biodegradability	%	/	/	100	100	100	95	95	95	60	60	60	60	100	100	100	95	95	95	60	60	60	60
matrix	availability		✓	✓	✓	✓	✓	✓	✓	✓	✓	✓	✓	✓	✓	✓	✓	✓	✓	✓	✓	✓	✓	✓
matrix	price	£/kg	1.58	1.58	0	0	0	47.5	47.5	47.5	20.3	20.3	20.3	20.3	0	0	0	47.5	47.5	47.5	20.3	20.3	20.3	20.3
MHC boards	Density	kg/m^3	680 ±40	720-735	450	278	639	773	579	327.2	493.8	521.7	688.3	671	536.3	/	471	355.3	425.2	345.5	545	500	578.6	561
MHC boards	thickness	mm	3 -32	9-12	3.1	2.5	2.9	3.4	2.9	2.9	3.2	3.3	3	3.4	3.1	/	3.6	4.1	3.4	2.5	3.7	3.5	3	3.5
MHC boards	MOR	MPa	36	27	0.886	0.207	1.5	3.9	1.1	0.327	4.4	11.5	18.1	8.4	0.865	/	0.616	0.94	1.3	0.127	7.8	11.2	7.9	3.9
MHC boards	Flexural modulus	GPa	16	3	5.3	3.0	10.4	21.4	13.5	4.4	26.4	68.4	714.3	64.8	13.5	/	4.8	7.2	11.6	3.4	70.6	176.7	181.4	45.1
MHC boards	Moisture content	%	8 ±3	8 ±3	6.1	7.5	6	5.9	5.1	4.9	5.5	5.8	5.8	7.6	5.8	/	5.5	3.8	3.5	5.6	7.7	5.1	3	5.6
MHC boards	Thickness swell	% 24h	25	15	/	/	/	/	/	/	/	/	/	/	/	/	/	/	/	/	/	/	22-29	48
manufacturing	fibre wetting	1-5$^{(5)}$	5	5	3	3	3	1	2	1	1	2	4	4	3	3	3	1	1	2	2	1	4	4
manufacturing	Mixing	1-5$^{(5)}$	5	5	2	2	3	1	3	4	2	3	4	4	1	3	2	2	2	3	1	2	4	3
manufacturing	surface appearance	A-D$^{(6)}$	D	D	B	B	A	B	A	C	B	C	C	B	A	A	A	A	A	B	A	B	C	C
manufacturing	structural appearance	1-5$^{(5)}$	5	5	2	1	4	2	3	1	2	3	3	2	1	1	2	1	2	2	1	2	3	3
manufacturing	voids	A-D$^{(6)}$	D	C	A	A	A	B	A	A	A	B	C	C	A	A	A	A	B	B	A	A	C	B
manufacturing	delamination		average	low	high	high	low	high	high	low	high	medium	low	low	high	high	low	high	average	low	high	high	low	low
manufacturing	retail price $^{(6)}$	£	5.9	6.8	/	/	/	/	/	/	/	/	/	/	/	/	/	/	/	/	/	/	4.2	3.5

(1) m^3 **(2)** mm^2 **(3)** breaking strength (N) **(4)** in Mexican peso exchange rate £1 = 25.58 MXP (23/11/2016) **(5)** 1= poor, 2= below average, 3= average, 4= good and 5= acceptable. **(6)** A= needs improvement, B= satisfactory, C= good, D= accomplished.

Figure_Apx 7-12 Data used for the Pugh matrix selection for 1st batch

Appendix G Engineering design materials

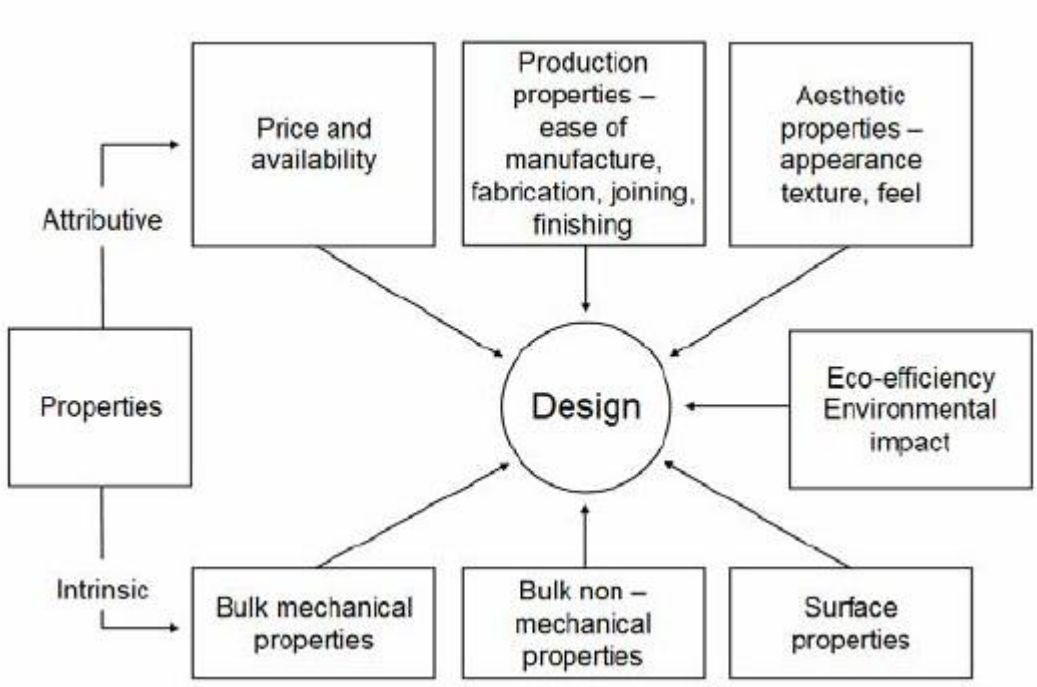

Figure_Apx 7-13 How the properties of engineering materials affect the way in which products are designed [208]

Appendix H General characteristics, applications and prices of WBF

Table_Apx 7-1 General characteristics, applications and prices of WBF in Mexico [200,201,223,231]

Board type	Board dimension (m)	Thickness (mm)	Density (kg/m^3)	Applications	Market price* (£)	Manufacturer
Thin MDF	1.22/1.52/1.83/2.15 x 2.44	3	730-820	Interior panels	4.45	Masisa
Light MDF	1.22/1.52/1.83/2.15 x 2.44	9	620-640	General use in dry environments	6.10	Duraplay
Standard MDF	1.22/1.52/1.83/2.15 x 2.44	6	730-830	General use in dry environments	5.01	EMMAN
Light MDF	1.22 x 2.44	6	640-740	Flooring base, furniture	5.10	Proteak
Particleboard	1.52 x 2.44	9	570-680	Furniture, non-structural wall claddings	3.90	Masisa

*** Mexican market exchange rate £1 = $ 26.91 Mexican pesos 18/01/2017**